The role of PI3K and ERBB family gene mutations and other abnormalities in resistance to HER2-targeted therapies in HER2-positive breast cancer

AUTHOR(S)

Naomi Elster

CITATION

Elster, Naomi (2016): The role of PI3K and ERBB family gene mutations and other abnormalities in resistance to HER2-targeted therapies in HER2-positive breast cancer. Royal College of Surgeons in Ireland. Thesis. https://doi.org/10.25419/rcsi.10809626.v1

DOI

10.25419/rcsi.10809626.v1

The role of PI3K and ERBB family gene mutations and other abnormalities in resistance to HER2-targeted therapies in HER2-positive breast cancer

Naomi Elster BSc

Medical Oncology Group, Department of Molecular Medicine

RCSI

A thesis submitted to the School of Postgraduate Studies, Faculty of Medicine and Health Sciences, Royal College of Surgeons in Ireland, in fulfilment of the degree of

Doctor of Philosophy

Supervisors: **Prof Bryan T Hennessy**

Dr Alex J Eustace

October 2016

I declare that this thesis, which I submit to RCSI for examination in consideration of the award of a higher degree of Doctor of Philosophy is my own personal effort. Where any of the content presented is the result of input or data from a related collaborative research programme this is duly acknowledged in the text such that it is possible to ascertain how much of the work is my own. I have not already obtained a degree in RCSI or elsewhere on the basis of this work. Furthermore, I took reasonable care to ensure that the work is original, and, to the best of my knowledge, does not breach copyright law, and has not been taken from other sources except where such work has been cited and acknowledged within the text.

Signed _____

Student Number _____

Date _____

Abbreviations

	Meaning		Meaning
2D	2-dimensional	LB	Luria Broth
3D	3-dimensional	LVI	Lymphovascular Invasion
AA	Amino Acid	mAb	Monoclonal Antibody
ADC	Antibody-Drug Conjugate	MAPK	Mitogen-Activated Protein Kinase
ADCC	Antibody-dependent cell-mediated ctyotoxicity	MDM2	Mouse double minute 2 homolog
ADP	Adenosine di-Phosphate	MEK	MAPK/ERK Kinase
ANOVA	Analysis of Variance	mg	milligrams
ATP	Adenosine tri-phosphate	min	minutes
BAD	Bcl-2 associated death protein	ml	millilitre
BCA	Bicinchronic Assay	mM	millimolar
BME	Beta Mercaptoethanol	MMP9	Matrix mettaloprotease 9
BMI	Body Mass Index	mTOR	Mammalian Target of Rapamycin
BRCA	Breast Cancer Susceptibility Gene	MUT	Mutated
BSA	Bovine Serum Albumin	NaCl	Sodium Chloride
BTC	Betacellulin	NaOH	Sodium Hydroxide
CF	Correction Factor	Neg	Negative
Chr	Chromosome	NEK1	NIMA-related kinase 1
CHO	Chinese Hamster Ovary	NFκB	Nuclear factor kappa-light-chain-enhancer of activated B cells
CI	Combination Index	NGS	Next Generation Sequencing
COSMIC	Catalogue of Somatic Mutations in Cancer	NI	Nonframeshift Insertion
CSA	Catalysed Signal Amplification	NK	Natural Killer
Ctrl	Control	nM	Nanomolar
DCIS	Ductal Carcinoma In Situ	NRG	Neuregulin
DFS	Disease-Free Survival	NSNV	Nonsynonymous Single Nucleotide Variation
dH2O	Distilled water	OS	Overall Survival
DMSO	Dimethyl Sulfoxide	OR	Odds Ratio
DNA	Deoxyribonucleic Acid	PBS	Phosphate Buffered Saline
dsDNA	Double stranded DNA	pCR	Pathologic Complete Response
ECOG	Eastern Cooperative Oncology Group Performance Status	PCR	Polymerase Chain Rea tion
ED_{25}	Effective Dose 25	PDK	Phosphoinositide-dependent kinase 1
ED_{50}	Effective Dose 50	PD-L1	Programmed Death Ligand 1
ED_{75}	Effective Dose 75	PFS	Progression Free Survival
EDTA	Ethylenediaminetetraacetic acid	PgR	Progesterone Receptor
EGF	Epidermal Growth Factor	PI3K	Phosphoinositide-3-kinase
EGFR	Epidermal Growth Factor Receptor	PIP_2	Phosphatidylinositol 4,5-bisphosphate
EPA	Environmental Protection Agency	PIP_3	Phosphatidylinositol (3,4,5)-trisphosphate
ER	Estrogen Receptor	PNPP	Para nitro phenol phosphate
Erk	Extracellular signal related kinase	Pos	Positive
EV	Empty Vector	PR	Progesterone Receptor
FBS	Fetal Bovine Serum	PTEN	Phosphatase and tensin homolog
FD	Frameshift Deletion	RFS	Relapse Free Survival
FFPE	Formalin Fixed Paraffin Embedded	RNA	Ribonucleic acid
FI	Frameshift Insertion	RPPA	Reverse Phase Protein Array
FISH	Flourescence in-situ hybridisation	RT	Room Temperature
FKHR	Forkhead Box Protein	RTK	Receptor Tyrosine Kinase
FOXO	Forkhead Box Protein subgroup	SAP	Shrimp alkaline phosphatase
g	Grams	SDS	Sodium dodecyl sulfate

GMO	Genetically Modified Organism	SFM	Serum Free Media
GSK3β	Glycogen Synthase Kinase 3	SGSNV	StopGain Single Nucleotide Variation
H&E	Hematoxylin and Eosin	SH2	Src Homology 2
HER1	Human Epidermal Growth Factor-like Receptor 1	SNV	Single Nucleotide Variation
HER2	Human Epidermal Growth Factor-like Receptor 2	STKLD1	Serine/threonine kinase-like domain-containing protein
HER3	Human Epidermal Growth Factor-like Receptor 3	T-DM1	Trastuzumab-emtansine
HER4	Human Epidermal Growth Factor-like Receptor 4	TCGA	The Cancer Genome Atlas
IC_{50}	Inhibitory Concentration 50	TFA	Trifluoroacetic acid
IDC	Invsive Ductal Carcinoma	TGF	Transforming Growth Factor
IGF1R	Insulin Growth Factor Receptor 1	TKI	Tyrosine Kinase Inhibitor
IHC	Immunohistochemistry	TRAIL	TNF-related-apoptosis-inducing ligand
ILC	Invasive Lobular Carcinoma	umol/L	micromoles per litre
IPTG	Isopropyl β-D-1-thiogalactopyranoside	UV	Ultraviolet
JNK	Jun Amino-terminated Kinase	VEGF	Vascular Epithelial Growth Factor
kDa	kilodalton	WT	Wild Type
KO	Knock Out	w/v	Weight/volume

Table of Contents

List of Figures

List of Tables

Summary

Trastuzumab resistance remains a challenge in the treatment of the 15-20% of breast cancers which are HER2-positive (HER2+ BC). Known mechanisms, including the PI3K pathway, account for some but not all cases of trastuzumab resistance.

The novel, pan-class I PI3K inhibitor copanlisib was tested alone and in combination with HER2-targeted therapies in a panel of HER2+BC cell lines, including models of acquired trastuzumab and/or lapatinib resistance. Reverse phase protein array was used to determine the effect of copanlisib on expression and activation of PI3K pathway components. 227 HER2+ BC tumours were assayed for ERBB family mutations using a custom-designed Sequenom panel. Two ERBB4 mutations, S303F and V721I, were created by site-directed mutagenesis and stably expressed in HER2+ BC cell lines to determine their effect on growth, invasiveness, signalling and response to HER2-targeted therapies.

Copanlisib is highly effective in HER2+ BC cell lines, including those with resistance to HER2-targeted therapies. The combination of HER2-targeted therapies and copanlisib is synergistic, and restores sensitivity to trastuzumab and lapatinib in cells with acquired resistance. Novel, somatic ERBB family mutations are present in 7.05% of HER2+BCs. There is a nonsignificant trend towards a survival effect after trastuzumab. The ERBB4 S303F mutation has increased HER4 kinase activity and is lethal to 2/3 cell lines. ERBB4 V721I increases HER4 overexpression, growth rate, and 3D colony formation. Both ERBB4 mutations studied alter sensitivity to copanlisib and the pan-HER inhibitor afatinib. The combination of copanlisib with HER2-targeted therapies is potentially an improved treatment for trastuzumab resistant HER2-positive breast cancer, which, due to our work presented herein, is now being evaluated in a Phase Ib/II clinical trial (Panther, ICORG 15-02). ERBB family mutations are present in 7.05% of HER2-positive breast cancers. ERBB4 S303F and V721I affect the biology of HER2+ BC and are potential predictive biomarker for copanlisib and afatinib.

Acknowledgements

This material is based upon works supported by the Irish Cancer Society Research Scholarship Award CRS11ELS.

I would like to firstly thank my mentor, Prof Bryan Hennessy, for giving me the opportunity to cut my teeth as a researcher on such an interesting and I will always believe worthwhile project. Looking back to how little naïve and inexperienced as a final year undergraduate student, it's hard to believe I had the potential to become the researcher (I hope) I am today. Thank you for not only seeing that potential, but nurturing and encouraging it. Every PhD project has its stumbling blocks, but I feel enormously proveleged in that I have never once doubted the relevance or value of what we were trying to achieve through this work. This is something for which I am profoundly grateful, and my role in providing the justification for the Panther study will always be one of my proudest achievements.

To my co-supervisor, Alex, it was you who taught me how to be a scientist. Thank you for your mentorship, which I value very much, for passing on so many skills, for being so generous with your time over the years, and most especially, for always pushing me to do better, and believing that I can. Without your support I would never have completed this project, and it certainly wouldn't have been the success we have made it. You also taught me how to persevere, even when (in your own words – I never have forgotten them) "This is science, and sometimes it kicks you in the face." Be assured that wherever life takes me, my fonts will be justified and my tables free of overhangs.

I hope that my subsequent career, for which you laid the foundations, will make you both proud.

I would like to thank Prof Hennessy's Medical Oncology group for all of their support, moral as well as practical, over the years. Particular thanks must go to Dr Sinead Toomey for her sequenom and next-generation sequencing work, Dr Mattia Cremona for his help with the proteomics studies in this project, and Dr Malgorzata Milewska for her help with microbiology

and molecular biology techniques. I acknowledge Prof Bryan Harvey for kindly providing us with working space in his Department of Molecular Medicine, and Lorraine Nolan and Dr Olive McCabe for taking care of administration and lab management. Your efforts keep the lab running smoothly, and I can't overstate how crucial this is to the the success of every researcher to pass through this lab. Thank you to the support staff and porters in the Smurfit building for their kindness and practical assistance. Special thanks also to Prof Niamh Moran and the RCSI School of Postgraduate Studies for their help, guidance and support.

I thank our collaborators for the expertise and time they lent to making this project a success. Prof Gallagher's Cancer Biology and Therapeutics group at University College Dublin for providing the bioinformatics support which helped us make sense of our next-generation data, Dr Madeline Murphy's group at the UCD Conway Institute for carrying out lentiviral transfections, the staff at Beaumont and St Vincent's Hospitals who assisted in the collection of tumours and patient data for our study, and Prof Elaine Kay's team at the Department of Pathology for their assistance reviewing and staining said tumours. Thanks to Dr Scott Wilhelm at Bayer Pharmaceuticals for his support, guidance and excellent communication during our copanlisib studies.

Special thanks must go to The Irish Cancer Society. It was their scholarship which made it possible for me to carry out this work, but their support over the years has gone much over and beyond what I would have expected of any funding body. Thank you also for the career development workshops, networking events, and opportunities to present research to the public, and for the sense of community these events created amongst the Irish Cancer Society scholars and fellows. Many of us now keep in touch socially and network professionally across different institutions, cities, and even countries. It was an honour to have part of the work presented in this thesis used in 2015's 'Paint It Pink' national campaign, and to speak at your press launch.

On a more personal note, thank you to my close friends who have supported me through this work, even when it's become so all-consuming I've struggled to keep in touch, even when life has taken us to different cities and countries.

Finally, I wish there were words powerful enough to thank my immediate and extended family as they deserve to be thanked, for seeing me through a life where I have never for a second been unloved and unsupported, and for being a constant source of inspiration. Thank you to my parents, Aoife and Steve, for welcoming me home when I became so ill I didn't feel like a human anymore, and for not turfing me out again when I recovered, so I could complete this PhD. Thank you for not just accepting that I might never leave university, but for keeping my spirits up by making a joke out of it – now that I'm finally finished (yes, finally, really, this time), I'm sure you'll have no difficulty coming up with another long-standing joke.

My beloved grandparents, Maureen and Ernie Elster, died while this work was being carried out. I dedicate it to their memory.

Chapter 1 Introduction

1.1 HER2(ERBB2) overexpression in breast cancer: An overview

Human epidermal growth factor-like receptor 2 (HER2) is a receptor tyrosine kinase (RTK) overexpressed by ERBB2 gene amplification in approximately 20 % of human breast cancers (HER2-positive breast cancers) and its overexpression is associated with shorter time to progression and decreased overall survival (OS)[1]. HER2-targeted therapies such as trastuzumab have significantly improved outcomes for HER2-positive breast cancer patients in both primary and metastatic settings (Table 1.1), but resistance to HER-targeted therapies remains a significant problem.

Table 1.1 Trastuzumab has improved outcomes for patients with metastatic HER2-positive breast cancer.

	Chemotherapy + Trastuzumab	Chemotherapy - Trastuzumab	P-value
Progression-Free Survival[74]	7.4 months	4.6 months	<0.001
Overall Survival[74]	25.1 months	20.3 months	0.046
Risk of Recurrence[73]	24% reduction		0.26

HER2 is a member of the HER (ERBB) RTK family. There are 20 known RTK families: members of over half of these have been found to be mutated or overexpressed in diseases marked by abnormal proliferation and were therefore considered potential targets for cancer therapy [2]. Following the successful targeting of RTKs such as EGFR and HER2 with anti-cancer agents such as erlotinib (Tarceva™, Astellas) and trastuzumab (Herceptin™, Genentech), there has been a focus on developing further inhibitors against other HER family members, with drugs such as pertuzumab (Omnitarg ™, Genentech) targeted to HER2 and HER3, and pan-HER family small molecule inhibitors such as afatinib (Boehringer Ingelheim) and neratinib (Pfizer) currently in clinical trials.

Please note that the following chapter has been published as a literature review.

1.1.1 Discovery and Characterisation of the HER2 gene and HER2-amplified Breast Cancer

A novel gene on Chr 17q12 encoding a 185 kDa protein was first discovered in the early 1980's. Initially named *neu*, this gene was subsequently cloned and characterised [3-5] and on

account of its similarity to human Epidermal Growth Factor Receptor (EGFR, now also known as HER1), the protein and gene were renamed HER2 (Human EGFR-like receptor 2).

HER2 was confirmed as an oncogene and its protein product as a potential therapeutic target when it was demonstrated that it could transform cells into a neoplastic phenotype [6], and that an antibody raised against HER2 [6] significantly inhibited tumour growth in nude mice implanted with HER2-transformed NIH 3T3 cells, but had no effect on mice infected with ras-transformed NIH 3T3 cells [7], indicating that anti-HER2 therapy could potentially attain high specificity and avoid off-target toxicity.

In 1985, it was found that the HER2 oncogene was amplified in 1 out of 10 breast cancer cell lines [8] and a ground-breaking study by Denis Slamon's group in 1987 found that amplification of the HER2 oncogene occurred in 30 % of breast cancers and correlates with a shorter time to relapse and reduced overall survival in women with breast cancer [9]. The tumourigenic potency of the HER2 oncogene was further confirmed in 1988 when Leder, Muller *et al* demonstrated that transfer of the activated oncogene is sufficient to produce malignant tumours in mice [10] and a study by Slamon *et al* that confirmed their original findings in a larger sample size [11].

1.1.2 Definition of HER2-positive breast cancer

According to current guidelines, HER2 testing is required on every primary invasive breast cancer (and on the metastatic site if applicable) in order to guide therapy decisions [12]. HER2 is currently detected using fluorescence in-situ hybridisation (FISH) and/or immunohistochemistry (IHC). FISH measures amplification of the *her2/erbb2* gene whereas IHC measures the levels of expression of the HER2 protein. According to the latest American Society of Clinical Oncologists/College of American Pathologists clinical practice guidelines, a tumour is defined as HER2-positive if it is IHC 3+, or IHC 2+ and FISH positive. In these cases HER2-targeted therapy should be recommended if clinically appropriate. An IHC score of 2+ or an equivocal FISH result defines a tumour as HER2 equivocal, and the decision to recommend HER2-targeted therapy should be delayed until further tests are carried out. A FISH negative or IHC 0/IHC +1 result confirms the tumour as HER2-negative and HER2-

targeted therapy is not recommended[12]. It has recently been proposed that HER2 gene copy number should also be considered as an indicator for whether a patient would benefit from HER2-targeted therapy[13].

1.1.3 HER2-positive breast cancer prognosis

Following the 1987 Slamon and Maguire paper which correlated HER2 oncogene amplification with a shorter time to relapse and reduced survival of breast cancer patients [9], Berger *et al* (1988) published a study demonstrating a statistically significant correlation of HER2 gene amplification with positive nodal status and poor nuclear grade, two factors commonly taken as independent indicators of poor prognosis [14]. The conclusions of this paper were drawn from a very small data set, but it paved the way for a larger study, published in 1989 by Wright *et al* (1989) [15], which examined 185 formalin-fixed, paraffin embedded (FFPE) primary breast tumours and found that the 17 % of tumours that exhibited strong staining for HER2 not only demonstrated a shorter time to progression and reduced survival, consistent with earlier studies, but also that patients who were HER2+ had reduced survival even if their tumours had other characteristics commonly associated with better prognosis, such as estrogen receptor (ER) positivity, EGFR negativity, and absence of lymph node metastasis. Patients with strong staining were highly unlikely to survive past two years. Further, this study found that "double positive" tumours, which also stained positive for EGFR, carried the poorest prognosis, arguably the first indication that EGFR and HER2 play a dual role in HER2-positive breast cancer.

While small tumours generally carry a better prognosis, a study carried out by researchers at MD Anderson found that women with tumours less than 1 cm in size were at a high risk of recurrence and metastasis if the tumours were HER2 positive, and that small HER2-positive tumours carried a risk of metastasis up to five times that of similar sized, HER2-negative tumours [16]. A meta-analysis in 2003 found that of 81 studies spanning sixteen years of research and incorporating 27,161 patients, and employing a wide range of techniques including immunohistochemistry, paraffin-embedded tissue, southern blot, fluorescence in situ-hybridisation and chromogenic in situ-hybridisation, 90% found that HER2 overexpression predicted poor breast cancer outcome [17]. HER2 normal status is one of the

factors used to define low-risk breast cancer by the ninth St Gallen Consensus panel, along with grade 1, node-negative, size ≤ 2cm, age at diagnosis ≥ 35 years, and a lack of peritumour vascular invasion. Amplification of HER2 alone is enough to place the patient in the intermediate risk category [18].

1.1.4 HER2 as a target and predictive marker

The high incidence of HER2-overexpression in breast cancer, along with its implications for disease-free and overall survival, makes it an attractive therapeutic target. Further, HER2 is amplified in human cancer cells compared to host normal tissue, with one study reporting up to a 25-fold increase in copy number (n=220)[19]. As HER2 levels have been found to be relatively homogenous amongst HER2-overexpressing tumour cells[20], HER2-targeted therapies could potentially target the vast majority of the cancerous cells residing in a given patient.

HER2-targeted therapies have dramatically improved outcomes for HER2-positive breast cancer patients. Trastuzumab (Herceptin™, Genetech Inc.) was the first HER2-targeted therapy to be approved by the U.S. Food and Drug Administration for HER2-positive breast cancer, and remains standard of care. Other therapies have since been developed to HER2 and other members of the HER family; these are discussed below.

Response to targeted anticancer agents varies widely across cancer subtypes and the use of predictive markers to enable the selection of patients most likely to benefit from a particular drug has proven to be advantageous. In addition to its role as a prognostic indicator, HER2 can act as a predictive biomarker, with a clear correlation between the level of HER2 amplification, as determined by FISH, and responsiveness to trastuzumab in the neoadjuvant setting (n=93) [21].

Initial clinical trials of trastuzumab reported modest benefits, and the inclusion of patients with 2+ HER2 immunostaining, indicative of a low level of HER2 overexpression, has been proposed as one likely reason for the low response rates initially seen [22]. It is also important to note that although trastuzumab has revolutionised treatment of HER2-positive breast

cancer, it is possible that its effects may have been missed entirely were trial patients not carefully selected on the basis of HER2 amplification. It has been estimated that without pre-selection, 23,586 randomly selected patients would have been required just to demonstrate a 1-year survival improvement of 2.4 %[18].

There is evidence that HER2's role as a predictive marker is not confined to HER2-targeted therapies. The twenty year Naples GUN trial (n=433) reported that HER2-positive tumours might not benefit from adjuvant treatment with tamoxifen (Nolvadex; AstraZeneca) [23], and that HER2-positivity is associated with better sensitivity to anthracycline-based adjuvant chemotherapy (n=628) [24].

1.2 HER (ERBB) Family Signalling

Receptor tyrosine kinases (RTK's) are a subclass of membrane bound, cell surface receptors with tyrosine kinase signalling activity, consisting of an extracellular ligand-binding domain, a transmembrane domain and an intracellular kinase domain. There are over 50 known RTKs consisting of 20 families: over half of these have been found to be mutated or overexpressed in diseases marked by abnormal proliferation and are therefore considered as potential targets for cancer therapy [2].

HER(ERBB) family signalling plays a key role in the pathogenesis of HER2-positive breast cancer and in the responsiveness of HER2-positive breast cancer to HER2-targeted therapies. The HER family, also known as the ERBB family or the epidermal growth factor receptor (EGFR) family, is a group of related receptor tyrosine kinases (RTK) comprising four currently known members, EGFR (HER1), HER2, HER3 and HER4. Each of these family members have distinct locations in the genome, with EGFR located on 7p12; HER2 on 17q12; HER3 on 12q13; HER4 on 2q33.3-34. Experiments with knock-out mice have shown the HER family to have essential roles in normal development, as KO mice for any of the four known HER family members are embryonic or perinatal lethal. EGFR seems to be involved in epithelial development in the skin, lungs and gastrointestinal tract [25]. Knock out of HER3 results in malformation of atrioventricular valves and defects in the development of the peripheral nervous system [26], and HER2 is responsible for the development of cardiac trabeculae [27]. HER4 knockout results in cardiac malformation [28] and HER4 is responsible for lobuloalveolar development and lactation in adults [29]. All four HER family members are expressed in the mammary gland, and have varying roles in ductal and lobuloalveolar development and lactation [30].

In contrast to the other known HER family members, no ligand has yet been identified for HER2. Crystallography studies report that when overexpressed, HER2 exists in a constitutively open conformation, leaving it intrinsically capable of interacting with any available binding partners even in the absence of ligand [31]. This is in contrast to the other HER family members which exist in an autoinhibited "closed" form and must undergo structural rearrangement upon ligand binding in order to participate in receptor dimerization [31]. It would appear that

the identity of activated receptors, rather than the number of activated receptors, is what determines the cellular response[32]. HER2-positive BC tumours are highly heterogeneous.

EGFR (HER1) was the first RTK to have its primary structure described and it is from early studies of EGFR that the signalling mechanism of the HER family was elucidated. Single molecule imaging studies revealed that the initial event in EGFR activation is the binding of a ligand to a preformed complex of an EGFR dimer and one EGF ligand. The binding of the EGF ligand to an EGFR dimer receptor is more than ten times stronger than the binding of an EGF molecule to an EGFR monomer, and EGFR becomes phosphorylated following dimerization [20].

Although kinase-deficient EGFR is expressed at normal levels and retains its binding affinities [33], it cannot stimulate DNA synthesis [33], transform cells [34], and kinase-deficient EGFR mutants display anti-oncogenic, anti-proliferative potencies in culture [35]. Moolenaar *et al* found that ATP binding is essential for tyrosine kinase signalling, as a mutation in the ATP-binding site abolishes signal transduction [36], a finding that would ultimately prove important in the targeting of tyrosine kinase receptors with small molecule inhibitors. A kinase-negative mutant EGFR can be phosphorylated by a WT EGFR, demonstrating that EGFR molecules form dimers and cross-phosphorylate [37].

Dimerization of HER2 with other receptors is mediated by the formation of disulphide bonds between cysteine residues in the juxtamembrane region of HER2, and disrupting the formation of these disulphide bonds disrupts the ability of HER2 to transform cells [38], indicating that the oncogenic potential of HER2 relies on receptor dimerization. HER family signalling is governed by a strict hierarchy, with HER2 being the preferred dimerization partner of all other HER family members [39]. Further, the recruitment sites on HER2 for downstream adapter proteins have been shown to be more promiscuous than the recruitment sites on other family members [40]. EGFR and HER3 have two multifunctional docking sites each, capable of numerous high-affinity interactions, whereas HER2 has many more sites, binding on average over 17 different proteins each [40]. 28 possible dimer combinations can form within this family [41] and signalling properties differ depending on the dimerization partner[39]. Dimerisation leads to receptor transphosphorylation, with each

member of a dimer phosphorylating the intracellular tyrosine kinase residues on its partner receptor.

Phosphorylated tyrosine residues on the receptor molecule then serve as recognition and docking sites for intracellular proteins containing Src Homology 2 (SH2) domains (Figure 1.1). SH2 domains are highly conserved domains of approximately 100 amino acids which interact with specific tyrosine phosphorylated ligands [42]. SH2 domains and SH2 containing proteins then serve as linker molecules, recruiting components of downstream signalling pathways through which the activated tyrosine kinase receptor exerts its biological effect(s) (Figure 1.2). SH2 domain interactions are highly dynamic, typically with a half-life of less than 10 seconds [40].

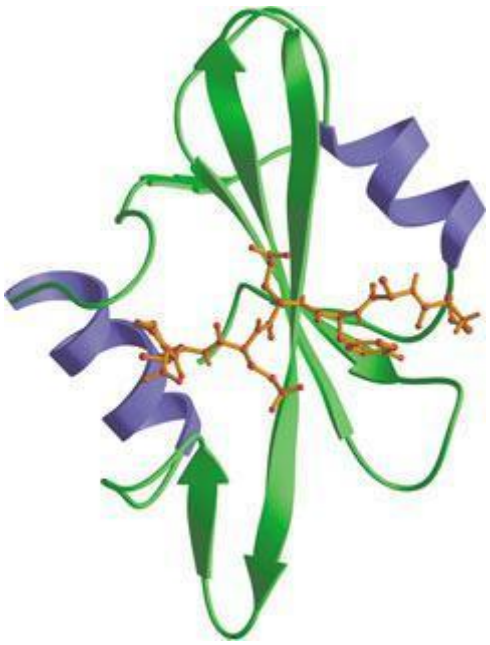

Figure 1.1 Structure of an SH2-domain bound to a phosphotyrosine peptide. The peptide is shown in red. From Waksman et al, Nature, 1992

The first evidence that the HER family members signal cooperatively to realise their oncogenic potential came when it was shown that cells transformed by HER2 displayed increased tyrosine phosphorylation of both HER2 and other proteins [44], and subsequently found that the EGF ligand could stimulate HER2 phosphorylation but only in the presence of EGFR [45]. Expression studies have confirmed the association between EGFR and HER2 positivity, and

have shown that HER3 overexpression is highly correlated with HER2 overexpression [46]. When EGFR and HER2 are co-expressed, heterodimerization occurs preferentially over homodimerization of either molecule [47]. HER2/HER3 heterodimers have been proposed to be the main oncogenic unit in HER2-positive breast cancer, with HER3 coupling activated HER2 to the downstream phosphoinositide 3-kinase (PI3K) pathway [48]. HER3 activation has been shown to attenuate the activity of anti-HER therapies[49] , and a correlation between simultaneous high HER2 and high HER3 levels and reduced sensitivity to trastuzumab has been shown. [50] The HER3 ligand neuregulin has been shown to confer resistance to chemotherapy, and has recently been implicated as a potential mechanism of resistance to T-DM1[51]. Synergistic targeting of HER2 and HER3 was demonstrated to achieve high therapeutic efficacy.[52] In contrast, some studies suggest an anti-oncogenic role for HER4 in HER2-positive breast cancer [53-56], although this is likely to be isoform-specific and context-specific [57, 58 51].

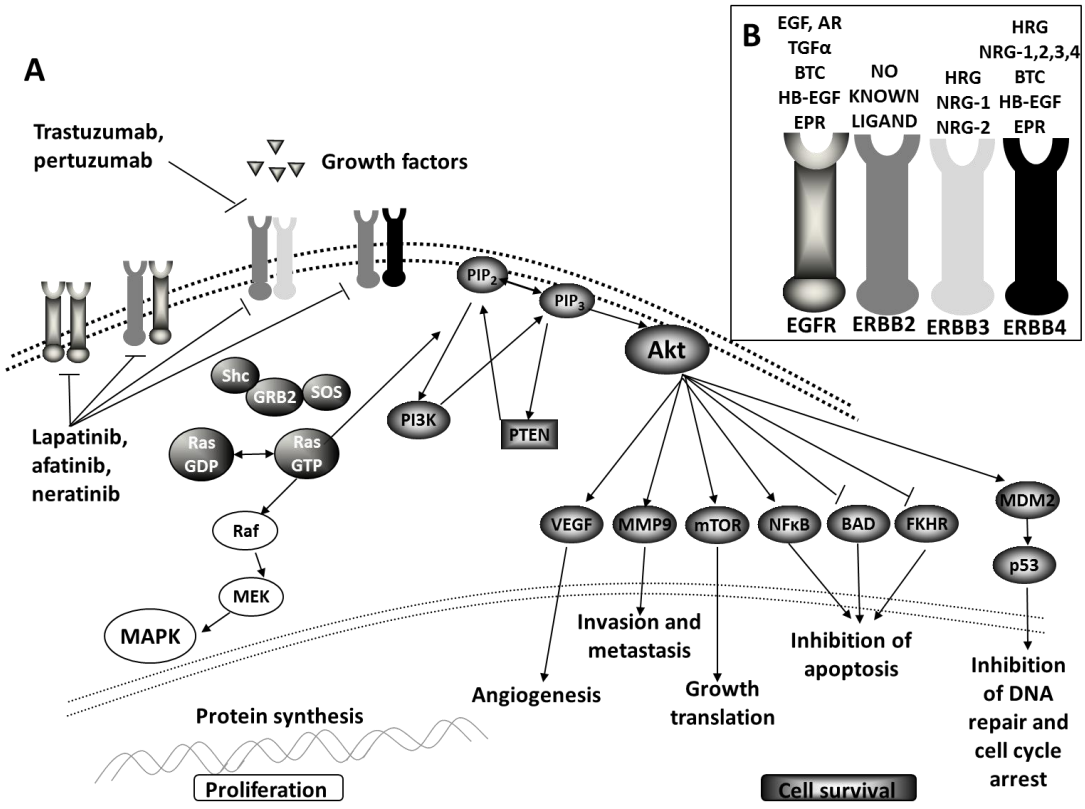

Figure 1.2 A: The HER Family signalling cascade and B: known ligands of each of the HER family receptors.

Activated HER (ERBB) family members homo- or heterodimerise and activate the downstream MAPK and PI3K pathways which confer growth and survival advantages respectively onto the cancer cell. The HER family signalling cascade can be targeted by anti-HER2 monoclonal antibodies such as trastuzumab, pertuzumab and T-DM1, by small molecule tyrosine kinase inhibitors lapatinib, afatinib and neratinib, and PI3K inhibitors such as copanlisib, GDC0971, GDC0980, and NVP-BEZ-235. B: Known ligands of each of the HER family receptors.

Two major downstream signalling pathways for the HER family receptors have been identified, the mitogen-activated protein kinase (MAPK) and the phosphatidylinositol-3-kinase (PI3K) pathways (Figure 1.3). Each of these pathways elicit different biological responses. The PI3K pathway confers survival advantages onto the cancer cell, and also has roles in growth, translation, transformation and inhibition of apoptosis [59]. The MAPK pathway may be critical for growth and metastasis of cancer cells [60].

Overexpression of extracellular signal related kinase (ERK5), a component of the MAPK pathway, is associated with decreased disease-free survival, and increased levels of HER2 correlate with increased ERK5 in patient samples *in vivo*. Inhibition of Erk5 *in vitro* sensitises HER2-positive cells to the HER2-targeted therapies trastuzumab and lapatinib [61]. However, it has been found in a panel of 12 breast cancer cell lines that activation of other MAPK pathway components, ERK1/2, does not uniformly correlate with EGFR or HER2 status. The same study noted that cells with a high basal activity of ERK1/2 were less sensitive to growth inhibition by EGFR inhibitors [62].

The PI3K pathway is one of the most frequently mutated pathways in cancer. Its functions include promoting survival by inhibiting pro-apoptotic genes such as Bcl-2associated death promoter (BAD) and forkhead box O (FOXO), regulation of cell motility, fatty acid synthesis, glucose homeostasis and metabolism [63].

PI3Ks can be subdivided into three distinct classes; Class I, Class II and Class III. Class I PI3Ks (PI3Kα,β,δ and γ) mediate HER2-induced activation of the PI3K pathway and its downstream effectors. Class I PI3Ks are heterodimers comprising two subunits called p85 and p110. p85 is

an inhibitory/adaptor regulatory subunit whereas p110 is the catalytic subunit of PI3K. Activating mutations in the *PIK3CA* gene, which encodes the catalytic subunit of PI3Kα, are common in several human cancers including HER2-positive breast cancer and can activate constitutive PI3K signalling through AKT to induce cell transformation [65].

p85 consists of two SH2 domains, an inter-SH2 (iSH2) domain, a breakpoint cluster domain and an SH3 domain. The iSH2 domain interacts with the p110 subunit and this interaction is required for the formation of enzymatically active PI3K [66]. The two SH2 domains associate with RTKs which contain a tyrosine-phosphorylated consensus sequence and in this way recruit the p85-p110 PI3K complex to activated membrane receptors such as the HER family receptors. Membrane localisation and activation of PI3K can activate several downstream kinases including AKT, JNK and p70S6K[67].

Upon membrane binding and activation by RTKs including HER family (e.g. HER2) dimers, PI3Ks phosphorylate phosphatidylinositol (4,5)-bisphosphate ($PIP_{2)}$, generating phosphatidylinositol (4,5)-trisphosphate (PIP_3) second messenger molecules which bind the pleckstrin-homology (PH) domains of downstream mediators such as AKT, recruiting them to the activation complex, thereby triggering downstream effects of PI3K activation, such as transformation, inhibition of apoptosis, translation, altered glucose metabolism and cytoskeletal rearrangement (Figure 1.3).

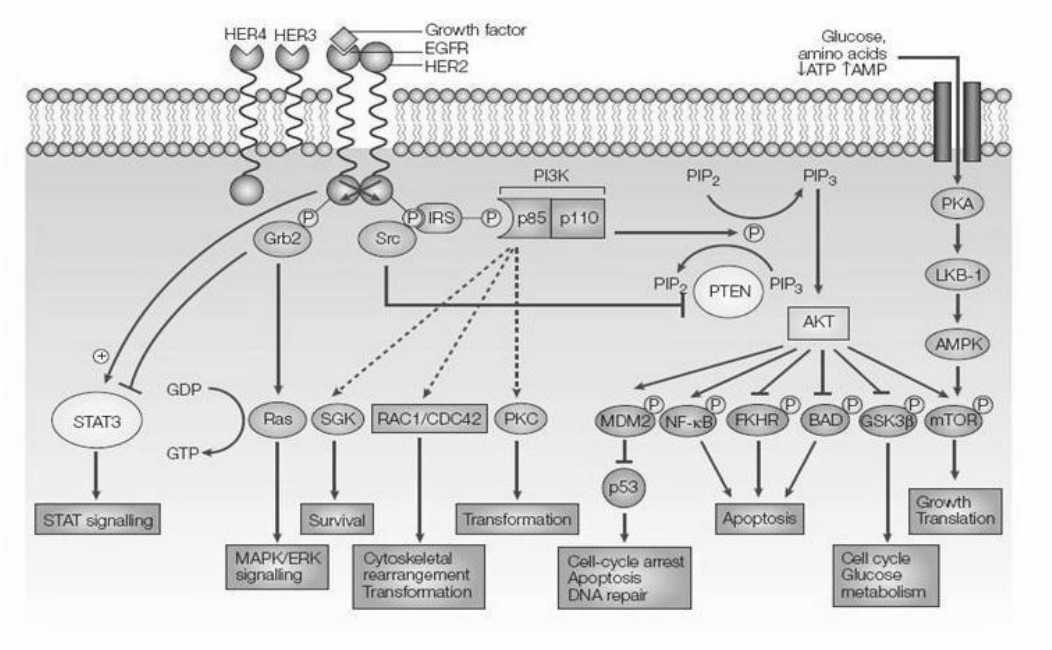

Figure 1.3 The PI3K/AKT and MAPK pathways signal downstream from HER2 and have multiple pro-oncogenic effects.

AKT is a serine/threonine kinase which is expressed as three different isoforms, AKT1, AKT2 and AKT3. AKT activation is dependent upon its being phosphorylated on serine 473 and threonine 308. Once AKT is localised to the cell membrane by PI3K-generated PIP_3 molecules, pyruvate dehydrogenase kinase (PDK) enzymes in the cell membrane cause its phosphorylation. Activated AKT then phosphorylates a number of downstream targets, leading to multiple oncogenic effects. By phosphorylating and thereby inactivating several members of the cell's apoptotic machinery, it promotes cellular survival under stressful conditions. Pro-apoptotic proteins inhibited by AKT include BAD, Caspase-9, the Forkhead family of transcription factors, and p53 [63, 68]. Other targets of AKT include mammalian target of rapamycin (mTOR) and S6K, both of which are involved in translation and which are activated by AKT, nuclear factor kappa-light-chain-enhancer of activated B cells (NFκB) and glycogen synthase kinase-3 beta (GSK3β), which are involved in glucose metabolism, a process

AKT also upregulates. AKT phosphorylation can be induced by all Class I PI3K isoforms and inhibits c-Myc mediated apoptosis and Caspase-3 like activity in rat1 fibroblasts [68]. Inactivation of AKT inhibits the survival advantage provided by activated PI3K, proving that AKT is a pivotal effector of the oncogenic effects of PI3K and thus HER2[68].

Phosphatase and tensin homolog deleted on chromosome ten (PTEN) is a dual lipid and protein phosphatase which counters PI3K signalling by dephosphorylating PIP_3 to PIP_2. PTEN is thus a crucial negative regulator of PI3K signalling and of the oncogenic effects of HER2.

PTEN consists of two major structural domains, a phosphatase and a C2 lipid-binding domain, both of which appear to play a role in membrane binding [69]. PTEN becomes inactive when it is phosphorylated and almost all phosphorylation occurs on serine residues [69]. When dephosphorylated it becomes active and in turn dephosphorylates PIP_3 to PIP_2, directly antagonising PI3K. One of the key methods by which PTEN suppresses tumours is by keeping PIP_3 levels low. As PIP_3 recruits AKT, a key mediator of the oncogenic effects of the PI3K pathway, suppressing PIP_3 levels effectively inhibits PI3K activity. However PTEN has multiple other roles in tumour suppression, including the induction of anoikis and the regulation of cell adhesion and migration [70]. PTEN also controls the protein levels and transcriptional activity of the tumour suppressor gene p53[71] with p53 protein levels dramatically decreased in *pten*-/- cells [72]. Although PTEN is a key negative regulator of the PI3K/AKT pathway, activation of AKT alone in transgenic mice does not account for all phenotypes related to PTEN loss [72], suggesting roles for PTEN other than regulation of PI3K signalling.

1.3 HER2-targeted therapies in clinical use

1.3.1 Trastuzumab

Trastuzumab is a monoclonal antibody (mAb) targeted to HER2 and now has well established efficacy in the treatment of women with HER2-positive breast cancer. It has significantly improved outcomes for patients, both in the metastatic setting (Table 1.1), and in the adjuvant setting (Figure 1.4) where it increases the cure rate of patients with HER2-amplified breast cancer [73, 74].

Drebin *et al* were the first to show that monoclonal antibodies to HER2 could significantly inhibit the tumourigenic growth of neu-transformed, but not ras-transformed cells injected into nude mice[2], suggesting HER2-targeted therapy had potential to be not only effective but also highly specific for HER2-positive cells, avoiding the high level of toxicity associated with the off-target effects of conventional chemotherapy. This study used a monoclonal antibody (mAb) against HER2 to bring about a dose-dependent, significant anti-tumour effect *in vivo*in both immune compromised and immune-competent animals. Subsequently, a combination of molecular modelling and gene mutagenesis was used to generate a humanised mAb against HER2, trastuzumab, with threefold-greater affinity for HER2 and comparable anti-proliferative potency to the parent molecule in HER2-positive breast cancer SKBR3 cells [75]. In addition to its *in vivo* efficacy as a single agent, trastuzumab was shown to increase the antitumour effect of paclitaxel and doxorubicin in xenograft models of HER2-positive breast cancer without causing additional toxicity [76].

Several clinical studies including the Herceptin Adjuvant (HERA) and the NSABPB1 and N9831 (Figure 1.4) trials found that the addition of trastuzumab to adjuvant chemotherapy results in highly significant reduction of recurrence and improved survival rates [77, 78]. Trastuzumab is thus now a standard front line therapy for the adjuvant treatment of HER2-positive breast cancer. A combined analysis of two large adjuvant clinical trials, NCCTG N9831 and NSABP B-31 with four-year follow up (n= 4,405), recorded significantly increased disease-free survival (DFS) ($P < 0.001$) and overall survival (OS) ($p < 0.001$) for patients treated with trastuzumab in addition to chemotherapy compared to patients in the chemotherapy-treated control group (Figure 1.4). Relative reduction in DFS event rate was 48% ($p < 0.001$) and the relative

reduction in the risk of death was 39% ($p < 0.001$) with the addition of trastuzumab to adjuvant chemotherapy[79].

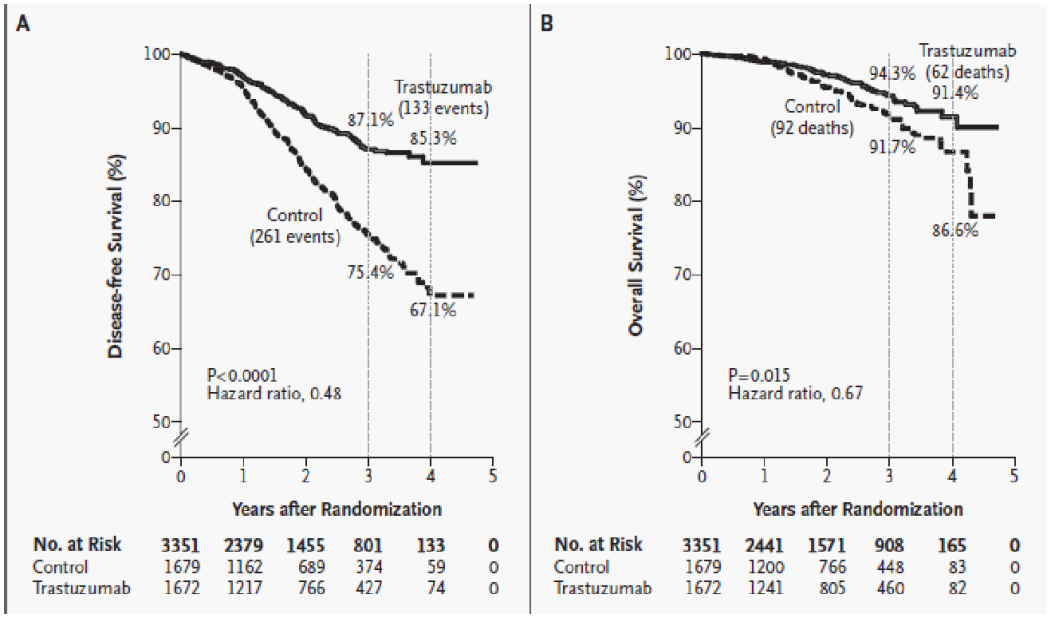

Figure 1.4 Kaplan-Meier estimates of disease-free survival (panel A) and overall survival (panel B) in trastuzumab vs. control groups from combined analyses of the NSABP-B1 and NCCTG N9831 adjuvant clinical trials at 4 year follow-up. From Perez *et al*, Journal of Clinical Oncology, 2011.

Trastuzumab also improves the efficacy of chemotherapy given prior to surgery (neoadjuvant chemotherapy) in patients with HER2-positive breast cancer. The NOAH trial evaluated the efficacy of neoadjuvant trastuzumab and chemotherapy versus neoadjuvant chemotherapy alone for women with locally advanced or inflammatory HER2-positive breast cancer. The addition of trastuzumab significantly improved the three year event-free survival rate, almost doubled the rate of pathological complete response (pCR) at surgery, and reduced the risk of breast cancer progression, relapse, and death (n=235) (Figure 1.5) [83].

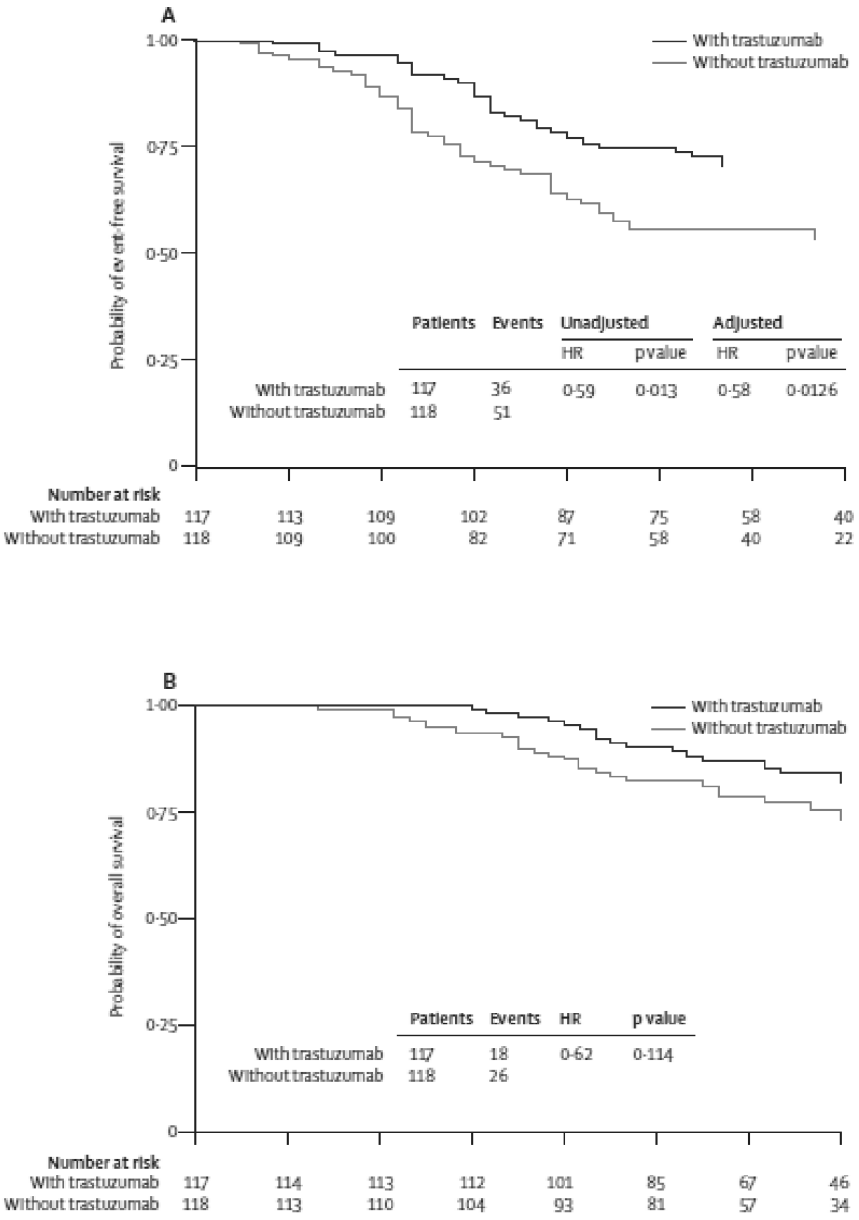

Figure 1.5 Probability of (A) event-free survival and (B) overall survival in patients with HER2-positive breast cancer from the NOAH trial which investigated the effect of the addition of neoadjuvant (and adjuvant) trastuzumab to neoadjuvant chemotherapy. From Gianni *et al*, Lancet, 2010.

Trastuzumab's mechanism of action remains incompletely defined. Trastuzumab contains two antigen-specific sites which bind to the juxtamembrane region of the extracellular domain of HER2, in a tight binding interaction mediated by three different regions on HER2 [84]. Binding at this site, which encompasses binding pockets for EGFR and HER3, may partially

inhibit homo- and heterodimerization of the HER2 molecule, which is a critical first step in HER2 signalling. Trastuzumab treatment has also been shown to downregulate HER2 expression in cell line models of HER2-positive breast cancer [85]. This trastuzumab-induced downregulation of HER2 was shown to enhance apoptosis mediated by tumour necrosis factor alpha-related apoptosis inducing ligand (TRAIL), a downstream mediator of the PI3K/AKT pathway which is known to have a significant role in the pathogenesis of HER2-positive breast cancer [85]. TRAIL expression is controlled by the transcription factor c-Jun, whilst AKT, a co-target of HER2, negatively regulates c-Jun. HER2-inhibition leads to suppressing of AKT phosphorylation, and the resulting increased expression of c-Jun allows TRAIL to be expressed, leading to an increase in TRAIL-mediated apoptosis [86]. It has been shown that the extent to which trastuzumab inhibits a tumour's growth is directly correlated to the extent to which it inhibits PI3K signalling [87].

Trastuzumab has also been shown to inhibit proteolytic cleavage of the ectodomain of activated HER2 [88], can generate a truncated form of HER2 known as p95 which is associated with a worse prognosis and has implications for therapy responsiveness [89]. It has also been suggested that trastuzumab-mediated internalisation and degradation of HER2 may inhibit receptor signalling, although some studies have also reported that receptor levels are unaffected by trastuzumab treatment [94]. Trastuzumab also induces the cyclin-dependent kinase inhibitor $p27^{KIP1}$ which prevents cancer cell proliferation by arresting cells in the G1 phase of the cell cycle [90].

As trastuzumab is a surface-binding antibody, it is logical that antibody-dependent cellular toxicity (ADCC) might be a possible mechanism of action. Trastuzumab treatment leads to an increase in the number of immune cells found inside a tumour, and increased numbers of natural killer (NK) cells are found inside trastuzumab-treated tumours with a clinically significant response compared to cancers with a poor response [91]. A role for immune effector cells in mediating trastuzumab's antitumour effects was further supported when it was shown that animals deficient in Fc receptors are insensitive to the breast cancer antitumour effects of trastuzumab [92], and trastuzumab has been shown to induce antibody-dependent cell-mediated cytotoxicity [93].

Despite its benefits, the effectiveness of trastuzumab is limited by *de novo* and acquired resistance in some HER2-positive breast cancers[95], and the fact that it cannot cross the blood-brain barrier. Approximately 35 % of metastatic HER2-positive breast cancer patients treated with trastuzumab go on to develop brain metastases [96].

1.3.2 Lapatinib

Lapatinib (Tykerb™, GlaxoSmithKline) is an orally bioavailable small molecule tyrosine kinase inhibitor targeted to EGFR and HER2. Tyrosine kinases (e.g. RTKs) catalyse the breakdown of adenosine tri-phosphate (ATP) into adenosine di-phosphate (ADP) and a free phosphate group. This dephosphorylation of ATP is the first step in receptor tyrosine kinase (RTK)-mediated signalling and TKIs function as ATP mimetics, sterically inhibiting ATP binding by blocking its binding site.

A preclinical study in 2001 reported that lapatinib inhibited the growth of three breast cancer cell lines including HER2-positive BT474 cells *in vitro* and *in vivo*[97]. Lapatinib also induced cell death and inhibited AKT phosphorylation in HER2-amplified BT474 cells [97].

The addition of lapatinib to capecitabine chemotherapy significantly improves time to progression in women with metastatic HER2-positive breast cancer compared to capecitabine alone in patients who had received prior trastuzumab (HR: 0.57, $P < 0.001$) with a trend towards improved OS (HR: 0.78, $p = 0.177$) [98] (Table 1.2, Figure 1.6). Preclinical [99] and clinical [100] evidence shows lapatinib is effective against trastuzumab-resistant HER2-positive breast cancer, and it is currently in use as a second line therapy for patients whose tumours have progressed despite trastuzumab treatment. Lapatinib inhibits HER2 phosphorylation more strongly than trastuzumab, and unlike trastuzumab it inhibits extracellular signal-related kinase (Erk) 1/2 *in vivo* [101]. It potently inhibits p-Akt, and resulted in a 23-fold increase in apoptosis in HER2-positive cell lines compared to cells treated with vehicle control *in vitro* and *in vivo*[102].

A functional genomics study in 2011 reported that lapatinib decreased AKT phosphorylation, and also that it induced transcription of estrogen receptor 1 (*ESR1*) and progesterone receptor (*PgR*) genes [103]. Lapatinib has inhibited tumour growth in p95HER2-overexpressing preclinical mouse models and has shown clinical benefit in patients refractory to trastuzumab whose tumours overexpressed p95HER2 (n=537) [100]. Lapatinib is effective in HER2-positive breast cancer cells resistant to trastuzumab, inhibiting activation of AKT, MAPK, IGF1R signalling and inducing p27 expression [99]. It inhibits the development of brain metastases *in vivo* [96] and has modest activity against HER2-positive brain metastases clinically (n=242) [104].

However, the success of lapatinib has been hit by a number of recent disappointing clinical trial results including the adjuvant study ALTTO[105], a number of neoadjuvant studies, and the NCIC CTG first-line metastatic study [106] (Table 1.2). These studies, along with the success of pertuzumab and T-DM1, mean that lapatinib's place in the clinic remains in patients with HER2-positive metastatic BC who have received at least 1-2 prior lines of therapy for metastatic disease.

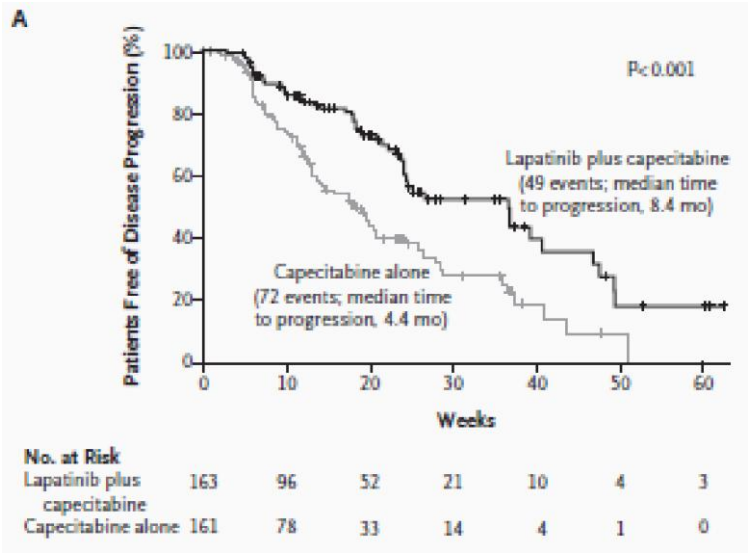

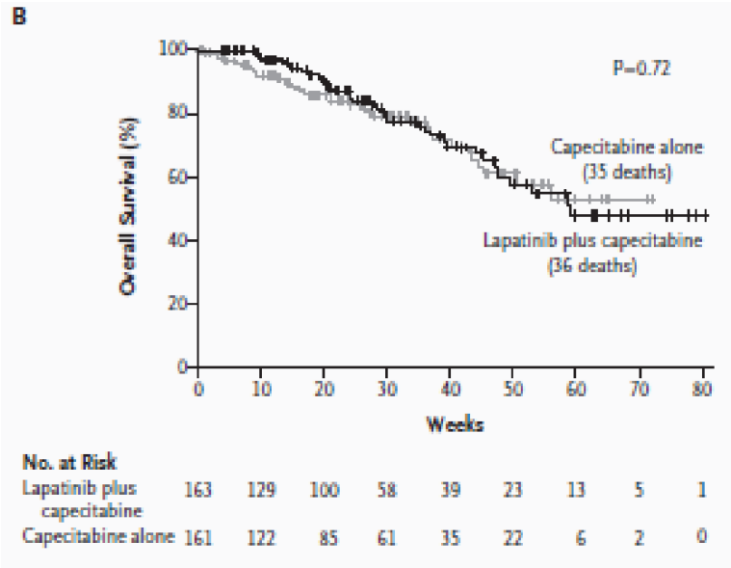

Figure 1.6 Kaplan-Meier Estimates of A Disease-Free Survival and B Overall Survival from NCT00078572, which investigated the addition of lapatinib to chemotherapy for women with locally advanced or metastatic HER2-positive breast cancer who have progressed on a trastuzumab-containing regimen. From Geyer *et al*, New England Journal of Medicine, 2006.

Table 1.2 Some significant clinical trials of HER2-targeted therapies completed to date in HER2-positive breast cancer

Clinical Trial	Details	Sample Size	Findings
TRASTUZUMAB-BASED TRIALS			
H0648g[80]	Adjuvant chemotherapy +/- trastuzumab in HER2-positive breast metastatic cancer patients	469	Addition of trastuzumab to adjuvant chemotherapy reduced relative risk of death by 20 % at median follow up of 30 months
HERA [81]	Adjuvant chemotherapy +/- trastuzumab	4,482	Addition of trastuzumab after adjuvant chemotherapy resulted in a 24% reduction of recurrence
NCCTG N9831/ NSABP B-31 [79]	Adjuvant chemotherapy +/- trastuzumab	4,405	48 % relative reduction in disease-free survival (DFS) ($p < 0.001$) and 39 % relative reduction in overall survival (OS) events ($p < 0.001$) with trastuzumab
BCIRG 006 [124]	Adjuvant chemotherapy +/- 1 year of trastuzumab	3,222	Addition of one year of trastuzumab significantly improved both DFS and OS at five-year follow up. Also showed excellent outcomes with docetaxel/carboplatin/trastuzumab (TCH) as an adjuvant regimen without anthracyclines.
NOAH [83]	Neoadjuvant chemotherapy +/- neoadjuvant trastuzumab for women with locally advanced or inflammatory breast cancer	235	Addition of trastuzumab significantly improved three year event-free survival, almost doubled the rate of pathological complete response (pCR) to therapy, and reduced risk of progression, relapse, and death
LAPATINIB-BASED TRIALS			
NCT00078572 [125]	Capecitabine +/- lapatinib in HER2-positive metastatic breast cancer patients who had progressed on trastuzumab treatment	399	51% reduced risk of progression and an improved DFS without a significant OS improvement with lapatinib
NSABP B-41[126]	Neoadjuvant lapatinib vs neoadjuvant trastuzumab in patients with operable HER2-positive breast cancer	519	Similar pCR rates between trastuzumab (52.5%) and lapatinib (53.2%), and a non-significant increase in pCR ($P=0.095$) with both trastuzumab and lapatinib compared to the use of either alone
CHER-LOB[127]	Neoadjuvant chemotherapy plus trastuzumab, lapatinib, or both in HER2-positive stage II to IIIA operable breast cancer	121	Significant relative increase in pCR (80%, $p=0.019$) with both trastuzumab and lapatinib compared to either alone

CALGB 40601[128]	Neoadjuvant paclitaxel and trastuzumab +/- lapatinib in newly diagnosed HER2-positive, stage II/stage III breast cancer patients	305	The addition of lapatinib resulted in higher pCR (51 % vs 40 %), although this did not reach statistical significance (p = 0.11)
ALTTO[105]	One year of trastuzumab alone, one year of lapatinib alone, their sequence or combination in the adjuvant treatment of HER2-positive early BC	8,381	Nonsignificant reduction in DFS with both lapatinib and trastuzumab compared to trastuzumab alone (88% vs 86%, P=0.048)
NeoALLTO[129]	Neoadjuvant trastuzumab, lapatinib or a combination of both +/- chemotherapy in HER2-positive primary breast cancer patients	455	Significantly improved pCR (p<0.01) rate with the combination of trastuzumab and lapatinib (51.3%) compared to that of trastuzumab alone (29.5%)
NCIC CTG[106]	Lapatinib + chemotherapy vs trastuzumab + chemotherapy as first-line treatment for women with metastatic HER2-positive BC	636	Singnificantly reduced PFS (P=0.01) with lapatinib + chemotherapy compared to trastuzumab + chemotherapy (8.8 months compared to 11.4 months)
PERTUZUMAB-BASED TRIALS			
CLEOPATRA [114]	Trastuzumab and docetaxel +/- pertuzumab in HER2-positive metastatic breast cancer	808	Prolonged DFS and significantly improved OS (p = 0.0008), 34 % reduced risk of death with pertuzumab
NeoSphere[130]	Neoadjuvant trastuzumab and docetaxel +/- pertuzumab	417	Significantly higher proportion of women achieved pathological complete response with pertuzumab, 17 % of patients given trastuzumab and pertuzumab without chemotherapy achieved pCR
T-DM1-BASED TRIALS			
EMILIA [131]	HER2-positive metastatic breast cancer	991	T-DM1 significantly improved progression-free survival compared to treatment with lapatinib plus capecitabine (median survival, 9.6 months, vs. 6.4 months, P<0.001) and also increased median overall survival with T-DM1 (30.9 months, vs. 25.1 months, P<0.001)
TH3RESA[132]	T-DM1 vs physician's choice in patients with advanced HER2-positive breast	602	T-DM1 significantly improved PFS compared to physician's choice (6.2 months vs 3.3 months, p<0.0001)

	cancer whose cancer had progressed despite previous HER2-targeted therapy		
NERATINIB-BASED TRIALS			
Phase II multicentre trial [133]	Evaluation of efficacy and safety of neratinib in patients with advanced HER2-positive breast cancer with and without prior trastuzumab treatment	136	Neratinib was well-tolerated, with objective response rates of 24% (prior trastuzumab treatment) and 56% (trastuzumab-naïve)
AFATINIB-BASED TRIALS			
Phase II Afatinib trial[134]	Safety and efficacy of afatinib monotherapy in patients with HER2-positive metastatic breast cancer who had failed prior trastuzumab treatment	52	Afatinib monotherapy induced PR and maintenance of stable disease in 46 % of patients
LUX-Breast 1	Afatinib + vinorelbine vs trastuzumab + vinorelbine in HER2-positive metastatic BC patients who have progressed on trastuzumab	508	No significant benefit to afatinib (PFS 5.5 months vs 5.6 months), with slightly worse adverse events in the afatinib arm
LUX-Breast 3	Vinorelbine +/- Afatinib in HER2-positive BC patients with brain metastasis	120	No benefit with the addition of afatinib

1.3.3 Pertuzumab

Pertuzumab (Omnitarg ™, Genentech) is a humanized monoclonal antibody which binds to the extracellular domain II of HER2, which is involved in dimerization [31] (unlike trastuzumab, which binds to HER2 domain IV) (Figure 1.7). Pertuzumab thus blocks the interaction of HER2 with HER3, diminishes ligand-activated HER2 signalling in breast cancer cell lines, and inhibits the growth of high- and low HER2-expressing HER2-positive breast xenografts *in vivo*[108]. Unlike trastuzumab, pertuzumab inhibits heregulin-beta 1 (HRG1; a HER3 ligand)-mediated HER2 phosphorylation, which has been shown to be vital for HER2-positive breast cancer tumorigenesis [109].

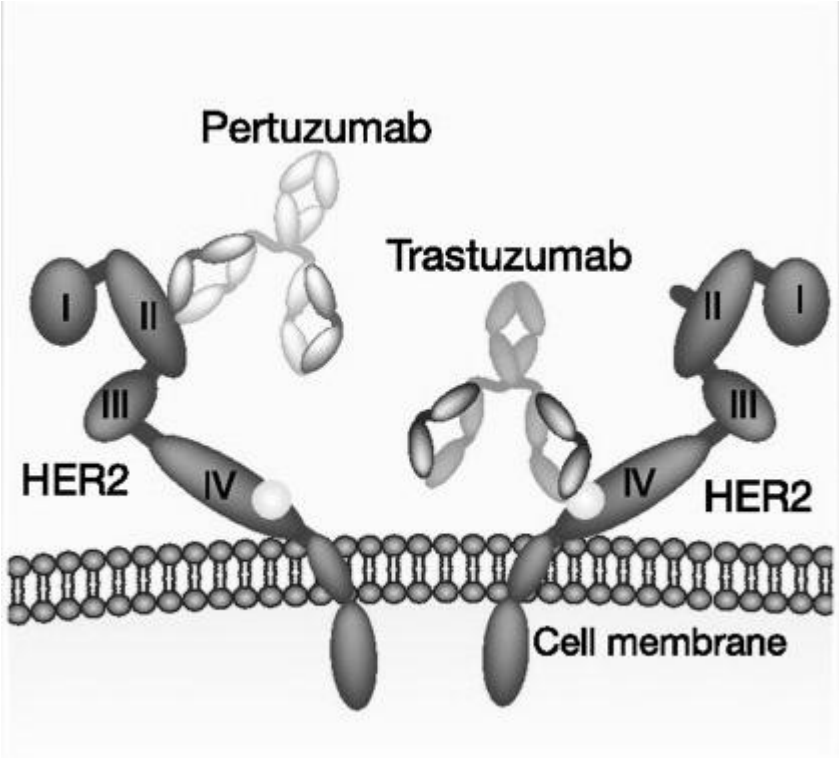

Figure 1.7: Trastuzumab and Pertuzumab bind to different domains on the HER2 receptor. From Pohlmann *et al*, Clinical Cancer Research, 2009.

Lee-Hoeflich *et al* confirmed the importance of the HER2-HER3 dimer in the proliferation of HER2-positive cells *in vitro* and *in vivo* and found that pertuzumab ablated tumour morphogenesis and proliferation normally mediated by heregulin, a HER3 ligand, *in vitro* and in xenograft mice, in particular in combination with

trastuzumab [110]. Combination treatment with trastuzumab and pertuzumab led to a survival advantage for these mouse models of HER2-positive breast cancer [111] , with a modest growth inhibitory effect on xenograft models for pertuzumab, and a strong enhancement of antitumour effect when trastuzumab and pertuzumab were used in combination. The combination of the two antibodies resulted not only in tumour regression but also in a complete inhibition of metastatic tumour spread in treated animals [112].

The combination of trastuzumab and pertuzumab *in vivo* results in an additive increase in ADCC [113] and in marked regression of metastatic HER2-positive breast cancer in treated animals [113].

Based on the the results of the clinical trials discussed below (Table 1.2), pertuzumab in combination with trastuzumab and chemotherapy is now approved for the first-line treatment of women with metastatic HER2-positive breast cancer (in Europe and the US) and for the neoadjuvant treatment of HER2-positive breast cancer (in the US).

Pertuzumab continues to be tested clinically in the adjuvant, metastatic and neoadjuvant settings. The largest completed trial to date is CLEOPATRA, which evaluated the addition of pertuzumab to first-line trastuzumab and docetaxel in women with HER2-positive metastatic breast cancer (n=808). The addition of pertuzumab to trastuzumab and docetaxel prolongs progression-free survival [114], and results in a statistically significant improvement in overall survival (p = 0.0008) and a 34% reduced risk of death. Kaplan-Meier estimates of OS rates show survival benefit with the combination of pertuzumab, trastuzumab and docetaxel at 1, 2, and 3 years [114]. The NeoSpere trial evaluated the addition of pertuzumab to neoadjuvant chemotherapy and trastuzumab (n=417). A significantly higher proportion of women achieved pathological complete response when given pertuzumab, trastuzumab and docetaxel compared with those receiving trastuzumab and docetaxel alone. 17% of

women who received both antibodies and no chemotherapy achieved a pathological complete response (pCR) to therapy, and this group had the lowest incidence of overall adverse events, highlighting the potential of neoadjuvant HER2 blockade alone as an effective treatment with better safety and quality of life than chemotherapy. However, a third of patients on this dual-antibody regimen without chemotherapy regimen did not respond to it [115].

On-going trials (Table 1.3) in the metastatic setting include PHEREXA, which is evaluating the combination of trastuzumab, capecitabine and pertuzumab versus trastuzumab and capecitabine in patients who have progressed following previous trastuzumab treatment (n=450) (NCT01026142), and MARIANNE, which is exploring the potential of combination pertuzumab and T-DM1 (n=1092) (NCT01120184). The APHINITY trial has recruited 3806 patients with early HER2-positive breast cancer. These patients were randomly assigned to either adjuvant chemotherapy plus trastuzumab and placebo or adjuvant chemotherapy plus trastuzumab and pertuzumab.

There is evidence that tumour immunology has a key role to play in the mechanism of action of both trastuzumab and pertuzumab. In the NeoSphere study, a high expression of the immune suppressor protein programmed death ligand 1 (PD-L1) was associated with lower pCR in response to trastuzumab and pertuzumab with or without chemotherapy[116]. Infiltration of lymphocytes into tumour has already been shown to predict trastuzumab benefit in early stage HER2-positive breast cancer.[117]

Table 1.3 Important ongoing clinical trials with novel HER2-targeted therapies in HER2-positive BC

Trial	Setting	Sample Size	Aims/Arms/Investigation	Results Expected
PERTUZUMAB-BASED TRIALS				
PHEREXA	Patients who progressed following trastuzumab	450	Trastuzumab and capecitabine +/- pertuzumab	June 2017
APHINITY	Early stage HER2-positive BC	3806 (estimated enrolment)	Adjuvant chemotherapy and trastuzumab +/- pertuzumab	December 2023
T-DM1-BASED TRIALS				
MARIANNE	Metastatic HER2-positive BC	1095	Combination pertuzumab and T-DM1	April 2016
KATHERINE	HER2-positive BC with residual tumour in breast/lymph nodes following pre-operative therapy	1484 (estimated enrolment)	Adjuvant trastuzumab vs adjuvant T-DM1	March 2023
NERATINIB-BASED TRIALS				
ExteNET	Early stage HER2-positive BC	2842	Effects of neratinib after adjuvant trastuzumab on overall survival	Completed, not yet reported
NALA	Metastatic HER2-positive BC	600 (estimated enrolment)	Neratinib plus capecitabine versus lapatinib plus capecitabine	May 2018

1.3.4 T-DM1

Trastuzumab-emtansine (T-DM1, Genentech) is an antibody-drug conjugate (ADC) composed of trastuzumab linked via a nonreductable thioether to a highly cytotoxic maytansinoid agent (Figure 1.8). Maytansinoid is about 100- to 1000-fold more toxic for a range of cell lines than most other cancer drugs. However, it failed in human clinical trials due to an unacceptable systemic toxicity [118]. The rationale for ADCs is that the antibody portion enables the specific delivery of a highly toxic chemotherapeutic agent to the cancer cells, leaving normal cells unscathed. The first ADC to be approved for cancer was gemtuzumab ozogamicin (Mylotarg™, Wyeth), which was approved by the US FDA in 2000 for leukaemia but had to be withdrawn in 2010 due to no benefit and systemic toxicity in patients, which resulted because the cytotoxic agent was released prematurely to its being internalised in the cancer cell [119].

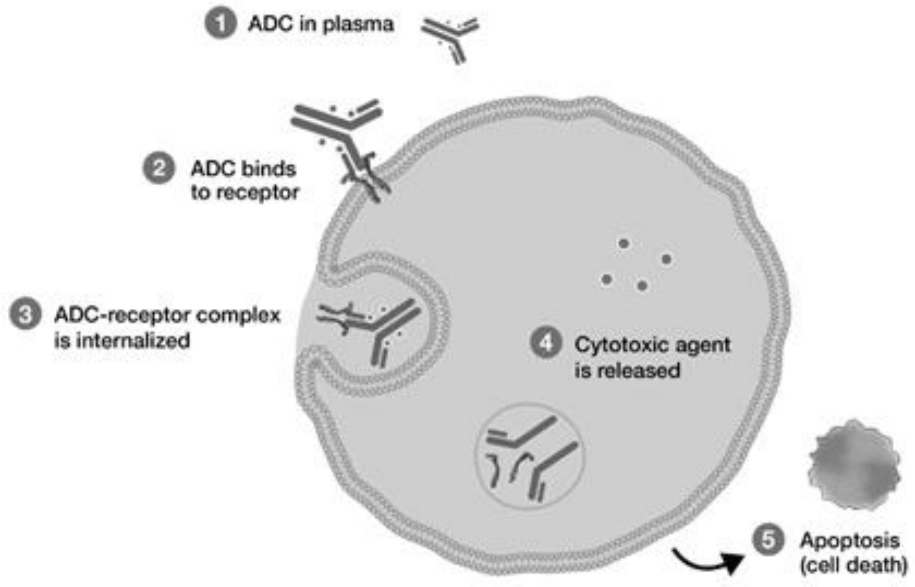

Figure 1.8 T-DM1 is an antibody-drug conjugate (ADC) which binds to the HER2 receptor and is internalised into the cell. Once internalised, the drug complex dissociates and the cytotoxic maytansinoid agent is released, becoming active. Figure from http://www.seagen.com

TDM-1 contains a highly sophisticated compound containing a non-disulfide linker which ensures that the cytotoxic portion of the ADC is not released and remains inactive until it is internalised into the cancer cell [120]. Following binding, receptor-mediated internalisation transports TDM-1 to the cytoplasm, where lysosomal degradation releases and activates the cytotoxic agent [121]. In addition to the anti-mitotic properties of emtansine, T-DM1 retains the effects of trastuzumab including initiation of ADCC, inhibition of HER2 cleavage, and inactivation of the PI3K/AKT pathway, and is effective in models of lapatinib-resistance *in vitro* [122]. A number of trials have shown it to be safe and well-tolerated in humans [123] and the recent EMILIA study found that T-DM1 significantly improved PFS (9.6 vs 6.4 months, $P < 0.0001$) compared to the combination of lapatinib and capecitabine (Table 1.2). This has lead to the approval of TDM-1 as a single agent in the US and Europe for the treatment of metastatic HER2-positive breast cancer patients who have previously received trastuzumab and a taxane. MARIANNE (NCT01120184) is an ongoing trial comparing T-DM1 to combination pertuzumab and trastuzumab, and TH3RESA (NCT01419197) is evaluating T-DM1 against physician's choice (Table 1.3).

1.4 Mechanisms of Resistance to HER-targeted therapy in HER2-positive breast cancer

Many potential mechanisms of trastuzumab resistance in HER2 positive BC have been proposed (Table 1.4); these include reduced receptor-antibody binding due to increased HER2 masking[135]; altered intracellular signalling involving loss of PTEN, reduced p27kip1, or increased PI3K/AKT activity (e.g. by PIK3CA mutations)[136]; and altered signalling via non-HER family RTKs[137, 138]. p95HER2, which lacks an extracellular domain but retains kinase activity, has also been proposed as a mechanism of resistance[139], although it was not shown to have a significant association with pCR rates clinically[127].

1.4.1 The PI3K/AKT Pathway

The PI3K pathway is the most frequently mutated pathway in breast cancer, with a number of possible activating abnormalities occurring including mutation and/or amplification of the oncogenes encoding the p110α subunit of PI3K (PIK3CA), the p110β subunit (PIK3CB), the p85 subunit of PI3K (PIK3R1), the PI3K effector protein AKT, upstream RTKs such as HER2, and others [140]. Loss of PTEN function can also occur due to gene mutations and deletions, and post-transcriptional and post-translational aberrations [69, 141].

PI3K/AKT aberrations occur in more than 25% of breast cancers, with PIK3CA alterations being the most common in HER2-positive and other breast cancer [59]. The most common activating PIK3CA mutations occur in three hotspots, taking the form of single base substitutions: E545K and E542K in the helical domain (exon 9) and H1047R in the kinase domain (exon 20).

The *PIK3CA* gene encodes the α isoform of the p110 subunit. When eight PI3K and 8 PI3K-like genes were sequenced in a variety of cancers with corresponding normal tissue it was found that *PIK3CA* was the only gene with frequent tumour-specific somatic mutations [142] (n=297). These mutations were observed in 70 of 234 colorectal cancers (32%), 4 of 15 glioblastomas (27%), 3 of 12 gastric cancers (25%), 1 of 12 breast cancers (8%), and 1 of 24 lung cancers (4%). A subsequent study focusing on breast cancer identified PIK3CA mutations in 25% of

breast cancers (n=53) [143]. A larger scale study found not only are PIK3CA mutations present in a high frequency of human breast cancers, but that they are associated with expression of estrogen and progesterone receptors, HER2 positivity, and lymph node metastasis, and they are mutually exclusive with PTEN loss (n= 342) [144]. PIK3CA mutations have been shown to occur at an early stage of carcinoma development, and to correlate with HER2 overexpression and lymph node metastasis which are independent factors indicative of poor prognosis. Tumours bearing PIK3CA mutations are less likely to respond to PI3K-inhibitor mediated growth inhibition than cells with PTEN loss [141].

PIK3CA mutation has been shown to predict resistance to anti-HER2/chemotherapy in HER2-positive BC[145], although this may be a true effect only in cancers that are HER2+/ER+[146], and to be associated with lower rates of pCR after neoadjuvant trastuzumab-based therapy[147]. However, recent reports have shown that PIK3CA mutation may not always be significantly correlated with worse survival[148]. Loi *et al* found that PIK3CA mutations were associated with a better outcome in HER2-positive BC, but that this effect disappeared after 3 years[149], suggesting that PIK3CA mutations may have a role in acquired but not *de novo* resistance.

O'Brien *et al* (2010) extensively profiled a panel of HER2-positive breast cancer cell lines incorporating cells with varying levels of sensitivity, with known *de novo* or acquired resistance to lapatinib and trastuzumab and searched for a correlation between drug sensitivity and PI3K/AKT phosphorylation and expression and PTEN status as determined by DNA sequencing and western blot [152]. This study found that trastuzumab response was not related to levels of HER2 phosphorylation, but that cell lines with PIK3CA mutations were less likely to respond to trastuzumab. AKT phosphorylation levels did not correlate to levels of HER2 phosphorylation, indicating that AKT can be activated independently of HER2. They report that PI3K pathway activation status as determined by levels of AKT phosphorylation correlates significantly with trastuzumab resistance *in vitro*. Inhibition of mTOR also improves lapatinib sensitivity in cells with trastuzumab resistance, and transfection of constitutively active AKT into lapatinib-sensitive cells abrogates lapatinib-response[3]. The finding that mTOR inhibition reduces p-AKT levels and increases lapatinib sensitivity suggests that combining

lapatinib with PI3K inhibition could be an improved treatment option for HER2-positive breast cancer patients [153].

Bitransgenic mice which were HER2-positive and had constitutive AKT activation displayed increased tumourigenesis despite decreased overexpression and phosphorylation of HER family members compared to control animals with normal AKT signalling [154]. This finding that activated AKT leads to less dependency on HER family signalling for tumorigenesis indicated that HER2 inhibition alone without co-inhibition of the PI3K pathway may not be sufficient to inhibit tumour growth. PTEN knockdown using antisense oligonucleotides confers trastuzumab resistance *in vitro* and *in vivo* and patients with PTEN-deficient breast tumours have significantly poorer responses to trastuzumab than patients whose tumours have normal PTEN (n= 47, $p<0.01$) [155].

Furthermore, activating mutations of *PIK3CA*, the oncogene that encodes the PI3K p110 alpha subunit, occur in 20-33% of HER2-amplified breast cancers and have the potential to deregulate kinase signalling in a HER2-independent fashion and thus to inhibit the antitumour efficacy of HER2-targeted therapies such as trastuzumab [59]. My mentor Prof Hennessy has shown that PTEN loss and PIK3CA mutations when used together predict prognosis after trastuzumab treatment better than either factor used alone, with the combined analysis reaching marked statistical significance as a negative prognostic biomarker [87]. In one clinical study, PTEN loss and PIK3CA mutations were found in 51.8% and 21.8% of HER2-positive breast tumours respectively, and patients with PI3K pathway activation (as defined by PTEN loss, PIK3CA mutation, increased p-AKT and increased p-p70S6K) had shorter OS and a worse response to trastuzumab (n=137) [156]. These findings are supported by a number of other clinical studies [87, 141].

1.4.2 IGF1R

HER2 homo- and heterodimer formation is important in HER family signalling. In addition to forming heterodimers with other members of its own family, HER2 can heterodimerise with other tyrosine kinase receptors such as MET and insulin-like growth factor receptor-1 (IGF1R).

Crosstalk between HER2 and IGF1R occurs in trastuzumab-resistant but not trastuzumab-sensitive parental SKBR3 cells. In resistant cells, stimulation of IGF1R resulted in increased HER2 phosphorylation, and inhibition of IGF1R tyrosine kinase activity with an IGF1R inhibitor and inhibition of HER2 dimerization with pertuzumab disrupted HER2-IGF1R interaction [157]. IGF-1R interacts with HER2 and HER3 to form a heterotrimer resulting in enhanced activation of downstream signalling in trastuzumab-resistant, but not parental, HER2-positive breast cancer cells. Knockdown of IGF-1R upregulates $p27^{Kip1}$ and resensitises resistant cells to trastuzumab [158]. A study involving two *in vitro* models of acquired trastuzumab resistance found that IGF1R expression was increased in one resistant model compared to the parental cell line, but not in the other. Interestingly, this study also found that co-targeting IGF1R and HER2 enhanced response to trastuzumab even in the BT474/TR model of acquired trastuzumab resistance, which did not display significantly altered IGF1R expression and phosphorylation compared to BT474 parental trastuzumab-sensitive cells [159].

The role of IGF1R in trastuzumab resistance is supported by clinical studies. IGF1R is overexpressed in 25% of HER2-positive breast carcinomas and patients with IGF1R overexpression had decreased progression-free survival when treated with adjuvant trastuzumab (n=155). The IGF1R inhibitor NVP-AEW541 was synergistic with trastuzumab in the HER2-positive breast cancer cell lines BT474 and SKBR3, [160] and co-targeting HER2 and IGF1R results in additive or greater than additive responses to a combination of trastuzumab and IGF1R inhibitors, including in models of trastuzumab and lapatinib resistance [161]. A phase two clinical trial of the anti-IGF1R mAb cixutumumab in combination with lapatinib and capecitabine is ongoing (NCT00684983).

1.4.3 $P27^{Kip1}$

One of trastuzumab's proposed mechanisms of action involves the induction of the cyclin-dependent kinase inhibitor $p27^{Kip1}$ which prevents proliferation by arresting cells in the G1 phase of the cell cycle. Increased $p27^{Kip1}$protein pushes cells out of the cell cycle and thereby halts proliferation, whereas reduced $p27^{Kip1}$protein leads to cells resuming proliferation. $P27^{KIP1}$ expression is significantly higher in HER2-positive than HER2-negative tumours [162].

Anti-HER2 antibodies increase the half-life of $p27^{Kip1}$protein, arresting cells in the G_1 phase of the cell cycle. Knockdown of $p27^{Kip1}$ expression by antisense cDNA significantly impairs this $p27^{Kip1}$ protein-induced G_1 arrest[90]. HER2-positive SKBR3 breast cancer cells with conditioned resistance to trastuzumab have decreased $p27^{kip1}$ levels compared to parental cells and expression of $p27^{kip1}$ restored trastuzumab sensitivity in these cells [163]. The PI3K inhibitor LY294002 increased levels of $p27^{kip1}$ and transfecting cells with constitutively active AKT abrogated the trastuzumab- and LY294002-mediated increases in $p27^{kip1}$ and corresponding inhibition of cell proliferation [164].

1.4.4 MET Receptor

MET is a tyrosine kinase receptor, which, along with its ligand, hepatocyte growth factor (HGF), have been found to be overexpressed in breast cancer, with overexpression correlating with a poorer prognosis as measured by significantly shorter DFS and OS (n=258)[165]. Higher levels of HGF also correlate to increasing size of primary breast tumours, node-positivity, and invasive breast cancers have been shown to have significantly higher HGF levels than DCIS (n=166) [166]. The association of HGF with invasion is supported by *in vitro* findings that HGF synergises with HER2 to promote invasion in breast cancer cell lines [167]. HGF has also been shown to synergise with IGF1R in promoting invasion, and MET inhibition nearly completely inhibited migration and invasion mediated by IGF1R in colon cancer cells [168].

In vitro, inhibition of MET sensitizes cells to trastuzumab, whereas Met activation results in both sustained HER2-independent AKT activation and abrogated p27 induction. HER2-positive breast cancer cells have been shown to rapidly upregulate Met in response to trastuzumab treatment thereby promoting their own resistance [169].

1.4.5 p95HER2

p95HER2, also called NH-terminal truncated HER2, is a truncated form of the HER2 receptor which lacks the extracellular domain and therefore lacks binding sites for trastuzumab and pertuzumab. However, it retains its intracellular and transmembrane domains and therefore its kinase activity. p95HER2 can be expressed via various mechanisms including proteolytic

cleavage, alternative initiation of translation and alternative mRNA splicing [89]. Expression of p95HER2 induces the formation of tumours in nude mice [170] and is associated with a worse prognosis in clinical studies. In one study, expression of p95HER2 but not full length HER2 was associated with 2.9 fold increased odds of developing lymph node metastasis (n=337) [171]. Other clinical studies support the role of p95HER2 as an indicator of poor prognosis, with high levels of p95HER2 correlating with shorter PFS and OS (n=576) [172, 173]. HER2-positive cells expressing p95HER2 are resistant to trastuzumab *in vitro* and in xenograft mice. Further, in a retrospective immunohistochemical analysis of HER2-positive breast cancer patient samples, only 11.1% of patients with tumours expressing p95HER2 responded to trastuzumab (partial response) whereas 51.4% of patients whose tumours had only full-length HER2 achieved either complete or partial response to trastuzumab (n = 46) [174]. However, efforts to date to develop a clinically robust p95HER2 assay have been unsuccessful, retarding the translation of this biomarker into clinical trials or clinical practice.

1.4.6 MUC4

MUC4 is a cell surface glycoprotein of the mucin family. It has been shown that overexpression of rat MUC4 inhibits the binding of HER2-targeted antibodies including trastuzumab [175]. *In vitro* studies with the trastuzumab-resistant HER2-positive breast cancer cell line JIMT-1 demonstrated that levels of MUC4 protein expression inversely correlates to the level of trastuzumab binding, and that antibodies binding to a HER2 epitope further removed from the membrane, bound more efficiently than did trastuzumab. Further, knockdown of MUC4 increased the sensitivity of JIMT-1 cells to trastuzumab. Taken together, these data suggest that MUC4 masks the trastuzumab binding domain, sterically inhibiting the antibody-target interaction and thereby leading to trastuzumab resistance [176].

1.4.7 HER2 and cancer stem cells

Human pluripotent stem cells are undifferentiated cells which are capable of self-renewal and have the potential to differentiate into any cell type[4]. Cancer stem cells (CSCs) are a subpopulation of tumour cells which retains these properties. The CSC hypothesis states that tumours contain this subpopulation of CSCs, which possess the properties of stem cells, drive

the growth of the tumour and mediate resistance to chemo- and radiotherapy. CSCs are heterogenous, with HER2+ CSCs shown to occur in HER2-positive breast cancer[5], and to differ in genotype from HER2-negative CSCs, with HER2+ CSCs displaying increased invasiveness and tumorigenesis, and increased expression of genes involved in control of progenitor cells and reduced expression of genes involved in differentiation and immune response[6]. *In vitro* and *in vivo*, HER2 overexpression increases the CSC population in breast cancer whereas HER2 blockade decreases it[7], and a pro-survival HER2 signalling pathway involving NFκB has been shown to be initiated within CSCs in response to radiotherapy[8], though the expression of HER2 on CSCs may mean they are still susceptible to HER2-targeted therapies. Interestingly, it has been shown that HER2-positive breast CSCs possess a high level of endocytic activity which renders then susceptible to T-DM1, leading the authors to speculate that the increased efficacy of T-DM1 relative to trastuzumab may be in part due to its ability to target CSCs[9].

1.4.8 HER family gene mutations

There is emerging evidence to suggest that gene mutations in the HER family may play a role in the pathogenesis of HER2-positive breast cancers and in response to HER2-targeted therapy. A T798M mutation in HER2 was identified in an *in vitro* screen using a randomly mutagenised HER2 library[177], and HER2-T798M was shown to confer resistance to lapatinib[178]. Mutations in the kinase domain of HER2 have also been reported to be associated with poorer response to trastuzumab clinically (n = 78) and to confer a more aggressive phenotype *in vitro*, with increased invasion and increased ability to form colonies in soft agar[179]. Further, it has recently been shown that activating mutations in HER2 could increase phosphorylation of EGFR and HER3 in breast cancers which were classed as HER2-negative by the standard diagnostic tests, IHC and FISH. Somatic mutations in HER3 have been discovered to be present in 11 % of gastric and colon cancers, and these mutations have oncogenic activity *in vitro* and *in vivo*, but only when in the presence of HER2[180]. Finally, somatic mutations in HER4 have been shown to affect signal transduction[181].

Intriguingly, my mentor Prof Hennessy has recently found activating somatic mutations in HER family members in ~20 % of a small cohort of HER2-positive breast cancers, suggesting a role

for these mutations in responsiveness of HER2-positive breast cancers to HER2-targeted therapies.

Table 1.4 Mechanisms of Resistance HER2-targeted therapies in HER2-positive BC

Title	**Mechanism**	**Known to mediate resistance to**	**Shown** *in vitro*	**Shown** *in vivo*	**Clinical Studies**	**Possible Strategies**
PIK3CA mutation	HER2-independent activation of the downstream PI3K pathway	Trastuzumab and Lapatinib	Yes[182]	Yes[150]	Yes[136]	Target the PI3K pathway in addition to targeting HER2
PTEN Loss	HER2-independent activation of the downstream PI3K pathway	Trastuzumab and Lapatinib	Yes[150]	Yes[150]	Yes[136]	Target the PI3K pathway in addition to targeting HER2
p95HER2	Lacks extracellular antibody binding domain but retains full kinase activity	Trastuzumab	Yes[184]	Yes[184]	Yes[50 139]	Lapatinib Novel TKI's
MUC4	Masks binding domain of HER2	Trastuzumab	Yes[135]	Yes[135]	No	Lapatinib Novel TKI's
MET Receptor	Upregulates AKT and abrogates p27 induction in response to trastuzumab	Trastuzumab	Yes[187]	No	Yes[188]	MET inhibition
IGF1R	Heterodimerizes with HER2 to activate downstream signalling	Trastuzumab	Yes[137]	No	Yes[137]	Co-target IGF1R and HER2
Inhibition of $P27^{Kip1}$	Impairs anti-HER2 antibody induced cell cycle arrest, thereby increasing proliferation	Trastuzumab	Yes[189]	No	Yes[190]	None to date

1.5 Strategies to overcome resistance to HER2-targeted therapies in HER2-positive breast cancer

1.5.1 Targeting the PI3K Pathway

Preclinical data suggest that targeting PI3K pathway signalling nodes downstream from HER2 (e.g. mammalian target of rapamycin (mTOR) in addition to targeting HER2 will overcome resistance of HER2-amplified breast cancer to HER2-targeted therapies in some cases [191].

Mammalian target of rapamycin (mTOR) is a serine/threonine kinase and a component of the PI3K pathway. As its name suggests, it is targeted by rapamycin, an immunosuppressant drug used in organ transplantation which binds irreversibly to mTOR complex 1 (mTORC1). Rapamycin and various "rapalogs" which target mTOR are in various stages of preclinical and clinical testing [192]. Two rapalogs, everolimus (Afinitor™, Novartis) and temsirolimus (Torisel, ™ Wyeth), have been FDA approved for the treatment of renal cell carcinoma. Everolimus was recently approved for metastatic, hormone receptor positive breast cancer in combination with anti-hormonal therapy [192]. The phase 3 BOLERO-2 study reported that everolimus improves the anti-tumour efficacy of trastuzumab in the second-line treatment of metastatic HER2-positive breast cancer. However, the benefits of the addition of everolimus to trastuzumab were minimal[193]. Overall, the efficacy of everolimus in the metastatic setting in HER2-positive breast cancer has been disappointing.

mTOR may thus not be not an optimal target for inhibition of the PI3K pathway. Firstly, mTOR is only one downstream target of PI3K and AKT (Figure 1.3). Targeting mTOR also leads to feedback loop-induced AKT activation, recently shown to significantly decrease the efficacy of mTOR inhibition [194]. This feedback loop may explain the modest efficacy of rapalogs in HER2-positive metastatic breast cancer (n=109) [195].

As a result newer inhibitors of PI3K and AKT are now being investigated including in combination with HER2-targeted therapies. Current studies are also attempting to define whether inhibition of specific or all isoforms of PI3K produces optimal antitumour activity in specific settings. Although the original PI3K inhibitors were pan-PI3K inhibitors, recent studies

suggest that isoform-specific PI3K inhibitors may achieve greater antitumour efficacy when used in the appropriate setting. It may be most relevant to target PIK3CA-mutated HER2-positive breast cancers with PI3Kα inhibitors[196].

Examples of novel PI3K inhibitors include NVP-BEZ235, a dual inhibitor of PI3K and mTOR [197, 198], GDC0980, a PI3K/mTOR inhibitor [199], GDC-0941, and BAY-80-6946 (copanlisib)[200]. Such compounds show clear *in vitro* [200] and *in vivo* [201] efficacy in HER2-positive breast cancers, and are now in early clinical trials in HER2-positive breast and other cancers [202]. The combination of the PI3K inhibitor buparlisib and trastuzumab inhibits PI3K and MAPK signalling in HER2-positive breast cancers resistant to trastuzumab [203], and has progressed to a phase II trial. The combination of trastuzumab with PI3K inhibitors such as GDC-0941 achieves improved blockade of the PI3K pathway compared with trastuzumab alone.[204]

1.5.1.1 BAY-80-6946 (copanlisib), a Novel, Potent, Selective PI3K Inhibitor

BAY-80-6946 is a novel, potent pan-class I PI3K inhibitor which is highly effective against PI3K, in particular isoforms α and δ, but has no activity against over 200 other serine/lipid kinases[200]. It has IC_{50}s in the low nanomolar range in 160 cell lines covering 14 tumour types and has been shown to induce apoptosis and inhibit VEGF-mediated angiogenic effects [200]. It inhibits tumour growth *in vivo* [201] and was well-tolerated in a phase 1 trial [202]. It has shown synergy with the EGFR inhibitor erlotinib in the treatment of non-small cell lung cancer (NSCLC) [205]. As an α PI3K isoform inhibitor, copanlisib may optimise anti-tumour activity in HER2-positive breast cancers, in particular those that are PIK3CA mutated.

1.4.2 Novel and Combination HER-targeted therapies

1.4.2.1 Neratinib

Neratinib (Table 1.4) is a potent, irreversible TKI which covalently binds the ATP binding pocket of EGFR and HER2. *In vitro,* it potently inhibits HER2 and EGFR kinase activity, inhibits MAPK and AKT phosphorylation, and enhances $p27^{KIP1}$ induction [206]. It is a more potent inhibitor of p95HER2 and EGFR and has greater inhibition of HER2 signalling activity than does lapatinib [207]. It also inhibits the growth of HER2-positive tumours *in vivo* [206]. Unlike

trastuzumab, it decreases phosphorylation of EGFR, HER2, HER4 and ERK, and the addition of neratinib to trastuzumab overcomes trastuzumab resistance *in vitro* [208]. The combination of neratinib and vinorelbine has shown significant antitumour effects with no synergistic toxicity [209]. Neratinib has been shown to be well-tolerated and has substantial clinical activity in patients who have and have not been pretreated with trastuzumab for HER2-positive breast cancer (n=136) [133]. It has also been reported that neratinib in combination with trastuzumab is well tolerated and displays efficacy in phase I/II trials, with a 27% objective response rate (n=33) [210].

Somatic, including activating, mutations, have recently been found to be present at a low frequency in HER2-negative breast cancers[211]. Several of those mutations were associated with resistance to lapatinib; one mutation increased the phosphorylation of EGFR and HER3, suggesting that HER signalling could be activated by HER2 somatic mutations as well as by HER2 gene overexpression. Although several of these mutations were associated with lapatinib resistance, neratinib potently inhibited the growth of cells bearing HER2 mutations, suggesting both a potential role for neratinib in overcoming lapatinib resistance, and that HER2-targeted therapy may benefit some patients whose tumours are HER2-negative as assessed by FISH and IHC, but bear HER2 somatic mutations.

1.4.2.2 Afatinib

Afatinib (Table 1.4) is a small molecule TKI which irreversibly binds to the ATP-pocket of the EGFR and HER2 tyrosine kinases. It was originally developed for lung cancer, where it was shown to be effective in a range of *in vitro* and *in vivo* preclinical models incorporating models which were sensitive and which were resistant to first generation TKIs such as erlotinib [212]. Afatinib inhibits ligand-dependent phosphorylation of HER3[212], and it has antitumour activity in patients with HER2-positive breast cancer whose tumours have progressed despite trastuzumab treatment[213]. It may also have potential in the treatment of some patients with triple-negative breast cancer, due to its anti-EGFR activity [214].

In a phase II clinical trial it was shown to confer clinical benefit including PR and maintenance of stable disease as monotherapy in patients with HER2-positive metastatic breast cancer

whose tumours had progressed on trastuzumab treatment [215]. Lux-Breast 1 (NCT01125566), a randomised Phase III trial investigating the addition of afatinib to the combination of trastuzumab and vinorelbine in HER2-positive metastatic breast cancer patients with prior trastuzumab treatment is ongoing, as is Lux-Breast 3, which is investigating the addition of afatinib to vinorelbine in patients with HER2-positive breast cancer suffering from brain metastasis (NCT01441596). Results presented at the ASCO meeting in 2012 showed afatinib monotherapy to have a higher overall response rate compared to both trastuzumab and lapatinib monotherapy in treatment naïve patients with HER2-positive, locally advanced breast cancer [216].

1.6 Conclusion

The HER family is a group of related RTKs which signal cooperatively to mediate oncogenic effects, primarily through the PI3K and MAPK pathways. One member, HER2, is overexpressed in approximately 20 % of human BC. HER2 overexpression in breast cancer correlates with a worse prognosis. Although the established HER2-targeted therapies trastuzumab and lapatinib have had some success, resistance remains a major clinical problem. Mechanisms of trastuzumab resistance include reduced receptor-antibody binding, increased signalling through alternative HER family RTKs, altered intracellular signalling and altered signalling via non-HER family RTKs.

There is an increasing awareness of the importance of HER family dimerization in the oncogenesis of HER2-positive breast cancer. The HER2/HER3 dimer is now thought to be the main oncogenic unit in HER2-positive breast cancer, and much of its effects are mediated through HER3's role in activating the PI3K pathway. Some studies have suggested that targeting the HER family alone without co-inhibition of PI3K will not be sufficient to treat some HER2-positive breast cancers. Other recent data have highlighted the heterogeneity of HER2-positive breast cancer, and suggested that mutations in the HER family may be sufficient to activate HER family signalling, even without HER2 overexpression. My mentor Prof Hennessy has also observed somatic mutations in ~20 % of a small cohort of HER2-positive breast cancers.

Emerging strategies to circumvent resistance to HER2-targeted therapies include co-targeting the PI3K pathway and HER family signalling, pan-HER family inhibition, and novel therapies such as T-DM1. In terms of PI3K inhibitors, although the original PI3K inhibitors were pan-PI3K inhibitors, recent studies suggest that isoform-specific PI3K inhibitors may achieve greater anti-tumour efficacy when used in the appropriate setting. For example, it may be most relevant to target PIK3CA-mutated HER2-positive breast cancers with PI3Kα inhibitors.
With our rapidly expanding understanding of HER2 signalling mechanisms along with the repertoire of HER family- and other targeted therapies including PI3K inhibitors, it is likely that

the near future holds further dramatic improvements to the prognosis of women with HER2-positive BC.

1.7 Aims

This project is based upon my mentor Prof Hennessy's previous and preliminary data that activation of the PI3K pathway is associated with resistance to HER2-targeted therapies, and that kinome aberrations including PIK3CA mutations and novel activating somatic gene mutations in the HER family members EGFR, HER2 and HER4 are present in up to 50% of HER2-amplified breast tumours. We hypothesise that there are other novel aberrations in the kinome of HER2-positive breast cancers which contribute to resistance of HER2-positive breast cancers to HER2-targeted therapies. We also hypothesize that these novel HER family gene mutations may have implications for signalling regulation, tumour pathogenesis and responsiveness of HER2-positive breast cancers to HER2-targeted therapies. Finally we hypothesise that the resistance of HER2-amplified breast tumours to trastuzumab and other drugs that inhibit multiple HER family members (e.g. lapatinib) will be reversed by combining these with a PI3K inhibitor with particular potency against the α isoform of PI3K.

Our investigation of these hypotheses will thus consist of three specific aims:

Specific Aim 1: To determine if the PI3K inhibitor copanlisib restores the antitumour efficacy of HER2-targeted therapies in HER2-amplified breast cancers.

Specific Aim 2: To determine the frequency and clinical and patient outcome implications of novel mutations in the kinome including the ERRB gene family in human HER2-amplified breast cancer.

Specific Aim 3: To determine the effects of novel mutations in the ERRB family on HER2-amplified breast tumour cell growth, signalling and responsiveness to HER2-targeted therapies using *in vitro* testing.

Chapter 2 Materials and Methods

2.1 Materials

Table 2.1 Reagents used to complete the experiments necessary to answer the objectives in this project, their suppliers and product codes.

Reagent	Supplier	Product Code	Reagent	Supplier	Product Code
2-propanol	Sigma-Aldrich®	B4252	p-CDF1-ERBB4-WT plasmid	Addgene®	29536
5-bromo-4 chloro-3-indoyl	Sigma-Aldrich®	I9516	pCDF1-MCS2-EF1 expression vector	System Biosciences®	CD110B-1
Afatinib	Sequoia Chemicals®	SRP03710a	Penicillin/Streptomycin	Gibco®	15070-063
Agarose	Sigma-Aldrich®	A9539	Pertuzumab	Genentech®	Under MTA
Ampicillin	Sigma-Aldrich®	A5354	Phosphate Buffered Saline	Sigma-Aldrich®	P4417
BAY80-6946	Bayer®	Under MTA	PhosStop phosphatase inhibitor cocktail	Roche®	4906837001
BD Matrigel	BD Biosciences®	Q32854	pPACKF1 Lentivector Packaging Kit	System Biosciences	LV100A-1
B-D-galactopyranoside	Sigma-Aldrich®	B4252	Primers	IDT®	N/A
Benchmark™ Pre-Stained Protein Ladder	Invitrogen®	10748-010	Puromycin	Sigma-Aldrich®	P9620
Biorad® DC Protein Assay Reagent A	Biorad®	500-0113	QIAamp AllPrep DNA/RNA Mini Kit	Qiagen®	80204
Biorad® DC Protein Assay Reagent B	Biorad®	500-0114	QIAamp DNA FFPE Tissue Kit	Qiagen®	56404
Biorad® DC Protein Assay Reagent S	Biorad®	500-0115	QIAfilter Plasmid Maxi Kit	Qiagen®	12263
Bovine Serum Albumin	Sigma-Aldrich®	A3059	QIAGEN Plasmid Maxi Kit	Qiagen®	12165
Complete Mini EDTA-Free	Roche®	11-836-170-001	QuBit® dsDNA BR Assay Kit	Life Technologies®	Q32853
Dimethylsulfoxide	Sigma-Aldrich®	D8418	QuBit® dsDNA HS Assay Kit	Life Technologies®	Q32854
Dulbeco's modified eagle medium	Sigma-Aldrich®	D6421	Quikchange XL II Site-Directed Mutagenesis Kit	Agilent®	200521
ERBB4-S303F plasmid	Created In-house	N/A	RPMI-1640	Sigma-Aldrich®	R8758
ERBB4-V721I plasmid	Created in-house	N/A	Select Agar	Sigma-Aldrich®	A5054
Ethanol	Sigma-Aldrich®	E7023	Sodium Acetate	Sigma-Aldrich®	S8625
Fetal Bovine Serum	Gibco®	10106-169	Sodium Chloride	Sigma-Aldrich®	S7653
Gel Star® Nucleic Acid Stain	Lonza®	50535	Sodium Hydroxide	Sigma-Aldrich®	80204
Glycerol	Sigma-Aldrich®	G5516	Trastuzumab	Roche®	H4289
Isopropyl-1-thio-B-D-galactopyranoside	Sigma-Aldrich®	I6758 – 1G	Triton-X 100	Sigma-Aldrich®	T9284
Lapatinib Tosylate	Sequoia Chemicals®	231277 – 92 – 2	Trizma-Hydrochloride	Sigma-Aldrich®	T5941
Luria-Bertani Agar	Sigma-Aldrich®	L2897	Trypsin-EDTA	Gibco®	15050 - 065
Luria-Bertani Broth	Sigma-Aldrich®	L3022	Water	Sigma-Aldrich®	W4502
Methanol	Sigma-Aldrich®	32213	Xylene	Sigma-Aldrich®	Q32853
ParaNitroPhenol Powder	Thermo Fisher®	34045	B-mercaptoethanol	Sigma-Aldrich®	M7154
Bolt ® 4-12 % Bis-Tris Plus Gel 15 well	Invitrogen®	NW00122BOX	iBLOT 2.0 Transfer Stacks, PVDF	Invitrogen®	IB24001
4X Bolt™ LDS Sample Buffer	Biosciences®	B0007	10X Bolt™ Sample Reducing Agent	Biosciences®	B0009

Table 2.2 Cell lines used in this thesis and their basal medium requirements for routine culture. With the exception of HEK293T, a human embryonic kidney line used as a transfection host, all cells are established HER2-positive breast cancer cell lines. All media was Supplemented with 10 % FBS and 1 % P/S. For HEK293T, heat-inactivated FBS was used. UCSF = University of California, San Francisico, NICB = National Institute of Biotechnology, Dublin City University, T = trastuzumab, L = lapatinib N/A = parental cell line with no acquired resistance. Fingerprinting was carried out by Source Bioscience

Cell Line	Source	Conditioned Resistance	Media	Maintenance Drug	Fingerprinted
BT474	NICB	N/A	RPMI-1640	None	4/4/13
BT474-Res	UCSF	T	RPMI-1640	100µg/ml T	4/4/13
SKBR3	NICB	N/A	RPMI-1640	None	4/4/13
SKBR3-T	NICB	T	RPMI-1640	10µg/ml T	4/4/13
SKBR3-TL	NICB	T/L	RPMI-1640	100µg/ml T + 250 nM L	4/4/13
SKBR3-L	NICB	L	RPMI-1640	250 nM/L	4/4/13
MDA-MB-453	NICB	N/A	RPMI-1640	None	4/4/13
MDA-MB-361	NICB	N/A	RPMI-1640	None	4/7/14
HCC1569	NICB	N/A	RPMI-1640	None	15/10/15
HCC1954	NICB	N/A	RPMI-1640	None	4/7/14
HCC1954-L	NICB	L	RPMI-1640	250 nM/L	4/7/14
HEK293T	ATCC	N/A	DMEM	None	Not done

Formalin-fixed paraffin embedded (FFPE) human HER2-positive breast cancer samples

135 HER2-positive breast tumours were acquired from Beaumont Hospital and 197 HER2-positive breast tumours acquired from St Vincent's University Hospital. All of these patients were HER2-positive and most had been treated with trastuzumab. Samples included primary HER2-positive breast cancer surgical specimens, initial staging biopsies, metastatic tumours and biopsies from patients who had received neoadjuvant trastuzumab. All tissue samples used in the study were histologically confirmed by the RCSI pathology department using H&E, and examined for tumour content. Samples confirmed to have at least 50 % tumour content were chosen for our sequencing studies. 84 tumours (with 27 matched normal lymph node samples) were used for an exploratory next generation sequencing study. A larger sample set

of 227 tumours were used in our subsequent sequenom validation study. All work was approved by the Ethics Committees of Beaumont and St Vincent's hospitals.

HER2-positive breast cancer cell lines

All cell lines used in this thesis originated from breast carcinoma and are HER2-positive. Details of the cell lines and their basal medium requirements for routine culture are listed in Table 2.2. Details of acquired resistant variants used in this thesis including the drugs they are resistant to, the concentrations used to maintain this resistance and their creators are listed in Table 2.3. BT474-Res cells were a kind gift from Dr Neil O'Brien (University of California San Francisco, San Francisco, USA). All other HER2-positive breast cancer cell lines used in this thesis were a kind gift from Dr Norma O'Donovan (National Institute of Cellular Biotechnology, Dublin, Ireland). SKBR3-T, SKBR3-L and SKBR3-TL cells were established in Dublin City University. 96-well dose response proliferation assays were performed in 0 – 600 nM lapatinib in order to select an appropriate concentration for conditioning. Each cell line was grown in duplicate flasks containing either control media or conditioned media, and media was replaced twice weekly for 6 months. SKBR3 cells were conditioned in trastuzumab (10 µg/ml (68 nM)) alone to create SKBR3-T cells, lapatinib (200 nM) alone to create SKBR3-L cells, or combined trastuzumab (5 µg/ml (34 nM)) and lapatinib (100 nM). After two months, the lapatinib concentration for SKBR3-L cells was increased to 250 nM. After six months of conditioning, dose-response assays were performed to monitor alterations in response to lapatinib and trastuzumab. BT474-Res cells were established at the University of California Los Angeles by culturing BT474 trastuzumab-sensitive cells in high dose Herceptin (100 µg/ml) for 18 months. BT474 and BT474-res cells were characterised for response to Herceptin and the dual EGFR-HER2 small molecule inhibitor, lapatinib by cell count and colony formation assay.

Table 2.3: Resistant cell line models used in this thesis

Cell Line	Source	Resistant To	Established By	Cultured In
SKBR3-T	National Institute of Cellular Biotechnology	Trastuzumab	Norma O'Donovan	10µg/ml trastuzumab
SKBR3-L	National Institute of Cellular Biotechnology	Trastuzumab and Lapatinib	Norma O'Donovan	250 nM lapatinib
SKBR3-TL	National Institute of Cellular Biotechnology	Trastuzumab and Lapatinib	Norma O'Donovan	10ug/ml trastuzumab and 250 nM lapatinib
BT474-Res	University of California, Los Angelus	Trastuzumab	Neil O'Brien	100µg/ml trastuzumab

Each cell line (Table 2.2) was manipulated separately, and the laminar flow cabinet was UV sterilised for a minimum of fifteen minutes between cell lines to minimize the likelihood of cross-contamination. Frozen cell suspensions were taken from liquid nitrogen storage, thawed and grown until 70 % confluent in 25 cm^2 flasks (T25) and subsequently maintained in 75 cm^2 flasks (T75) at 37 °C in a humidity controlled incubator with 5 % CO_2 and 20.9 % O_2. The culture medium was changed as required. Cell line identity was confirmed by DNA fingerprinting, which was performed by Source Biosciences™. Drug-resistant variants were treated twice weekly with the relevant drug and grown for a week in drug-free media prior to experiments. All cell lines were grown and maintained in 1% P/S, which was removed prior to experiments.

2.2 Methods

2.2.1 Doubling Time Assays

1 x 10^4 cells/well were seeded in duplicate into 6-well plates. Plates were incubated overnight at 37 °C to allow cells to adhere and cell counts performed on subsequent days until cells two doublings had been reached. To count cells, all media was removed and the well rinsed with 500 µl trypsin. 500 µl trypsin was added to each well and the plate incubated at 37°C for approx. 4 min to allow cells to detach. 500 µl RPMI-1640 was then added to inactivate the trypsin and a minimum of 4 cell counts were performed per well using a haemocytometer. Results were graphed using Graphpad Prism and the doubling time extrapolated from the curve.

2.2.2 Acid Phosphatase Toxicity Assays

1-5 x 10^4 cells/well at a volume of 100 µl were seeded in 96-well plates depending on the proliferation rate of the cell line. Plates were incubated overnight at 37 °C to allow cells to adhere. Drugs were serially diluted 1:2. 100 µl drug at 2X the test concentration was then added to the cells. Following a 5 day incubation at 37 °C, during which control cells attained 80-90% confluency, all media was removed from the plates, and the plates washed with PBS. 10 mM para-Nitrophenyl phosphate (PNPP) substrate in 0.1 M sodium acetate buffer with 0.1 % Triton X was added to each well and incubated at 37 °C for approximately 1 hour, at which stage the control cells stained yellow. 50 µl of 1 M NaOH was added to halt the reaction. Absorbance was read at 405 nM for 0.1 sec. For combination assays, drug was made up at 4X the desired concentration and 50 µl of the first inhibitor was added to 100 µl cells/media, followed by 50 µl of the second inhibitor or 50 µl media control. For scheduling combination assays, cells were pre-treated with one drug of a combination at a specific concentration and incubated at 37°C for 6 hours. The other drug in the combination was then added at a specific concentration and the plate incubated for 5 days before being processed as outlined above.

2.2.3 3D Soft Agar Assays

3D soft agar assays were carried out in triplicate in a 24-well plate Cells were counted and resuspended at 4.2 x 10^4 cells/ml in 1.5 ml RPMI-1640 medium supplemented with 10 % FBS. 3 % w/v agar was melted in a microwave and immediately transferred to a 65 °C water bath. 5.6 ml and 7.4 ml media were aliquoted into 15 ml tubes for the bottom and top layer, respectively, and placed in the 65 °C water bath. Drugs were made up at 3X the desired concentration and 1.5 ml drug was added to the cells. Pertuzumab was tested at a dose at which it is expected to saturate its target receptors; BAY80-6946 was tested at its IC_{50}. Heated media and agar were then sprayed with ethanol and brought into the hood. 1.2 ml agar was added to both tubes, and the layers returned to 65 °C water bath. The bottom layer, consisting of 0.5 % agar, was removed from 65 °C and brought to the hood. 500 µl of the bottom layer was added to each well dropwise, ensuring an even layer without air bubbles, and allowed to solidify. The top layer was then removed from the water bath and allowed to cool to 37 °C. Once the top layer had cooled, 1.5 ml was added to the cell/drug mixture, resulting in a 5:1 media/agar mix. 500 µl of this mix was added to each well on top of the solidified 0.5 % agar, resulting in a density of 7 x 10^4 cells per well. Cells were seeded in triplicate. PBS was added to the remaining wells on the plate to prevent dehydration. The plate, wrapped in parafilm, was incubated at 37 °C for 21 days. During this time, plates were regularly checked macroscopically and microscopically to ensure no dehydration or contamination presented. Prior to counting, 20 µl of sterile filtered neutral red was added to each well and left at 37 °C overnight to allow the dye to permeate the agar matrix. The following day each well was divided into 8 quadrants and visualised at 10 x under a light microscope. 4 quadrants were selected at random and live colonies (2 or more cells), which stained red, were counted. 3 planes from each quadrant were visualised and counted. The results were averaged and the average multiplied by 8, with the answer being taken to represent the total number of colonies per well. Separate wells were stained with Sytox Green overnight and imaged using a LSM510 confocal microscope.

2.2.4 Invasion and Migration Assays

Invasion and migration assays were performed in biological triplicate using the Boyden chamber method. For invasion assays, 100 µl 1 mg/ml matrigel was applied to porous (8 µm pore size) transwell migration chambers in a 24 well plate and left to solidify at 4˚C O/N. The plate was then equilibrated to 37 ɜ for an hour prior to the addition of the cells. Excess matrigel was removed and the insert washed with 100 µl with serum free RPMI-1640 media (SFM) and then with serum-containing media. 1 x 10^6 cells/ml in SFM was added dropwise to the centre of the insert, followed by 100 µl test media (SFM containing 5 nM BAY 80-6946 or DMSO-TFA vehicle control). 500 µl of serum-containing media was added to the bottom of the well as a chemo attractant and the plate incubated at 37 ɜ for 24 hours, during which time it was expected cells would digest the matrigel and migrate through the transwell. After incubation, matrigel and media were removed from the top of the insert and the bottom of the insert placed into 500 µl of crystal violet for ten minutes, and rinsed three times in distilled water. When dry, inserts were visualised, counted and imaged at 100 X using a light microscope. Cells which had successfully crossed the transwell and reached the bottom of the chamber stained purple.

2.2.5 DNA Extraction from HER2-positive breast cancer cell lines

DNA extraction was performed using an AllPrep™ DNA/RNA Mini Kit from Qiagen as per manufacturer's protocol. The AllPrep™ protocol is based on DNA binding to a spin column. Wash buffers remove cellular debris, prior to purified DNA being eluted. Cells were grown on a 10 cm petri dish until 80 – 90 % confluent. Media was removed and cells were washed with PBS prior to harvesting with 350 µl RLT buffer containing 1 % β-Mercaptoethanol (Qiagen buffer; composition not disclosed) supplemented with β-mercaptoethanol. Cells were scraped and the sample was homogenized by passing it through a blunt 20 G needle 16 times and transferred to a DNA spin column. 500 µl AW1 buffer (Qiagen buffer; composition not disclosed) was added and the column spun down for 15 sec at 15,000 RPM. 500 µl of AW2 buffer (Qiagen buffer; composition not disclosed) was then added and the column spun down for 2 minutes

at ≥ 14,000 RPM. 100 µl EB buffer, pre-warmed to 70 ℃, was added to the centre of the column and the column was incubated at room temperature for one minute before being centrifuged at ≥ 14,000 RPM for one minute. The eluted DNA was then quantified using QuBit™ technology (Invitrogen™). Typically 100 ng would be sent to Source Bioscience for fingerprinting analysis, and 20 ng used for Sequenom analysis.

2.2.6 Protein Extraction from HER2-positive breast cancer cell lines

4.5×10^5 cells were seeded into six well plates and left to adhere overnight. They were then treated with either 1 nM BAY-806946 or an equivalent concentration of DMSO-TFA (vehicle control). Protein was extracted 30 min, or 6 h, or 24 h post treatment (depending on the experiment) and stored at -80 ℃. To extract protein all media was removed and cells were twice washed with ice-cold PBS. 100µl lysis buffer (15 % NaCl 1M, 1 % triton X-100, 5 % Tris, 14 % phosphatase inhibitors 7X, 65 % dH_2O) was added to the plate and the plate scraped with a plastic 25 cm cell scraper. This lysis buffer was developed by our collaborators in MD Anderson to be suitable for phosphoprotein. Although typical lysis buffers (such as RIPA buffer, for western blot) are more stringent, they are not suitable for subsequent use on RPPA. The cell lysate was collected into a microcentrifuge tube and vortexed vigorously for 10 sec before being spun at 14,000 rpm for 10 min at 4 ℃. Supernatant was transferred to a fresh microcentrifuge tube. Protein concentration was determined using a bicinchoninic acid assay (BCA) as per manufacturer's protocol, using the lysis buffer as a blank. Absorbance was read at 750 nm. 1 µg/ml protein at 30 µl was used for RPPA. 30µg protein was used for western blotting.

2.2.7 Reverse Phase Protein Analysis of HER2-positive breast cancer cell lines

RPPA experiments were carried out by Dr Mattia Cremona and Dr Clare Morgan. Protein extraction lysates were normalized to 1.5 µg/µL concentration as assessed by bicinchoninic acid assay (BCA) and boiled with 1% SDS. Supernatants were manually diluted in four-fold serial dilutions with lysis buffer.

A QArray 2 arrayer (Molecular Device, Wokingham, UK) created a 378 sample array on Oncyte Avid nitrocellulose-coated slides (Grace Bio-Labs, Bend, OR). The slides were stored with desiccant (Drierite, Xenia, OH) at −20 °C prior to immunostaining.

Immunostaining was performed on an automated slide stainer according to the manufacturer's instructions (Autostainer catalyzed signal amplification (CSA) kit - Dako, Carpinteria, CA). Each slide was incubated with a single primary antibody at room temperature for 30 min. Each array was probed with a validated primary antibody. Please see Table 2.4 for a list of all primary antibodies used for the RPPA experiments. The secondary antibodies used were goat anti-rabbit IgG heavy + light (1:5000) (Vector Laboratories, Burlingame, CA) or rabbit anti-mouse IgG (1:10) (Dako). Dako Secondary antibodies were used as a starting point for amplification via horseradish peroxidase-mediated biotinyl tyramide with chromogenic detection (diaminobenzidine) according to the manufacturer's instructions (Dako).

Scanned TIFF images of slides were analyzed using Microvigene software, version 5.1 (VigeneTech Inc., Carlisle, MA) to generate spot signal intensities. The QRPPA module of Microvigene uses a 4 parameter logistic-log model ("SuperCurve" algorithm) which uses all spots within one array to form a sigmoid antigen-binding kinetic curve.

Finally, spots were normalized by protein loading, using the entire antibody panel. Briefly, the normalization process is as follows: we determined the median for each antibody across the sample set and divided each raw linear value by the median within each antibody to get the median-centered ratio. We then calculated the median from median-centered ratio for each sample across the entire antibody panel. This median functions as a correction factor (CF) for protein loading adjustment. We considered a sample to be alike if the CF was above 2.5 or below 0.25. Finally, we divided the raw data in linear values by the CF to obtain the normalized value.

Table 2.4 Primary antibodies used in our RPPA experiments

Antibody	Manufacturer	Catalogue number	Species	Dilution
Akt	Cell Signaling	9272	Rabbit	1:3000
Akt (S473)	Cell Signaling	9271	Rabbit	1:250
Akt (T308)	Cell Signaling	9275	Rabbit	1:500
Akt2 (5B5)	Cell Signaling	2964	Rabbit	1:50
C-Raf	Millipore	04-739	Rabbit	1:250
C-Raf (S338) 56A6)	Cell Signaling	9427	Rabbit	1:200
EGFR	Santa Cruz	SC-03	Rabbit	1:100
EGFR (Y1173)	Epitomics	1124	Rabbit	1:50
EGFR (Y992)	Cell Signaling	2235	Rabbit	1:100
EGFY (Y1068)	Cell Signaling	2234	Rabbit	1:100
MAPK – ERK 1/2	Cell Signaling	9102	Rabbit	1:200
HER2	Lab Vision	MS-325-P1	Mouse	1:1000
HER2 (Y1248)	Upstate	06-229	Rabbit	1:750
HER3	Santa Cruz	285	Rabbit	1:500
HER3 (Y1289)	Cell Signaling	4791	Rabbit	1:50
MAPK (T202/Y204-ERK 1/2	Cell Signaling	4377	Rabbit	1:1200
MEK1	Epitomics	1235-1	Rabbit	1:1200
MEK1/2 (S217/S221)	Cell Signaling	9121	Rabbit	1:1000
mTOR	Cell Signaling	2972	Rabbit	1:400
mTOR (S2448)	Cell Signaling	2971	Rabbit	1:100
mTOR (S2481)	Cell Signaling	2974	Rabbit	
NF-kB-p65 (S536)	Cell Signaling	3033	Rabbit	1:100
p38_MAPK	Cell Signaling	9212	Rabbit	1:300
p38 MAP Kinase (T180/Y182)	Cell Signaling	9211	Rabbit	1:250
p53	Cell Signaling	9282	Rabbit	1:3000
p70 S6 Kinase	Epitomics	1494-1	Rabbit	1:250
p70 S6 Kinase (T389)	Cell Signaling	9205	Rabbit	1:250
PDK1 (S241)	Cell Signaling	3061	Rabbit	1:100
PI3K-p110-alpha	Cell Signaling	4255	Rabbit	1:100
PTEN	Cell Signaling	9552	Rabbit	1:1000
S6 Ribosomal Protein (S235/S236) (2F9)	Cell Signaling	2211	Rabbit	1:200
S6 Ribosomal Protein (S240/S244)	Cell Signaling	2215	Rabbit	1:3000

2.2.8 Western Blot

Samples containing 30 µg protein were mixed with Bolt™ LDS buffer, Bolt™ reducing agent (composition not disclosed) to a final volume of 40 µl and incubated at 95°C for 2 min prior to being loaded into Bolt™ precast 4 – 12 % SDS gel. The gel was run at 200 V for 35 minutes and rinsed in 20 % ethanol with gentle shaking for 10 min . The gel was then blotted onto PVDF membrane using an iBlot 2.0™ dry transfer system, for 9 min at 25 V. The membrane was blocked in 5 % milk-TBST for 1 hr and the primary anti-rabbit HER4 antibody (Cell signalling, 4795S)) incubated at 1:1000 overnight at 4°C. Following 3 TBST 10 min washes with shaking, the secondary antibody was incubated at 1:3000 for 1 hr at RT. Following secondary antibody incubation, the blot was rinsed with TBST (2 x 5 min) and placed in a cassette. ECL prime was applied and the blot developed for 1 min. The blot was exposed to x-ray film and the film developed in a darkroom.

2.2.9 HER4 Protein Immunoprecipitation and Kinase Assay

HER4 immunoprecipitation was carried out by adding 20 µl Protein A magnetic beads to 200 µl cell lysate at 1 mg/ml protein (quantified by BCA). The mixture was rotated at 4^{o}C for 1 hour to clear cellular debris from the sample. The beads were then separated by magnetic rack and the supernatant removed and incubated with anti-rabbit HER4 antibody (Cell signalling, 4795S) at 1:50 dilution at 4^{o}C O/N with rotation. 20 µl Protein A magnetic beads for rabbit IgG (Cell Signaling, 8687) were added to the sample, mixed, and incubated with rotation at 4^{o}C for 30 min. Beads were separated using a magnetic rack and rinsed three times in cell lysis buffer. Purified HER4 protein was eluted from the beads in 20 µl ultra-pure water (Sigma) and assayed for its kinase activity using an ADP-Glo kinase assay kit (Promega, V9391).

The ADP-Glo system is a luminescence assay based on the conversion of ATP to ADP. Standard curves are prepared with fixed ratios of ATP:ADP. 50 µM of ADP was added to 10 µl sample (the substrate), 10 µl HER4 enzyme and 5 µl DMSO in a well of a 96-well white opaque plate. The plate was covered in tin foil and the kinase reaction

allowed to proceed in the dark for an hour at RT. A standard ATP-to-ADP conversion curve was generated by combining appropriate volumes (µl) of 1 µM ADP and 1 µM ATP stock solutions (provided with the kit) as follows: ADP:ATP 100:0, 80:20, 60:40, 40:40, 20:80, 10:90, 5:95, 4:96, 3:97, 2:98, 1:99, 0:100. 25 µl ADP-Glo reagent (Promega™ reagent, composition not disclosed), was then added to standards and samples and the reaction allowed to proceed at RT for 40 min. 50 µl kinase detection reagent (Promega™ reagent, composition not disclosed) was added to standards and samples and the plate incubated in the dark at RT for 30 min. Luminescence was read on a PerkinElmer plate reader and the kinase activity calculated by the level of unconverted ATP remaining in the sample.

2.2.10 DNA Extraction from FFPE clinical samples

DNA was extracted from 5 x 10 µm sections of FFPE tissue per sample using a Qiagen™ FFPE Kit as per manufacturer's protocol. Samples were scored by RCSI pathology and those with less than 50 % tumour were macrodissected to enrich for tumour content. The FFPE kit is based on spin column extraction. Xylene is used to remove the tissue from the paraffin as a first step. DNA then binds to the column whilst cellular waste is removed through wash buffers and centrifugation. 5 x 10 µm sections of tissue were cut and were placed into a 1.5 ml microcentrifuge tube (Sarstedt, 72.690.001). 1 ml xylene was added to the tube and the sample vortexed vigorously for 10 seconds before being centrifuged at 14,000 RPM for 2 min at room temperature. The supernatant was removed and discarded. This step was repeated twice more. 1 ml 100 % ethanol was then added to the sample, which was again vortexed vigorously for 10 seconds and spun at ≥ 14,000 RPM for 2 min at room temperature. This step was repeated twice more. The supernatant was discarded and the pellet air dried for approx 10 min until all the ethanol had evaporated. The pellet was resuspended in 180 µl Qiagen buffer ATL. 20 µl proteinase K was added and mixed by vortexing. Samples were incubated for 36 hours at 56 ɜ. 20 µl proteinase K was added and samples incubated for a further 2 hours at 56 ɜ. The samples were incubated at 90 ɜ for 1 hour. Following a brief centrifugation, 200 µl Qiagen AL buffer

and 200 µl 100 % ethanol were added and mixed immediately and thoroughly by vortexing for 10 sec. Following a brief centrifugation the lysate was transferred to a QIAamp minielute column and centrifuged at 8000 RPM for 1 min. Flow through was discarded and 500 µl Qiagen Buffer AW1 added to the column. The column was spun at 8000 RPM, the flowthrough discarded, and 500 µl Qiagen Buffer AW2 applied to the column. Columns were spun at 8000 RPM for 1 min and then at ≥ 14,000 RPM for 3 min to dry the membrane. The QIAamp minielute column was placed in a sterile 1.5ml microcentrige tube. 20µl Buffer ATE was added to the centre of the column and the column incubated at RT for 5 min before being centrifuged at full speed for 1 min. The elution step was repeated once more in order to maximise DNA yield. DNA samples were concentrated by being placed in an oven at 55 ɜ until all elution buffer had evaporated. They were then resuspended in 11 µl Qiagen Buffer ATE and quantified using QuBit™ technology according to manufacturer's instructions.

2.2.11 Next-generation sequencing

Next-generation sequencing was carried out by Dr Alex Eustace and Dr Sinead Toomey. DNA (200-300 bp) was extracted from FFPE samples and quantified with QuBit™ technology as outlined above. Using SPRIbeads (Beckman Coulter) DNA samples were size selected using a ratio of 0.7x to obtain only DNA fragments between 100 bp and 250bps. Following SPRIbead size selection samples were purified using the SureSelect™ Agilent Target Enrichment System Kit protocol. 27 µl AMPure XP™ magnetic beads were added to the DNA fragments in a Lo-bind 1.5 ml tube, mixed by vortexing and incubated 5 min. The tube was then placed in a magnetic stand and the sample allowed to clear. Beads were rinsed twice with 500 µl fresh 70 % ethanol. The tube was then incubated at 37 ɜ until residual ethanol evaporated and DNA was eluted from the beads in 50 µl nuclease-free water. Following this sample purification an end repair reaction was performed to generate blunt-end fragments with 5'-phosphorylated ends. Samples were mixed with nuclease-free water, End Repair buffer (Agilent reagent, composition not disclosed), dNTP mix, T4 DNA polymerase, T4 Polynucleotide Kinase and Klenow DNA

polymerase as per manufacturers guidelines to a final volume of 100 µl and the mixture incubated in a thermal cycler for 30 min at 20 ɜ. The sample was again purified with AMPure XP™ magnetic beads as described above. 30 µl DNA sample was mixed with 11 µl nuclease-free water, 5 µl Klenow Polymerase Buffer, 1 µl dATP and 3 µl Exo(-) Klenow, and the reaction incubated for 30 min at 30 ɜ in order to add "A" bases to the 3'-end of the DNA fragment. The adapters (5'GATCGGAAGAGCTCGTATGCCGTCTTCTGCTTG3') and (5'ACACTCTTTCCCTA-CACGACGCTCTTCCGATCT3') were used in a 10:1 molar ratio to raw genomic DNA. Samples were again purified with AMPure XP™ magnetic beads. Amplification of the library was performed with the Herculase II Fusion DNA Polymerase kit for 14 cycles of PCR. DNA was then quantified on a Bioanalyser to determine its concentration and purity.

For the hybrid selection the libraries were adjusted to at least 750 ng in 3.4 µl dH_2O and added to the SureSelect Block solutions. This mixture was heated at 95°C for 5 min and held for 5 min at 65°C. The library was then mixed with the prewarmed hybridization buffer (5 min at 65°C) and SureSelect oligo capture library mix (2 min at 65°C). After 24 h incubation at 65°C, the hybridization mix was added to 500 ng (50 µl) of M-280 streptavidin Dynabeads (Invitrogen), and the incubation was continued for 30 min at room temperature (RT). The beads were pulled down and washed once at RT for 15 min with 500 µl of SureSelect Wash Buffer 1, followed by three 10 min washes at 65°C with 500 µl of prewarmed SureSelect Wash Buffer 2. Hybrid-selected DNA was eluted with 30 µl of Elution Buffer and incubated for 5 min at RT. The post amplification step was performed with the Herculase polymerase and the SureSelect GA PCR-Primer-mix for 12 cycles. DNA was once again quantified on a Bioanalyser to determine the efficiency of the proceedure.

The original manufacturer's protocol resulted in large losses of DNA. Table 2.5 summarises the modifications we made to the manufacturer's protocol in order to minimise DNA loss prior to sequencing.

Table 2.5 Optimisation of the NGS sample preparation procedure in order to minimise DNA loss prior to sequencing.

Proceedure	1. Starting 3µg DNA 2. Fragmented Sample 3. Normal Prep 4. Gel Post PCR	1. Starting 3µg DNA 2. No Fragment 3. Normal Prep 4. SPRIbead separation	1. Starting 3µg DNA 2. No Fragment 3. TCD Indexes 4. Gel Post PCR
Post Fragmentation	453 ng	2005 ng	1523 ng
Post End Repair	303 ng	1491 ng	1413 ng
Post T-Base Addition	330 ng	909 ng	909 ng
Post Ligation	203 ng	441 ng	447 ng
Post PCR	68.9 ng	1332 ng	187.6 ng
Post Gel clean-up	42 ng	480 ng	13.42 ng

2.2.2.12 Sequenom Analysis of FFPE HER2-positive breast cancer samples

Sequenom analysis was carried out by Dr Sinead Toomey. Mutations were identified in the DNA isolated from our HER2-positive cell line panel and from 227 patient samples using the Sequenom MassArray system (Sequenom, San Diego, CA). A custom panel was designed containing ERRB family mutations discovered in our next-generation sequencing study, as well as potentially deleterious mutations identified in TCGA, and which had been previously published[180, 181] (Table 2.6). The technique involves a PCR reaction which amplifies the region of the DNA to be sequenced, followed by a clean-up reaction where shrimp alkaline phosphatase (SAP) is added to each assay to remove excess nucleotides. PCR and extension primers for the multiplexed assay were designed with the Sequenom Assay Design software. An iPLEX assay was carried out, where the primer and amplified target DNA were incubated with dideoxynucleotide terminators which have a modified mass. Using these terminators the DNA is extended by one base. Prior to sequencing, a nanodispenser was used to spot the samples from the PCR plate onto a Sequenom spectrochip. Transferred volumes were checked to ensure they were greater than 5 nL and less than 20nL. When the volume was less than or greater than this, the speed

of the machine was adjusted until the target volume was achieved. Spotted spectrochips were then placed onto the Sequenom MassArray and through the use of MALDI-TOF mass-spectrometry, the mass of the extended primer can be determined. The mass of the primer indicates the sequence and therefore the genotype of the sample. Visual inspection and Sequenom Typer software were used to perform genotyping based on mass spectra. Reactions where >15% of the resultant mass ran in the mutant site were scored as positive.

Table 2.6 The mutations in EGFR, ERRB2, ERRB3, ERRB4 and PIK3CA assayed in our sequenom study.

EGFR	HER2	HER3	HER4	PIK3CA
A839T	D769H	A232V	D595GV	R38H
D761NY	G776S	D297Y	E810K	Q60K
E709AVG	G776V	E928G	E872K	R88Q
E709KQ	H878Y	G284R	E872V	K111N
E884K	L755S	G325R	E874X	G118D
G719AD	P1119S	P262H	E934K	N345K
G719CSR	S310FY	Q809R	G599W	S405F
G863D	V777A	S505F	G936R	E418K
H870R	V777LM	S846I	K935E	C420R
K846R	V842I	T355A	K935TRI	E453K
L858M		T355I	N861Y	P539R
L858R		T389K	P854Q	E542K/Q/V/G
L861QR		V104M	R782Q	E545D/K/Q/A/V/G
N700D		V714M	R81X	Q546H/E/K/L/P/R
R836C			S303Y/F	C901F
S720TP			T926M	F909L/L
T273S			V348ML	M1004I
T783A			V721I	G1007R
V398I				Y1021C/H/N
V689M				R1023Q
V769LM				T1025A/S/I/T
				A1035T/V
				M1043I/I/I/V
				A1046V
				H1047R/L/Y
				G1049R
				I1058F
				H1065L

2.2.13 Plasmid-transformed bacterial culture and plasmid preparation

A plasmid encoding for wild-type (WT) ERBB4 was obtained from Addgene (29536). pCDF1-MCS2-EF1-puro (Systems Biosciences; CD110-B1) was obtained to serve as an empty vector control. Plasmids were provided as a bacterial stab, transformed into *Escherichia coli* bacteria. Transformed bacteria were streaked onto 3.5 % (w/v) LB agar plates containing 100 µg/ml ampicillin and incubated overnight at 37 °C. A single

colony was used to inoculate a starter culture of 4 ml LB broth containing 50 µg/ml ampicillin. This culture was incubated at 37 °C with vigorous shaking (225 rpm) for approximately 8h and then diluted 1 in 500 into 250ml LB agar broth containing 50 µg/ml ampicillin, which was cultured O/N at 37 °C with vigorous shaking (225 rpm) . Bacterial cells were harvested by centrifugation at 6,000 x g for 15 min at 4 °C. Plasmid DNA was extracted and purified using a QIAGEN™ plasmid maxi kit and QIAfilter in accordance with the manufacturer's instructions. Eluted DNA was dissolved in 20 µl ATE Buffer (Qiagen) and quantified using Nanodrop technology.

2.2.14 Site-directed mutagenesis

Site-directed mutagenesis was performed using the QuikChange II XL Site-Directed Mutagenesis Kit (Agilent®). Primers were designed using Agilent's QuikChange Primer Design programme at www.agilent.com/genomics/qcpd, which was specifically designed to be used with this site-directed mutagenesis kit. Briefly, the mutations we wished to introduce were a single base C to T substitution at position 908 (S303F) and a single base G to A substitution at position 2161 (V721I) of ERBB4. We selected the base we wished to substitute and a number of bases (at least 5 codons) either side of it. We then introduced a "mistake" into the sequence, substituting a T for a C, at position 908, or a G for an A at position 2161. This mismatch was at the centre of the primer sequence, as if it were too close to an end of the primer the primer may not anneal to the sequence due to the mismatch. However, with the mismatch flanked by correct bases either side, the primers should anneal tightly, maximising the chance that the substitution will be introduced. GC content, melting temperature, and primer length were optimised by the software. Primers were then synthesised and purified by IDT™.

Table 2.7 Primers used to perform site-directed mutagenesis to create ERBB4 S303F and V721I

Gene (Human)	Primer Sequence (Forward/Reverse)	Final concentration (pmol)
ERBB4-S303F	5’ - ggcacgcacacaaaaactggaatctaccacaaagttat – 3’	1.25
	3’ – ataactttgtggtagattccagtttttgtgtgcgttgcc – 5’	1.25
ERBB4-V721I	5'-gaaactgagctgaagaggataaaagtccttggctcag-3' 3'-ctgagccaaggacttttatcctcttcagctcagtttc-5'	1.25 1.25

Mutagenesis and control reactions were prepared in sterile PCR tubes and carried out according to the manufacturer’s instructions. The technique involves a PCR reaction using template (ERBB4 WT) DNA and the mutation-specific primers detailed above. Cycling parameters were set according to the size of the template plasmid in line with manufacturer's guidelines. Mutated DNA was then transformed into the XL-10 supercompetent *E coli* bacteria supplied with the kit. The XL-10 strain was necessary as our plasmids were too large to be transformed into other competent species. Plasmid-transformed bacteria were grown and plasmids purified as outlined above. Sequenom analysis was used to confirm that the mutation had been generated.

2.2.15 Transduction of exogenous DNA into HER2-positive breast cancer cells

ERBB4 WT, ERBB4 S303F and ERBB4 V721I plasmids, along with the pCDF1-MCS2-EF1-puro empty vector plasmid, were stably expressed in three HER2-positive breast cancer cell lines (Table 2.6) by researchers in Dr Madeline Murphy’s group at the Conway Institute, University College Dublin. Prior to transfection, HEK293T cells were seeded so as to be approximately 70% confluent in a T75 flask on the day of transfection. Lentiviral expression constructs were prepared using 20 µl of the pPACKF1 Lentivector Packaging Kit (Systems Biosciences®) with 20 µg plasmid containing the DNA to be transfected, which were diluted in serum-free DMEM, mixed in a sterile 1.5 ml Eppendorf tube and added dropwise to the HEK293T cells, which were then incubated at 37˚C for 48 hours, in which time these producing cells

create and secrete pseudoviral particles. 48 hours post transfection the viral-enriched supernatant was collected from the HEK293T cells and filtered through a 0.45 µM syringe filter. 3.5 ml of supernatant was then added to T75's containing host cells at approximately 30 % confluence. 48 hours after transfection selective media was added to the cells. Successfully transfected cells were selected in 2 µg/ml puromycin for a minimum of 10 days prior to experiments, and were maintained in this concentration of puromycin thereafter.

Table 2.8 Established HER2-positive cell line models used for development of ERRB family mutation constructs in this thesis

Cell Line	HER Family	PIK3CA	ER Status
HCC1569	WT	WT	Neg
HCC1954	WT	H1047R	Neg
BT474	WT	K111N	Pos

2.2.16 Statistical analysis

All experiments described in this thesis were carried out in biological triplicate, unless otherwise stated. Error bars are representative of the standard deviation of biological replicates. Statistical tests were performed when n ≥ 3. Statistical significance was denoted by a p–value ≤ 0.05. IC_{50} and Combination Index (CI) values were calculated using CalcuSyn software (BioSoft) which is based on the Chou-Tallalay synergy quantification method. A CI value of < 1 is considered synergistic, 1 is considered additive and > 1 is considered antagonistic. The Student's *t*-test (two-tailed with equal variance) was used to compare the effect of BAY80-6946 on invasion and migration, and the effect of BAY80-6946 on AKT, mTOR and PI3K-p110-alpha expression and phosphorylation. A Kruskal-Wallis non-parametric test was performed to compare tratsuzumab alone, BAY80-6946 alone and the combination. Kaplan-Meier analysis was performed using GraphPad prism to determine the impact of mutations on overall survival and relapse-free survival. Fisher's Exact Test (2 variables) or Chi-Squared Test (≥ 3 variables) were used to determine any significant correlations between mutations and clinical or pathological features in our study group.

Chapter 3 : A preclinical evaluation of the PI3K alpha/delta dominant inhibitor BAY80-6946 in HER2-positive breast cancer models with acquired resistance to the HER2-targeted therapies trastuzumab and lapatinib.

3.1 Introduction

HER2-positive breast cancer accounts for 15-20 % of all breast cancers and is associated with shorter time to progression and decreased overall survival[10]. Trastuzumab, a monoclonal antibody targeted to HER2, has significantly improved outcomes in both the adjuvant and metastatic settings[1], but resistance to trastuzumab remains a problem. Lapatinib, a small molecule tyrosine kinase inhibitor (TKI) against HER2 and EGFR, currently in use as a second-line therapy in patients who have progressed on trastuzumab therapy[11], is effective in some patients who acquire resistance to trastuzumab. However, the efficacy of lapatinib is also limited by the development of acquired resistance.

The phosphatidylinositol-3-kinase (PI3K) pathway, a major signalling mediator in cancer[12] is activated downstream of HER2. This pathway has been strongly implicated as a mediator of trastuzumab resistance in breast cancer[13, 14] and has recently been associated with lapatinib resistance[3]. Preclinical data suggest that targeting a PI3K signalling node called mammalian target of rapamycin (mTOR) in combination with HER2-inhibition could overcome HER2-positive breast cancer resistance to HER2-targeted therapy[12]. However, the clinical efficacy of mTOR inhibitors in HER2-positive breast cancer has been disappointing[15], likely in part due to inhibition of mTOR activating a feedback loop which upregulates PI3K activity, thereby attenuating the anti-tumour efficacy of mTOR inhibitors[16].

We hypothesise that directly targeting PI3K can overcome the limitation of feedback activation mediated by mTOR inhibition. BAY 80-6946, a novel, potent, highly selective PI3K inhibitor[17-20], able to induce apoptosis *in vitro*[20] , was well-tolerated in a Phase I clinical trial[21]. In the study presented here, we show that the novel PI3K inhibitor, BAY 80-6946, potently inhibited the growth of 5 HER2-positive cell lines and 5 HER2-positive lines with acquired trastuzumab/lapatinib resistance. We found that the combination of BAY 80-6946 and HER2-targeted therapies more effectively

inhibited cell growth than either therapy used alone, with clear synergy in many cases, and that the addition of the PI3K inhibitor could restore sensitivity to HER2-targeted therapies in cells with acquired resistance to trastuzumab and lapatinib.

The objectives of the work described in this chapter were to:

1. Profile a panel of HER2-positive breast cancer cell lines including models of acquired resistance to trastuzumab and/or lapatinib for their response to BAY 80-6946, and to the established HER2-targeted therapies trastuzumab, lapatinib, and pertuzumab, and to the novel HER2-targeted therapy afatinib
2. Characterise the above mentioned cell line panel for their PIK3CA mutational status, PTEN status and PI3K pathway activation status, in order to determine if any of these affected sensitivity to the PI3K inhibitor
3. Investigate whether BAY 80-6946 treatment inhibited PI3K signalling
4. Determine if combining PI3K inhibition with HER2-targeted therapy results in improved growth inhibition compared to either therapy used alone
5. Investigate if a non-lethal dose of BAY 80-6946 affects invasion and/or migration of HER2-positive breast cancer cells

The work described in this chapter has been published[22] and based on the results presented herein Bayer pharmaceuticals have agreed to support a phase Ib/II clinical trial of copanlisib in combination with trastuzumab in women with metastatic HER2-positive breast cancer whose tumours have progressed despite previous treatment with trastuzumab.

3.2 HER2-positive breast cancer cell lines respond to BAY 80-6946 regardless of their mutational status and response to trastuzumab, lapatinib, afatinib or pertuzumab.

A panel of HER2-positive cell lines including matched models of acquired trastuzumab, lapatinib and combined trastuzumab and lapatinib-resistance, were analysed by Sequenom MassArray for somatic mutations in 53 different genes (Table 3.1). Mutations in the PIK3CA gene were identified in BT474 (K111N), HCC1954 (H1047R) and MDA-MB-453 (H1047R) cells, and although all of our cell lines had activated PI3K signalling. The cell lines bearing the H1047R mutation were intrinsically relatively resistant to trastuzumab and lapatinib, however a similar innate resistance was observed in HCC1569, which are PIK3CA WT, and the BT474 model, which bears a K111N mutation was our most sensitive model to both trastuzumab and lapatinib. The mutational status of PI3K, TP53 or the expression of PTEN did not change between parental cell lines and models of acquired resistance to trastuzumab and/or lapatinib (Table 3.1). Taken together, these data suggest that PIK3CA mutation alone is not sufficient to predict PI3K pathway activation status or sensitivity to trastuzumab and/or lapatinib.

BAY 80-6946 achieved an IC_{50} in this panel of cell lines ranging from 3.9 ± 0.8 nM in BT474 cells to 29.4 ± 4.7 nM in MDA-MB-453 cells and was effective in cell lines regardless of their PI3K or P53 mutational status (Table 3.1). Models of acquired resistance to trastuzumab had a higher IC_{50} to BAY 80-6946 than their matched parental cell lines (SKBR3 = 7.2 ± 0.8 nM; SKBR3-T = 26.2 ± 6.2 nM : BT474 = 3.9 ± 0.8 nM; BT474-Res = 6.25 ± 0.8 nM).

Whereas SKBR3, SKBR3-L and SKBR3-TL had similar IC_{50} values to BAY80-6946, the SKBR3-T model was relatively insensitive (Table 3.1). It has been shown that activated

AKT leads to less dependence on HER2 for downstream signalling (including through the PI3K pathway). Although an elucidation of the mechanisms by which SKBR3-T acquired trastuzumab resistance was beyond the scope of this study, an upregulation of HER2-independent PI3K signalling in this cell line model could potentially account for its increased IC_{50} to copanlisib, as a higher level of signalling would require a higher dose to inhibit it. We subsequently designed a reverse phase signalling array (RPPA) experiment in part to answer the question of why this cell line is more resistant to copanlisib than the other SKBR3 models.

We also studied the effect of lapatinib and afatinib (dual EGFR/HER2 inhibitors) in our panel of cell lines. Lapatinib IC_{50}s ranged from 33.3 ± 9.5 nM in BT474 cells to cells lines which did not achieve an IC_{50} at concentrations greater than 2μM lapatinib; such as the cell lines with acquired lapatinib resistance. The cell lines with acquired lapatinib resistance SKBR3-L, -TL and HCC1954-L did not achieve an IC_{50} at greater than 500nM lapatinib whilst MDA-MB-453 cells did not achieve an IC_{50} at greater than 2μM lapatinib. Afatinib IC_{50}s ranged from 3.8 ± 2.4 nM in SKBR3-T cells to greater than 1μM in MDA-MB-453 cells. Interestingly the SKBR3-L and SKBR3-TL cells had a greater IC_{50} to afatinib than that seen in SKBR3 cells; however the same affect was not observed in the HCC1954-L cell line relative to HCC1954 cells. Spearman rank correlation failed to identify any correlation between response to BAY 80-6946 and response to either lapatinib or afatinib in our panel of cells (results not shown), suggesting that PI3K independent effects at least partly drive the proliferation of these cells. Cells had varying sensitivity to trastuzumab when used alone, achieving between 43.6% ± 4.1 % growth inhibition in BT474 cells to no growth inhibition (e.g. in HCC1954 cells).

Table 3.1 IC_{50} values assessing for BAY 80-6946, lapatinib and afatinib, and the effect of trastuzumab and pertuzumab on % growth inhibition in a panel of HER2-positive cell lines including matched models of acquired trastuzumab (-T amd -Res) resistance and a model of acquired resistance to both lapatinib and trastuzumab (-TL). Comparative mutational analysis was determined by sequenom MassARRAY of mutations in PIK3CA and TP53; PTEN status as assessed by western blotting with median expression level used for high/low cutoff; PI3K Signalling as defined by expression and activation of PI3K signalling factors as determined by RPPA. Standard deviations are representative of triplicate independent experiments. IC_{50} values determined using Calc u s yn s o f t w a r e (B i t w o - t a i l e d e q u a l v a r i a n c e ' = p ≤ S t u d e n t ' s t e s t r e l a t i v e to matched parental cell line. N/A indicates parental cell lines that do not have acquired resistance. Wt = wild type

Cell Line	Acquired Resistance	Mutational Status		PI3K Signalling Factors		Response to Targeted Therapies (IC_{50})				
Name		PIK3CA	TP53	PTEN	PI3K Signalling	BAY80-6946 (nM)	Lapatinib (nM)	Afatinib (nM)	Trastuzumab % growth inhibition at 10 µg/ml	Pertuzumab % growth inhibition at 10 µg/ml
SKBR3	N/A	Wt	wt	Low	Active	7.2 ± 0.8	65.1 ± 11.8	6.2 ± 1.7	39.8 ± 5.2	1.0 ± 20.0
SKBR3-L	L	Wt	wt	Low	Active	7.6 ± 4.0	<50% inhibition @ 500nM	32.1 ± 6.1	15.9 ± 8.2	-2.8 ± 7.1
SKBR3-T	T	Wt	wt	Low	Active	26.2 ± 6.2*	51.2 ± 2.8	3.8 ± 2.4	12.5 ± 4.7	-3.0 ± 1.0
SKBR3-TL	T+L	Wt	wt	Low	Active	8.0 ± 1.4	<50% inhibition @ 500nM	38.5 ± 1.1	11.2 ± 6.1	-6.6 ± 8.0
BT474	N/A	K111N	wt	High	Active	3.9 ± 0.8	33.3 ± 9.5	6.3 ± 1.9	43.6 ± 4.1	-2.5 ± 3.7
BT474-Res	T	K111N	wt	High	Active	6.25 ± 0.8 *	108.7 ± 0.8	4.6 ± 1.5	-1.2 ± 2.7	6.4 ± 5.8
HCC1954	N/A	H1047R	wt	Low	Active	4.9 ± 1.0	291.4 ± 42.2	44.2 ± 9.7	-10.0 ± 19.0	-4 ± 20.0
HCC1954-L	L	H1047R	wt	Low	Active	9.2 ± 2.3	<50% inhibition @ 500nM	54.0 ± 12.2	-2.0 ± 14.0	2.0 ± 12.0
HCC1569	N/A	Wt	wt	High	Active	29.4 ± 4.7	291.4 ± 4.70	19.8 ± 7.4	7.9 ± 8.1	1.9 ± 6.8
MDA-MB-453	N/A	H1047R	wt	Low	Active	3.9 ± 1.9	> 2000	> 1000	-1.5 ± 2.1	-1.7 ± 2.6

3.3 The combination of BAY 80-6946 and the HER2-targeted therapies improve response to either drug used alone in HER2-positive breast cancer cells including those with acquired trastuzumab resistance

Having established its single-agent efficacy in the results presented above, and based upon the evidence described in Chapter 1 that argues for the co-targeting of HER2 and PI3K in HER2-positive breast cancer, we investigated whether the addition of copanlisib to the established HER2-targeted therapies trastuzumab and lapatinib would restore the efficacy of these drugs in HER2-positive breast cancer cell lines with acquired or innate resistance.

The combination of trastuzumab and BAY 80-6946 resulted in statistically improved growth inhibition compared to either therapy alone in 3/4 parental cell lines tested (BT474, HCC1954 and SKBR3) (Figure 3.1). Combinations of BAY 80-6946 with trastuzumab significantly enhanced growth inhibition in models of acquired trastuzumab and/or lapatinib resistance (BT474-Res, SKBR3-L, -T, -TL ($p < 0.05$)) but not in HCC1954-L cells.

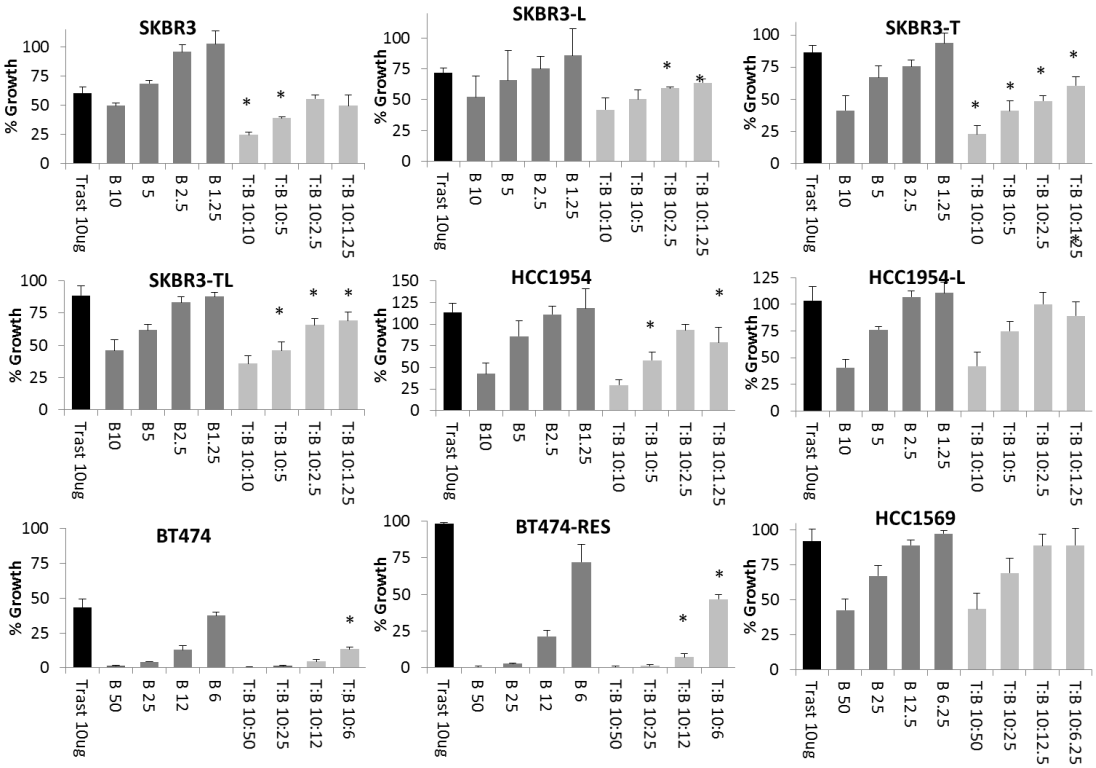

Figure 3.1 Combining trastuzumab (T) and BAY 80-6946 (B) inhibits growth more effectively than testing either drug alone using acid phosphatase assays in our panel of HER2-positive breast cancer lines including matched models of acquired trastuzumab and/or lapatinib resistance. '*' indicates a p-value < 0.05 relative to trastuzumab alone and the corresponding dose of BAY 80-6946 alone as calculated by tukey multiple ANOVA analysis. Standard Deviations are representative of independent triplicate experiments.

Combinations of lapatinib and BAY 80-6946 enhanced growth inhibition relative to testing either drug alone in all cell lines tested including those with acquired lapatinib resistance (Figure 3.2). Lapatinib had a synergistic response in the majority of HER2-positive breast cancer cell lines when tested in combination with BAY 80-6946 (BT474 CI @ ED_{50} = 0.12 ± 0.09 ranging to SKBR3-L CI @ ED_{50} = 0.85 ± 0.23) (Table 3.2). Despite lapatinib resistant models SKBR3-L, HCC1954-L and SKBR3-TL having limited sensitivity to lapatinib, the combination of lapatinib and BAY 80-6946 was still synergistic with clear restoration of sensitivity to lapatinib in these cell lines. This trend was also observed in the trastuzumab resistant cell lines BT474-Res and SKBR3-T, whereby the combination of lapatinib plus BAY 80-6946 remains highly synergistic with a CI at ED50 of 0.32 +/- 0.20 as calculated by Calcusyn (Biosoft), which is based on the Chou-Tallaly Synergy Quantification method (Table 3.2).

The combination of afatinib and BAY 80-6946 enhanced growth inhibition relative to testing either drug alone (Figure 3.3). Afatinib and BAY 80-6946 had an additive response in SKBR3 cells (CI @ ED_{50} = 0.91 ± 0.13) and a synergistic response in the remaining cell lines (SKBR3-TL CI @ ED_{50} = 0.48 ± 0.02 to HCC1569 CI @ ED_{50} = 0.58 ± 0.13) (Figure 3.3, Table 3.2). Indeed, the combination is far more synergistic in BT474-Res, SKBR3-T, SKBR3-L and SKBR3-TL than in the corresponding parental cells. Interestingly, synergy is enhanced in cell line models of acquired resistance to trastuzumab and/or lapatinib.

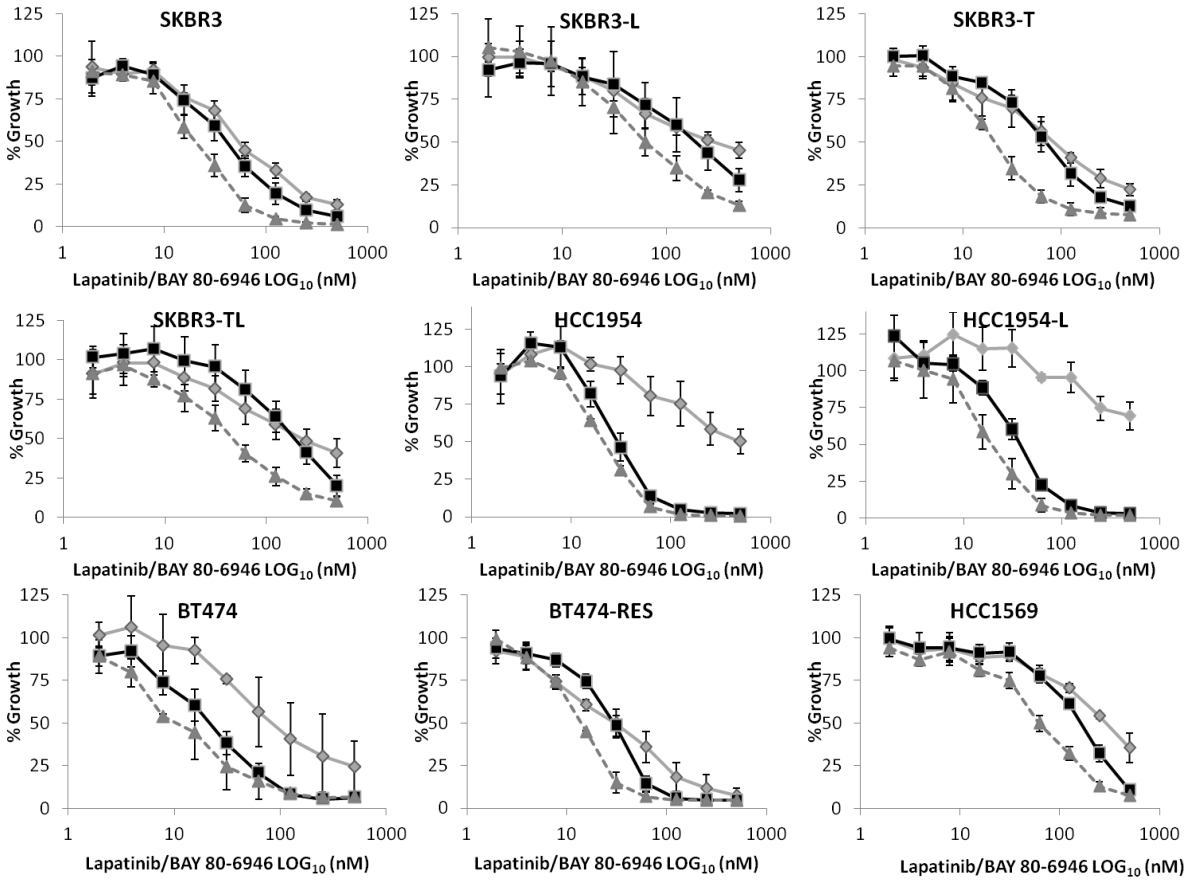

Figure 3.2 Efficacy of lapatinib (-◊-), BAY 80-6946 (-□-) and a combination of lapatinib and BAY 80-6946 (--Δ--) in a panel of HER2-positive cell lines, including those with acquired resistance to either trastuzumab (-T or -Res), lapatinib (-L) or the combination of trastuzumab and lapatinib (-TL). Acid phosphatase toxicity assays were used to generate dose-response curves to each drug alone and in combination over 5 days, with Calcusyn (Biosoft), which is based on the Chou-Tallalay Synergy Quantification method, subsequently used to calculate IC_{50} and CI values. Error bars are representative of standard deviations across triplicate experiments. The ratio of lapatinib:BAY 80-6946 in this assay is fixed at 5:1 with a top concentration for serial dilution set at 500 nM and 100 nM resepectively.

Table 3.2 The IC_{50}s of lapatinib and afatinib in combination with BAY 80-6946 compared to the IC_{50} of each as a single agent and Combination Index (CI) values at ED_{50} for the combination of lapatinib or afatinib with BAY 80-6946. Acid phosphatase toxicity assays were used to generate dose response curves to the agents alone and in combination over a 5 day period, with lapatainib:BAY 80-6946 tested at a 5:1 ratio (500 nM:100 nM), and afatinib:BAYn80-6946 at a 1:1 Ratio (100 nM:100 nM). Calcusyn (Biosoft), which is based on the Chou-Tallalay Synergy Quantification method, subsequently used to calculate IC_{50} and CI values. A CI value of 1 indicates a drug combination is additive, a CI value > 1 indicates a combination is antagonistic, and a CI value of < 1 indicating a combination is synergistic, with lower CI values denoting greater synergy. Standard deviations are representative of independent triplicate experiments.

Cell line	IC_{50} (nM)	Lap:80-6846	Afat:80-6946	IC_{50} (nM)	IC_{50} (nM)	IC_{50} (nM)	IC_{50} (nM)
	BAY 80-6946	ED_{50}	ED_{50}	Lapatinib	Lap + BAY80-6946	Afatinib	Afat + BAY80-6946
SKBR3	7.2 ± 0.8	0.68 ± 0.08	0.91 ± 0.13	65.1 ± 11.8	17.8 ± 8.1	6.2 ± 1.7	2.7 ± 0.3
SKBR3-L	7.6 ± 4.0	0.85 ± 0.23	0.50 ± 0.09	<50% inhibition @ 500nM	68.5 ± 11.0	32.1 ± 6.1	7.8 ± 4.5
SKBR3-T	26.2 ± 6.2	0.44 ± 0.19	0.59 ± 0.18	51.2 ± 2.8	24.1 ± 6.9	3.8 ± 2.4	3.0 ± 0.8
SKBR3-TL	8.0 ± 1.4	0.59 ± 0.09	0.48 ± 0.02	<50% inhibition @ 500nM	55.1 ± 6.0	38.5 ± 1.1	9.1 ± 1.5
BT474	3.9 ± 0.8	0.12 ± 0.09	0.50 ± 0.05	33.3 ± 9.5	9.6 ± 4.3	6.3 ± 1.9	2.5 ± 0.1
BT474-Res	6.25 ± 0.8	0.32 ± 0.20	0.52 ± 0.13	108.7 ± 10.5	5.4 ± 7.3	4.6 ± 1.5	4.0 ± 1.0
HCC1954	4.9 ± 1.0	0.63 ± 0.10	0.73 ± 0.02	291.4 ± 42.2	17.8 ± 6.0	44.2 ± 9.7	1.4 ± 0.5
HCC1954-L	9.2 ± 2.3	0.83 ± 0.07	0.46 ± 0.22	<50% inhibition @ 500nM	40.6 ± 7.5	54.0 ± 12.2	1.8 ± 0.7
HCC1569	29.4 ± 4.7	0.80 ± 0.11	0.58 ± 0.13	291.4 ± 60.0	65.2 ± 3.8	19.8 ± 7.4	6.8 ± 0.5

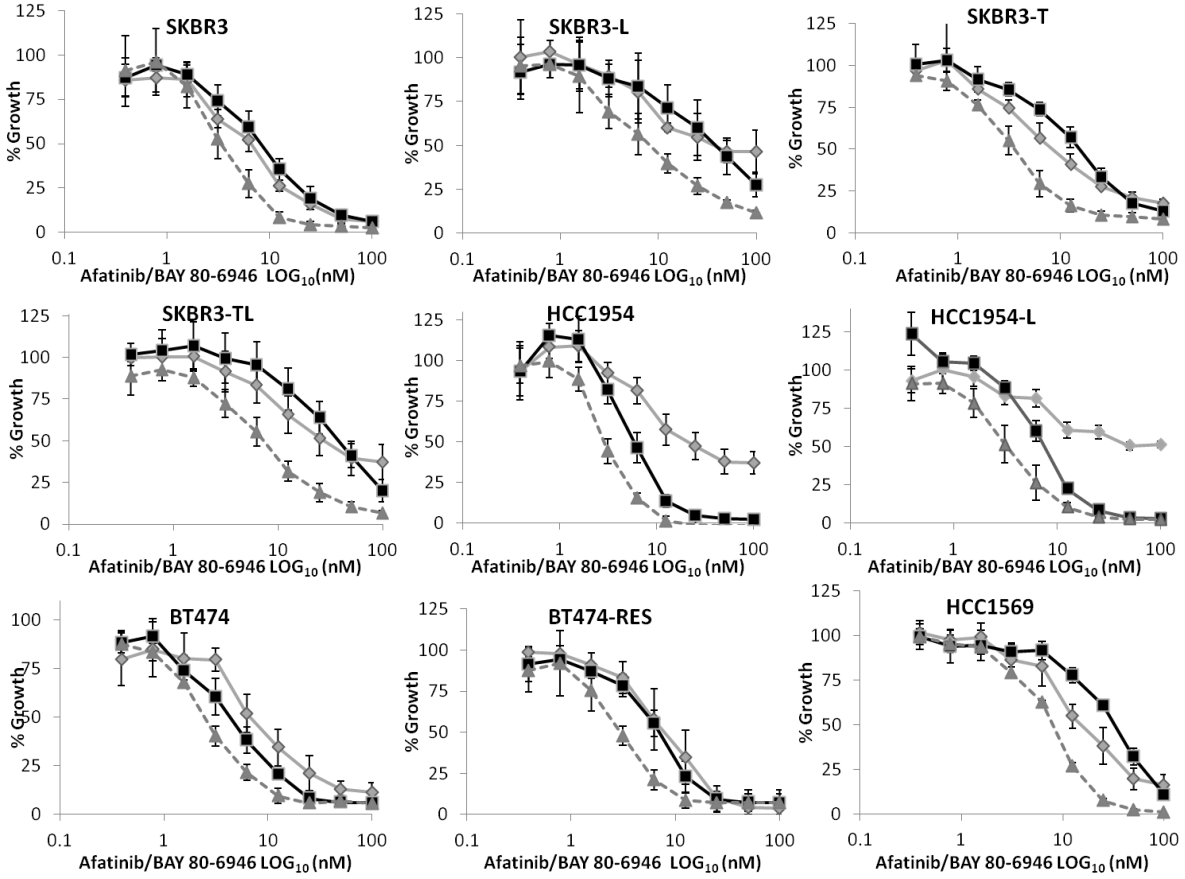

Figure 3.3 Efficacy of afatinib (-◊-), BAY 80-6946 (-□-) and a combination of afatinib with BAY 80-6946 (--Δ--) in a panel of HER2-positive cell lines, including those with acquired resistance to either trastuzumab (-T or -Res), lapatinib (-L) or the combination of trastuzumab and lapatinib (-TL). Acid phosphatase toxicity assays were used to generate dose-response curves to each drug alone and in combination over 5 days, with Calcusyn (Biosoft), which is based on the Chou-Tallalay Synergy Quantification method, subsequently used to calculate IC_{50} and CI values. Error bars are representative of standard deviations across independent triplicate experiments. The ratio of lapatinib: BAY 80-6946 in this assay is fixed at 1:1 with a top concentration for serial dilution of 100 nM for each drug.

3.4 Effects of BAY 80-6946 on cell signalling

As described previously, we found the BAY 80-6946 to potently inhibit the growth of HER2-positive breast cancer cells regardless of PIK3CA mutational status. Although all of our cell lines had activated PI3K signalling, they did not respond equally to the PI3K inhibitor (Table 3.1), and further, the lack of correlation between lapatinib/afatinib efficacy and BAY 80-6946 efficacy suggests that our cell line-panel are not entirely dependent on the PI3K pathway. We designed an RPPA experiment to elucidate the effects of BAY 80-6946 on signalling across the HER family receptors, the PI3K and MAPK pathway in order to elucidate a basic mechanism and search for biomarkers for its efficacy.

HER2 activation (Y1248) was significantly increased in HCC1954, BT474 and HCC1569 cells treated for 6 and 24hrs with BAY 80-6946 (Table 3.3, Figure 3.4). HER3 expression or activation (Y1289) was not altered after BAY 80-6946 treatment in parental HER2-positive cells. We also saw a significant increase in MAPK activation (T202/Y204) in HCC1954, BT474 and MDA-MB-453 cells after treatment with BAY 80-6946 after 6 hrs. Interestingly in models of acquired lapatinib resistance (SKBR3-L and HCC1954-L), treatment with BAY 80-6946 significantly reduced HER3 phosphorylation (Y1289), whilst no similar effect was seen in the SKBR3-TL cells or in models of acquired trastuzumab resistance (SKBR3-T and BT474-RES).

The expression of PI3K-P110-alpha was not significantly affected by BAY 80-6946 treatment in any cell line tested including models of acquired resistance to either trastuzumab and/or lapatinib (not shown). AKT phosphorylation (S473) was significantly reduced in 3/5 cell lines tested (SKBR3, BT474 and MDA-MB-453); however it remained unchanged in HCC1569 and increased in HCC1954 cells (Table 3.3, Figure 3.4). HCC1569 had very high endogenous phosphorylation of AKT (S473) relative to the remaining cell lines, whilst HCC1954 had higher phosphorylation of both SRC kinase (Y416) and STAT3 (Y705) relative to the other cell lines (results not shown). In SKBR3 and BT474 cells which had diminished AKT activation (S473) in response to 6hr BAY 80-6946 treatment, a corresponding decrease in phosphorylation of mTOR (S2481) was observed (Fig 3.4). In the models of acquired resistance AKT

phosphorylation (S473) was reduced in SKBR3-L, -T, -TL but not in HCC1954-L and BT474-RES cells whose AKT phosphorylation remains unchanged.

We found in all models tested that treating cells with 1nM BAY 80-6946 did not result in increases in PARP cleavage or in cleavage of caspase-7, -8, or -9 at 6 hr (results not shown), indicating that BAY 80-6946 does not induce apoptosis in our cells at the concentration tested.

Table 3.3 Percentage changes in protein expression or phosphorylation as calculated from RPPA analysis following treatment of cells with 1nM BAY80-6946 for 6 hours relative to DMSO-treated controls. BAY80-6946 must result in a significant change in protein expression or phosphorylation of greater than 15% relative to untreated control as calculated by Coefficient of Variability to be included. Standard deviations are calculated from triplicate independent results. * indicates a p-value of < 0.05; ** indicates a p-value < 0.01. N/S indicates result is not significant.

Sample	Akt	Akt S473	mTOR	mTOR S2481	HER2	HER2 Y1248	HER3	HER3 Y1289	MAPK-ERK1/2	MAPK T202/Y204
SKBR3	N/S	-25.3 ± 9.7*	N/S	-11.3 ± 3.7*	N/S	N/S	N/S	N/S	N/S	N/S
SKBR3-L	N/S	-41.1 ± 11.8*	N/S	25.5 ± 10.9*	N/S	N/S	N/S	-19.7 ± 10.4*	N/S	N/S
SKBR3-T	N/S	-14.1 ± 9.9*	N/S	N/S	N/S	N/S	N/S	N/S	N/S	76.7 ± 23.0*
SKBR3-TL	N/S	-30.4 ± 10.3**	N/S	-25.8 ± 8.9*	N/S	N/S	N/S	N/S	N/S	N/S
BT474	N/S	-53.8 ± 3.3**	N/S	-43.6 ± 29.9*	N/S	81.1± 25.0*	N/S	N/S	32.9 ± 15.9*	97.2 ± 24.1*
BT474-Res	N/S	N/S	N/S	N/S	N/S	N/S	N/S	-33.8 ± 7.1*	N/S	N/S
HCC1954	N/S	13.6 ± 2.0**	N/S	N/S	N/S	15.4 ± 1.1*	N/S	N/S	15.6 ± 11.2*	23.2 ± 6.6*
HCC1954-L	N/S	N/S	N/S	N/S	N/S	N/S	N/S	-16.4 ± 11.8*	N/S	N/S
HCC1569	N/S	N/S	N/S	N/S	N/S	12.8 ± 5.7*	N/S	N/S	N/S	N/S
MDA-MB-453	N/S	-22.8 ± 15.2*	N/S	N/S	N/S	N/S	N/S	N/S	N/S	27.8 ± 5.2*

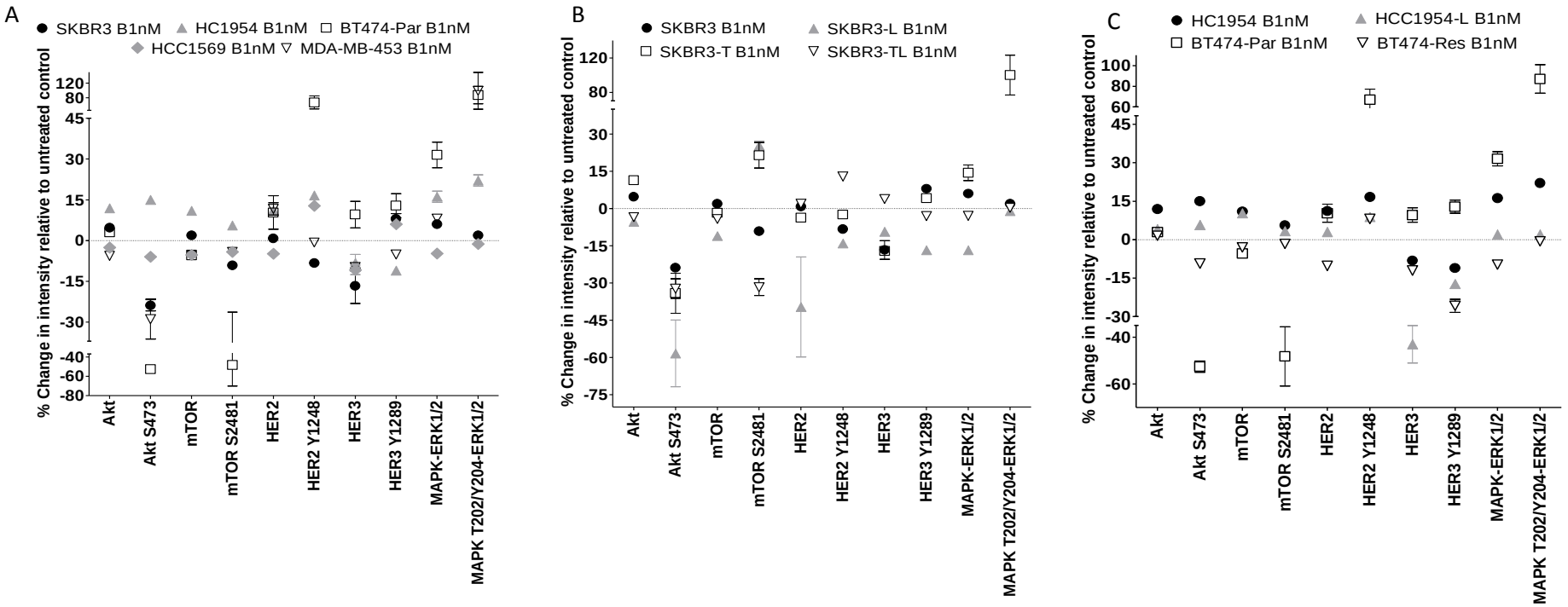

Figure 3.4 Percentage changes in protein expression or phosphorylation as calculated from RPPA analysis following treatment of cells with 1nM BAY80-6946 for 6 hours relative to DMSO-treated controls in A) panel of HER2 positive BC cells, B) SKBR3 parental and resistant models C) HCC1954 and BT474 parental and resistant models. BAY80-6946 must result in a significant change in protein expression o phosphorylation of greater than 15% relative to untreated control as calculated by Coefficient of Variability to be included. Standard deviations are calculated from triplicate independent results.

As described above, MAPK (T202/Y204) phosphorylation was significantly increased in 3 of the 5 parental cell lines following 6 hr treatment with BAY 80-6946 (Fig 3.4). Lapatinib targets EGFR, which activates the MAPK pathway, and we found the addition of lapatinib to BAY 80-6946 to be highly synergistic (Table 3.2). We therefore designed a 30 minute RPPA experiment in the SKBR3 and HCC1954 models and in the matched models of acquired lapatinib resistance to test the hypothesis that the synergy between lapatinib and BAY 80-6946 may in part relate to a lapatinib-mediated MAPK inhibition while BAY 80-6946 inhibits PI3K signalling.

Treatment with BAY 80-6946 for 30 minutes increased MAPK (T202/Y204) and MEK (S217/221) phosphorylation in SKBR3 and SKBR3-L cells, whilst there was an increase in MAPK (T202/Y204) signalling in HCC1954 and HCC1954-L cells (Figure 3.5). BAY 80-6946 alone decreased MEK (S217/221) phosphorylation in HCC1954 cells. Treatment with lapatinib reduced MAPK (T202/Y204) phosphorylation relative to treatment with BAY 80-6946 in all cell lines tested; however it only reduced MEK (S217/221) phosphorylation in the SKBR3-L and HCC1954-L cell lines (Fig 3.5). Finally treatment with the combination of BAY 80-6946 and lapatinib inhibited MAPK (T202/Y204) phosphorylation by BAY 80-6946 but did not reduce further the phosphorylation of either MAPK (T202/Y204) or MEK (S217/221) relative to treatment with lapatinib alone in all cell lines tested (Fig 3.5).

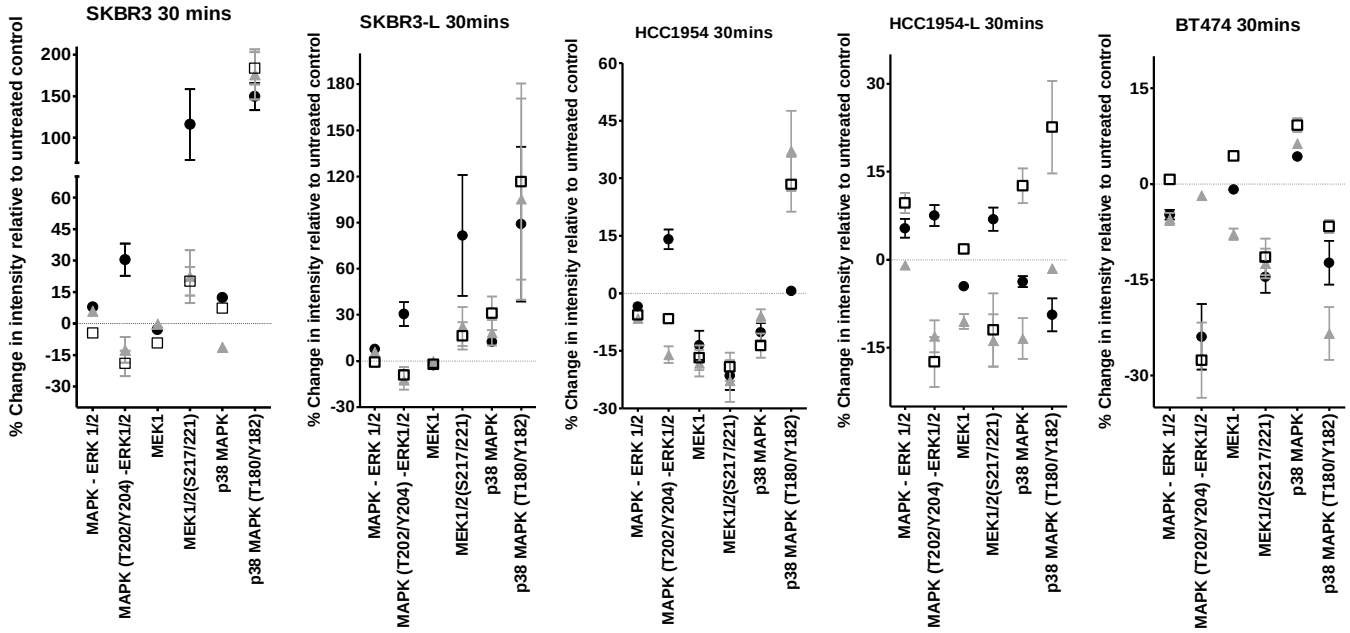

Figure 3.5 Percentage changes in protein expression or phosphorylation as calculated from RPPA analysis following 30 min treatment of cells with '●' -GW4786, Lapatinib at its IC_{50} or '□' a combination (IC_{50} and BAY80-6946 (1 nM) for 30 mins relative to DMSO controls SKBR3 and HCC1954 parental and lapatinib resistant cells and BT474 cells. BAY80-6946 must result in a significant change in protein expression or phosphorylation of greater than 15% relative to untreated control as calculated by Coefficient of Variability to be included. Standard deviations are calculated from triplicate independent results.Standard deviations are calculated using propogation of error from triplicate independent biological experiments.

3.5 PI3K Inhibition does not sensitise *de novo* resistant HER2-positive breast cancer cell lines to HER2 inhibitors

Although the data presented so far show increased benefit for the combination therapy compared with either therapy alone in cells which were sensitive to or had acquired resistance to HER2-inhibitors, the combination of BAY 80-6946 with HER2 inhibition displayed no benefit compared to the PI3K inhibitor alone in HER2-positive cells with innate trastuzumab and lapatinib resistance (Figure 3.6). MDA-MB-453 did not respond to any of the HER inhibitors used in this study when they were tested alone (Table 3.1). While MDA-MB-361 had some response to lapatinib and afatinib, this was much lower than observed in other cell lines (with the exception of MDA-MB-453) (Table 3.1). Both cell lines were however sensitive to the PI3K inhibitor. As neither cell line displayed a meaningful response to HER2-inhibitors, their HER2 status was tested and confirmed by FISH analysis. As the HER2-targeted therapies did not achieve IC_{50}s it was not possible to calculate CI values.

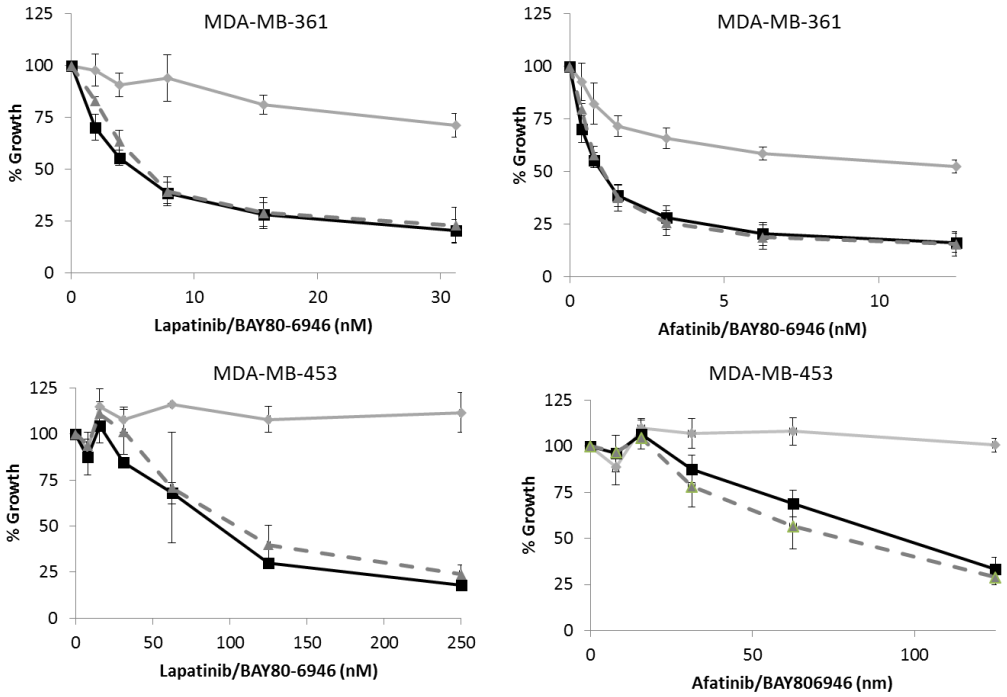

Figure 3.6 Efficacy of lapatinib or afatinib (-◊-), BAY 80-6946 (-□-) and a combination of lapatinib or afatinib with BAY 80-6946 (--Δ--) in MDA-MB-361 and MDA-MB-453 cell lines which have *de novo* resistance to HER2-inhibitors. Acid phosphatase toxicity assays were used to generate dose-response curves of the cells to each of the drugs tested alone and in combination over a 5 day period. Lapatinib:BAY 80-6946 was tested at a 5:1 ratio (top conc for serial dilution 500 nM:100 nM). Afatinib:BAY 80-6946 was tested at a 1:1 Ratio (100 nM top conc for both drugs). Standard Deviations are representative of independent triplicate experiments. As 50% growth inhibition was not achieved by either of the HER inhibitors tested as single agents in either of these cell lines, it was not possible to calculate an IC_{50}. As one of the agents in combination did not achieve an IC_{50} as a single agemt, the Chou-Tallalay method could not be applied to robustly calculate synergy between the two agents in combination. However, the dose response curves for the combination overlap (in the case of MDA-MB-361) with or closely resemble (in he case of MDA-MB-453) the doe response of the PI3K inhibitor alone.

3.6 There is no benefit to scheduling the PI3K inhibitor and the HER family inhibitors 6 hours apart compared to adding the agents simultaneously

BT474 and BT474-Res cells were pretreated with BAY 80-6946 or a HER-targeted therapy (trastuzumab, lapatinib, afatinib, pertuzumab) 6 hours prior to the addition of the other drug. Although the combination remained effective when the anti-PI3K agent and the HER-targeted therapy were scheduled 6 hours apart, there was no benefit to scheduling the treatments apart compared to administering them together (Figure 3.7, Figure 3.8, Figure 3.9, Figure 3.10).

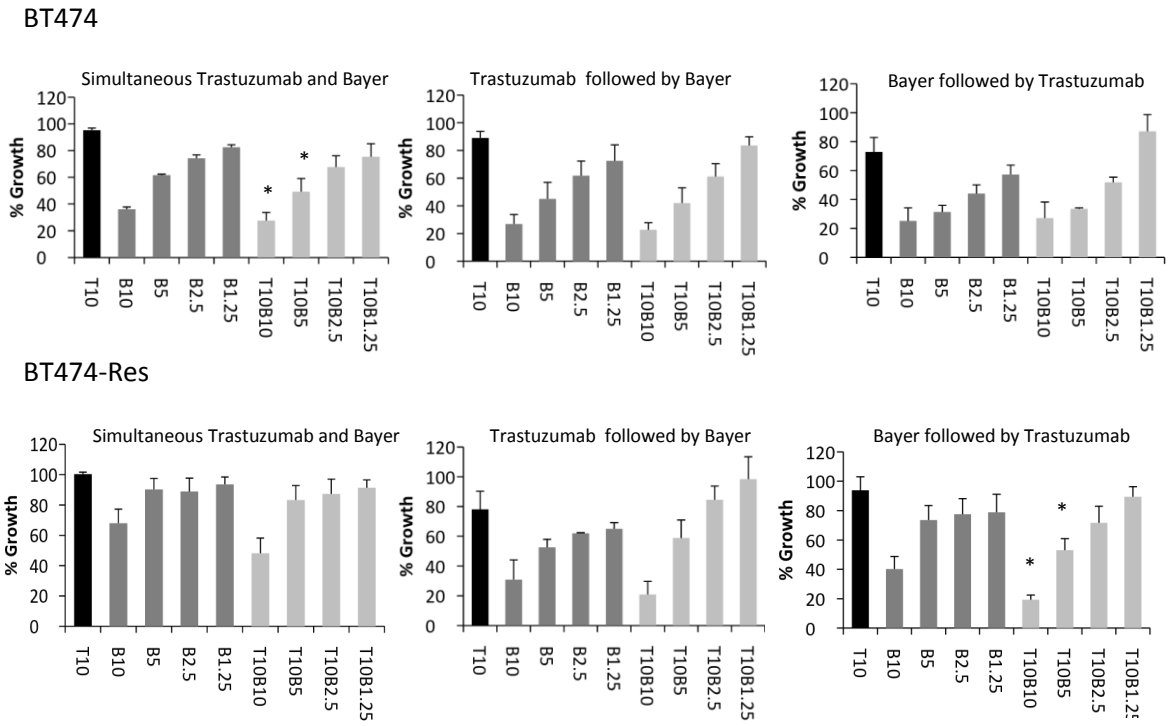

Figure 3.7 The effect of pre-treating BT474 and BT474-Res cells with either BAY 80-6946 or trastuzumab for 6 hours prior to the addition of the other drug, to assess the impact of scheduling of treatment on growth inhibition. Acid phosphatase toxicity assays tested the effect of the drugs on proliferation over a 5 day period. '*' = p-value, 2-tailed, equal variance t-test relative to trastuzumab alone and the corresponding dose of BAY 80-6946 alone. Error bars are representative of standard deviations across triplicate independent experiments.

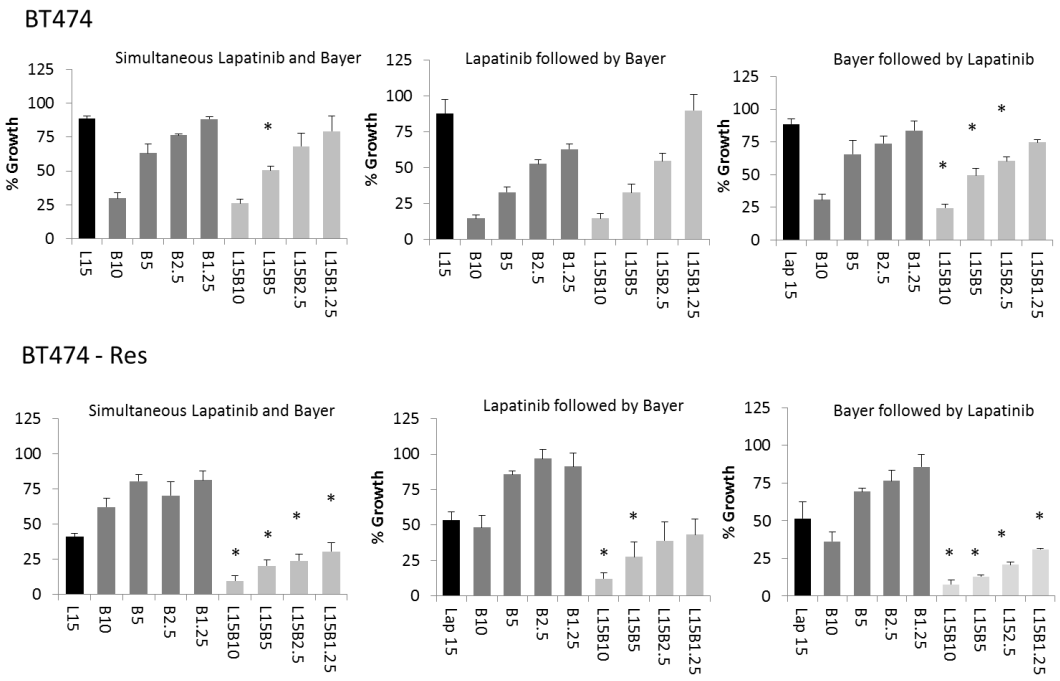

Figure 3.8 The effect of pre-treating BT474 and BT474-Res cells with either BAY 80-6946 or laptinib for 6 hours prior to addition of the other drug, to assess the impact of scheduling of treatment on growth inhibition. Acid phosphatase toxicity assays tested the effect of the drugs on 0.05 by 2-tailed, equal variance ttest relative to trastuzumab alone and the corresponding dose of BAY 80-6946 alone. Error bars are representative of standard deviations across triplicate experiments.

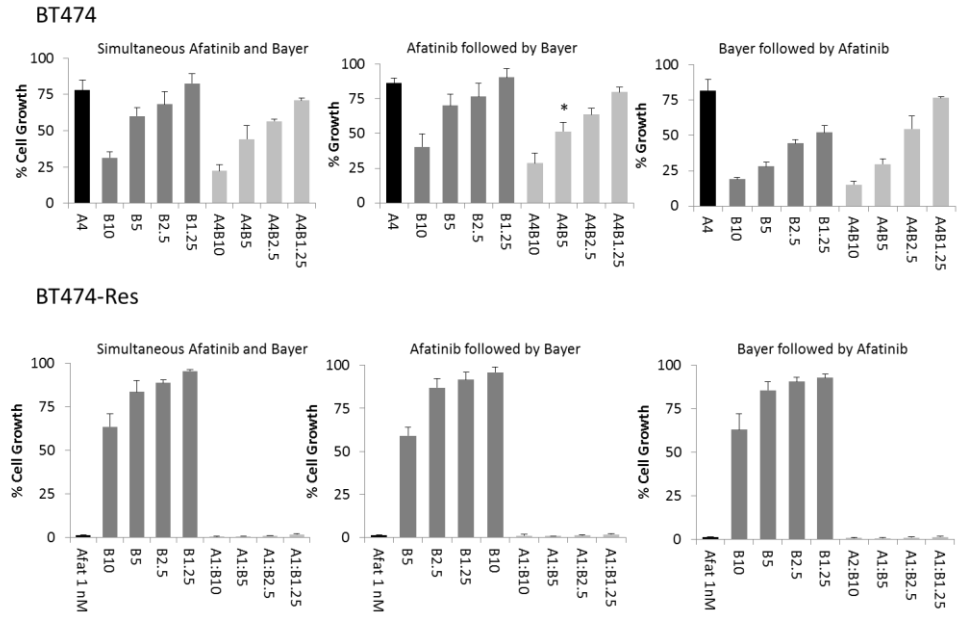

Figure 3.9 The effect of pre-treating BT474 and BT474-Res cells with either BAY 80-6946 or afatinib for 6 hours prior to addition of the other drug, to assess the impact of scheduling of treatment on growth inhibition. Acid phosphatase toxicity assays tested the effe c t of the drugs on proliferatio

0.05 by 2-tailed, equal variance ttest relative to trastuzumab alone and the corresponding dose of BAY 80-6946 alone. Error bars are representative of standard deviations across independent triplicate experiments.

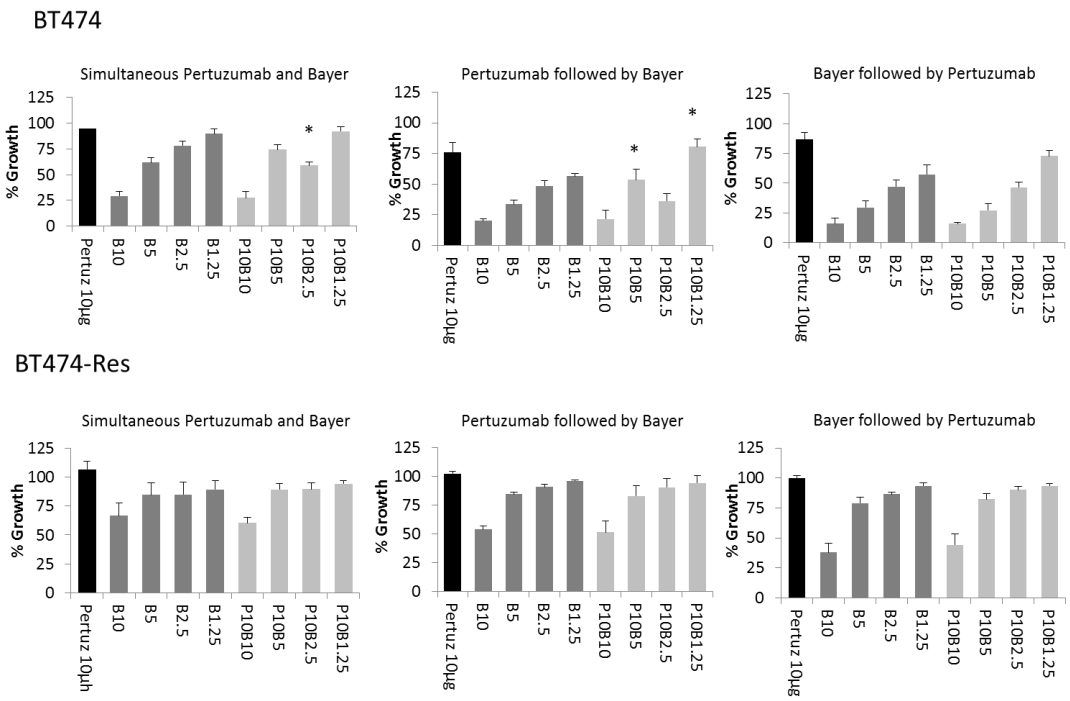

Figure 3.10 The effect of pre-treating BT474 and BT474-Res cells with either BAY 80-6946 or pertuzumab for 6 hours prior to addition of the other drug, to assess the impact of scheduling of treatment on growth inhibition. Acid phosphatase toxicity assays tested the effect of the drugs on

0.05 by 2-tailed, equal variance ttest relative to trastuzumab alone and the corresponding dose of BAY 80-6946 alone. Error bars are representative of standard deviations across independent triplicate experiments.

3.7 Pertuzumab, despite its proven efficacy in the clinic, is ineffective in 2D culture as a single agent and its addition to BAY 80-6946 confers no benefit compared to the PI3K inhibitor alone. It inhibits growth of BT474 and BT474-Res cells when tested in 3D soft agar assays.

We found pertuzumab to be ineffective in all cell lines tested when used alone (Table 3.1), and that the combination of pertuzumab and BAY 80-6946 rarely resulted in improved growth inhibition relative to the PI3K inhibitor alone (Figure 3.13). This lack of *in vitro* efficacy is in striking contrast to clinical data[23].

When tested in 3D culture, pertuzumab treatment results in a statistically significant inhibition of colony forming ability relative to untreated controls (Figure 3.14). BAY 80-6946 treatment and the combination of BAY 80-6946 also resulted in inhibition of 3D colony-forming ability, but there was no significant difference between the inhibition of colony formation achieved by any of the three treatments tested.

Untreated colonies grew outwards and formed a necrotic core, whereas colonies treated with copanlisib looked healthy throughout, likely due to their much smaller size (Figure 3.15). Colonies treated with combination pertuzumab and copanlisib showed increased cellular stress relative to single treatments or control cells (Figure 3.15).

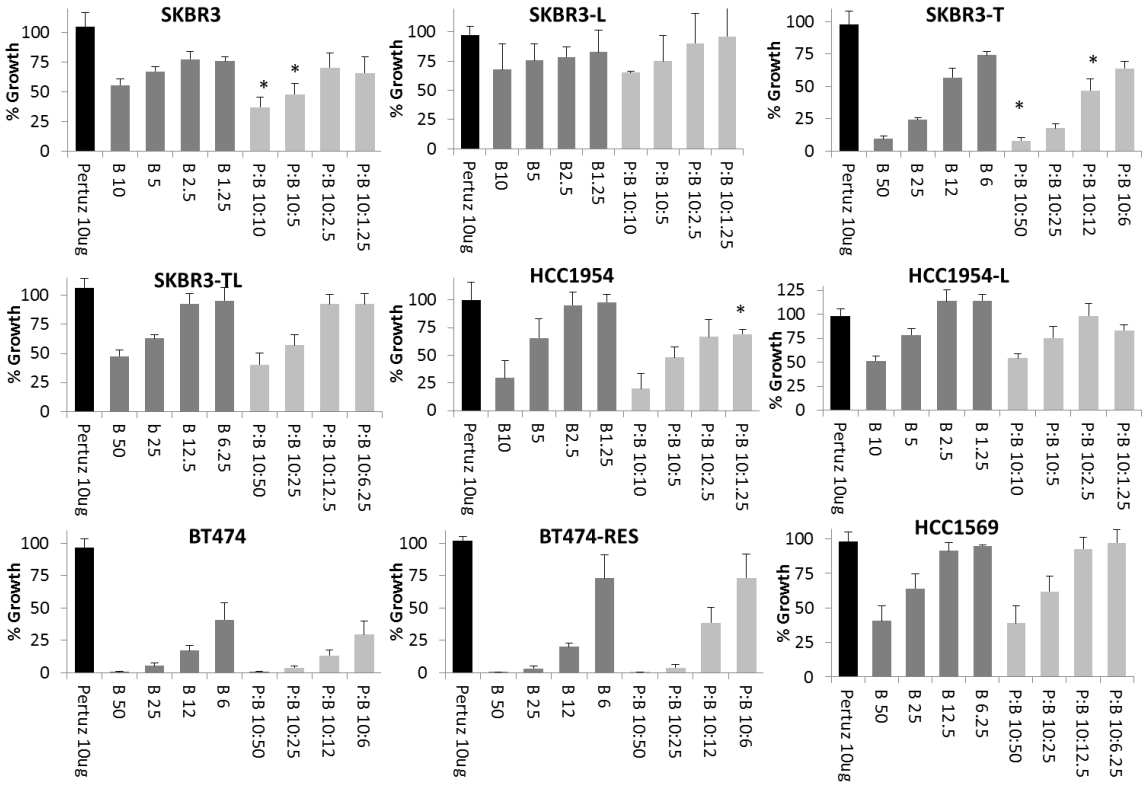

Figure 3.11 The efficacy of combining pertuzumab (P) and BAY 80-6946 (B) in a panel of HER2-positive cell lines including matched models of acquired trastuzumab and/or lapatinib resistance. Acid phosphatase toxicity assays tested the effect of the drugs on proliferation over a 5 day period. Standard Deviations are representative of independe- value < 0.05 as calculated by 2-tailed Student's t-test with equal variance relative to pertuzumab alone and the corresponding dose of BAY 80-6946 tested alone.

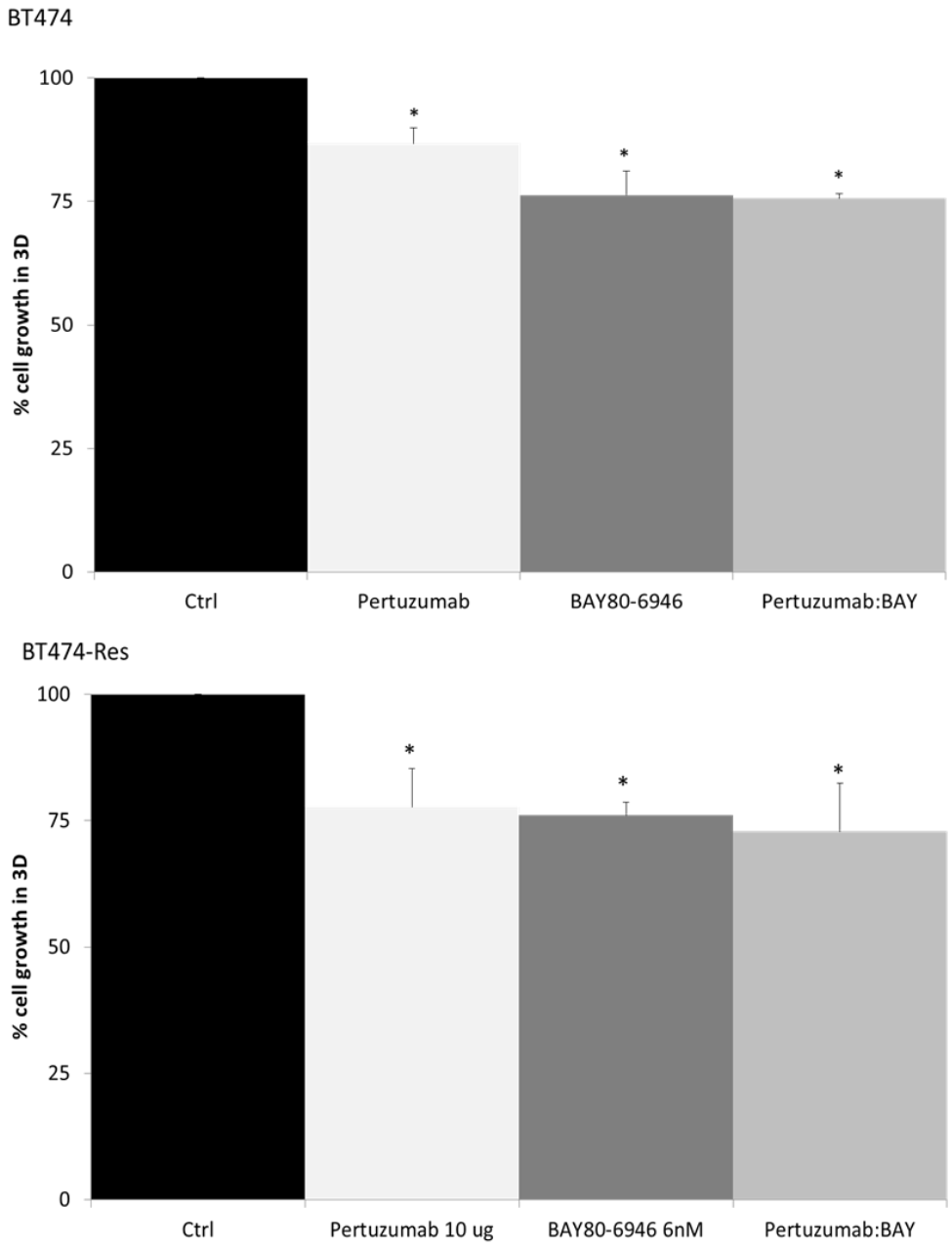

Figure 3.12 Pertuzumab, BAY 80-6946 and the combination of pertuzumab inhibits colony forming ability in a 3D soft agar matrix. Cells were treated, seeded into an agar matrix and left to form colonies for 21 days. Error bars are representative of independent triplicate experiments. * = p < 0.05 as assessed by 2-tailed Student's t-test with equal variance relative to untreated control.

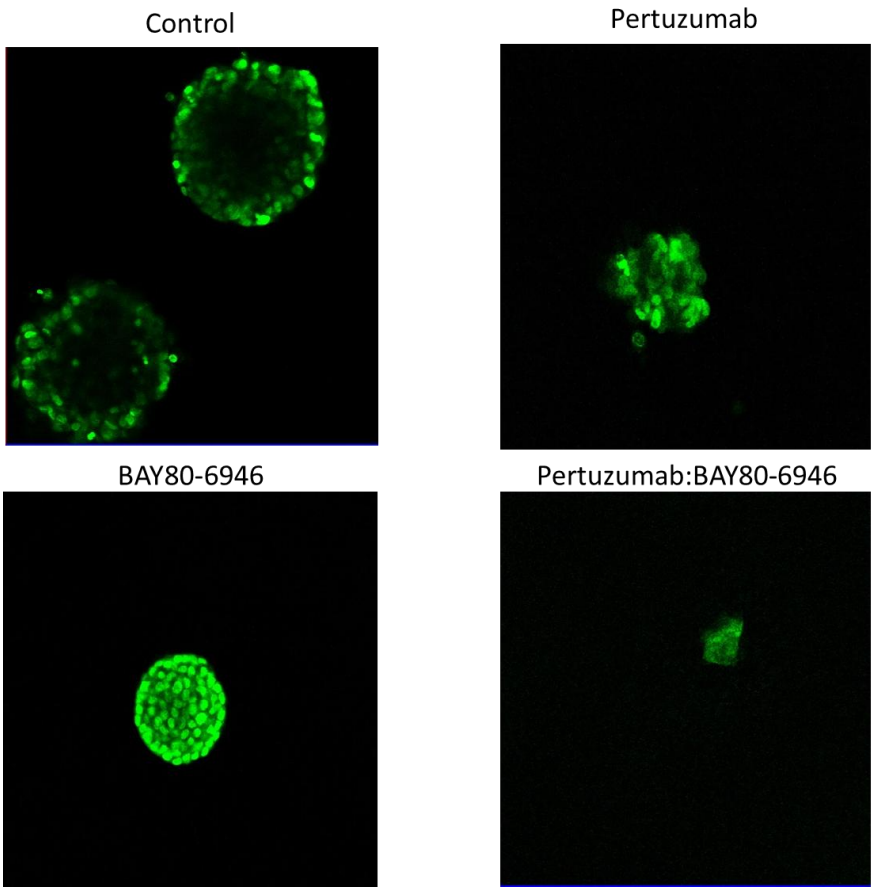

Figure 3.13 Laser scanning microscopy images of BT474 colonies grown in a 3D soft agar matrix for 21 days, stained with Sytox Green (nucleic acid stain) as per manufacturer's protocol and imaged using an LSM 510 confocal microscope (Zeiss).

3.8 BAY 80-6946 inhibits the invasion of HER2-positive breast cancer cell lines

5nM BAY 80-6946 was found to be non-lethal to cells over a 24 hour period using acid phosphatase toxicity assays. MDA-MB-453 and BT474 cells were treated 5nM BAY 80-6946 or DMSO-TFA (vehicle control) for 24 hours. Treatment with BAY 80-6946 significantly decreased invasion in both cell lines (BT474 p = 0.008; MDAMB453 p = 0.008) but had no effect on migration (Figure 3.16).

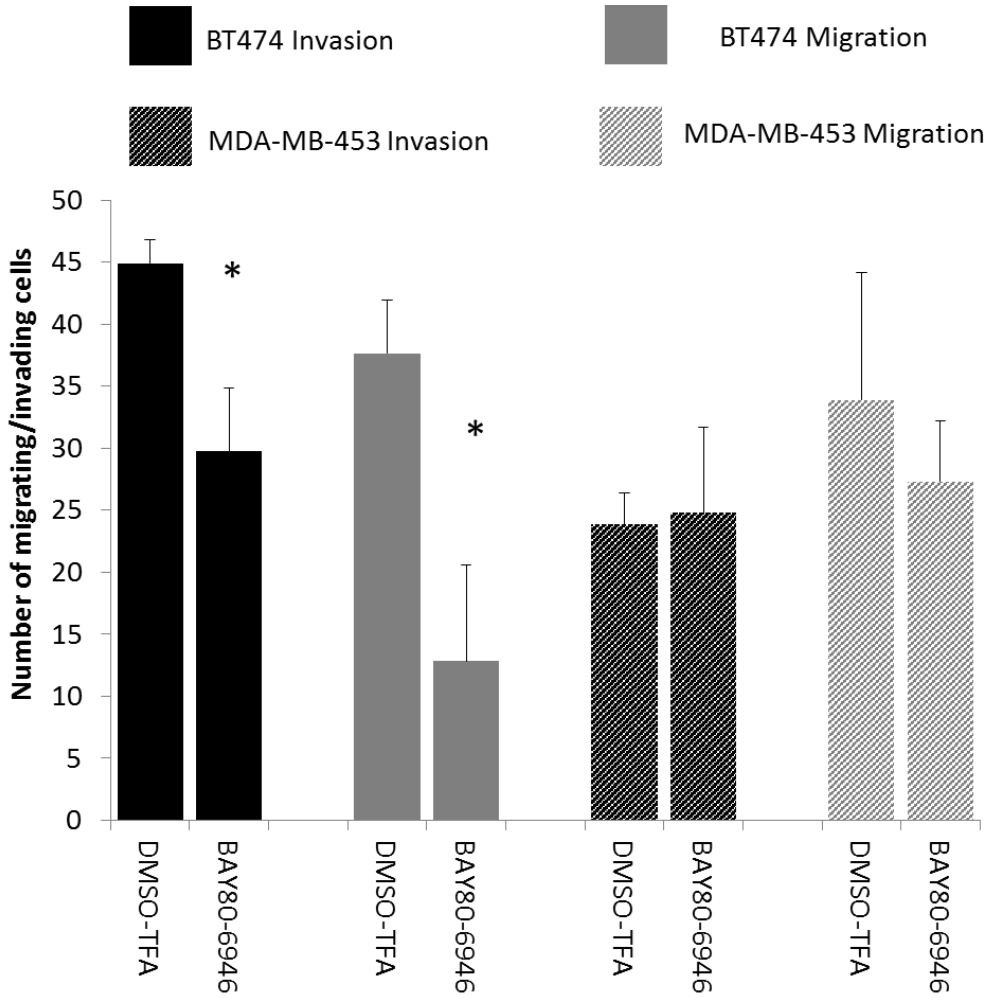

Figure 3.14 5nM BAY 80-6946 (a) inhibits invasion through matrigel and seubsequent migration through a Boyden Chamber containing 8 µM pores or (b) doesn't affect migration of cells through a Boyden Chamber containing 8 µM pores in MDA-MB-453 and BT474 cells over a 24 hour period. Error bars represent standard deviations of triplicate experiments. * p<0.05 relative to DMSO-TFA vehicle control as calculated by 2-tailed Student's t-test with equal variance.

3.9 Discussion

3.9.1 Discussion

Resistance to trastuzumab remains a significant clinical problem, with up to 30 % of patients not responding to it in the metastatic setting[24]. Strong evidence has implicated the PI3K pathway in trastuzumab and lapatinib resistance[13, 14, 25], although data supporting the involvement of PI3K signalling in lapatinib resistance are somewhat conflicting[3, 26]. Preclinical testing of mTOR inhibitors led to anticipation that resistance to HER2 targeted therapies could be overcome, but their clinical benefit has been somewhat disappointing[15], reflected in the results of the Phase 3 BOLERO-3 clinical trial[27]. We therefore hypothesized that targeting PI3K directly would represent a more optimal strategy, and that combined PI3K- and HER2-inhibition may represent an improved treatment strategy for HER2-positive breast cancer.

BAY 80-6946, a novel, potent PI3K inhibitor with *in vitro* and *in vivo* efficacy[17-20] was well-tolerated in a phase I clinical trial[21] and we found it to have anti-proliferative effects in HER2-positive breast cancer cell lines regardless of their PI3K mutational status. We also report that BAY 80-6946 inhibited invasion but had no effect on migration. The PI3K pathway has previously been shown to upregulate invasion[28, 29], a crucial step in metastasis[30]. It is therefore encouraging that in addition to inhibiting proliferation, BAY 80-6946 also inhibited invasion in HER2-positive cell lines, and may also suggest a potential role for BAY 80-6946 in the adjuvant treatment of breast cancer as well as in the metastatic setting.

In our cell line panel we tested BAY 80-6946 at 1nM to observe pure signalling effects, without the signalling interference associated with cell death. BAY 80-6946 did not effectively inhibit AKT phosphorylation in all our cell lines at the concentration tested. However previous reports have indicated that AKT phosphorylation is effectively inhibited in other models of cancer at higher concentrations (200 μmol/L)[18]. We believe that the reduction of PI3K signalling

observed in some, but not all cell lines may thus in part reflect the dose of BAY 80-6946 used in our RPPA signalling experiment (1 nM). In addition, we have previously observed that pharmacokinetics including cellular uptake of kinase inhibitor drugs vary across cell lines and also that PI3K promotes oncogenic activity through both AKT-dependent and AKT-independent mechanisms. However, an elucidation of the exact reason(s) for the reduction of PI3K signalling in some but not all cell lines by BAY 80-6946 is beyond the scope of our study.

In what is arguably the most important observation of this study, we found that combining BAY 80-6946 with the HER2-targeted therapies trastuzumab, lapatinib and afatinib resulted in significantly greater proliferation inhibition relative to testing either drug alone in our panel of cells, including those with acquired resistance to trastuzumab and/or lapatinib. To evaluate BAY 80-6946's potential to restore the efficacy of the HER-targeted therapies in cells with acquired resistance; we compared the IC_{50}'s of lapatinib and afatinib used in combination with BAY 80-6946 against the IC_{50} of lapatinib and afatinib alone. In all cases the IC_{50} of the HER-targeted therapy was less in combination with BAY 80-6946 than as a single agent. In SKBR3-L and HCC1954-L cells, lapatinib when used with BAY 80-6946 achieved an IC_{50} that was similar or less than the IC_{50} of lapatinib used alone in the corresponding parental cell line, indicating that the addition of BAY 80-6946 restores sensitivity to lapatinib. Importantly, combinations of BAY 80-6946 with lapatinib and afatinib were synergistic in all cell lines with acquired resistance to lapatinib and/or trastuzumab, indicating a potential clinical benefit to using combinations of the PI3K inhibitor BAY 80-6946 with HER-targeted agents in patients whose cancers have developed resistance to these HER2-targeted agents.

Although PI3K inhibition has previously been shown to activate HER3[31], possibly attenuating the antitumor effect of some PI3K inhibitors[32], we found that BAY 80-6946 did not activate HER3 phosphorylation in any cell line tested. We did however find that when used alone, BAY 80-6946 activated HER2 phosphorylation. PI3K inhibition has previously been shown to enhance HER signalling resulting in compensatory MAPK signalling in HER2-positive breast cancer[33]. Because we

observed increases in MAPK signalling, in some cases associated with increases in HER2 phosphorylation, after treatment with BAY 80-6946, we hypothesised that combining BAY 80-6946 with lapatinib would overcome this MAPK activation. We report that combining BAY 80-6946 with lapatinib inhibited MAPK (T202/Y204) phosphorylation by BAY 80-6946 and instead resulted in a reduction of MAPK signalling in all cell lines tested (with a parallel reduction in MEK signalling in some models of acquired lapatinib resistance). This finding may underlie, at least in part, the synergy between BAY 80-6946 and HER2 inhibitors, and further supports the argument that PI3K inhibition should be used in combination with HER2-inhibitors.

3.9.2 Summary and Conclusion

In summary, BAY 80-6946 is effective as monotherapy in HER2-positive breast cancer cells including models of acquired resistance to trastuzumab and/or lapatinib. Combinations of BAY 80-6946 with HER2-targeted therapies offer greater benefit than testing these drugs alone and can restore sensitivity to HER2-inhibitors in cells with acquired resistance to trastuzumab and lapatinib. BAY 80-6946 also inhibits the invasion of HER2-positive breast cancer cells. Taken together, our data argue that the addition of the PI3K inhibitor BAY 80-6946 to HER2-targeted therapy should be considered for clinical trial evaluation in patients with HER2-positive breast cancer whose disease has become refractory to HER2-targeted therapies such as trastuzumab or lapatinib.

Chapter 4 Determining the ERBB family and PIK3CA mutational status of HER2-positive breast cancer and their clinical significance

4.1 Introduction

It is well-established that all four known members of the HER family interact with each other and work cooperatively; EGFR positivity is associated with HER2 positivity, HER2 overexpression highly correlated with HER3 overexpression[34], and HER3 activation has been shown to attenuate the activity of therapies targeting HER2[35,36]. We feel therefore that a study of the mutational background of HER2-positive breast cancer should not merely profile ERRB2 itself, but should also examine the mutational status of EGFR (HER1), ERRB3 and ERRB4.

The role of EGFR mutations in lung cancer is well documented[37]. More recently, mutations in other ERBB family members have been reported in breast, gastric and colon cancers. Mutations in the kinase domain of ERBB2 have also been reported to be associated with poorer response to trastuzumab clinically in HER2-positive breast cancer (n = 78) and to confer a more aggressive phenotype *in vitro*, with increased invasion and increased ability to form colonies in soft agar[38]. Further, it has been shown that activating mutations in ERRB2 could increase phosphorylation of EGFR and ERBB3 in breast cancers which were classed as HER2-negative by the standard diagnostic tests, IHC and FISH. A transmembrane domain somatic mutation in ERRB2, V659E, was recently identified in a sporadic lung tumour and was subsequently shown to increase phosphorylation of AKT and p38 MAPK *in vitro*[39]. The rat ERBB2 V664E mutation, which corresponds to human V659E, induces oncogenic transformation *in vivo*[40]. Somatic mutations in ERBB3 have been discovered in 11 % of gastric and colon cancers, and these mutations have oncogenic activity *in vitro* and *in vivo*, when expressed in the presence of HER2[41]. Somatic mutations in ERBB4 have been shown to affect signal transduction[42] and ERBB4 has been shown to be highly mutated in melanoma, where ERBB4 mutations increase ERBB4 kinase activity despite similar expression of the HER4 protein, and sensitise cells to lapatinib [43].

Preclinical evidence argues that PI3K pathway activation induces trastuzumab[26] and lapatinib resistance[3], and that co-targeting PI3K and HER2 potentially represents an improved treatment for patients whose HER2-positive breast cancer has acquired resistance to trastuzumab[22]. It has been reported that somatic PIK3CA mutations are

associated with decreased relapse-free survival (RFS) and overall survival (OS)[44, 45] following treatment with trastuzumab, but other publications suggest PIK3CA mutations are predictive of prognosis only in ER+/HER2- breast cancer[46], and that in HER2-positive breast cancer, the magnitude of trastuzumab benefit may not differ according to PIK3CA genotype[46]. A recent study reported that PIK3CA mutations are associated with decreased benefit to neoadjuvant trastuzumab and lapatinib as measured by pathologic complete response (pCR) rate, but that overall survival (OS) and relapse-free survival (RFS) do not differ between patients with PIK3CA mutated and PIK3CA WT breast cancers[47].

Taken together, these studies suggest a potential role for somatic mutations in the ERBB gene family as well as in other genes of the kinome (including PIK3CA) in the pathogenesis and therapy responsiveness of HER2-positive breast cancer. We hypothesise that mutations in EGFR, ERBB2, ERBB3, ERBB4 and PIK3CA are frequently present in HER2-positive breast cancer, and that these mutations may affect therapy response and outcomes after adjuvant trastuzumab-based therapy.

The objectives of the work described in this chapter were thus to:

1. Identify, validate and determine the frequency of somatic mutations in genes of the kinome including the ERBB family and PIK3CA in HER2-positive breast cancer surgical samples from patients who received adjuvant trastuzumab-based therapy (n = 227)

2. Determine if somatic mutations in ERBB gene family members in HER2-positive breast cancers influence overall survival (OS) and relapse free survival (RFS) times following adjuvant treatment with trastuzumab-based chemotherapy and correlate with clinical and histological features

4.2 Clinical characteristics of patients in our HER2-positive breast cancer surgical sample set

Our sample set was obtained from 227 HER2-positive breast cancer patients at Beaumont Hospital and St Vincent's University Hospital. Tumours were classed as HER2-positive by the relevant hospital's pathology department based on a HER2 IHC score of 3+ or by an IHC score of 2+ combined with FISH-positivity. All surgical samples were reviewed by RCSI Pathology and those confirmed to contain ≥50% tumour were selected for an exploratory next-generation sequencing (NGS) study, and a subsequent mass-spectrometry based Sequenom study.

Tables 4.1, 4.2 and 4.3 summarise histological, clinical and outcomes data for the patients in this sample set. Briefly, our sample set included 56.0 % estrogen receptor (ER) positive and 30.8 % ER-negative tumours. 6.2 % of patients were 35 years or less at diagnosis (an independent predictor of high risk according to the St Gallen consensus panel[48]). 56.8 % patients had tumours greater than 20 mm in size, which is an independent high risk factor[48]. 22.0 % patients were classed as overweight or obese at diagnosis based on body mass index (BMI). Survival data was available for all patients (n = 227).

Table 4.1 Patient age, body mass index (BMI), Eastern Cooperative Oncology Group (ECOG) performance status, and laterality at diagnosis. Healthy (normal) weight is defined as a BMI of 18.5 – 24.9, overweight: BMI 25-29.9, obese: BMI 30. A cut off of 35 years was used for age at diagnosis (in accordance with the St Gallen Consensus Panel). ECOG performance status is a scale used to assess the impact of a disease upon the daily living activities of the patient, with a higher ECOG score generally denoting lower activity levels and fitness.

Age at Diagnosis (median age = 49 years)	**Patients n, %**
≤ 35 years	14, 6.2
≥ 36 years	201, 88.5
Not Available	12, 5.3
BMI	**Patients n, %**
Underweight	0, 0.0
Normal	38, 16.7
Overweight/Obese	50, 22.0
Not Available	139, 61.3
Grade	**Patients n, %**
Grade 1	5, 2.2
Grade 2	71, 31.3
Grade 3	141, 62.1
Not Available	10, 4.4
Laterality	**Patients n, %**
Left	47, 20.7
Right	39, 17.2
Bilateral	2, 0.9
Not Available	139, 61.2
ECOG Status at Diagnosis	**Patients n, %**
ECOG 0	51, 22.5
ECOG 1	35, 15.4
ECOG 2	2, 0.9
Not Available	139, 61.2

Table 4.2 Estrogen receptor (ER), progesterone receptor (PR), lymphovascular invasion (LVI) status, histological subtype and stage at diagnosis data for the HER2-positive breast cancers in our dataset.

ER Status	**Patients n, %**
Positive	127, 56.0
Negative	70,30.8
Not Available	30, 13.2
PR Status	**Patients n, %**
Positive	31, 13.7
Negative	82, 36.1
Not Available	114, 50.2
Grade	**Patients n, %**
Grade 1	5, 2.2
Grade 2	71, 31.3
Grade 3	141, 62.1
Not Available	10, 4.4
Histological Subtype	**Patients n, %**
DCIS	1, 0.4
IDC	189, 83.3
ILC	8, 3.5
Not Available	29, 12.8
T Stage	**Patients n, %**
T0 (no evidence of primary tumour)	4, 1.8
T1 (≤ 20 mm)	62, 27.3
T2 (21 – 50 mm)	104, 45.8
T3 (> 50 mm)	25, 11.0
Not Available	32, 14.1
N Stage	**Patients n, %**
N0	91, 40.1
N1	62, 27.3
N2	30, 13.2
N3	17, 7.5
Not Available	27. 11.9
M Stage	**Patients n, %**
M0	211, 93.0
M1	11, 4.8
Not Available	5, 2.2

At the time of our analysis (median follow up 5 (0 – 25) years), 30 % patients had died and 31.7 % patients had developed recurrent breast cancer in one or more sites. The

majority of patients in our sample set had received chemo and radiotherapy, and trastuzumab was most commonly administered in the adjuvant setting (Table 4.3).

Table 4.3 Treatment and outcome data at a median follow up of 5 (0 – 25) years for patients in our dataset. All patients received trastuzumab as part of their treatment.

Surgery	**Patients n, %**
No Surgery	10, 4.4
Surgery	184, 81.1
Not Available	33, 14.5
Adjuvant trastuzumab-based chemotherapy	**Patients n, %**
None	15, 6.6
Yes	172, 75.8
Not Available	40, 17.6
Neoadjuvant trastuzumab-based chemotherapy	**Patients n, %**
None	75, 33.0
Yes	27, 11.9
Not Available	125, 55.1
Adjuvant anti-hormonal therapy	**Patients n, %**
None	77, 34.0
Yes	132, 58.1
Not Available	18, 7.9
Adjuvant radiotherapy	**Patients n, %**
None	12, 5.3
Yes	155, 68.3
Not Available	60, 26.4
Recurrence	**Patients n, %**
No recurrence	140, 61.7
Recurrence of which first recurrence at 1 Site	45, 19.8
Recurrence of which first recurrence at 2 Sites	13, 5.7
Recurrence of which first recurrence at 3 Sites	7, 3.1
Recurrence of which first recurrence at 4+ Sites	2, 0.9
Not Available	20, 8.8

Recurrence sites, listed in decreasing order of frequency, were liver, locoregional, bone, lung, and brain (Table 4.4), the sites which have been shown previously to be where breast cancer preferentially metastasises[49].

Table 4.4 Sites of recurrence in those 67 patients in our sample set who developed recurrent breast cancer

Site of Recurrence	Patients n, %	Site of Recurrence	Patients n, %
Liver	20, 29.9	Bone	17, 25.4
Lung	19, 28.4	Brain	13, 19.4
Locoregional	18, 26.9	Other	16, 23.9

4.3 Discovery and validation of novel kinome mutations (including in the ERBB family) by next generation kinome sequencing (NGS) and Sequenom MassARRAY analysis

We sequenced 612 genes of the kinome and related genes in 84 FFPE-preserved, HER2-positive breast cancer surgical samples (as well as 27 matched normal tissues) using the Agilent kinome panel and an Illumina MiSeq™ sequencer. Fragments of between 100 and 250 base pairs were size selected and purified prior to library generation and amplification. FASTQ raw data files from the sequencer were QC'ed, trimmed and aligned, and variants were then filtered and called by our bioinformatics collaborators. Any sample with less than 30X coverage (38 % samples) was subsequently excluded from this analysis as it has previously been shown that low coverage can yield false positives and false negatives[50].

We identified a number of genes with hotspots (Table 4.5), genes which contained somatic mutations in the same region across multiple samples. The most frequent of these was in C9orf96, which encodes Serine/threonine kinase-like domain-containing protein (STKLD1), an ATP and nucleotide binding protein. The next most frequently occurring hotspot mutation was in NEK1, which encodes NIMA-related kinase 1, which is involved in cell cycle regulation. Neither C9orf96 nor NEK1 were mutated in TCGA's HER2-positive breast cancer set (n = 120). Although we found these mutations to be absent from our matched normal samples, both mutations occurred in both the 1,000 genome[51] and 6500 exome[52] studies, suggesting that they are germline, as well as having COSMIC IDs, suggesting that they are somatic. The COSMIC IDs for both of these mutations have since been removed. We thus hypothesise that these mutations are likely germline, but that further study is needed

into the nature f these mutations and whether this varies across populations. Further study may also be needed into whether the same NGS methods can be used to sequence cancerous and normal tissue. However, both of these questions are beyond the scope of our studies. PIK3CA, encoding the catalytic subunit of PI3K, was one of the most commonly mutated genes in our sample set, with an overall somatic mutation rate of 20.83% in this NGS study (including hotspot mutations), a lower rate than reported by TCGA (31 %), but similar to previous publications that reported rates of 21.3% (n=80)[44] and 23 % (n = 355)[47].

Table 4.5 The identity, Ensembl ID and chromosome location of those genes in which mutations were most frequently identified in our kinome study (n = 84), with the amino acid change, functional domain and frequency of all mutations in the gene in question and of the most common mutations in each gene. Chr = chromosome. DNA was extracted from 84 FFPE HER2-positive breast cancer clinical samples and sequenced using the Agilent 612-gene SureSelect™ plan Illumina MiSeq™.

Gene	Ensembl ID	Chr	Total Mutation Frequency n, %	Most Common Mutation	Domain of Mutation	Frequency n, %
C9orf96	ENSG198870	9	8, 9.5	R568Q	Function Unknown	7, 87.5
TRIM24	ENSG122779	7	5, 6.0	R1009S	Function Unknown	4, 80.0
NEK1	ENSG137601	4	6, 7.1	E655G	Function Unknown	6, 75.0
DGKZ	ENSG149091	11	3, 3.6	A10D	Function Unknown	3, 75.0
PIK3CA	ENSG121879	3	4, 4.8	I391M	C2	4, 40.0
PIK3CA	ENSG121879	3	4, 4.8	E524K	Helical	3, 30.0

PIK3CA was mutated in 10 different cases, with I391M the most frequent PIK3CA mutation in our sample set based on NGS. I391M was not reported in TCGA's HER2-positive breast cancer database, unlike PIK3CA E542K, which had a frequency of 4.2 % in TCGA and 6.25 % in our sample set. 8 genes from the PI3K pathway were mutated in this HER2-positive breast cancer sample set (Table 4.6). These genes encode subunits of PI3K, the PIP second messengers, the PI3K inhibitory protein PTEN, and the downstream effectors mTOR and p53. Several MAPK pathway genes were also mutated in this sample set (Table 4.7), with the mutated genes encoding

activating ligands (e.g. EGFR) or kinases involved in the MAPK signalling cascade. Many of our samples had mutations in both the PI3K and MAPK pathways (Figure 4.1). In fact, MAPK pathway mutations more commonly co-occured with PI3K pathway mutations than alone (Figure 4.1). In our kinome study, 14 tumours had PI3K pathway mutations but WT MAPK genes, 4 had mutations in the MAPK pathway but WT PI3K pathway genes, 19 were WT for both and 11 had mutations in both.

Table 4.6 The identity, Ensembl ID and chromosome locations of genes involved in the PI3K pathway which were mutated in our kinome study (n = 84), and the type, functional domain, frequency and amino acid consequence of each mutation. Chr = chromosome; ND = nonframeshift deletion; FI = frameshift insertion; NSNV = nonsynonymous single nucleontide variation; FD = frameshift deletion; SGSNV = stopgain single nucleotide variation. DNA was extracted from 84 FFPE HER2-positive breast cancer clinical samples and sequenced using the Agilent 612-gene SureSelect™ panel and an Illumina MiSeq™.

Gene	Ensembl ID	Chr	Mutation	Domain of Mutation	Type	Frequency n, %
PIK3C2A	ENSG11405	11	1596_1605del	C2	ND	1, 1.2
PIK3C2G	ENSG139144	12	F64fs	Function Unknown	FI	1, 1.2
PIK3C2G	ENSG139144	12	H1058fs	Kinase	FD	1, 1.2
PIK3CA	ENSG121879	3	C604R	Helical	NSNV	1, 1.2
PIK3CA	ENSG121879	3	H1047R	Kinase	NSNV	1, 1.2
PIK3CA	ENSG121879	3	G1049R	Kinase	NSNV	1, 1.2
PIK3CA	ENSG121879	3	I391M	C2	NSNV	4, 4.8
PIK3CA	ENSG121879	3	E542K	Helical	NSNV	3, 3.6
PIK3R1	ENSG145675	5	219_221del	RhoGAP	ND	1, 1.2
PIK3R4	ENSG196455	3	G1206D	Function Unknown	NSNV	1, 1.2
PIK3R4	ENSG196455	3	P761S	Function Unknown	NSNV	1, 1.2
PIK3R4	ENSG196455	3	N574S	Function Unknown	NSNV	1, 1.2
PTEN	ENSG171862	10	H141P	Phosphataase	NSNV	1, 1.2
PTEN	ENSG171862	10	319_320del	PTEN C2	FD	1, 1.2
TP53	ENSG141510	17	F209fs	DNA-binding domain	FD	1, 1.2
TP53	ENSG141510	17	R205L	DNA-binding	NSNV	1, 1.2
TP53	ENSG141510	17	R141H	DNA-binding	NSNV	1, 1.2
TP53	ENSG141510	17	E126K	DNA-binding	NSNV	1, 1.2
TP53	ENSG141510	17	122_124del	DNA-binding	FD	1, 1.2
TP53	ENSG141510	17	R116Q	DNA-binding	NSNV	1, 1.2
TP53	ENSG141510	17	G113V	DNA-binding	NSNV	1, 1.2
TP53	ENSG141510	17	91_92del	DNA-binding	FD	1, 1.2
TP53	ENSG141510	17	R64X	Function Unknown	SGSNV	1, 1.2
TP53	ENSG141510	17	C9G	P53 transactivation motif	NSSNV	1, 1.2
TP53	ENSG141510	17	S88F	Function Unknown	NSSNV	1, 1.2
TP53	ENSG141510	17	E12fs	P53 transactivation motif	FD	1, 1.2

TP53	ENSG141510	17	H47R	Function Unknown	NSNV	2, 2.4
mTOR	ENSG198793	1	E2181Q	Rapamycin binding	NSNV	1, 1.2
mTOR	ENSG198793	1	A519T	Function Unknown	NSNV	1, 1.2

Table 4.7 The identity, Ensembl ID and chromosome locations of genes involved in the MAPK pathway which were mutated in our kinome study (n = 84), and the type, functional domain, frequency and amino acid consequence of each mutation. DNA was extracted from 84 FFPE HER2-positive breast cancer clinical samples and sequenced using the Agilent 612-gene SureSelect™ panel Illumina HiSeq™. Chr = chromosome; ND = nonframeshift deletion; NSNV = nonsynonymous single nucleotide variation; FD = frameshift deletion; FI = frameshift insertion; NI = nonframeshift insertion.

Gene	Ensembl ID	Chr	Mutation	Domain of Mutation	Type	Frequency n, %
EGFR	ENSG146648	7	903_909del	Kinase	ND	1, 1.2
MAP2K1	ENSG169032	15	G392V	Functionally Unannotated	NSNV	1, 1.2
MAP2K4	ENSG65559	17	K357fs	Kinase	FD	1, 1.2
MAP3K1	ENSG95015	5	T457fs	Functionally Unannotated	FI	1, 1.2
MAP3K1	ENSG95015	5	A887fs	Functionally Unannotated	FD	1, 1.2
MAP3K1	ENSG95015	5	S1002fs	Functionally Unannotated	FI	1, 1.2
MAP3K19	ENSG176601	2	464_474del	Functionally Unannotated	FD	1, 1.2
MAP3K19	ENSG176601	2	R163I	Functionally Unannotated	NSNV	1, 1.2
MAP3K5	ENSG197442	6	P987delinsPD	Functionally Unannotated	NI	4, 4.8
MAPK13	ENSG73803	6	R354W	Functionally Unannotated	NSNV	1, 1.2
MAPK15	ENSG180815	8	T221K	Kinase	NSNV	1, 1.2
MAPK3	ENSG102882	16	162_172del	Kinase	ND	1, 1.2
MAPK6	ENSG69956	15	489_490del	Functionally Unannotated	ND	1, 1.2
MAPK6	ENSG69956	15	H683N	Functionally Unannotated	NSNV	1, 1.2

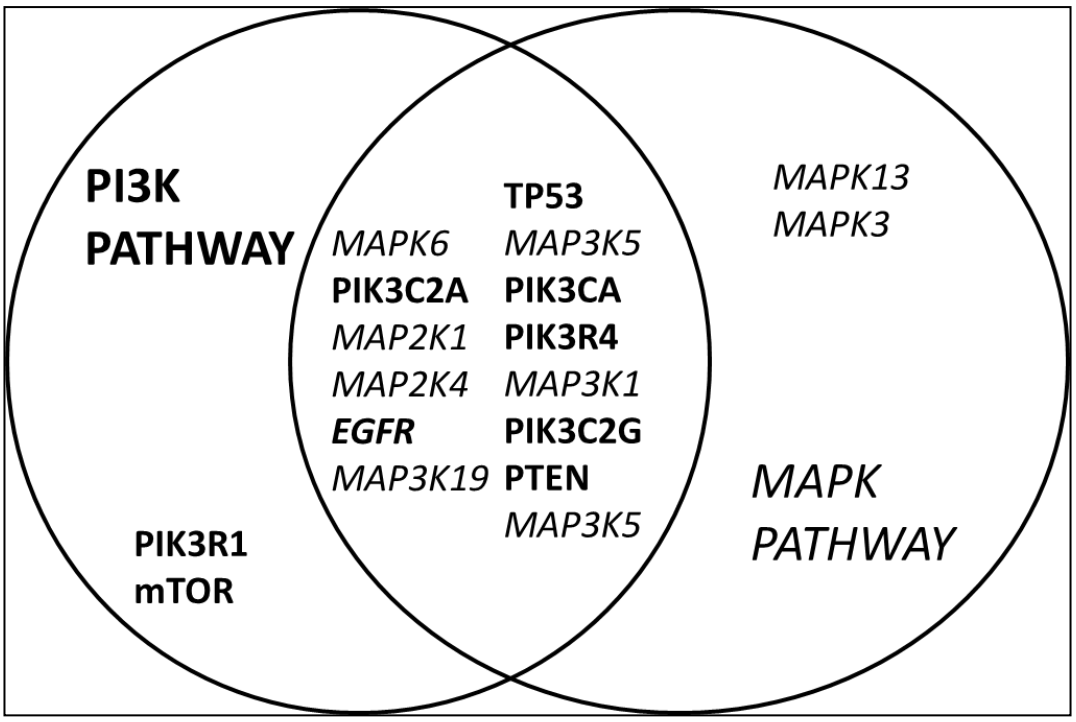

Figure 4.1 Genes from the PI3K (bold) and MAPK (italics) pathways in which mutations occurred separately or together with mutations in the other pathway in our kinome sequencing study. DNA was extracted from 84 FFPE HER2-positive breast cancer clinical samples and sequenced using the Agilent 612-gene S u r e S e l e c t ™ p m á m e a l M á r S d e q á ™ n I l l u

We designed this project to discover if ERBB family mutations were present in HER2-positive breast cancers, and their role in resistance to HER2-targeted therapy. We discovered 10 mutually exclusive somatic mutations in ERBB family genes in our NGS study as follows: 5 EGFR mutations, 1 ERBB2 mutation, 2 ERBB3 mutations and 2 ERBB4 mutations (Table 4.9). EGFR R836C had a reported frequency of 0.00154 in the 6500 exome study. None of the other mutations were reported in the 1000 genome[53] or the 6,500 exome studies[52] further suggesting they are somatic, rather than germline mutations. These mutations occurred in the ligand-binding domains, kinase domain, or the furin-like domains, which are involved in receptor aggregation. We also found 5 somatic PIK3CA mutations (Table 4.8) in the helical, kinase and C2 domains.

Table 4.8 Genes of the ERBB family and PIK3CA, with their Ensembl ID and chromosome location, in which we discovered somatic variants in our kinome study (n=84), along with the amino acid consequence, type, functional domain and frequency of each mutation, and whether the mutation was subsequently confirmed by Sequenom. N/A = not applicable as Sequenom cannot detect deletions (in the case of EGFR) or the panel did not contain that particular mutation (PIK3CA). NSNV = nonsynonymous single nucleotide variation; ND = nonframeshift deletion; SGSNV = stopgain single nucleotide variation

Gene	Ensembl ID	Chromosome	Mutation	Domain of mutation	Type	Frequency n, %	Confirmed by Sequenom
EGFR	ENSG146648	7	R836C	Kinase	NSNV	1, 1.2	NO
			903_909del	Kinase	ND	1, 1.2	N/A
			V398I	Ligand-binding	NSNV	1, 1.2	NO
			T273S	Kinase	NSNV	1, 1.2	NO
			1182_1184del	Cytosolic Tail	ND	1, 1.2	NO
ERBB2	ENSG141736	17	P1089S	Functionally Unannotated	NSNV	1, 1.2	NO
ERBB3	ENSG65361	12	S505F	Furin-like	NSNV	1, 1.2	NO
			158_167del	Ligand-binding and Furin-like	ND	1, 1.2	NO
ERBB4	ENSG178568	2	R81X	Ligand-binding	SGSNV	1, 1.2	NO
			G599W	Furin-like	NSNV	1, 1.2	YES
PIK3CA	ENSG121879	3	E542K	Helical	NSNV	3, 3.6	YES
			G1049R	Kinase	NSNV	1, 1.2	YES
			C604R	Helical	NSNV	1, 1.2	N/A
			H1047R	Kinase	NSNV	1, 1.2	YES
			I391M	C2	NSNV	4, 4.8	N/A

Having discovered a set of somatic ERBB family and PIK3CA mutations, we then moved to validate them using the highly sensitive Sequenom MassARRAY platform in 227 HER2-positive breast cancers using a panel designed to detect the ERBB family mutations identified in our kinome sequencing study, as well as a wide range of other cancer-associated somatic ERBB family mutations published in the literature[41, 42, 54] or found in the TCGA database.

Ultimately only one somatic ERBB mutation from our kinome sequencing study was validated by sequenom's more sensitive technology, that being ERBB4 G599W.

Our sequenom analysis identified 12 somatic mutations in the ERBB family, which break down as follows: (Table 4.10) 3 EGFR mutations, 1 ERBB2 mutation, 3 ERBB3 mutations, and 5 ERBB4 mutations. 16/227 (7.05 %) of our samples thus contained somatic HER family mutations, which in all cases were mutually exclusive with each other. These mutations occurred in the kinase and furin-like domains of the ERBB genes, and our Sequenom study mutations were not detected in the 1,000 genome study or the 6,500 exome study. Two mutations, ERBB3 Q809R and ERBB4 S303F, occurred in more than one sample and thus are hotspot mutations. Three of these mutations were reported in the cancer genome atlas (TCGA); an EGFR mutation (V769L) in lung adenocarcinoma, an ERBB3 mutation (E928G) which was found in both invasive breast carcinoma and colon cancer, and an ERBB4 mutation (S303F) found in both invasive breast and uterine carcinoma.

60/227 or 26.43 % of our samples contained somatic PIK3CA mutations. The most frequent mutation was H1047R, which occurred in 13 % of samples (Table 4.10). Many of the PIK3CA mutations we report here were not reported in either the 1,000 genome or the 6,500 exome study (Table 4.10). ERBB family and PIK3CA somatic mutations co-occurred in 3/227 (1.32 %) samples, with the specific co-occurring mutations being EGFR A839D with PIK3CA E545D, ERBB3 Q809R with PIK3CA E545D, and ERRB3 Q809R with PIK3CA H1047R.

Table 4.9 The identity and properties of somatic ERBB family mutations discovered in our sequenom study in 227 HER2-positive breast cancers. A low AVSIFT value predicts that a mutation is likely to be deleterious. Mutation Assessor is a bioinformatics tool which predicts the likely effect of a mutation. All ERBB family mutations listed here were confirmed somatic by sequencing matched normal DNA. N/A = not available

Gene/Mutation	Frequency n, %	Domain	AVSIFT Value	Predicted Effect (Mutation Assessor)	Identified in TCGA HER2-positive breast cancer study (n = 120)	COSMIC ID
EGFR V769L	1, 0.44	Kinase	0.24	Tolerated but probably damaging	Not Reported	6242
EGFR A839T	1, 0.44	Kinase	0	Deleterious, probably damaging	Not Reported	13430
EGFR K846R	1, 0.44	Kinase	0.03	Deleterious, borderline damaging/benign	Not Reported	13431
HER2 H878Y	1, 0.44	Kinase	0.03	Deleterious, probably damaging	Not Reported	21985
HER3 P262H	1, 0.44	1st furin-like	N/A	NA	Not Reported	NA
HER3 Q809R	3, 1.32	Kinase	N/A	NA	Not Reported	NA
HER3 E928G	1, 0.44	Kinase	0	Deleterious, probably damaging	Not Reported	94228, 1363010
HER4 S303F	3, 1.32	1st furin-like	0	Deleterious, probably damaging	Not Reported	NA
HER4 V721I	1, 0.44	Kinase	N/A	NA	Not Reported	NA
HER4 G599W	1, 0.44	2nd furin-like	0	Deleterious, probably damaging	Not Reported	NA
HER4 D595G	1, 0.44	2nd furin-like	0.27	Tolerated, possibly damaging	Not Reported	1405173
HER4 K935R	1, 0.44	Kinase	0.1	Tolerated, benign	Not Reported	1405163
All ERBB Mutations	16, 7.05					

Table 4.10 The identity, frequency and properties of somatic PIK3CA mutations discovered in our sequenom study (n = 227) in HER2-positive breast cancers. A low AVSIFT value predicts that a mutation is likely to be deleterious. Mutation Assessor is a bioinformatics tool which predicts the likely effect of a mutation. ALL PIK3CA mutations listed here were confirmed somatic by sequencing matched normal DNA. N/A = not available

Mutation	Domain	Frequency n, %	AVSIFT	Predicted Effect (Mutation Assessor)	Identified in TCGA HER2-positive breast cancer study	COSMIC ID
R88Q	p85 binding	1, 0.44	0.19	Tolerated	Not Reported	COSM746
H1047R	Kinase	33, 14.54	0.06	Deleterious, possibly damaging	10/120, 8.3 %	COSM775
E542K	Helical	10, 4.41	0.04	Deleterious, possibly damaging	5/120, 4.2 %	COSM760
N345K	C2	3, 1.32	0.09	N/A	Not Reported	COSM754
E545D	Helical	2, 0.88	0.29	Tolerated	Not Reported	COSM765
M1043V	Kinase	1, 0.44	0.01	Deleterious, Damaging	Not Reported	COSM12591
E545K/G	Helical	2, 0.88	N/A	N/A	Not Reported	Not Available
E545K	Helical	5, 2.20	0.25	Tolerated	9/120, 7.5 %	COSM763
A1035V	Kinase	1, 0.44	0.02	Deleterious, Damaging	Not Reported	COSM17445
G1049R	Kinase	1, 0.44	0.15	Tolerated	Not Reported	COSM12597
M1043I	Kinase	1, 0.44	1	Tolerated	1/120, 0.8 %	COSM773
All PIK3CA Mutations		60, 26.43				

4.4 Correlation of ERBB family and PIK3CA somatic mutations with histological and clinical features and with survival outcomes following trastuzumab-based therapy

The presence of ERBB family or PIK3CA mutations did not correlate with clinicopathological features such as ER and PR status, or age at diagnosis (Table 4.11, Table 4.12), although the low numbers in our test groups (especially for ERBB mutations) preclude confidently drawing conclusions. As the PI3K pathway is downstream of HER2, we decided to group PIK3CA mutations with ERBB family mutations and analyse them together. Table 4.13 groups patients which had a mutation in either PIK3CA or the ERBB family, and grouping these mutations and analysing both together did not alter trends or significance regarding correlation with clinical features.

Table 4.11 Correlation between ERBB family mutations and clinical/pathological features at diagnosis / surgery - square calculat test as appropriate. ER = estrogen receptor; PR = progesterone receptor; LVI = lymphovascular invasion; BMI = body mass index; WT = wild type

Variable		WT Patients n (%)	MUT Patients n (%)	P value
ER Status	Negative	70 (35.7)	6 (46.2)	0.5536
	Positive	126 (64.3)	7 (53.8)	
PR status	Negative	75 (72.2)	7 (77.8)	1.000
	Positive	29 (27.8)	2 (22.2)	
LVI	Negative	64 (36.8)	6 (42.9)	0.7751
	Positive	110 (63.2)	8 (57.1)	
Grade	Grade 1	4 (2.1)	1 (6.7)	0.4033
	Grade 2	60, (31.8)	6 (40.0)	
	Grade 3	125 (66.1)	8 (53.3)	
BMI	Healthy	21 (32.3)	1 (14.3)	0.4270
	Overweight	44 (67.7)	6 (85.7)	
T Stage	T1	59 (33.3)	3 (21.4)	0.6969
	T2	94 (53.1)	10 (71.4)	
	T3	24 (13.6)	1 (7.2)	
N stage	N0	85 (46.4)	6 (42.8)	0.7582
	N1	58 (31.8)	4 (28.6)	
	N2	28 (15.3)	2 (14.3)	
	N3	12 (6.5)	2 (14.3)	
Age at Diagnosis	≤ 35 years	14, (7.0)	0, (0.0)	0.6053
	≥ 36 years	186 (93.0)	15 (100.0)	
	≤ 50 years	103 (49.8)	9 (60.0)	0.5880
	≥ 51 years	104 (50.2)	6 (40.0)	
M Stage	M0	197 (95.2)	14 (93.3)	0.5453
	M1	10 (4.8)	1 (6.7)	

Table 4.12 Correlation between PIK3CA mutations and clinical/pathological features at diagnosis/surgery - square calculat test as appropriate. ER = estrogen receptor; PR = progesterone receptor; LVI = lymphovascular invasion; BMI = body mass index; WT = wild type.

Variable		WT Patients	MUT Patients	P value
ER Status	Negative	54 (36.2)	16 (33.3)	0.8625
	Positive	95 (63.8)	32 (66.7)	
PR status	Negative	64 (64.3)	18 (64.3)	0.3289
	Positive	21 (35.7)	10 (35.7)	
LVI	Negative	52 (36.3)	18 (39.1)	0.8609
	Positive	90 (63.4)	28 (60.9)	
Grade	Grade 1	4 (2.6)	1 (2.0)	0.5422
	Grade 2	47 (30.3)	19 (38.8)	
	Grade 3	104 (67.1)	29 (59.2)	
BMI	Healthy	16 (40.0)	6 (40.0)	0.3676
	Overweight	41 (60.0)	9 (60.0)	
T Stage	T1	21 (43.8)	21 (43.8)	0.1627
	T2	22 (45.8)	22 (45.8)	
	T3	5 (10.4)	5 (10.4)	
N stage	N0	66 (44.3)	25 (52.1)	0.5372
	N1	51 (34.2)	11 (22.9)	
	N2	22 (14.8)	8 (16.7)	
	N3	10 (6.7)	4 (0.3)	
Age at Diagnosis	≤ 35 years	11 (6.7)	3 (5.8)	1.0000
	≥ 36 years	152 (93.3)	49 (94.2)	
	≤ 50 years	84 (49.7)	25 (47.2)	1.0000
	≥ 51 years	85 (50.3)	28 (52.8)	
M Stage	M0	161 (95.3)	50 (94.3)	0.7265
	M1	8 (4.7)	3 (5.7)	

Table 4.13 Correlation between ERBB/PIK3CA mutations and clinical/pathological features at diagnosis / surgery - square calculat test as appropriate. ER = estrogen receptor; PR = progesterone receptor; LVI = lymphovascular invasion; BMI = body mass index; WT = wild type

Variable		WT Patients	MUT Patients	P value
ER Status	Negative	54 (36.5)	22 (36.1)	1.0000
	Positive	94 (63.5)	39 (63.9)	
PR status	Negative	57 (75.3)	2, (67.6)	0.5010
	Positive	19 (24.7)	12 (32.4)	
LVI	Negative	46 (35.9)	18 (40.0)	0.6291
	Positive	82 (64.1)	28 (60.0)	
Grade	Grade 1	3 (2.6)	2 (3.1)	0.3246
	Grade 2	41 (30.3)	25 (39.1)	
	Grade 3	96 (67.1)	37 (57.8)	
BMI	Healthy	15 (30.0)	7 (31.8)	1.0000
	Overweight	35 (70.0)	15 (78.2)	
T Stage	T1	38 (27.7)	24 (38.7)	0.2633
	T2	72 (55.4)	32 (51.6)	
	T3	19 (13.5)	6 (9.6)	
N stage	N0	60 (44.3)	31 (50.0)	0.4408
	N1	47 (34.2)	15 (24.2)	
	N2	20 (14.8)	10 (16.2)	
	N3	8 (6.7)	6 (9.6)	
Age at Diagnosis	≤ 35 years	11 (7.4)	3 (4.5)	0.5567
	≥ 36 years	137 (92.6)	64 (95.5)	
	≤ 50 years	83 (47.7)	35 (53.8)	0.3876
	≥ 49 years	91 (52.3)	30 (46.2)	
M Stage	M0	147 (95.5)	64 (94.1)	1.0000
	M1	7 (4.5)	4 (5.9)	

We found no significant correlation between ERBB family and/or PIK3CA mutations and survival in all patients (Figure 4.2) or after adjuvant trastuzumab-based therapy (Figure 4.3).

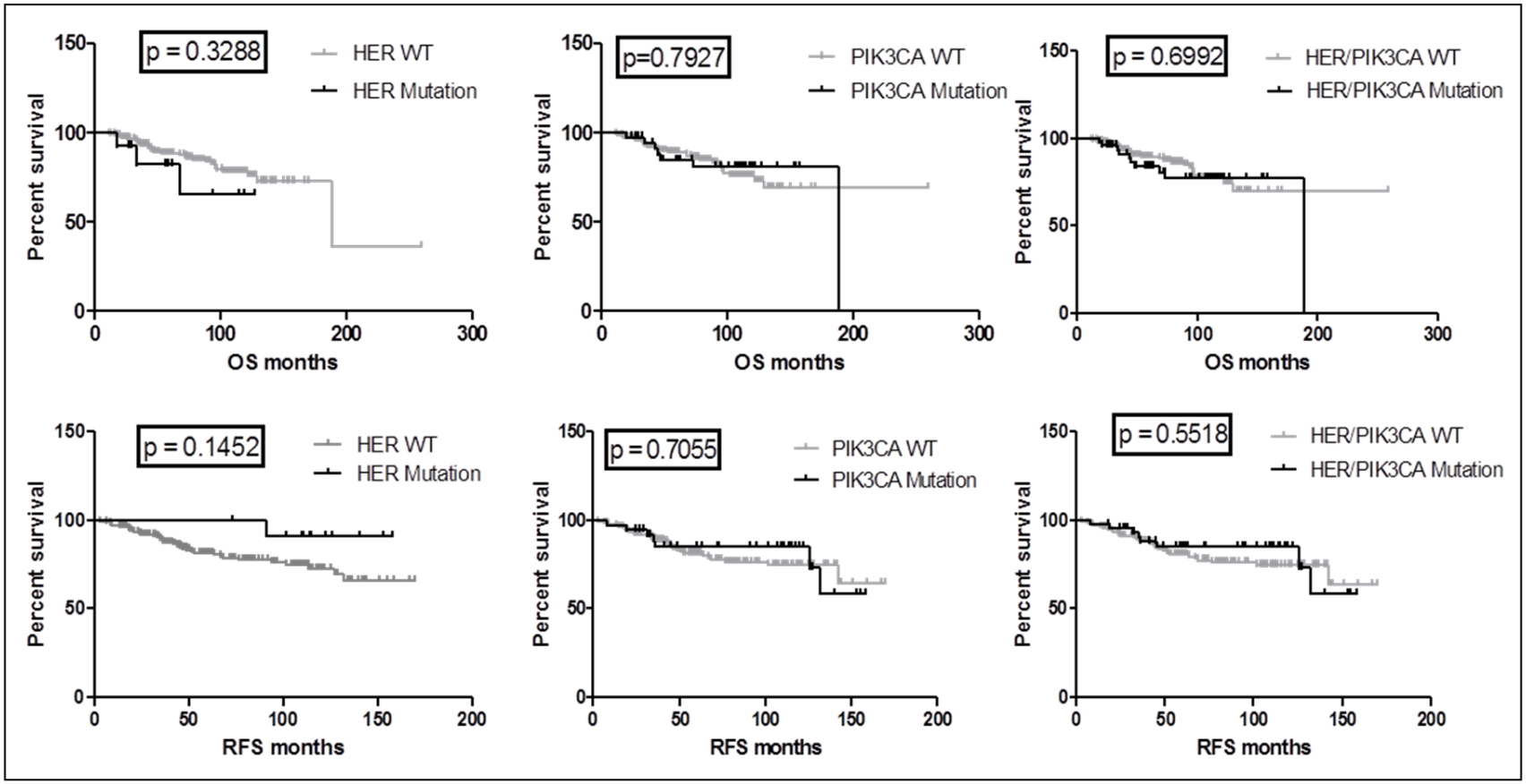

Figure 4.2 Impact of somatic ERBB Family and PIK3CA mutations on relapse-free survival (RFS – above, n=191) and overall survival (OS – below, n=195) in all patients in our sample set. p-values were calculated using the log-rank (Mantel-Cox) test with Graphpad Prism. ERBB Family and PIK3CA mutations were identified using Sequenom's MassARRAY based genotyping platform.

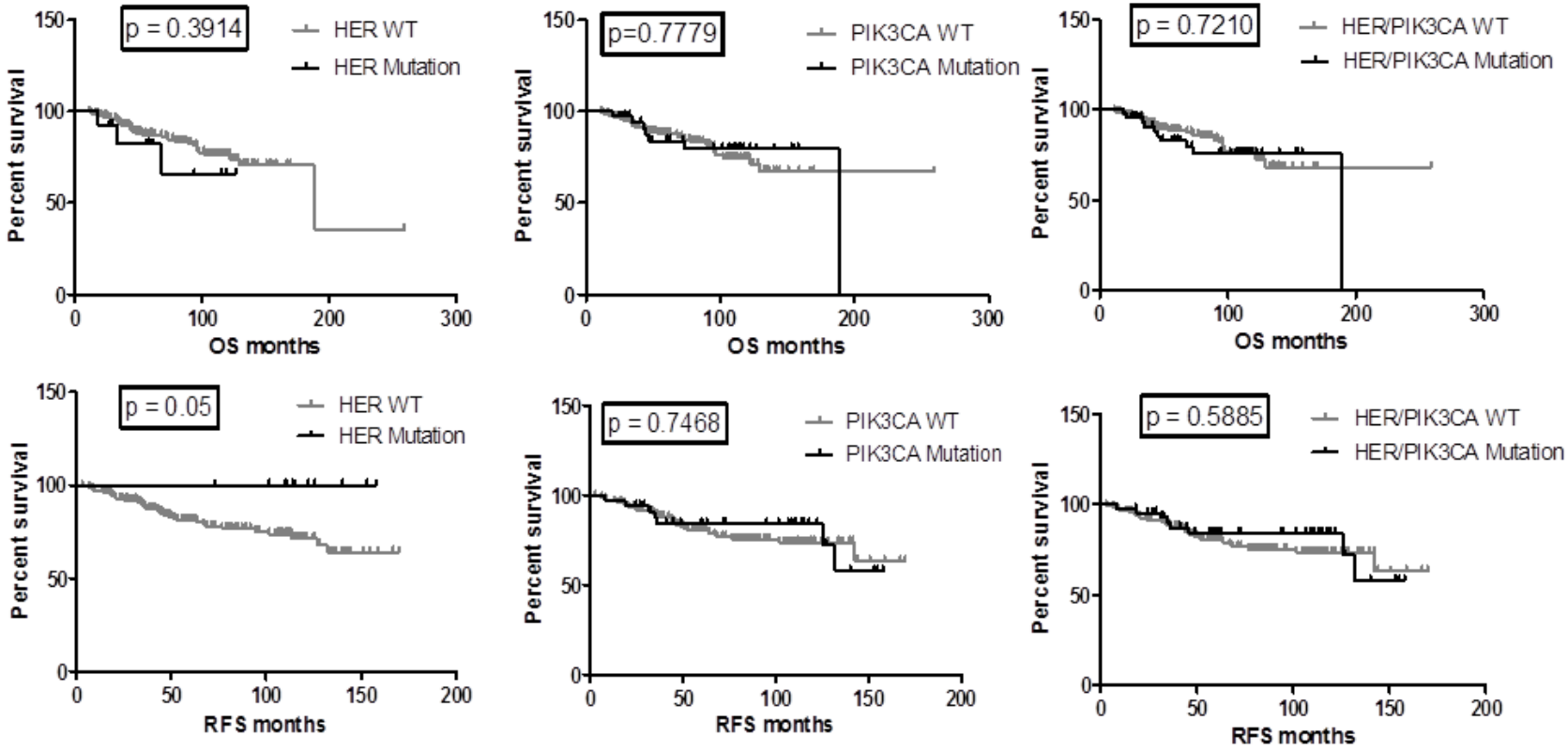

Figure 4.3 Impact of somatic ERBB Family and PIK3CA mutations on relapse-free survival (RFS – above, n=177) and overall survival (OS – below, n=181) after adjuvant trastuzumab-based therapy in our sample set. p-values were calculated using the log-rank (Mantel-Cox) test with Graphpad Prism. ERBB Family and PIK3CA mutations spectrometry based genotyping platform.

PIK3CA mutations were slightly more frequent in the tumours of patients who recurred at more than 1 versus 1 site (17.8 % vs 27.3 %, p = 0.07, Table 4.14). In terms of the site of first recurrence, liver and lung recurrences were most likely to be associated with ERBB and PIK3CA mutations (Table 4.15).

Table 4.14 Frequency of ERBB family and PIK3CA mutations in the tumours of patients whose HER2-positive breast cancer recurred at one or more sites

	ERBB Mutation Frequency	PIK3CA Mutation Frequency	HER/PIK3CA Mutation Frequency
Recurrence at 1 site	2/45, 4.4 %	8/45, 17.8 %	10/45, 22.2 %
Recurrence at 2 sites	0/17, 0.0 %	4/13, 30.1 %	4/13, 30.1 %
Recurrence at 3 sites	1/7, 14.3 %	1/7, 14.3 %	2/7, 28.6 %
Recurrence at 4+ sites	0/2, 0.0 %	1/2, 50.0 %	1/2, 50.0 %

Table 4.15 Frequency of ERBB family and PIK3CA mutations in the tumours of patients whose HER2-positive breast cancer recurred, according to first site of recurrence

	ERBB Mutation Frequency	PIK3CA Mutation Frequency	HER/PIK3CA Mutation Frequency
Locoregional	0/18, 0.0 %	2/18, 11.1 %	2/18, 11.1 %
Bone	1/17, 5.9 %	3/17, 17.7 %	4/17, 23.6 %
Lung	1/19, 5.3 %	5/19, 26.3 %	6/19, 31.6 %
Liver	3/20, 15.0 %	4/20, 20.0 %	7/20, 35.0 %
Brain	0/13, 0.0 %	1/13, 7.7 %	1/13, 7.7 %
Other	0/11, 0.0 %	4/11, 36.4 %	4/11, 36.4 %

4.5 Discussion

4.5.1 Discussion

Using the Agilent kinome platform, we were able to carry out a next generation sequencing (NGS) study of 612 kinome-related genes. The ERBB family and PIK3CA mutations we discovered in this exploratory analysis were then carried forward for validation in a larger sample set of HER2-positive breast cancers using Sequenom's mass spectrometry based genotyping tool, which is highly sensitive in clinical tumour specimens, exceeding the sensitivity of NGS platforms and Sanger sequencing[55]. All of the E542K, H1047R and G1049R PIK3CA mutations discovered in our kinome sequencing study were validated by Sequenom. However, only one of the ERBB family mutations identified in the kinome study was validated by sequenom, that being ERBB4 G599W.

The discrepancy between our results is most likely due to our use of archived formalin-fixed paraffin embedded (FFPE) samples. Another potential cause is that whereas Sequenom is highly sensitive, the kinome panel we used may be less capable of detecting low frequency mutations. Although FFPE-derived DNA can be used for NGS[56], there may be higher variability and a resulting greater number of false positives compared to fresh frozen tissue-derived DNA due to DNA damage[57]. The kinome sequencing method we used may be more suitable for DNA derived from fresh frozen tumour tissue, but as few centres have been preserving their specimens this way, we were unable to collect enough samples with sufficient follow up to adequately power a study. This is in contrast to the Sequenom technology which is ideally suited for DNA derived from FFPE tumour samples because it utilises very short DNA fragments[55].

More frequent mutations in the ERBB family and in PIK3CA were identified by sequenom than in our kinome study. This was not unexpected, due to sequenom's greater sensitivity. The MassARRAY platform can detect a mutation even if it is only present in as little as 5 % of the sample. Similar work carried out by Sueta *et al* confirmed that more sensitive technologies will reveal a higher mutational frequency even across the same tumour samples. These authors analysed 43 HER2-positive

breast cancers for PIK3CA mutations by direct sequencing and digital PCR, and found that 12% of their samples contained mutations detectable only by the latter, more sensitive method[58].

Overall, we found a rate of 7.05 % for somatic ERBB mutations in HER2-positive breast cancer. The ERBB family mutations we discovered in our sequenom study were not reported by the cancer genome atlas (TCGA) in HER2-positive breast cancer (n = 120). Within the full TCGA breast cancer study, ERBB3 E928G was reported as occurring in 1 % of breast cancers whereas we found it in 0.44 % in our samples; similarly, ERRB4 S303F occurred in 1.32 % of our samples and in 1 % of breast cancers in TCGA (Table 4.9). While they have been reported in other cancer types, to the best of our knowledge, most of the somatic ERBB family mutations discovered in our sequenom study have neither been previously published nor shown to occur in HER2-positive breast cancer.

We found ERRB4 to be the most frequently somatically mutated ERRB gene in our sample set, being mutated in 2.85 % of samples (Table 4.9). ERRB4 has an ambiguous role in HER2-positive breast cancer, with some studies suggesting an anti-oncogenic effect[59] and others suggesting a pro-oncogenic role[60]. Further functional work on this gene and its known mutations could shed light on whether hitherto unknown ERBB4 mutations could in part account for HER4's ambigious role in breast cancer.

PI3K/AKT aberrations occur in more than 25% of breast cancers, with PIK3CA alterations being the most common in HER2-positive and other breast cancers[12]. Our overall PIK3CA mutation rate of 26.43 % is similar to the TCGA HER2-positive breast cancer study in which PIK3CA was mutated in 31 % of cases (n = 120), and similar to previous publications reporting 21.3% (n=80)[44], and 23 %(n = 355)[47]. In keeping with the established knowledge that PIK3CA mutations cluster in the kinase and helical domains[25], most of the mutations in our study clustered in these regions, although we also detected a p85-binding domain mutation and a C2 domain mutation (Table 4.10). We found the frequency of the H1047R mutation to be greater than reported in TCGA (Table 4.10) although this is not significant (p = 0.09), which may be due to

the sensitivity of the sequenom platform, and/or to differences in the genetic backgrounds of the two patient populations. We found a number of PIK3CA mutations at low frequencies in our sample set which were not reported in TCGA, which is likely a further testament to Sequenom's sensitivity. We also observed the PIK3CA mutation E545K in a significantly lower percentage of our sample set compared to TCGA ($p = 0.02$).

The impact of PIK3CA mutations on survival in HER2-positive breast cancer has been controversial, with some studies arguing that they are associated with poorer outcomes[14, 44, 61], but most studies suggest that they do not influence survival after adjuvant trastuzumab-based chemotherapy[46, 47, 61, 62]. Despite this, it has been shown that PIK3CA mutations are associated with significantly lower pathological complete response (pCR) rates after treatment with neoajduvant HER2-targeted therapies in HER2-positive breast cancer[47, 61]. Here we report that in the adjuvant setting, PIK3CA mutations do not influence survival outcomes after HER2-targeted therapy. These results are in keeping with other findings that PIK3CA mutations are not significantly associated with altered OS and RFS in HER2-positive breast cancer after adjuvant trastuzumab-based chemotherapy+[46, 47, 61, 62], with the observation in one study that initially patients with PIK3CA mutations in their tumours had a better OS and RFS for only the first three years[46] not being supported by our study (Figure 4.2). We also observed that somatic ERBB mutations do not influence survival after adjuvant trastuzumab-based therapy (OS: $p = 0.32$, RFS: $p = 0.15$). Given that these are relatively rare mutations, it would be interesting to see our study replicated in a larger sample size. As both HER family proteins and PI3K signal through the same pathway, we investigated whether analysing PIK3CA and ERBB family mutations together would reveal an overall impact on survival. Grouped together, these mutations do not affect survival (OS: $p = 0.70$, RFS: $p = 0.55$).

The lack of significant association we observe between PIK3CA mutations and clinicopathological features is in line with previous work[44]. It is notable that the greater proportion of patients in our sample set were classed as overweight or obese according to their body mass index (BMI) (Table 4.1). 5 % of all cancers in

postmenopausal women in the UK are attributable to being overweight or obese and increasing BMI has been associated with increased breast cancer incidence and mortality in postmenopausal women[63]. A statistically significant correlation has recently been discovered between rising BMI and a worse clinical outcome in patients with early stage HER2-positive breast cancer; however, adjuvant trastuzumab improves outcomes for patients regardless of BMI[64]. Levels of the hormone leptin correlate with adiposity, and, signalling through the ObR1 receptor, leptin activates three major pathways, JAK2/STAT3, MAPK/ERK, and PI3K/AKT[65]. Two of these, MAPK and PI3K, are major pathways downstream of HER2[1], and the leptin/ObR system is coexpressed with HER2 in a large fraction of human breast cancers[65]. It might therefore have been logical to expect a significant correlation between ERBB family and/or PIK3CA mutations and a high BMI. However, an inverse association between BMI and HER2 overexpression has also been reported[66], which may explain the lack of an association between BMI and HER mutations in our sample set, as might the relatively low proportion of patients for whom we could collect BMI data.

The lack of an association between ERBB family gene mutations and clinical or histologic variables or survival outcomes does not mean that these mutations are not functional or good therapeutic targets (this is also the case for PIK3CA mutations). We hypothesise that the clustering of the somatic mutations we discovered in functional regions of each gene, along with their low AVSIFT values, increases the likelihood that they have functional implications. It has been proposed that the importance of rare functional mutations may be overlooked through lack of statistical power, and that the functional interpretation of mutations may be improved by analysing mutations in terms of domain hotspots rather than gene hotspots (preprint, Miller at al http://biorxiv.org/content/biorxiv/early/2015/02/26/015719.full.pdf).

Further, some limited evidence suggests ERBB family mutations, including some reported here, may have functional effects in other cancers. EGFR V769L has been reported as a rare mutation in non-small cell lung cancer, in which it confers

resistance to gefitinib[67]. ERBB3 Q809R was previously reported in a study of gastric and colon cancer, where it was shown to be oncogenic *in vitro* when it was expressed in the presence of HER2[41]. ERBB4 has been shown to be highly mutated in melanoma, but there is controversy over whether these are driver[43] or passenger mutations[68]. Given the current ambiguity over its role in breast cancer, the fact that it is the most frequently mutated ERBB gene in our sample set (Table 4.11), and that it contains a hotspot mutation, we hypothesise that ERBB4 mutations should be carried forward for functional analysis and the study of optimal therapeutic targeting strategies.

4.5.2 Summary and conclusion

Employing next-generation and mass spectrometry based sequencing methods, we uncovered a set of mutations in the ERBB family and in the PIK3CA gene in a sample set of 227 HER2-positive breast cancers. ERBB family mutations occurred in 7.05 % (16/227) of samples, and were mutually exclusive with each other, although ERBB family and PIK3CA mutations co-occurred in three cases. PIK3CA mutations occurred in 26.43 % or 60/227 samples. The ERBB family mutations uncovered here did not correlate significantly with histological or clinical features, or with outcomes after trastuzumab-based therapy, but this could be due to a low sample number. However, it is important to determine the functional relevance of these novel ERBB gene mutations in HER2-positive breast cancer, and if breast cancers with these mutations are more likely to benefit from specific therapeutic strategies.

Chapter 5 Functional effects of the ERBB4 kinase domain mutation V721I and furin-like domain mutation S303F on HER2-positive breast cancer cell growth, signalling and response to HER2-targeted therapies

5.1 Introduction

We discovered a number of novel somatic mutations in the four ERBB genes encoding the 4 proteins of the HER family in HER2-positive breast cancer. These were present in 7.05 % of HER2-positive breast tumours (n = 227). These mutations were mutually exclusive and clustered in the furin-like and kinase domains of each gene.

ERBB4 was the most frequently mutated gene of all four ERBB family members in our sample set, carrying five mutations in all (Table 4.9). In contrast with other known HER family members, increased HER4 protein expression has been associated with a better prognosis[59], and increased sensitivity to trastuzumab in metastatic breast cancer[59]. However, some studies have argued that knockdown of ERBB4 reverses resistance to trastuzumab and that high HER4 expression is associated with a poor outcome in HER2-positive breast cancer[69]. ERBB4 mutations have been associated with increased tyrosine kinase phosphorylation and increased HER4 kinase activity in melanoma, and cells transfected with these mutations displayed higher AKT activation but no increase in ERK activation relative to ERBB WT[43], although none of the mutations in this study matched those in our study and melanoma findings may not translate to HER2-positive breast cancer. ERBB4 mutations also increased the transforming ability of NIH 3T3 cells[43]. Of the five mutations in ERBB4 uncovered in our sequenom study, 3 were located in the furin-like domains, which have been shown to be involved in receptor dimerisation[70], a key early step in HER family signalling[37].

The HER2/HER3 heterodimer has been proposed as the main oncogenic unit in HER2-positive breast cancer, with activated HER3 coupling HER2 to the PI3K pathway[71], and there is evidence that HER3 signalling may mediate resistance to both HER family inhibitors[35] and to PI3K inhibitors[32]. Crystallography studies of HER3 domain interactions suggest that HER4 and HER3 may interact to form a mutually inhibitory heterodimer[72], resulting in the sequestration of HER3 away from EGFR and HER2. This hypothesis may explain the finding that the combined expression of HER3 and HER4 was associated with better OS and DFS[73], whereas co-expression of the other HER family proteins predict worse OS and DFS in invasive breast cancer.

Therefore, our discovery of a hotspot somatic mutation in the furin-like domain of ERBB4 was particularly interesting. ERBB4 S303F occurs in tumours from three different patients in our sample set of 227 patients. We discovered two ERBB hotspot mutations in our sample set, and whereas ERBB3 Q809R had been previously published, albeit in colon cancer[41], ERBB4 S303F has not been previously studied. We therefore selected ERBB4 S303F as a candidate for functional analysis. As our mutations occurred in kinase as well as furin-like domains, we also selected the kinase domain mutation ERBB4 V721I (Table 4.11) to carry forward for *in vitro* testing.

Miller et al (http://biorxiv.org/content/biorxiv/early/2015/02/26/015719.full.pdf) analysed mutations in protein domains using data from over 5,000 tumour normal pairs from 22 cancers profiled in TCGA and found that kinase and furin-like domains of oncogenes are significantly enriched for somatic mutations in cancer. The top three genes found to carry the most kinase domain mutations were BRAF, EGFR, and ERBB2, and the genes with the most furin-like domain mutations were EGFR, ERBB3 and ERBB2. This study predicted ERBB4 S303F to be a gain-of-function mutation in breast and ovarian cancers, that will increase sensitivity to small molecule inhibitors, and speculated that it may be analogous to the activating ERBB2 S310F somatic mutation, which has been reported in invasive lobular carcinoma[74] and micropapillary urothelial carcinoma, a rare form of bladder cancer[75]. ERBB2 S310F was also found in a lung adenocarcinoma in a patient whose advanced tumour was refractory to multiple lines of chemotherapy but who was subsequently and successfully treated with afatinib[76].

ERBB4 V721I was previously reported in colorectal adenocarcinoma[77] and was subsequently shown not to affect kinase activity, tyrosine phosphorylation or sensitivity to gefitinib in COS-7 or MCF-7 cells compared to ERBB4 WT cells[42].

To the best of our knowledge this is the first study to functionally characterise both ERBB4 S303F and ERBB4 V721I in HER2-positive breast cancer cells.

The objectives of the work described in this chapter were:

1. To determine the effects of ERBB4 S303F and ERBB4 V721I mutations on HER2-positive breast cancer cell growth, 3D soft agar colony forming ability, HER4 protein expression and kinase activity
2. To determine the effects of the ERBB4 S303F and ERBB4 V721I mutations on the sensitivity of HER2-positive breast cancer cells to the HER2-targeted therapies trastuzumab, lapatinib and afatinib and the PI3K inhibitor copanlisib
3. To determine if the combination of HER2-targeted therapies and copanlisib remains synergistic in HER2-positive breast cancer cells carrying the ERBB4 S303F and ERBB4 V721I mutations
4. To determine the effects of ERBB4 S303F and ERBB4 V721I mutations on cell signalling

5.2 Characterisation of ERBB4-transfected cell lines

We selected three HER2-positive breast cancer cell lines as hosts for transfection based on their PIK3CA mutation status. HCC1569 is PIK3CA wild type, HCC1954 carries the PIK3CA H1047R mutation known to be common in HER2-positive breast cancer, and BT474 carries a rare PIK3CA mutation, K111N. All cell lines are WT for ERBB family genes. Mutations were confirmed by Sequenom.

Although we were able to stably express empty vector, ERBB4 WT, and ERBB4 V721I in all of our host cell lines, ERBB4 S303F was lethal to 2/3 cell lines (Figure 5.1). We note that in our clinical study, S303F did not co-occur with a PIK3CA mutation, and correspondingly, the PIK3CA WT cell line was the only one in which stable S303F transfection could be established.

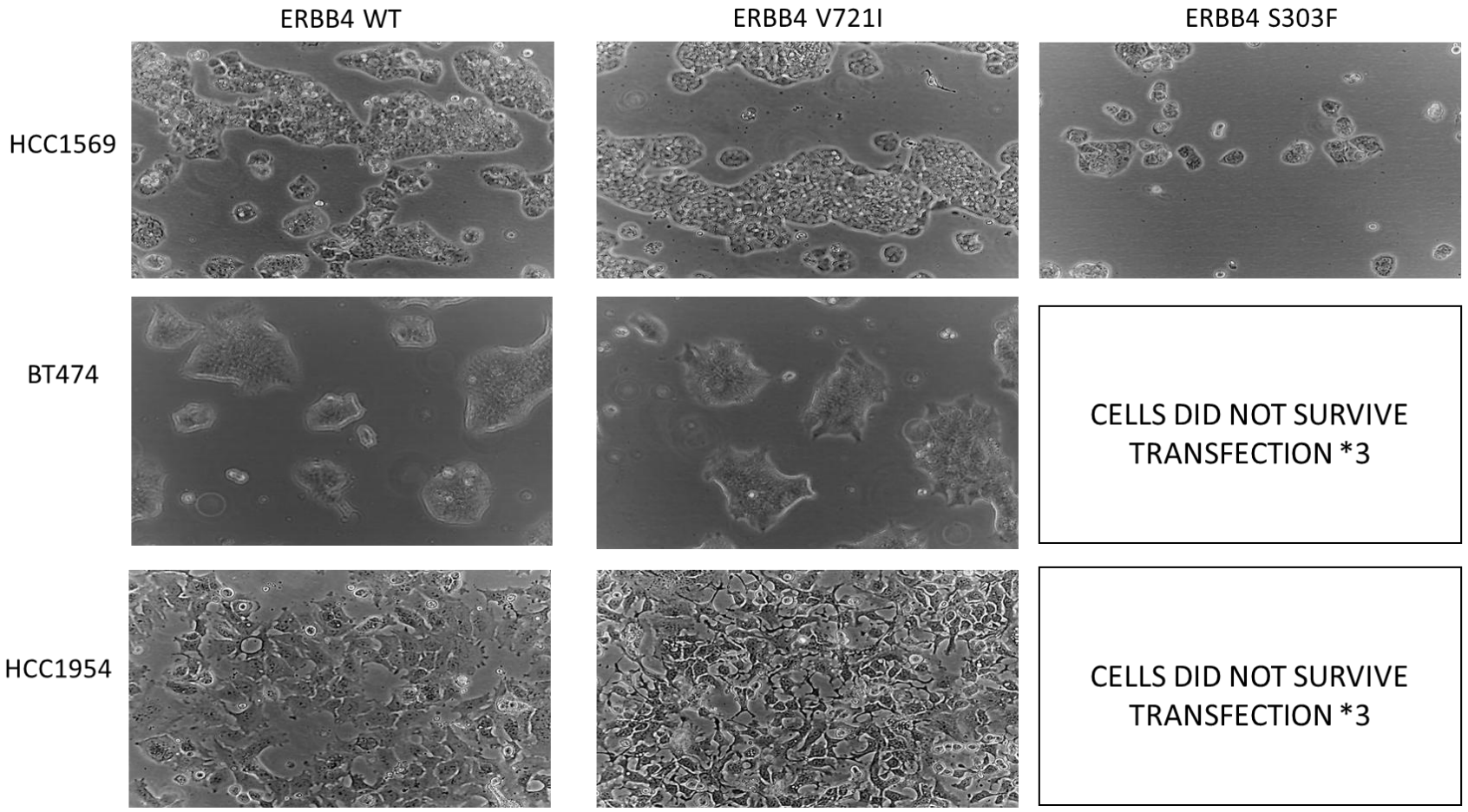

Figure 5.1 Morphology of three established HER2-positive breast cancer cell lines transfected with ERBB4 WT, ERBB4 V721I, ERBB4 S303F, and the corresponding empty vector, pCDF1 visualised in T75 flasks at 100X with a light microscope (Nikon).

Stable transfection of the ERBB4 mutation V721I appeared to increase levels of the HER4 protein relative to empty vector and ERBB4 WT controls. This effect was significant in the BT474 cell line (p = 0.01). HCC1569 cells carrying the ERBB4 S303F mutation expressed lower levels of HER4 protein than cells transfected with ERBB4 V721I, EV and ERBB4 WT controls.

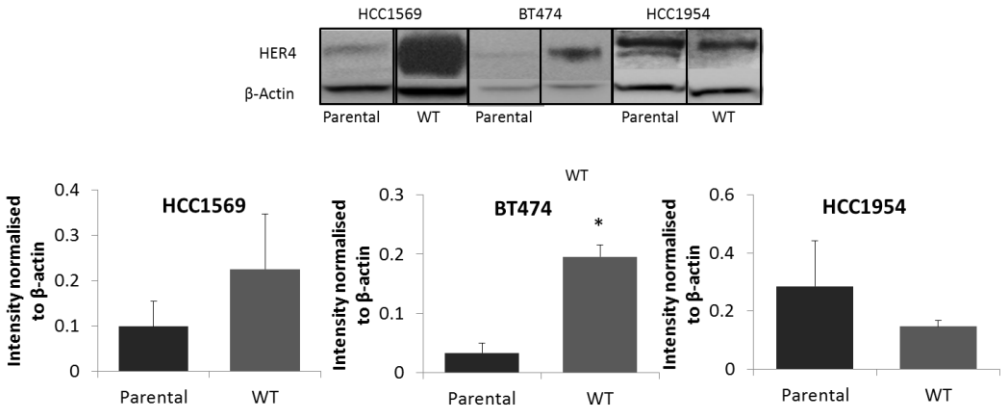

Figure 5.2 Total levels of HER4 protein were analysed by western blot and densitometry was performed on EV-, ERBB4 WT-, ERBB4 V721I- and ERBB4 S303F-transfected cell lines. Error bars are representative of biological triplicates. * = p < 0.05 as calculated by the 2-tailed Student's t-test with equal variance relative to both EV and WT. EV = empty vector WT = wild type

The V721I mutation increased the growth rate in all HER2-positive breast cancer cell lines tested, as assessed by doubling time assay (Figure 5.3).

Table 5.1 Doubling times of parental (from the literature), empty vector (EV) expressing and wild-type ERBB4 (WT) expressing HER2-positive breast cancer cell lines. Standard deviations are representative of triplicate experiments. P-values calculated by 2-tailed Student's t-test with equal variance

	Doubling Time (Days)			
	Parental	**EV**	**WT**	**p-value**
HCC1569	1.04[26]	1.39 +/- 0.25	1.08 +/- 0.19	0.18
BT474	3.79[78]	3.13 +/- 0.03	2.95 +/- 0.08	0.46
HCC1954	1.92[78]	2.10 +/- 0.19	1.69 +/- 0.23	0.06

The doubling times of Empty vector (EV)- and ERBB4 WT-transfected cell lines were similar to published doubling times of the corresponding parental cell lines (Table 5.1)[26, 78]. ERBB4 V721I-transfected cell lines had a significantly increased growth

rate in comparison with ERBB4 WT cells in 2/3 cell lines, BT474 ($p = 0.03$) and HCC1954 ($p = 0.01$). In HCC1569 cells neither the ERBB4 S303F mutation nor the ERBB4 V721I mutation increased growth rate relative to ERBB4 WT-transfected cells (Figure 5.3).

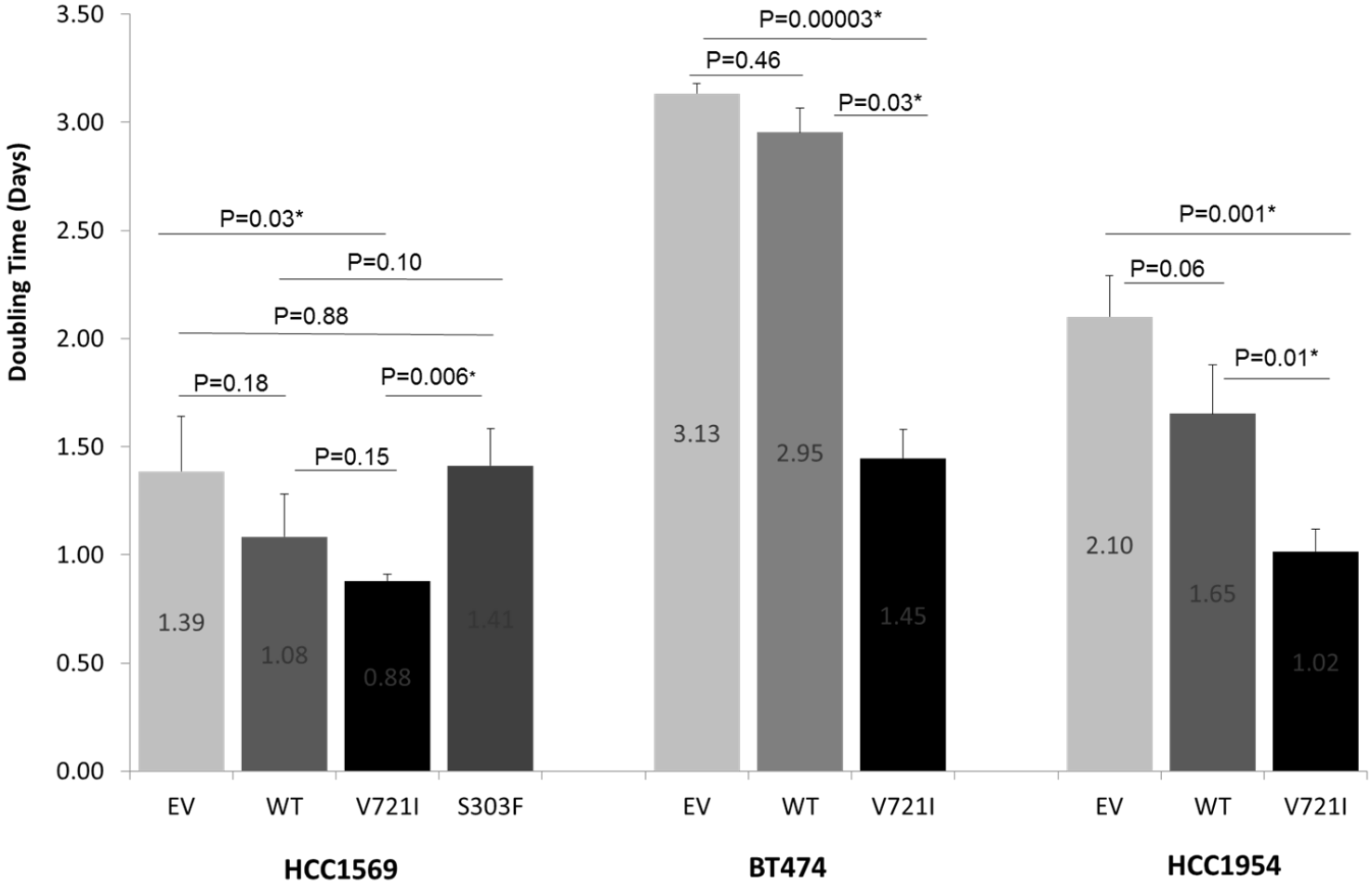

Figure 5.3 Doubling times of HCC1569, BT474 and HCC1954 HER2-positive breast cancer cell lines stably expressing WT ERBB4, ERBB4 V721I, ERBB4 S303F, or the pCDF1 empty vector. Doubling times were assessed by plating 1 x 10^4 cells in 6 well plates at day 0, lysing and counting with a haemacytometer until two doublings had been reached, and plotting the resulting curves with Graphpad Prism. Error bars are representative of independent triplicate experiments. * = $p < 0.05$ as calculated by the t-test (2-tailed with equal variance).

When grown in 3D soft agar, V721I expressing cells formed more colonies than the corresponding WT ERBB4-transfected cell lines (Figure 5.4). The S303F-transfected cell line showed reduced colony forming ability relative to ERBB4 WT-transfected HCC1569 cells, but this was not significant (Figure 5.4). 3D colony-formation is a surrogate for anchorage-independent growth, one of the hallmarks of cancer and a key determinant of metastatic ability.

Overall, HER4 expression was significantly increased in V721I-transfected cell lines relative to EV- and WT-cell lines, as is growth rate and 3D colony forming ability.

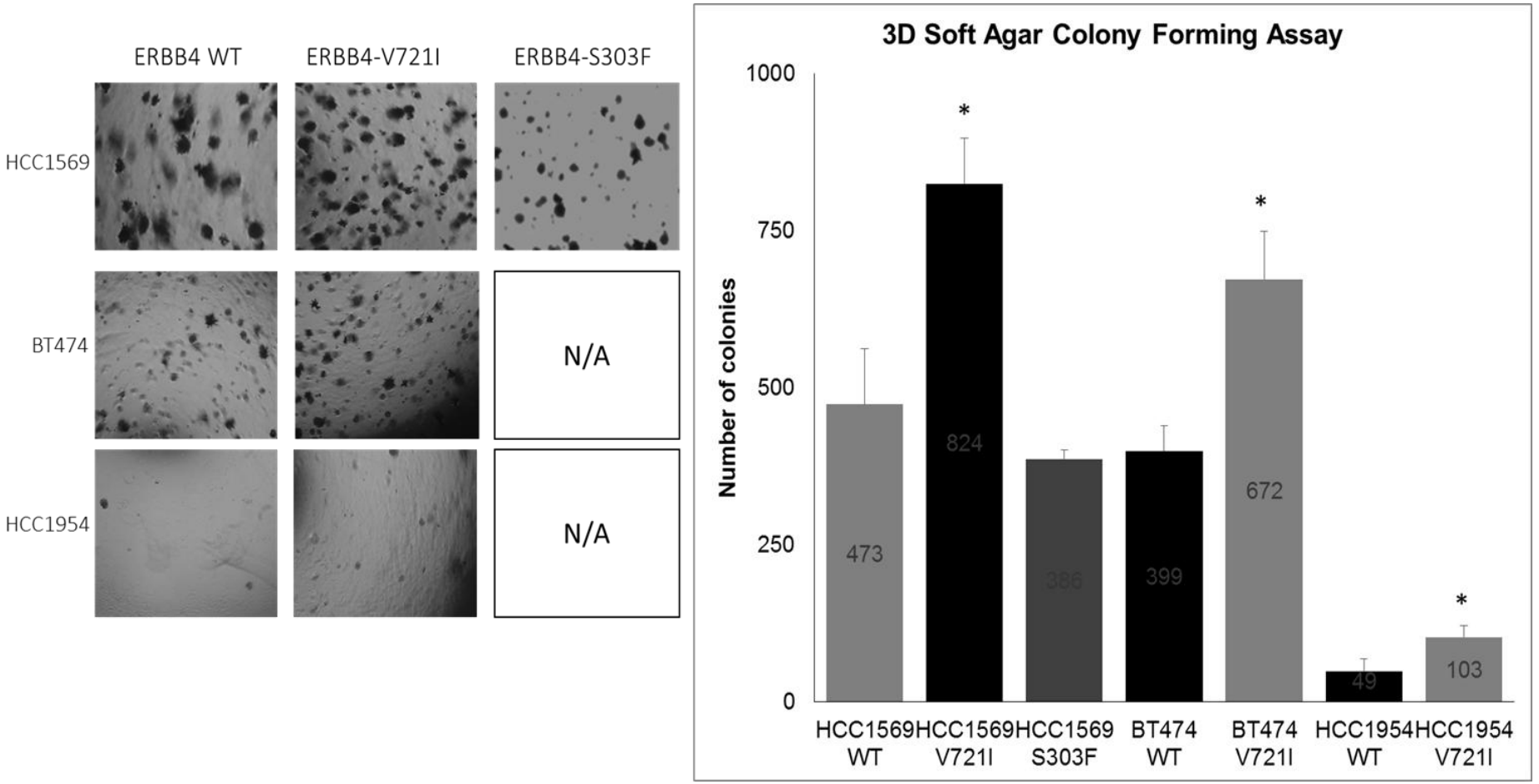

Figure 5.4 The effect of the ERBB4 V721I and S303F mutations on 3D colony-forming ability of the HER2-positive breast cancer cell lines HCC1569, BT474 and HCC1954 in 3D soft agar. Cells were seeded into a media/agar matrix and prior to staining with Neutral Red and being counted in three planes. Error bars are representative of independent triplicate experiments. * = $p < 0.05$ as calculated by the S-test (2-tailed with equal variance). N/A = experiment not carried out as these cells did not survive post-transfection.

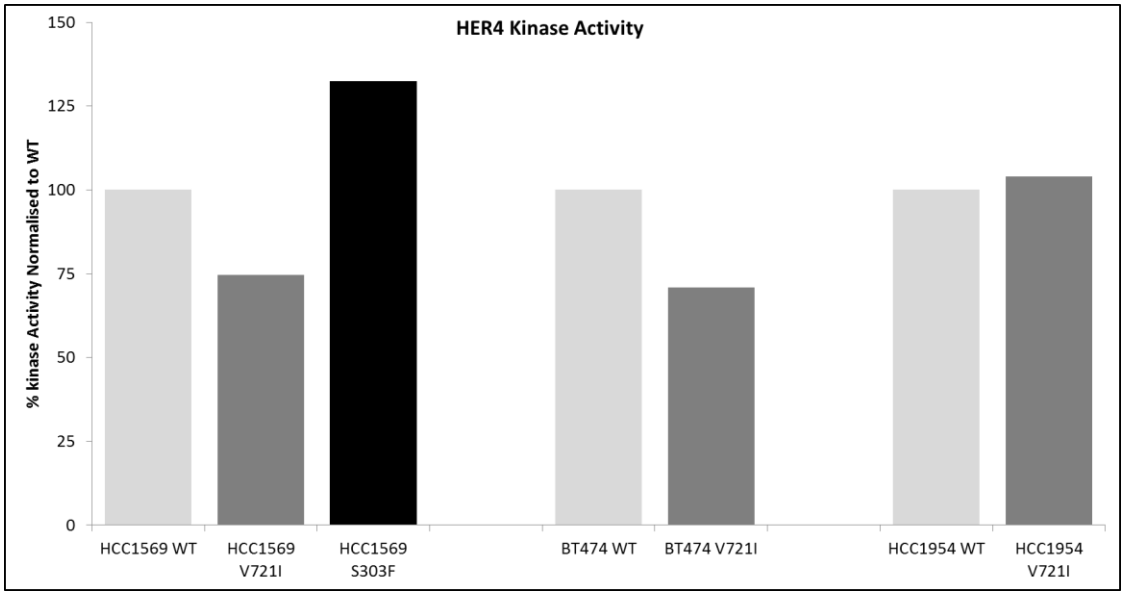

Figure 5.5 The effect of transfection of the ERBB4 V721I and S303F mutations on HER4 kinase activity of the HER2-positive breast cancer cell lines HCC1569, BT474 and HCC1954. HER4 protein was purified by immunoprecipitation and kinase activity determined using the ADP-Glo Assay (Promega). Due to the cost and time demand of the experiment it was only possible to complete it once over the course of this thesis and this is a preliminary result.

A preliminary result suggested that the kinase domain mutation V721I decreased HER4 kinase activity in 2/3 transfected cell lines, whereas HCC1569 cells transfected with the furin-like domain mutation S303F had a marked increase in HER4 kinase activity relative to ERBB4 WT-transfected HCC1569 cells (Figure 5.5).

5.3 Influence of the ERBB4 V721I and S303F mutations on sensitivity to HER2-targeted therapies, and to the PI3K inhibitor copanlisib

Trastuzumab sensitivity is not significantly affected by transfection of either of these ERBB4 mutations in any cell line tested (Table 5.2). This is consistent with the clinical data presented in Chapter 4.

The expression of ERBB4 WT increased sensitivity to the pan-HER inhibitor afatinib in most cell lines tested relative to cells transfected with empty vector control, being significant in all but the BT474 model (IC_{50} (nM): HCC1569 EV 8.91 +/- 1.04 vs WT 6.93 +/- 0.51, p = 0.04; BT474 EV 2.25 +/- 0.33 vs WT 1.49 +/- 0.13, p = 0.09; HCC1954 EV 51.39 +/- 2.36 vs WT 6.54 +/- 2.15, p = 0.004). Transfection of the ERBB4 V721I kinase domain mutation in HCC1569 and HCC1954 increasd resistance to afatinib relative to cells transfected with ERBB4 WT (HCC1569 p = 0.02, HCC1954 p = 0.005) (Table 5.2). Transfection of the ERBB4 furin-like domain mutation S303F rendered HCC1569 cells sensitive to afatinib in comparison with the HCC1569 cells transfected with WT ERBB4 (IC_{50} (nM) WT 6.93 +/- 0.51 vs S303F 2.98 +/- 0.46) (Table 5.2).

There was no significant influence of ERBB4 V721I transfection on lapatinib sensitivity in 2/3 cell lines tested, but a significant sensitization was observed in the HCC1954 model transfected with ERBB4 V721I relative to cells transfected with WT ERBB4 (IC_{50} (nM) WT 894.24 +/- 42.16 vs V721I 789.48 +/- 89.44 p = 0.00005). ERBB4 S303F transfection was associated with resistance to lapatinib in the HCCC1569 model (IC_{50} (nM) WT 503.67 +/- 33.42 vs V721I 736.41 +/- 51.55).

Transfection of both V721I and S303F mutations significantly increased sensitivity to the PI3K inhibitor in the PIK3CA WT cell line HCC1569 (IC_{50} (nM) WT 74.74 +/- 9.69 vs V721I 43.20 +/- 9.22, S303F 47.09 +/- 5.09) but transfection of the V721I mutation increased resistance to copanlisib in the PIK3CA mutated cell line HCC1954 in comparison with cells transfected with WT ERBB4 (IC_{50} (nM) WT 5.96 +/- 0.29 vs V721I 9.25 +/- 0.63).

Overall, transfection of WT or mutated ERBB4 had the least influence on copanlisib, afatinib and lapatinib sensitivity of the BT474 model, the most sensitive of the three cell lines to the inhibitors tested.

Table 5.2 IC_{50} values of copanlisib, lapatinib and afatinib, and the effect of trastuzumab on % growth inhibition in a panel of HER2-positive breast cancer cell lines stably expressing ERBB4 WT, ERBB4 V721I, ERBB4 S303F or the pCDF1 empty vector (EV). Standard Deviations are representative of triplicate independent experiments. * = p < 0.05 compared to the matched cell line transfected with ERBB4 WT by Student's t test • = p < 0.05 compared to the matched cell line transfected with EV by Student's t test ^ = p < 0.05 compared to the matched cell line transfected with ERBB4 WT by Student's t test. Statistical tests were 2-tailed with Equal Variance. EV = empty vector WT = wild type

Mutation	Copanlisib IC_{50} (nM)	Afatinib IC_{50} (nM)	Lapatinib IC_{50} (nM)	Trastuzumab % inhibition at 10 µg/ml
HCC1569 (PIK3CA WT)				
EV	85.39 +/- 6.37	8.91 +/- 1.04	541.82 +/- 48.77	8.29 +/- 5.35
ERBB4 WT	74.74 +/- 9.69	6.93 +/- 0.51•	514.02 +/- 30.50	3.59 +/- 2.21
ERBB4 V721I	43.20 +/- 9.22*•	12.34 +/- 2.38*•	503.67 +/- 33.42	2.98 +/- 2.03
ERBB4 S303F	47.09 +/- 5.09*•	2.98 +/- 0.46*•^	736.41 +/- 51.55*•^	0.26 +/- 2.89
BT474 (PIK3CA Mutated)				
EV	5.31 +/- 0.58	2.25 +/- 0.33	32.67 +/- 7.74	49.03 +/- 5.51
ERBB4 WT	4.72 +/- 0.65	1.49 +/- 0.13	42.69 +/- 4.97	43.02 +/- 5.63
ERBB4 V721I	4.27 +/- 1.04	1.13 +/- 0.25	44.78 +/- 4.12	42.05 +/- 5.34
HCC1954 (PIK3CA Mutated)				
EV	21.21 +/- 1.65	51.39 +/- 2.36	872.43 +/- 76.90	8.74 +/- 4.72
ERBB4 WT	5.96 +/- 0.29•	6.54 +/- 2.15 •	894.24 +/- 42.16	3.58 +/- 2.76
ERBB4 V721I	9.25 +/- 0.63*•	13.74 +/- 0.27* •	789.48 +/- 89.44*	1.41 +/- 0.73

We have previously shown that co-targeting PI3K and HER2 has the potential to be an improved treatment strategy for patients with HER2-positive breast cancer[22]. This formed the rationale for testing our construct cell lines to determine if combining copanlisib with trastuzumab, or afatinib, or lapatinib remained synergistic in cells with ERBB4 mutations. In general, additivity or synergy was noted between afatinib and copanlisib in the HCC1569 and HCC1954 cell models utilised herein (Table 5.3). As noted above, relative afatinib resistance was induced by the V721I mutation in HCC1569 cells compared with matched WT ERBB4-transfected cells (Table 5.2), but this was overcome by combining it with copanlisib (Figure 5.7, Table 5.3, CI @ ED_{50}: HCC1569 WT 1.04 +/- 0.23 vs V721I 0.83 +/- 0.27; HCC1954 WT 0.54 +/- 0.08 vs V721I 0.42 +/- 0.10). There was a trend towards enhancement of Afatinib:Copanlisib synergy in HCC1569 and HCC1954 cells transfected with ERBB4 V721I relative to cells transfected with WT ERBB4, although this did not reach significance (Table 5.3). The sensitising effect of the S303F mutation to afatinib also held true for the combination of afatinib with copanlisib in HCC1569 cells; this combination was more synergistic in this cell line when transfected with S303F relative to HCC1569 cells transfected with WT ERBB4 (Figure 5.7, Table 5.3, CI @ ED_{50}: HCC1569 WT 1.04 +/- 0.23 vs S303F 0.46 +/- 0.09, $p = 0.01$).

No additivity or synergy between afatinib and copanlisib occured in the BT474 model, regardless of ERBB4 status. However, both drugs were highly potent as single agents in this cell line and the combination was highly effective at inhibiting growth at low nanomolar concentrations.

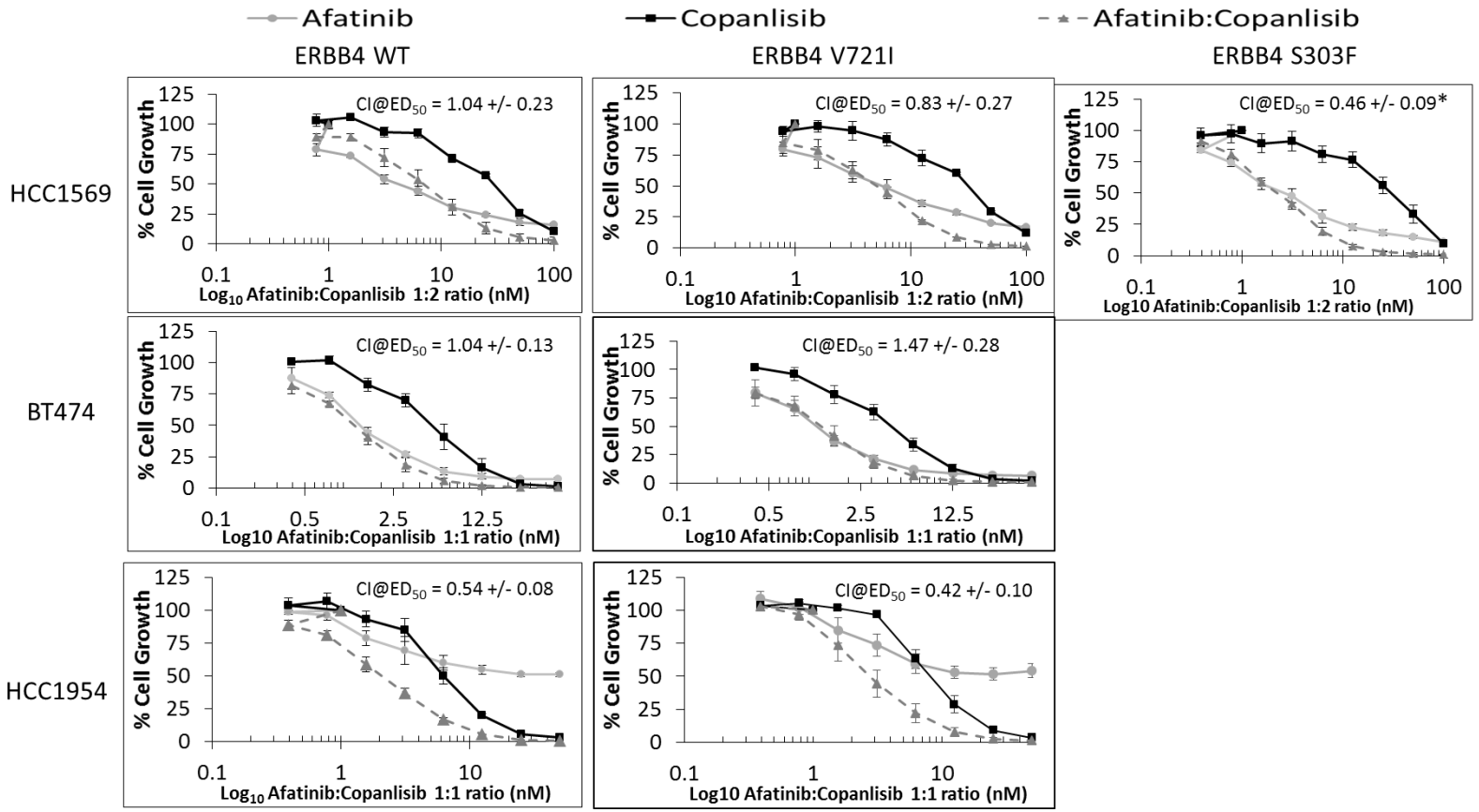

Figure 5.6 Efficacy of afatinib (-o-), copanlisib (-□-) and a combination of afatinib and copanlisib (--Δ--) in a panel of HER2-positive cell lines stably expressing ERBB4 WT, V721I or S303F. Acid phosphatase toxicity assays were used to investigate the effect of a serial dilution of the drugs on these HER2-positive breast cancer cell lines over a 5 day period and the resulting dose-response curves were analysed with Calcusyn (Biosoft). Error bars are representative of standard deviations across triplicate experiments * = p < 0.05 relative to WT as calculated by t-test (2-tailed with equal variance). CI (Combination Index) values were calculated using Calcusyn software according to the Chou-Tallalay method. A CI value of 1 denotes additivity, with a CI < 1 denoting synergy and of > 1 denoting the two drugs in combination are antagonistic. Afatinib:Copanlisib was tested at a 1:1 ratio (top conc 100nM:100nM).

Table 5.3 The IC_{50}s of afatinib in combination with copanlisib compared to the IC_{50} of each as a single agent and Combination Index (CI) values at ED_{25}, ED_{50} and ED_{75} for the combination of afatinib and copanlisib. IC_{50} and CI values were calculated with CalcuSyn software (Biosoft) according to the Chou-Tallalay Synergy Quantification method. A CI of 1 denotes additivity, < 1, synergy, and > 1, antagonism. Lower CI values denote higher synergy. Standard deviations are representative of independent triplicate experiments. * = p < 0.05 compared to ERBB4 WT-transfected cells (2-tailed t-test with equal variance) ^ = p < 0.05 compared to cells transfected with ERBB4 V721I-test (2-tailed with equal variance)

	Afatinib IC_{50} (nM)	Afatinib IC_{50} in combination with copanlisib	CI @ ED_{25}	CI @ ED_{50}	CI @ ED_{75}
HCC1569					
ERBB4	6.93 +/- 0.51	5.91 +/- 0.19	2.41 +/- 0.30	1.04 +/- 0.23	0.52 +/- 0.16
ERBB4 V721I	12.34 +/- 2.38*	1.45 +/- 0.35	2.06 +/- 1.14	0.83 +/- 0.27	0.42 +/- 0.05
ERBB4 S303I	2.98 +/- 0.46	2.28 +/- 0.50	0.88 +/- 0.23*	0.46 +/- 0.09*	0.27 +/- 0.06*^
BT474					
ERBB4	1.49 +/- 0.13	1.17 +/- 0.11	1.42 +/- 0.16	1.04 +/- 0.13	0.81 +/- 0.22
ERBB4 V721I	1.13 +/- 0.25	1.10 +/- 0.24	2.29 +/- 0.44	1.47 +/- 0.28	1.01 +/- 0.22
HCC1954					
ERBB4	6.54 +/- 2.15	2.09 +/- 0.18	0.67 +/- 0.17	0.54 +/- 0.08	0.51 +/- 0.12
ERBB4 V721I	13.74 +/- 0.27*	2.34 +/- 0.38	0.49 +/- 0.13	0.42 +/- 0.10	0.41 +/- 0.09

The combination of lapatinib and copanlisib remained synergistic in our cell line models regardless of ERBB4 mutational status (Figure 5.7, Table 5.4). In HCC1569 the combination of lapatinib: copanlisib is synergistic in all models utilised herein (Table 5.4). Although the use of combination indices for our HCC1569 model is limited due to the failure of lapatinib to reach an IC_{50} as a single agent, our dose response curves also clearly showed that the combination is an effective treatment in this cell line (Figure 5.8). Synergy between copanlisib and lapatinib was also noted in the BT474 model, which was sensitive to single agent lapatinib (CI @ ED_{50}: BT474 WT 0.28 +/- 0.03 vs V721I 0.23 +/- 0.01), although no difference was noted between the synergy of ERBB4-WT and ERBB4-V721I expressing BT474 cells.

Combination indices indicate less lapatinib:copanlisib synergy in HCC1954 V721I-transfected cells relative to ERBB4 WT-transfected cells. However, this may partly relate to a limitation of the Chou-Tallalay method as the lapatinib IC_{50} was significantly higher in the WT ERBB4-transfected HCC1954 model. Dose response curves indicate that the combination is similarly effective in both ERBB4 WT- and V721I-transfected HCC1954 cells. Overall, the combination of lapatinib:copanlisib remains synergistic in our call line panel regardless of either if the ERBB4 mutations tested. In some cases synergy is affected by the presence of an ERBB4 mutation (HCC1945 cells bearing V721I are less synergistic than their WT counterparts, whereas HCC1569-S303F cells have more synergy albeit only at one dose than theirWT counterparts), but statistical significance between WT and ERBB4 mutated cells is not universal.

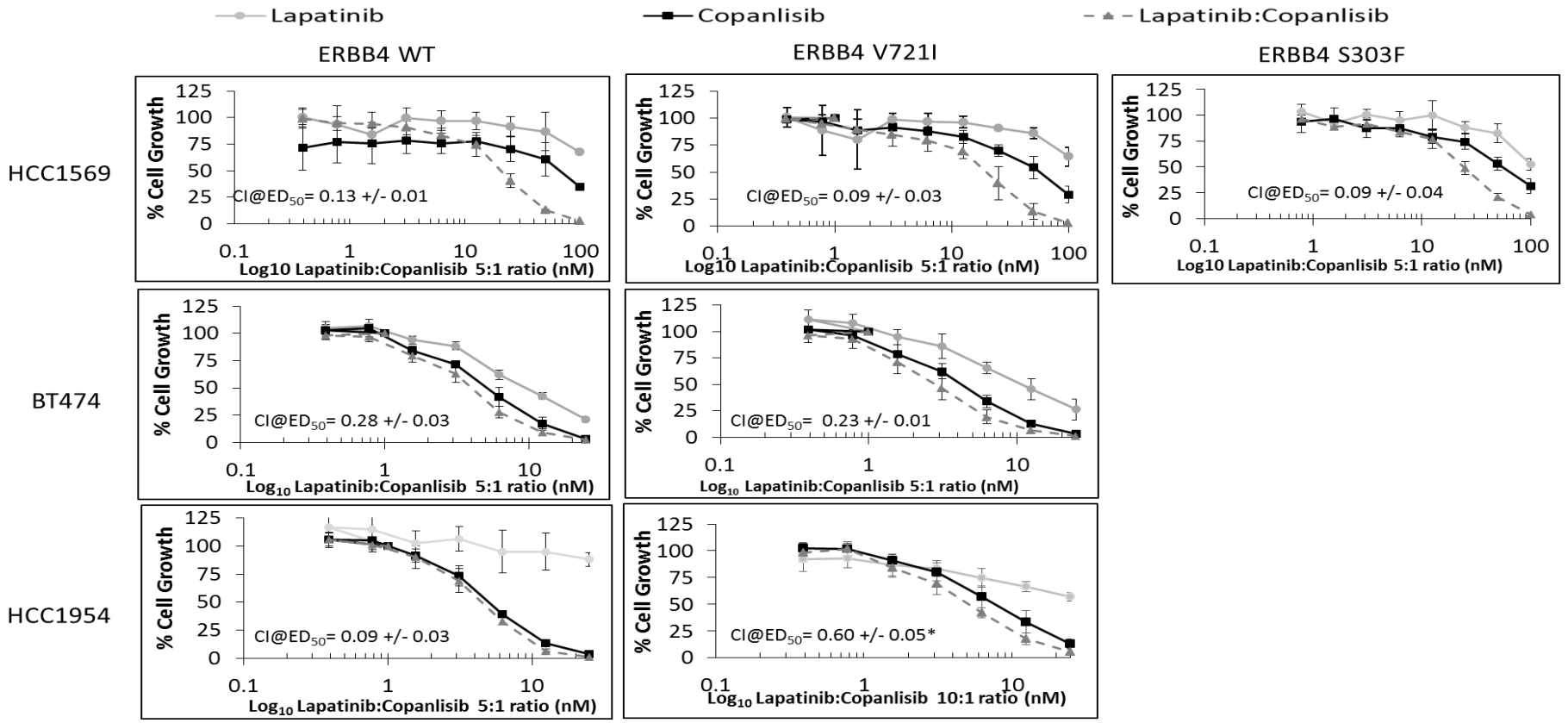

Figure 5.7 Efficacy of lapatinib (-◊-), copanlisib (-□-) and a combination of lapatinib and copanlisib (--Δ--) in a panel of HER2-positive cell lines stably expressing ERBB4 WT, V721I or S303F. Acid phosphatase toxicity assays were used to investigate the effect of a serial dilution of the drugs on these HER2-positive breast cancer cell lines over a 5 day period and the resulting dose-response curves were analysed with Calcusyn (Biosoft).Error bars are representative of standard deviations across triplicate experiments. * b= p < 0.05 compared to cells transfected with WT (2-tailed Student's T-Test with equal variance). CI (Combination Index) values were calculated using Calcusyn software according to the Chou-Tallalay method. A CI value of 1 denotes additivity, with a CI < 1 denoting synergy and of > 1 denoting the two drugs in combination are antagonistic. Lapatinib:Copanlisib was tested at a 5:1 ratio (top conc 500nM:100nM).

Table 5.4 The IC_{50}s of lapatinib in combination with copanlisib compared to the IC_{50} of each as a single agent and Combination Index (CI) values at ED_{25}, ED_{50} and ED_{75} for the combination of lapatinib and copanlisib. IC_{50} and CI values were calculated with CalcuSyn software (Biosoft) according to the Chou-Tallalay Synergy Quantification method. A CI of 1 denotes additivity, < 1, synergy, and > 1, antagonism. Lower CI values denote higher synergy. Standard deviations are representative of independent triplicate experiments. * = p < 0.05 compared to cells transfected with WT pER<BB04. 0b5y cSotmupdaernetd' st ot cells tra t-test (2-tailed with equal variance)

	Lapatj(nniM $_{50}$	Lapatjinnibcdin $_{50}$ with copanlisib	CI @ED $_{25}$	CI @ED $_{50}$	CI @ED $_{75}$
HCC1569					
ERBB4 W	514.02 +/- 30.50	22.21 +/- 4.88	0.16 +/- 0.01	0.13 +/- 0.01	0.11 +/- 0.01
ERBB4 V	503.67 +/- 33.42	25.36 +/- 4.26	0.17 +/- 0.03	0.09 +/- 0.03	0.06 +/- 0.04
ERBB4 S	736.41 +/- 51.55	17.12 +/- 3.81 (vs VI p = 0.07)	0.09 +/- 0.01*^	0.09 +/- 0.04	0.10 +/- 0.07
BT474					
ERBB4 W	42.69 +/- 4.97	3.59 +/- 1.18	0.37 +/- 0.10	0.28 +/- 0.03	0.22 +/- 0.01
ERBB4 V	44.78 +/- 4.12	2.69 +/- 0.89	0.29 +/- 0.02	0.23 +/- 0.01	0.20 +/- 0.01
HCC1954					
ERBB4 W	894.24 +/- 42.16	3.79 +/- 0.11	0.13 +/- 0.04	0.09 +/- 0.03	0.07 +/- 0.01
ERBB4 V	789.48 +/- 89.44*	5.63 +/- 0.09*	0.69 +/- 0.16*	0.60 +/- 0.05*	0.57 +/- 0.01*

We previously found the combination of trastuzumab and copanlisib to inhibit the growth of HER2-positive breast cancer cells better than either agent used alone[22]. Here, we demonstrate that trastuzumab:copanlisib inhibited the growth of the following cell line models more effectively than either therapy alone, although this was significant only at certain doses (Figure 5.8): BCC1569-ERBB4 WT, HCC1569-ERBB4 S303F, BT474-ERBB4 WT, BT474-ERBB4 V721I and HCC1954-ERBB4 V721I.

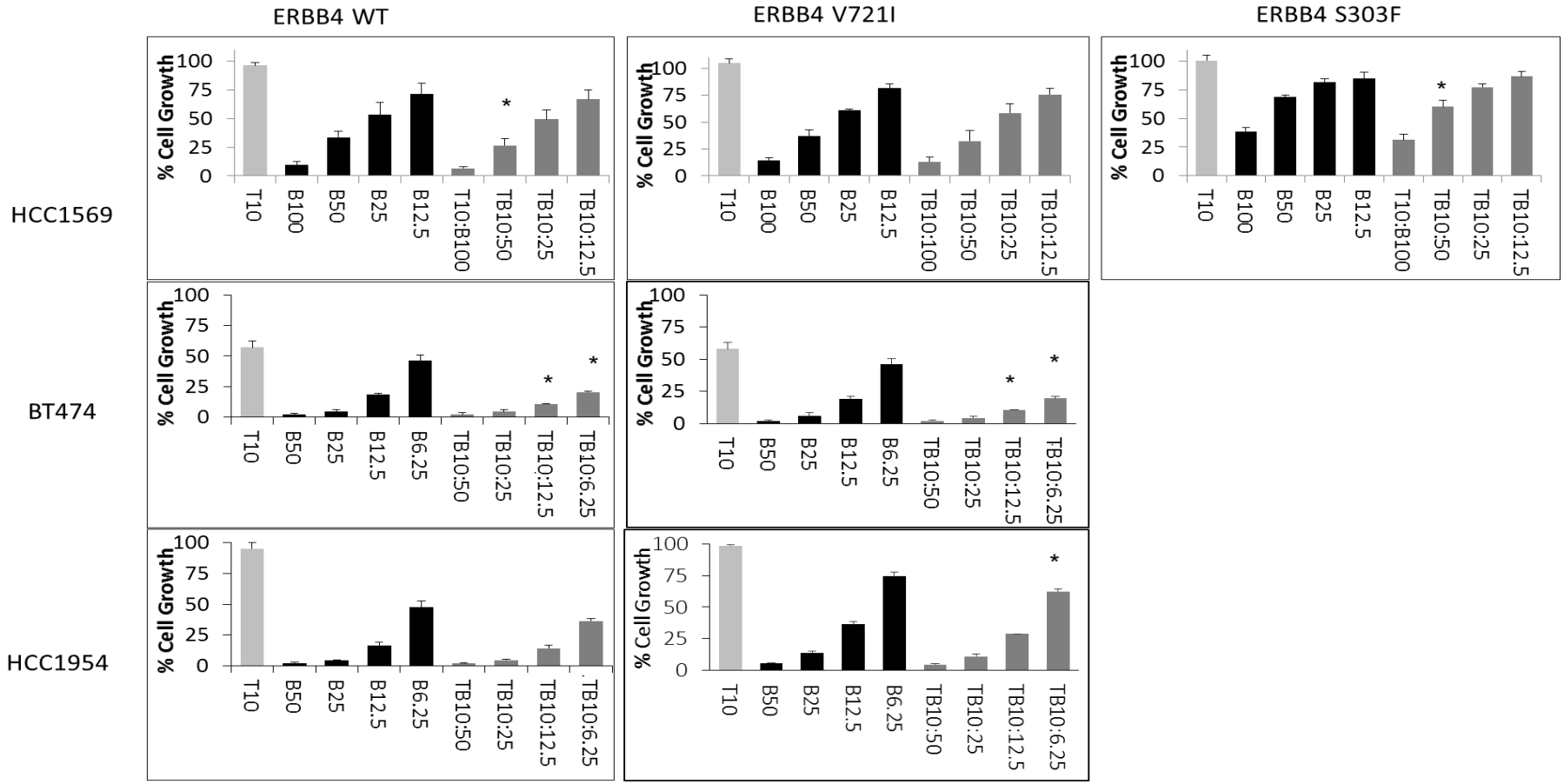

Figure 5.8 The efficacy of combining trastuzumab (T) and copanlisib (B) in a panel of HER2-positive cell lines stably expressing ERBB4 WT, V721I, or S303F. Acid phosphatase assays were used to investigate the effect of trastuzumab, copanlisib or the combination of both cell proliferation over a 5 day period. % growth is relative to untreated controls, which were normalised to 100 %. Error bars are representative of standard deviations across triplicate experiments. * = $p \leq 0.05$ compared to control (2-tailed t-test with both equal variance)

5.4 Discussion

5.4.1 Discussion

Little functional work has been done on ERBB mutations in HER2-positive breast or any cancer to date, but there is evidence to suggest that mutations in the ERBB family may have functional consequences for the cancer cell. EGFR mutations occur in approximately 5% of lung cancers and mostly sensitize these cancers to EGFR inhibitors. EGFR-V769L has been reported as a rare mutation in non-small cell lung cancer, in which it confers resistance to gefitinib[67]. ERBB3 Q809R was previously reported in a study of gastric and colon cancer, where it was shown to be oncogenic *in vitro* when it was expressed in the presence of HER2[41]. Further, it has been shown that somatic activating ERBB2 mutations are present in HER2-negative breast tumours and render these breast cancer cells sensitive to the HER2-targeted therapy neratinib[54].

Here, we show that in both the presence and absence of PIK3CA mutations, the ERBB4 kinase domain mutation V721I has profound functional effects on HER2-positive breast cancer cells, increasing HER4 protein expression (Figure 5.2), growth rate (Figure 5.3) and 3D colony forming ability (Figure 5.4), and altering sensitivity to HER family and PI3K inhibition (Table 5.2). This is in contradiction to what was seen previously, when ERBB4 V721I was shown not to result in altered HER4 kinase activity *in vitro* in the murine and human HER2-negative breast cancer cell lines 32D and MDA-MB-468[42]. We propose that the supposedly conflicting results between these published results and ours may point to a role for HER2 in the activity of this ERBB4 mutation. HER family proteins signal cooperatively through the formation of dimers[1]. HER family signalling is governed by a strict hierarchy with HER2 being the preferred dimerization partner of all other HER family proteins[79] and disrupting the ability of HER2 to heterodimerise interferes with the ability of HER2 to transform cells[70]. Further, Jaiswal *et al* reported that mutations in ERBB3 promote anchorage independent growth, interleukin-3 (IL-3)-independent survival and increases in HER2, HER3 and AKT phosphorylation only when co-expressed with HER2[41].

We also report that two different mutations in the same gene have significantly different effects. This may relate to the mutations being in different functional domains of the gene, with S303F in the furin-like domain, involved in dimerization, and V721I in the kinase domain. The functional effects of the mutations may also be influenced by the specific amino acids changed and resulting structural revisions – for example, alterations to a binding site – as different mutations within the same region have previously been shown to differently affect function. A computational study to predict the effects of these mutations *in silico* would likely yield useful mechanistic information on these mutations, but this was beyond both the scope and resources of this study.

While the ERBB4 kinase domain mutation V721I increased the HER4 expression and growth rate of HCC1569 cells, the ERBB4 furin-like domain mutation S303F did not increase HER4 expression or growth rate (Figure 5.3), and compared to V721I-transfected cells, the S303F-transfected cells grow more slowly (Figure 5.3) and form significantly fewer colonies (Figure 5.4). The effect of each mutation on the expression of the HER4 protein is also different (Figure 5.2). HER4 kinase activity has previously been shown to be necessary and sufficient for an anti-proliferative effect in breast cancer cells[80] and correspondingly, our V721I mutation induced lower levels of HER4 kinase activity and a faster growth rate than ERBB4 WT cell lines. Our furin-like domain mutation S303F induced a higher level of HER4 kinase activity and the expected increased anti-proliferative response may explain why this mutation was lethal to 2/3 cell lines. Although previous studies on the impact of HER4 have focused on protein expression, it may be that the kinase activity of this protein is as or more relevant and as or more likely to affect the behaviour of HER2-positive breast cancer than its expression.

The difference of effects between cell lines may partially relate to the PIK3CA genotype of each parent. Neither S303F nor V721I occurred in the presence of PIK3CA mutations in our clinical study, and the PIK3CA WT cell was the only one of our models in which we could establish S303F. PIK3CA mutations also affect HER2-

positive breast cancer in their own right. Although PIK3CA mutations probably do not affect survival in the adjuvant setting in HER2-positive breast cancer[44-46], PIK3CA H1047R, which is present in HCC1954, has previously been shown to enhance HER2-mediated transformation via upregulation of the HER3 ligand neuregulin *in vitro,*[81] and to promote lung metastasis and resistance to trastuzumab, lapatinib and pertuzumab *in vivo*.[82] The co-occurrence of ERBB and PIK3CA mutations in 3/227 samples in our clinical study demonstrates that mutations in these genes can co-occur, and the PI3K pathway is established to be a key downstream mediator of the oncogenic effects of HER family signalling[12].

Transfecting HER2-positive breast cancer cell lines with ERBB4, whether in its WT form or carrying the V721I/S303F mutations, largely induced sensitivity to the pan-HER inhibitor afatinib and to the PI3K inhibitor copanlisib in 2/3 cell lines but did not have the same effect on lapatinib sensitivity (Table 5.2). Although lapatinib and afatinib are both anti-HER2 TKI's, their mechanism differs in that lapatinib is a reversible inhibitor of HER2 and EGFR, whereas afaitinib is an irreversible, pan-HER inhibitor, which has been shown to bind strongly to HER4[83]. The increased expression of HER4 within a cell could therefore improve the affinity of afatinib. The kinase domain mutation V721I does not induce sensitivity to the same extent as WT ERBB4 in 2/3 cell lines tested. Another hypothesis is that the large increase in HER4 expression observed in the V721I-transfected cells (Figure 5.2) may either supply more receptors, hence increasing the affinity threshold, or act as a decoy to stop afatinib binding so strongly to HER2, and hence a higher dose may be needed to attain an IC_{50} (Table 5.2).

HER4 expression has been shown clinically to prolong OS in trastuzumab treated patients[84] ($p = 0.013$), to increase metastasis-free survival in the neoadjuvant setting ($p = 0.04$) and improve PFS ($p = 0.03$) and OS ($p = 0.47$) in the metastatic setting[85]. However, it has also been shown to mediate acquired resistance to trastuzumab and lapatinib *in vitro*[86]. We did not see any effect of ERBB4 WT or either ERBB4 mutation on trastuzumab sensitivity in any of our transfected cell lines (Table 5.2).

The combinations of copanlisib with the HER2-targeted therapies afatinib, lapatinib and trastuzumab, which were previously shown to be synergistic by us in established HER2-positive breast cancer cell lines[22] and are now in a clinical trial in Ireland of women with metastatic HER2-positive breast cancer, largely remain synergistic regardless of ERBB4 mutation status, and, in the case of the S303F hotspot mutation, synergy between afatinib and copanlisib is significantly enhanced (Table 5.3).

5.4.2 Summary and Conclusion

ERBB4 mutations do not affect trastuzumab efficacy *in vitro*. The ERBB4 mutations V721I and S303F occur in different functional domains of the same gene, and have different effects on HER2-positive breast cancer cells, altering growth, HER4 expression, colony formation, and sensitivity to therapies. The finding that ERBB4 mutations may enhance the efficacy of the PI3K inhibitor copanlisib relative to ERBB4 WT and enhance afatinib:copanlisib synergy suggests that patients on our ongoing clinical trial of trastuzumab:copanlisib should be profiled for their ERBB mutational status in order to evaluate the potential of ERBB mutations as clinical biomarkers. Here, we show that ERBB4 mutations have potential to alter the sensitivity of HER2-positive breast cancer cells to pan-HER and PI3K inhibition *in vitro*. Our phase Ib/II study gives us the opportunity to investigate whether these effects may hold true clinically.

Chapter 6 General Discussion and Future Directions

6.1 General Discussion

6.1.1 Targeting the PI3K pathway for the treatment of HER2-positive breast cancer

Breast cancer remains one of the most commonly diagnosed cancers and a leading cause of mortality in women[87]. 20-25 % of breast cancers are HER2-positive, with overexpression of the HER2 receptor associated with shorter time to relapse and decreased overall survival[10]. Trastuzumab was the first therapy to exploit HER2-positive breast cancer's addiction to HER2. HER2-targeted therapies have significantly improved outcomes for HER2-positive breast cancer patients, but *de novo* or acquired resistance to HER2-targeted therapies remains a challenge[1].

The PI3K pathway is one of the most frequently deregulated pathways in cancer and is thought to drive the oncogenesis of up to 30 % of cancers, with mutations, amplifications and other abnormalities found in a number of PI3K pathway components across several cancer types[12]. For example, somatic mutations in PTEN, a negative regulator of the PI3K pathway, are found in melanomas, endometrial and ovarian cancers, and PIK3CA amplification can be found in cervical and lung cancers[12]. PIK3CA has been confirmed as a transforming oncogene, and PTEN loss stimulates tumour development in mice.

Specifically in breast cancer, PIK3CA mutations have consistently been shown to occur at high frequencies: 34.5 % in hormone receptor positive, 22-26 % in HER2-positive, and 8.3 % in triple-negative tumours[13]. PIK3CA mutations are significantly associated with HER2 overexpression ($p = 0.04$)[25]. Other indications that the PI3K pathway is deregulated in breast cancer include AKT1 (1.4 %) and PTEN mutations (2.3 %) in hormone receptor-positive breast cancers[13] and the discovery that PIK3CA mutations are mutually exclusive with PTEN loss[25].

The PI3K pathway was highly mutated in our HER2-positive breast cancer sample set, with alterations in a number of different PI3K pathway components. PIK3CA mutations in our human tumour study occurred at a frequency (26 %) similar to what

has been previously reported[13, 44, 46], suggesting that PI3K is likely to be a useful therapy target in HER2-positive breast cancer.

As part of our preclinical study, we characterised a panel of HER2-positive breast cancer cell lines for their PI3K signalling by RPPA and their PIK3CA status by Sequenom. We demonstrated that our HER2-positive breast cancer cell lines have activated PI3K signalling, regardless of PIK3CA mutation or PTEN expression status. This *in* vitro work adds support to the notion of the PI3K pathway being deregulated in HER2-positive breast cancer.

Initial attempts to inhibit the PI3K pathway targeted mTOR. Despite promising preclinical efficacy for mTOR inhibition[88], the BOLERO3 trial of the mTOR inhibitor everolimus in combination with trastuzumab reported that the addition of everolimus did not greatly improve survival outcomes and led to significant toxicity[89]. mTOR may not be an ideal target as mTOR inhibition triggers a negative feedback loop which results in further activation of AKT[16], likely limiting the efficacy of mTOR inhibitors in blocking PI3K pathway signalling.

A primary function of the PI3K pathway is cell survival. It may thus be more effective to preferentially target PI3K mediators which inhibit apoptosis, rather than mTOR, which regulates growth translation. Further, mTOR itself is only one downstream target of PI3K/AKT. When selecting a PI3K inhibitor to use in our studies, we hypothesised that a direct PI3K inhibitor could circumvent mTOR inhibition-induced feedback and more thoroughly inhibit all downstream mediators of PI3K. We also drew on the knowledge that, although three distinct classes of PI3Ks exist, Class I PI3Ks are most involved in human breast cancer, with the alpha isoform (PIK3CA) likely to be the predominant target in this cancer type[26].

Copanlisib (BAY 80-6946) is a novel, potent pan-class 1 PI3K inhibitor which is highly effective against PI3K, in particular isoforms α and δ, but has no activity against over 200 other serine/lipid kinases against which it was tested [200]. It has IC_{50}s in the low nanomolar range in 160 cell lines covering 14 tumour types and has been shown to

induce apoptosis and inhibit VEGF-mediated angiogenic effects [200]. It has been shown to inhibit tumour growth *in vivo* [201] and was well-tolerated in a phase 1 trial [202]. It has shown synergy with the EGFR inhibitor erlotinib in the treatment of non-small cell lung cancer (NSCLC) [205]. As an α PI3K isoform inhibitor, copanlisib may optimise anti-tumour activity in HER2-positive breast cancers, in particular those that are PIK3CA mutated. Ours is the first study of copanlisib in HER2-positive breast cancer.

We show that copanlisib potently inhibits the proliferation of HER2-positive breast cancer cells, achieving low nanomolar IC_{50}s in a panel of HER2-positive breast cancer cell lines incorporating models which were sensitive to, as well as models of acquired and *de novo* resistance to trastuzumab and lapatinib. We also demonstrate that copanlisib diminishes the ability of HER2-positive breast cancer cells to invade through matrigel and to form anchorage-independent 3D colonies. Copanlisib was effective in PIK3CA WT and PIK3CA mutated cell lines.

While our proteomic work confirmed copanlisib inhibits PI3K signalling, neither inhibition of AKT phosphorylation at S473 nor PIK3CA mutations were associated with any significant differences in copanlisib IC_{50}s, arguing that neither of these is a reliable biomarker for the efficacy of copanlisib. However our panel of cell lines was limited and more studies are required for definitive demonstration of this.

Feedback upregulation of HER3 expression and phosphorylation has been shown to limit the activity of the PI3K inhibitor XL147[32]. We did not observe a significant change in total HER3 expression in our cell line panel following treatment with copanlisib. Further, we found that HER3 phosphorylation significantly decreased in response to copanlisib treatment in 3/10 cell lines tested, suggesting that HER3 may not be a mediator of resistance to copanlisib. 4/10 cell lines had an increase in MAPK phosphorylation at T202/Y204 in response to copanlisib. This suggests the MAPK pathway may compensate for PI3K inhibition in some cases, enabling resistance to PI3K inhibitors, and argues that the co-targeting of PI3K and MAPK pathways should be tested preclinically in HER2-positive breast cancer. The combination of copanlisib

with a MEK inhibitor has potential in the treatment of non-small-cell lung cancer and colorectal cancer[19].

There is evidence that the PI3K pathway confers a survival advantage on cells subjected to stress, and confers resistance to anti-cancer strategies such as chemotherapy, radiotherapy, and targeted drugs. While clinical studies on the predictive benefit of PIK3CA mutations are conflicting[44-46], strong preclinical evidence points to PI3K pathway activation as a major determinant of trastuzumab resistance[3, 26, 90]. The ability of trastuzumab and lapatinib to inhibit tumour growth has been associated with their ability to inhibit AKT signalling, and most of the currently known mechanisms of trastuzumab resistance directly or indirectly involve the PI3K pathway, e.g., IGF1R signals upstream of PI3K, whereas MET receptor upregulates AKT, and PIK3CA mutation and PTEN loss directly increase activation of the PI3K pathway[1]. *In vitro* studies have clearly shown the PI3K pathway to be involved in trastuzumab resistance[26]; although reports on its role in lapatinib resistance have been conflicting[3, 26].

We show clear synergy between copanlisib and HER2-targeted therapies in trastuzumab/lapatinib sensitive models and models of acquired resistance. In all models of acquired resistance, co-targeting the HER family and PI3K led to a restoration of sensitivity to the HER2-targeted therapy. We also show an inhibition of 3D colony formation when copanlisib is tested both alone and in combination with the HER2/HER3 dimerization inhibitor pertuzumab.

The upregulation of MAPK signalling in response to copanlisib treatment was inhibited when copanlisib was tested in combination with lapatinib, which further supports a combination rather than a single-agent approach as the best strategy in HER2- positive breast cancer.

The addition of copanlisib did not improve the efficacy of HER2-targeted therapies in *de novo*resistant cell lines, suggesting that co-targeting PI3K and HER proteins is most appropriate for those patients whose HER2-positive breast cancer has

progressed after an initial period of response. However, copanlisib alone still achieved a low nanomolar IC_{50} in *de novo* trastuzumab/lapatinib- resistant cell lines.

Copanlisib had been previously shown to be safe and well-tolerated in humans, to induce apoptosis *in vitro* and to have potent and selective antiproliferative activity across 160 cell lines in a range of cancers including breast[18], when tested as a single agent. Ours is the first preclinical study of copanlisib in HER2-positive breast cancer[22], but its previous success in a Phase I trial in solid tumours (including two breast cancer patients, one of whom was HER2-positive) ensured that any promising *in vitro* effects we discovered could be quickly translated to a clinical study.

Based on our work a clinical trial, the Panther study (ICORG 15-02), is about to start accruing women with recurrent or metastatic HER2-positive breast cancer which has been previously treated with trastuzumab in the adjuvant setting. The trial will test trastuzumab in combination with copanlisib in these patients. Trastuzumab is a monoclonal antibody with a well-established safety profile. Although our most promising results, both in terms of synergy and ablation of the potential MAPK resistance mechanism, were derived from the combination of lapatinib and copanlisib, combining two potent small molecule inhibitors has a greater potential for toxicity, especially in light of the diverse functional effects of the PI3K pathway[12].

A translational study within the Panther trial aims to identify and validate biomarkers for copanlisib efficacy based on the clinical and functional ERBB mutation studies presented in this thesis. We have demonstrated that the combination of copanlisib with HER2-targeted therapies is a promising strategy for the treatment of HER2-positive breast cancer with acquired trastuzumab resistance and this will be tested in our clinical trial. We subsequently discovered that the ERBB4 kinase domain mutation V721I alters sensitivity to copanlisib, in addition to rendering HER2-positive breast cancer cells less sensitive to HER inhibitors. Our translational study within the Panther trial will determine if any of the patients enrolled have somatic ERBB family mutations in their tumours, and if patients with ERBB mutations do better with

copanlisib-trastuzumab treatment. This will potentially identify another biomarker for copanlisib efficacy.

6.1.2 The suitability of the next-generation kinome sequencing platform for the discovery and validation of ERBB and PIK3CA Mutations in HER2-positive breast cancer

We considered a number of approaches for our sequencing study. These included Sanger sequencing and next-generation sequencing (NGS), in collaboration with other academic institutions, or outsourcing the sequencing to industry.

The only tissue available to us with sufficient follow-up was formalin-fixed, paraffin-embedded (FFPE). We wished to sequence the full length of five genes (the four ERBB genes and PIK3CA), which, had we used conventional Sanger methods, would have demanded high quantities of DNA, which were unlikely to be obtained from FFPE tumour tissue. NGS was more efficient in terms of financial cost and quantity of DNA needed. NGS techniques at the time were optimised for fresh-frozen tissue samples but a small number of publications had claimed that NGS could be used for FFPE, even though FFPE samples do tend to be of lower quality[56].

The MiSeq instrument can generate 24-30 million sequence reads passing QC filters on a single 2x150bp run in 24 hours. This approximates to 3.7 Gb of sequence data. As we were targeting <500kb of genomic DNA (and assuming 75% of the sequence reads align back to our target region) we expected to obtain over 100X coverage per target base, allowing us to accurately detect variants in our samples.

Given the high coverage we expected, and that an NGS approach was ultimately better value than Sanger sequencing, we decided to maximise on the high throughput nature of NGS sequencing. By expanding our focus to include several hundred genes of the kinome beyond our key genes of interest, we aimed to reach a more comprehensive understanding of the genetic background of HER2-positive breast cancer.

Following an extensive consultation process with third parties including Source Bioscience and TrinSeq, the Trinity College Dublin sequencing laboratory , we

selected the Agilent SureSelect™ 612-gene Kinome Panel to use with an Illimina MiSeq™ benchtop sequencer. The cost of purchasing our own sequencing technology was prohibitive, and we had access, through collaborators, to the Illumina MiSeq.

Many NGS panels do not provide full coverage of the ERBB3 gene, which was of particular interest to us given the established role of HER3 in the oncogenesis of HER2-positive breast cancer[71]. A key factor in our decision to use the SureSelect™ panel was that it provided full coverage of ERBB3, as well as of the other genes of the ERBB family.

Ultimately, the coverage we achieved was lower than we had anticipated based on the best knowledge available to us at that time. Several of our samples had to be excluded due to not reaching a threshold coverage of 30X. Our use of archival FFPE samples may partially explain the low coverage attained. FFPE DNA is frequently fragmented or sheared, which may reduce the ability of probes to bind. As they are less frequently sequenced than other genes, for example PIK3CA, the kinome panel may contain fewer probes for the ERBB genes, possibly also contributing to low coverage.

With the exception of ERBB4 G599W, none of our validated ERBB mutations were detected by our NGS panel. The NGS panel detected a number of ERBB gene mutations which failed to validate by sequenom. In contrast, our PIK3CA mutation results were generally concordant between Sequenom and NGS at 30X coverage.

Illumina recommends a sequencing depth of 10X – 30X for detecting human genome mutations. This proved sufficient for us to detect mutations in the relatively well-characterised PIK3CA gene, which we successfully validated and found to occur at a frequency of 26 % in HER2-positive breast cancer. However, based on our findings and the discrepancy between our NGS and Sequenom results for the ERBB family (a similar discrepancy between NGS and digital PCR has been reported by other authors[58]), we argue that a higher depth of up to 100X is necessary to detect rare mutations such as those observed in ERBB family genes in 7 % of cases in our study.

We also found that the manufacturer's protocol resulted in large losses of DNA quantity post-sample preparation, which was a significant concern given the relatively low yield of our FFPE tissue samples (extracted DNA ranged from <1 µM to >5 µM). Newer techniques contain fewer steps during the sample preparation procedure in order to retain as much DNA as possible.

In summary, our experience is that the NGS Agilent SureSelect™ kinome panel is a useful exploration tool, but that 30X coverage is not sufficient to uncover low frequency mutations. Our sequenom study revealed two hotspot mutations in ERBB genes in HER2-positive breast cancer, ERBB3 Q809R and ERBB4 S303F, neither of which were picked up on our NGS panel at 30X coverage, or in other NGS studies of HER2-positive breast cancer. Strong bioinformatics support is essential to eliminate false positives, and any mutations discovered through an NGS platform must be validated.

Our study investigated the frequency of functional somatic mutations in the ERBB family, and of the overall somatic mutation rate in PIK3CA in HER2-positive breast cancer. We report these frequencies to be 7.05 % and 26.43 %, respectively (n = 227 tumours). The frequency of PIK3CA mutations matches that in other published studies[44, 46]. The frequency of ERBB family mutations in our sample set was lower than we had anticipated based on Prof Hennessy's unpublished preliminary data that ERBB mutations are present in up to 20 % of HER2-positive breast cancers. This may in part reflect that the preliminary study did not sequence matched normal tissue, so a number of the variants uncovered may have been germline SNPs.

Recent studies confirm that ERBB gene mutations are relatively rare, across several cancer types. Publications report mutations at frequencies from 1/253 (lung[39]) to 5% (4/78) of HER2-positive breast tumours[38] (ERBB2), to 11 % ERBB3 mutations (gastric and colon[41]) and ERBB4 mutations in ~2 % of gastric, colorectal, breast and NSCLC cancers[77]. Mutations in individual ERBB genes occur at frequencies of 0.5 % to 6.9 %

in TCGA's breast cancer studies, and at frequencies of 1 % to 7 % within the TCGA HER2-positive breast cancer study.

We propose that in addition to determining the frequency of a mutation, the biology of the gene and location of the mutation, coupled with computational tools to predict amino acid and structural changes, should all be considered when selecting candidate mutations for further analysis.

Our ERBB mutations clustered in two domains with likely functional relevance. The kinase domain is involved in kinase signalling, and mutations in this domain have previously been shown to affect cell signalling and drug sensitivity, for example, mutations in exon 19 and 21 of EGFR are known to sensitise lung cancers to TKIs such as gefitinib and erlotinib[91]. The furin-like domain, the location of our ERBB4 hotspot mutation S303F, is of interest as it mediates the formation of homo- and heterodimers, and this dimerisation is a crucial first step in HER family signalling[1]. Further, our mutations were predicted as likely deleterious by two independent bioinformatic tools.

We demonstrate that even rare mutations can have functional relevance. Miller and colleagues argue that analysing domains that are enriched for mutations, or "domain hotspots" can enable the detection of rare mutations with novel functional effects. Their analysis of data from over 5000 tumours across 22 cancer types from TCGA found that mutations cluster in domains involved in tyrosine kinase receptor signalling, including the kinase and furin-like domain, which is reflected in the ERBB family mutations which we discovered. Excitingly, they identified ERBB S303F as a mutation warranting further study, as it aligns with ERBB2 S310F/Y, which is an activating mutation in a rare form of bladder cancer. Here, we confirm their hypothesis by showing the ERBB4 S303F is lethal to 2/3 cell lines and in general does not promote growth, invasiveness, or protein expression, and renders HER2-positive breast cancer cells exquisitely sensitive to afatinib. We also confirm that two mutations from different functional domains in the same gene have different effects.

Although we did not see any significant association between ERBB family mutations and clinical/histological features or survival after adjuvant trastuzumab therapy in HER2-positive breast cancer, we speculate that an assay for ERBB family mutations in a larger sample set will reveal definitively if ERBB mutations affect survival outcomes after trastuzumab.

A limitation of grouping our ERBB family mutations together for the purposes of survival analyses is that individual mutations within our set may have opposing effects which cancel each other out; this is particularly relevant in light of our *in vitro* findings that the ERBB4 mutations S303F and V721I have different effects when stably expressed *in vitro*: while V721I is strongly oncogenic, S303F is not, and is even lethal to 2/3 cell lines we transfected.

Compared to the ERBB family, PIK3CA mutations are well studied in HER2-positive breast cancer. Our PIK3CA mutation frequency is consistent with previous reports. Our finding that PIK3CA mutations are not associated with survival outcomes in early stage HER2-positive breast cancer is also consistent with previous work[46].

6.1.3 The Role of wild-type and mutated ERBB4 in HER2-positive Breast Cancer

ERBB mutations occur in 7 % of HER2-positive breast cancers in our clinical study. A limited number of ERBB mutations have been comprehensively functionally characterised to date. We selected the ERBB4 gene as a candidate for functional analysis as it was the most frequently mutated gene in our study, and contained the hotspot S303F, which had not been previously published (unlike our ERBB3 hotspot Q809R, which had been characterised, albeit in gastric rather than breast cancer[41]).

An ERBB4 WT lentiviral plasmid was available from Addgene, which we used as a template to construct the ERBB4 S303F and V721I mutations. Our plasmids thus had a lentiviral backbone and we had access, through our collaborators, to expertise in this transfection system, which was well-validated, in comparison to newer technologies like CRISPR which was relatively untested at the time.

We investigated antibodies for total and phospho-HER4 and realising that none were validated, we chose to carry out kinase assays to investigate HER4 signalling activity. We show that cells carrying the kinase domain ERBB4 mutation V721I overexpress HER4 protein and are less kinase-active than ERBB4 WT cells. HER4 kinase activity has been shown to mediate an antiproliferative effect[80]. Accordingly, our V721I cells with the fastest growth rate had the lowest level of HER4 kinase activity. The S303F ERBB4 furin-like domain mutation had increased kinase activity compared to ERBB4 WT cells, and did not increase growth rate. Further, this mutation was lethal to 2/3 cell lines transfected.

Our results are in accordance with published work showing increased HER4 kinase activity decreases cell proliferation[80] but disagree with a previous report that ERBB4 mutations do not affect HER4 kinase activity[42]. The finding that ERBB4 mutations have no impact on HER4 kinase activity came from a study using HER2-negative cell lines, whereas our results, showing a clear effect of V721I and S303F on HER4 kinase activity, are based on HER2-positive breast cancer models. Jaiswal *et al* reported that ERBB3 mutations promote ligand-independent signalling *in vitro* and tumorigenesis *in vivo* but only when expressed in the presence of HER2[41]. Although we did not test

HER2-negative models, we show similar results with ERBB4 mutations when stably expressed in HER2-positive breast cancer cell lines, with effects on kinase activity, growth rate, 3D colony formation and drug sensitivity. Taken together, our findings and others' potentially point to the importance of HER2 signalling in HER4 activity, and reflect the knowledge that HER-family signalling is controlled by a strict hierarchy, with HER2 the preferred dimerization partner of all other HER family members[92].

The formation of 3D colonies within a soft agar matrix is a surrogate for anchorage-independent growth, one of the hallmarks of cancer. HER2-positive breast cancers carrying the V721I mutation form significantly more colonies in soft agar than corresponding cells transfected with ERBB4 WT. S303F cells form fewer 3D colonies than ERBB4 WT cells, although this is not significant. Taken together, these data suggest that the V721I mutation is oncogenic, and the S303F mutation likely less so.

Having shown that ERBB4 mutations affect the biology of HER2-positive breast cancer cells, and given that ERBB gene mutations affect drug sensitivity in other cancers[54, 67] we investigated the effect of ERBB4 mutations on responsiveness of HER2-positive breast cancer cells to HER2-targeted therapies and the PI3K inhibitor copanlisib.

We discovered that transfection of WT ERBB4 increased sensitivity to the pan-HER inhibitor afatinib relative to parental cells. This is a particularly relevant finding as some authors have argued that pan-HER inhibition is not an ideal therapeutic strategy for HER2-positive breast cancer as it may negate the anti-oncogenic effects of HER4[84]. This argument has largely been refuted by recent clinical trial results reaffirming the potential of drugs such as afatinib and neratinib[1], but here we show that afatinib has potential in the treatment of HER2-positive breast cancer bearing an ERBB4 mutation. Further, we present convincing evidence that a hotspot ERBB4 mutation, S303F, renders HER2-positive breast cancer cells exquisitely sensitive to afatinib *in vitro* and may be applicable as a biomarker to identify patients most likely to benefit from pan-HER inhibition. We also show that the kinase domain mutation

V721I potentially decreases sensitivity to afatinib. In our cell line panel, cells with reduced HER4 kinase activity are more resistant to afatinib whereas cells with increased kinase activity are more sensitive.

The S303F mutation increased resistance to lapatinib, despite increasing sensitivity to afatinib. It has been reported that ERBB2 mutations sensitise HER2-negative breast cancer cells to neratinib (which is in the same drug class as afatinib), but that lapatinib was not effective in inhibiting the growth of these cells[54].

In a PIK3CA WT cell line (HCC1569), both ERBB4 mutants we studied increased sensitivity to the pan class I PI3K inhibitor copanlisib, whereas the ERBB4 V721I mutation increased resistance to it in the HCC1954 cell line, which carried the H1047R PIK3CA mutation. It is particularly interesting that the hotspot mutation S303F which occurs in multiple patient samples in our clinical study may be a biomarker of sensitivity to copanlisib. It has been shown that copanlisib is effective in PIK3CA mutated cell lines[18]. Our preclinical study demonstrated that it is also effective in PIK3CA WT HER2-positive breast cancer cell lines[22].

Our results indicate that PIK3CA mutations may not be a robust biomarker for copanlisib sensitivity in HER2-positive breast cancer, but that ERBB mutations may be useful to identify patients more likely to benefit from copanlisib. We found that combining copanlisib with trastuzumab, or lapatinib, or afatinib remains an effective treatment strategy in HER2-positive breast cancer cells regardless of ERBB4 mutation status.

One aim of this thesis was to determine the effect of ERBB gene mutations on sensitivity to HER2-targeted therapies. Several clinical studies have reported that HER4 expression is associated with more favourable outcomes, significantly correlating with increased cumulative survival ($p = 0.01$)[92], and prolonged OS ($p = 0.01$)[84], RFS ($p = 0.001$) and breast cancer specific survival ($p = 0.001$) after trastuzumab[93].

Our study was focused on the mutational status and *in vitro* functional interrogation of the ERBB4 gene as opposed to HER4 protein overexpression, but we did note that the transduction of the ERBB4 WT gene into a panel of HER2-positive breast cancer cells resulted in overexpression of the HER4 protein relative to the corresponding parental cell line. However, no difference was observed between control and WT-transduced cell lines' sensitivity to trastuzumab, and neither the V721I nor the S303F ERBB4 mutations alter the efficacy of trastuzumab in inhibiting HER2-positive breast cancer cell growth, suggesting that ERBB4 mutational status does not affect sensitivity or resistance to trastuzumab.

In contrast to its fellow HER family members, HER4 overexpression is associated with a better outcome clinically[84, 93] and an antiproliferative response *in vitro*[80]. However, there are some reports that HER4 may promote the proliferation of breast cancer cells *in vitro*[94], but these reports have not been validated clinically, and there is some evidence to suggest HER4 has a role in resistance to therapy in breast and other cancers[86].

It is important to note that many clinical studies of HER4 to date have limitations. The lack of a validated HER4 antibody reduces confidence in overexpression studies, especially when one publication reported that HER4 could predict outcome when it was quantified by FISH, but not by IHC[59]. Similarly, a recent study has shown that in both HER2-positive and triple negative breast cancer, HER4 was significantly associated with a favourable prognosis in a univariate analysis, but that this significance disappeared when a multivariate analysis was carried out taking known risk factors such as age and tumour grade into account[95].

It has been proposed that different isoforms of HER4 may explain some of the conflicting results thus far. However, it has recently been shown that only one HER4 isoform is expressed in breast cancer (JM-a)[85]. My work provides the first convincing evidence that mutations within ERBB4 may account for some of the conflicting results reported so far: we clearly demonstrate that ERBB4 WT, V721I and S303F have distinct effects on a panel of HER2-positive breast cancer cell lines.

6.1.4 Summary and Conclusion

Through the work presented in this thesis, we build on previous knowledge of the PI3K pathway as a major determinant of trastuzumab resistance by demonstrating the potential of combining the pan-class I PI3K inhibitor copanlisib with HER2-targeted therapies as a treatment for trastuzumab-resistant cells. My published work in this regard has led to the initiation of the Panther clinical trial. We identify novel, somatic ERBB family mutations in 7 % of our HER2-positive breast cancer samples, and demonstrate that two of these, the ERBB4 mutations S303F and V721I, have functional effects on the biology of HER2-positive breast cancer cells. We also demonstrate that these ERBB4 mutations have potential as predictive biomarkers, as they affect the efficacy of the pan-HER inhibitor afatinib and the PI3K inhibitor copanlisib *in vitro*.

6.2 Future Directions

The data presented in this thesis argue that further research should be directed to unravelling the role of ERBB mutations, and the role of ERBB4, wild-type and mutated, in the biology and therapy responsiveness of HER2-positive breast cancer.

ERBB4 mutations are functional *in vitro,* and particularly our finding that mutants which trigger increased HER4 protein expression are associated with decreased kinase activity, argues that a thorough investigation of the signalling differences between WT and mutated ERBB4 should be carried out.

The ideal way to do this would be to carry out an extensive reverse phase protein array (RPPA) study using a range of different antibodies covering the HER family proteins and the PI3K and MAPK pathways. The panel should include both total and phospho protein antibodies to compare the effect of mutations on activation as well as expression of a number of pathway components relative to ERBB4 WT cells. This RPPA study could be expanded to further understand how ERBB4 mutations affected the efficacy of afatinib and copanlisib we observed in our study, by treating our construct cell lines with sub-lethal doses of these drugs prior to lysing them.

As stated previously, the formation of homo- and heterodimers within the HER family is known to be a crucial first step in HER family signalling, and the furin-like domain, which contains our hotspot mutation S303F and generally exerts anti-oncogenic effects, is involved in dimerization. There is some published evidence that the HER receptors present in breast tissue may influence the dimers that can form, and that HER4 may not dimerise as readily as other HER family members[92]. Separate studies have shown a positive correlation between HER3/4 at the mRNA level[93, 96] and increased levels of ERBB3/4 mRNA correlate with a longer OS[96]. The HER2/3 heterodimer has been proposed to be the main oncogenic unit in HER2-positive breast cancer[71] and it has been suggested that HER4 may act as a decoy receptor, preventing HER2 from binding to HER3 or EGFR[97]. We propose that the ability of ERBB4 mutations, in particular furin-like domain mutations such as S303F, to alter

the dimerization patterns of HER2-positive breast cancer cells should be investigated by proximity ligation assays.

Finally, we have already demonstrated that the combination of the PI3K inhibitor copanlisib and HER2-targeted therapy is potentially an improved treatment option for HER2-positive breast cancer patients whose tumours have acquired resistance to trastuzumab[22]. It was our work which convinced Bayer Pharmaceuticals to fund the Panther phase Ib/II study of copanlisib and trastuzumab for Irish women with pre-treated recurrent or metastatic breast cancer (ICORG 15-02). The study has received regulatory approval and the phase I stage will open at three Irish sites in Q2 of 2016, the recruitment stage lasting twelve months. The study will open to five Irish sites for phase II, and recruitment will be open for 18 months. It is exciting that, thanks to our work, Irish patients will be amongst the first patients in the world to gain access to this promising new treatment.

The data presented in this thesis also show that ERBB family mutations can predict sensitivity to HER2-targeted therapy and copanlisib *in vitro*, and sequencing biopsies from the patients on the Panther study for their ERBB mutational status and carrying out a prospective study to determine if these mutations are associated with a better or worse outcome to the test compounds on the clinical trial would help determine if our *in vitro* results translate to the clinic.

Mutations in ERBB2 have been shown to sensitise triple negative breast cancer cells to HER2-targeted therapies[54] and a phase II clinical trial testing neratinib in patients with solid tumours containing mutated ERBB2 (including bladder, colorectal, endometrial, and ovarian cancers) is currently recruiting patients (NCT01953926). We show that the efficacy of afatinib, which is also in use for lung cancer, may be affected by ERBB4 mutations. We propose that the frequency of ERBB mutations and their impact on sensitivity to pan-HER inhibitors and PI3K inhibitors should be evaluated in other cancer types, particularly NSCLC, for which afatinib is being used, and leukaemia, in which copanlisib is being studied[17].

Bibliography

1. Slamon DJ, Clark GM, Wong SG, Levin WJ, Ullrich A, McGuire WL. Human breast cancer: correlation of relapse and survival with amplification of the HER-2/neu oncogene. Science 1987;235(4785): 177-82.
2. Gschwind A FO, Ullrich A. The discovery of receptor tyrosine kinases:targets for cancer therapy. Nature Reviews Cancer 2004;4.
3. Semba K KN, Toyoshima K, Yamamoto T. . A v-erbB-related protooncogene, c-erbB-2, is distinct from the c-erbB-1/epidermal growth factor-receptor gene and is amplified in a human salivary gland adenocarcinoma. PNAS 1985;82(19): 6497-501.
4. Yamamoto T IS, Akiyama T, Semba K, Nomura N, Miyajima N, Saito T, Toyoshima K. Similarity of protein encoded by the human c-erb-B-2 gene to epidermal growth factor receptor. 1986;319(6050): 230-4.
5. Coussens L Y-FT, Liao YC, Chen E, Gray A, McGrath J, Seeburg PH, Libermann TA, Schlessinger J, Francke U, et al. Tyrosine kinase receptor with extensive homology to EGF receptor shares chromosomal location with neu oncogene. . Science 1985;230(4730): 1132-9.
6. Drebin JA LV, Stern DF, Weinberg RA, Greene MI. Down-modulation of an oncogene protein product and reversion of the transformed phenotype by monoclonal antibodies Cell 1985;41: 697-706.
7. Drebin JA LV, Weinberg RA, Greene MI. Inhibition of tumor growth by a monoclonal antibody reactive with an oncogene-encoded tumor antigen. PNAS 1986;83(23): 9129-33.
8. King CR KM, Williams LT, Merlino GT, Pastan IH, Aaronson SA. Human tumor cell lines with EGF receptor gene amplification in the absence of aberrant sized mRNAs Nucleic Acids Research 1985;13: 8477-86.
9. Slamon DJ CG, Wong SG, Levin WJ, Ullrich A, McGuire WL. . Human breast cancer: correlation of relapse and survival with amplification of the HER-2/neu oncogene Science 1987;235: 177-82.
10. Muller W, et al. . Single-step induction of mammary adenocarcinoma in transgenic mice bearing the activated c-neu oncogene. . Cell 1988;54: 105-15.
11. DJ Slamon WG, LA Jones, JA Holt, SG Wong, DE Keith, WJ Levin, SG Stuart, J Udove, A Ullrich, Press and MF. . Studies of the HER-2/neu proto-oncogene in human breast and ovarian cancer. . Science 1989;244(4905): 707=12.
12. Wolff AC, Hammond ME, Hicks DG, et al. Recommendations for human epidermal growth factor receptor 2 testing in breast cancer: American Society of Clinical Oncology/College of American Pathologists clinical practice guideline update. J Clin Oncol 2013;31(31): 3997-4013.
13. Borley A, Mercer T, Morgan M, et al. Impact of HER2 copy number in IHC2+/FISH-amplified breast cancer on outcome of adjuvant trastuzumab treatment in a large UK cancer network. Br J Cancer 2014;110(8): 2139-43.
14. Berger M, et al. . Correlation of c-erbB-2 gene amplification and protein expression in human breast carcinoma with nodal status and nuclear grading. . Cancer Res. 1988;48: 1238-43.
15. Wright C ea. Expression of c-erbB-2 Oncoprotein: A Prognostic Indicator in Human Breast Cancer. . Cancer Research 1989;49: 2087- 90.

16. Gonzalez-Angulo AM ea. High risk of recurrence for patients with breast cancer who have human epidermal growth factor receptor 2-positive, node-negative tumors 1 cm or smaller. J Clin Oncol 2009;1(27(34)): 5700-6.
17. Ross J, et al. . The HER2/neu Gene and Protein in Breast Cancer 2003: Biomarker and Target of Therapy. . The Oncologist 2003;8: 307-25.
18. Duffy M, et al. . Use of molecular markers for predicting therapy response in cancer patients. . Cancer Treatment Reviews 2011;37: 151-59.
19. Gschwind A, Fischer OM, Ullrich A. The discovery of receptor tyrosine kinases: targets for cancer therapy. Nat Rev Cancer 2004;4(5): 361-70.
20. Sako Y MS, Yanagida T. Single-molecule imaging of EGFR signalling on the surface of living cells. Nature Cell Biology 2000;2.
21. Arnould L ea. Pathologic complete response to trastuzumab-based neoadjuvant therapy is related to the level of HER-2 amplification. . Clin Cancer Res 2007;1(13(21).): 6404-9.
22. C. H. Trastuzumab – Mechanism of Action and Use in Clinical Practice. . N Engl J Med 2007;357: 39-51.
23. De Placido S ea. Twenty-year results of the Naples GUN randomized trial: predictive factors of adjuvant tamoxifen efficacy in early breast cancer . Clin Cancer Res 2003;9: 1039-46.
24. Kathleen I. Pritchard MD, Lois E. Shepherd, M.D., Frances P. O'Malley, M.D., Irene L. Andrulis, Ph.D.,, Dongsheng Tu PD, Vivien H. Bramwell, M.B., B.S., and Mark N. Levine, M.D.,. HER2 and Responsiveness of Breast Cancer to Adjuvant Chemotherapy. N Engl J Med 2006;354(20).
25. Miettinen PJ, Berger JE, Meneses J, et al. Epithelial immaturity and multiorgan failure in mice lacking epidermal growth factor receptor. Nature 1995;376(6538): 337-41.
26. Riethmacher D, Sonnenberg-Riethmacher E, Brinkmann V, Yamaai T, Lewin GR, Birchmeier C. Severe neuropathies in mice with targeted mutations in the ErbB3 receptor. Nature 1997;389(6652): 725-30.
27. Lee KF, Simon H, Chen H, Bates B, Hung MC, Hauser C. Requirement for neuregulin receptor erbB2 in neural and cardiac development. Nature 1995;378(6555): 394-8.
28. Gassmann M, Casagranda F, Orioli D, et al. Aberrant neural and cardiac development in mice lacking the ErbB4 neuregulin receptor. Nature 1995;378(6555): 390-4.
29. Tidcombe H, Jackson-Fisher A, Mathers K, Stern DF, Gassmann M, Golding JP. Neural and mammary gland defects in ErbB4 knockout mice genetically rescued from embryonic lethality. Proc Natl Acad Sci U S A 2003;100(14): 8281-6.
30. Olayioye MA, Neve RM, Lane HA, Hynes NE. The ErbB signaling network: receptor heterodimerization in development and cancer. EMBO J 2000;19(13): 3159-67.
31. Cho HS, Mason K, Ramyar KX, et al. Structure of the extracellular region of HER2 alone and in complex with the Herceptin Fab. Nature 2003;421(6924): 756-60.
32. Riese DJ, Kim ED, Elenius K, et al. The epidermal growth factor receptor couples transforming growth factor-alpha, heparin-binding epidermal growth factor-like factor, and amphiregulin to Neu, ErbB-3, and ErbB-4. J Biol Chem 1996;271(33): 20047-52.

33. Livneh E RN, Berent A, Ullrich A, Schlessinger J. An insertional mutant of epidermal growth factor receptor allows dissection of diverse receptor functions. The EMBO Journal 1987;6(9): 2669-76.
34. Honegger AM SD, Schmidt A, Lyall R, Van Obberghen E, Dull TJ, Ullrich A, Schlessinger J. A Mutant Epidermal Growth Factor Receptor with defective Protein Tyrosine Kinase Is Unable To Stimulate Proto-Oncogene Expression and DNA Synthesis. Molecular and Cellular Biology 1987: 4568-71.
35. Redemann N HB, von ruden T, Wagner EF, Schlessinger J, Ullrich A. Anti-Oncogenic Activity of Signalling-Defective Epidermal Growth Factor Receptor Mutants. Molecular and Cellular Biology 1992: 491-98.
36. Moolenaar WH BA, Tilly BC, Verlaan I, Defize LHK, Honegger AM, Ullrich A, Schlessinger J. A point mutation at the ATP-binding site of the EGF-receptor abolishes signal transduction. The EMBO Journal 1988;7(3): 707-10.
37. Honegger AM KR, Ullrich A, Schlessinger J. Evidence that autophosphorylation of solubilized receptors for epidermal growth factor is mediated by intermolecular cross-phosphorylation. PNAS USA 1989;86: 925 - 29.
38. Siegel PM MW. Mutations affecting conserved cysteine residues within the extracellular domain of Neu promote receptor dimerization and activation. PNAS USA 1996;93: 8878-83.
39. Graus-Porta D, Beerli RR, Daly JM, Hynes NE. ErbB-2, the preferred heterodimerization partner of all ErbB receptors, is a mediator of lateral signaling. EMBO J 1997;16(7): 1647-55.
40. Jones RB GA, Krall JA, MacBeath G. A quantitative protein interaction network for the ErbB receptors using protein microarrays. Nature 2006;439.
41. Roskoski R, Jr. The ErbB/HER family of protein-tyrosine kinases and cancer. Pharmacol Res 2014;79: 34-74.
42. Moran MF KC, Anderson D, Ellis C, England L, Martin GS, Pawson T. Src homology region 2 domains direct protein-protein interactions in signal transduction. PNAS 1990;87: 8622-26.
43. Waksman G KD, Robertson SC, Pant N, Baltimore D, Birge RB, Cowburn D, Hanafusa H, Mayer BJ, Overduin M, Resh MD, Rios CB, Silverman L, Kuriyan J. Crystal structure of the phosphotyrosine recognition domain SH2 of v-src complexed with tyrosine-phosphorylated peptides. Nature 1992;358(6388): 646-53.
44. Stern DF KM, Cao H. Oncogenic Activation of p185neu Stimulates Tyrosine Phosphorylation In Vivo. Molecular and Cellular Biology 1988: 3969-73.
45. Kokai Y DK, Weiner DB, Myers JN, Nowell PC, Greene MI. Phosphorylation process induced by epidermal growth factor alters the oncogenic and cellular neu (NGL) gene products. PNAS 1988;85: 5389-93.
46. Witton CJ RJ, Going JJ, Cooke TG, Bartlett JMS. . Expression of the HER1-4 family of receptor tyrosine kinases in breast cancer. . J Pathol 2003;200: 290-7.
47. Qian X LC, Freeman JK, Dougall WC, Greene MI. Heterodimerization of epidermal growth factor receptor and wild-type or kinase-deficient Neu: A mechanism of interreceptor kinase activation and transphosphorylation. PNAS 1994;91: 1500-04.
48. Holbro T, Beerli RR, Maurer F, Koziczak M, Barbas CF, 3rd, Hynes NE. The ErbB2/ErbB3 heterodimer functions as an oncogenic unit: ErbB2 requires ErbB3 to drive breast tumor cell proliferation. Proc Natl Acad Sci U S A 2003;100(15): 8933-8.

49. Sergina NV, Rausch M, Wang D, et al. Escape from HER-family tyrosine kinase inhibitor therapy by the kinase-inactive HER3. Nature 2007;445(7126): 437-41.
50. Lipton A, Goodman L, Leitzel K, et al. HER3, p95HER2, and HER2 protein expression levels define multiple subtypes of HER2-positive metastatic breast cancer. Breast Cancer Res Treat 2013;141(1): 43-53.
51. Phillips GD, Fields CT, Li G, et al. Dual targeting of HER2-positive cancer with trastuzumab emtansine and pertuzumab: critical role for neuregulin blockade in antitumor response to combination therapy. Clin Cancer Res 2014;20(2): 456-68.
52. Garner AP, Bialucha CU, Sprague ER, et al. An antibody that locks HER3 in the inactive conformation inhibits tumor growth driven by HER2 or neuregulin. Cancer Res 2013;73(19): 6024-35.
53. Fujiwara S, Ibusuki M, Yamamoto S, Yamamoto Y, Iwase H. Association of ErbB1-4 expression in invasive breast cancer with clinicopathological characteristics and prognosis. Breast Cancer 2012.
54. Witton CJ, Reeves JR, Going JJ, Cooke TG, Bartlett JM. Expression of the HER1-4 family of receptor tyrosine kinases in breast cancer. J Pathol 2003;200(3): 290-7.
55. Sassen A, Diermeier-Daucher S, Sieben M, et al. Presence of HER4 associates with increased sensitivity to Herceptin in patients with metastatic breast cancer. Breast Cancer Res 2009;11(4): R50.
56. Monsey J, Shen W, Schlesinger P, Bose R. Her4 and Her2/neu tyrosine kinase domains dimerize and activate in a reconstituted in vitro system. J Biol Chem 2010;285(10): 7035-44.
57. Machleidt A, Buchholz S, Diermeier-Daucher S, Zeman F, Ortmann O, Brockhoff G. The prognostic value of Her4 receptor isoform expression in triple-negative and Her2 positive breast cancer patients. BMC Cancer 2013;13: 437.
58. Sassen A, Rochon J, Wild P, et al. Cytogenetic analysis of HER1/EGFR, HER2, HER3 and HER4 in 278 breast cancer patients. Breast Cancer Res 2008;10(1): R2.
59. Hennessy BT ea. Exploiting the PI3K/AKT Pathway for Cancer Drug Discovery. . Nature Reviews Drug Discovery 2005;4(12): 988-1004.
60. Cronin MR NK, Johnson NL, Granger DA, Cuevas BD, Wang J-G, Mackman N, Scott JE, Dohlman HG, Johnson GL. Defining MAP3 kinases required for MDA-MB-231 cell tumour growth and metastasis. Oncogene 2012;31: 3889-900.
61. Montero JC OA, Abad M, Ortiz-Ruiz MJ, Pandiella A, Esparis-Ogando A. Expression of Erk5 in Early Stage Breast Cancer and Association with Disease Free Survival Identifies this Kinase as a Potential Therapeutic Target. PLoSONE 2009;4(5).
62. Lev DC KL, Melnikova V, Ruiz M, Ananthaswamy HN, Price JE. Dual Blockade of EGFR and ERK1/2 phosphorylation potentiates growth inhibition of breast cancer cells. Br J Cancer. 2004;91(4): 795-802.
63. CJ WJaW. Signalling downstream of PI3 kinase in mammary epithelium: a play in 3 Akts. Breast Cancer Research 2010;12(202).
64. Chang HW AM, Fruman D, Auger KR, Bellacosa A, Tsichlis PN, Cantley LC, Roberts TM, Vogt PK. Transformation of Chicken Cells by the Gene Encoding the Catalytic Subunit of PI 3-Kinase. Science 1997;276(5320): 1848-50.
65. Liu Z RT. Human Tumor Mutants in the p110a Subunit of PI3K. Cell Cycle 2006;5(7): 675-77.

66. Klippel A EJ, Hirano M, Williams LT. The Interaction of Small Domains between the Subunits of Phosphatidylinositol 3-Kinase Determines Enzyme Activity. Molecular and Cellular Biology 1994: 2675-85.
67. Klippel A RC, Kavanaugh WM, Apell G, Escobedo M-A, Williams LT. Membrane Localization of Phosphatidylinositol 3-Kinase Is Sufficient To Activate Multiple Signal-Transducing Kinase Pathways. Molecular and Cellular Biology 1996: 4117-27.
68. Link W RA, Fominaya J, Thomas JE, Carnero A. Membrane Localization of all Class I PI 3-Kinase Isoforms Suppresses c-Myc-Induced Apoptosis in Rat1 Fibroblasts via Akt. Journal of Cellular Biochemistry 2005;95: 979-89.
69. Gericke A MM, Ross AH. Regulation of PTEN phosphatase. Gene 2006;374.
70. Di Christofano A PP. The Multiple Roles of PTEN in Tumor Supppression. Cell 2000;100: 387-90.
71. Freeman DJ LA, Wei G, Li H-H, Kertesz N, Lesche R, Whale AD, Martinez-Diaz H, Rozengurt N, Cardiff RD, Liu X, Wu H. PTEN tumor suppressor regulates p53 protein levels and activity through phosphatase-dependent and -independent mechanisms. Cancer Cell 2003;3.
72. Blanco-Aparicio C RO, Leal JFM, Carnero A. PTEN, more than the AKT pathway. Carcinogenesis 2007;28(7): 1379-86.
73. Piccart-Gebhart MJ PM, Leyland-Jones B, et al. Trastuzumab after adjuvant chemotherapy in HER2-positive breast cancer. N Engl J Med 2005;353(1659-1672).
74. Slamon DJ L-JB, Shak S, et al. Use of chemotherapy plus a monoclonal antibody against HER2 for metastatic breast cancer that overexpresses HER2. N Engl J Med 2001;353.
75. Carter P PL, Gorman CM, Ridgway JBB, Henner D, Wong WLT, Rowland AM, Kotts C, Carver ME, Shepard HM. Humanization of an anti-p185HER2 antibody for human cancer therapy. PNAS 1992;89: 4285-89.
76. Baselga J NL, Albanell J, Kim YM, Mendelsohn J. Recombinant humanized Anti-HER2 Antibody (Herceptin) Enhances the Antitumour Activity of Paclitaxel and doxorubicin against HER2/neu Overexpressing Human Breast Cancer Xenografts. Cancer Research 1998;58: 2825-31.
77. Piccart-Gebhart MJ PM, Leyland-Jones B, et al Trastuzumab after adjuvant chemotherapy in HER2-amplified breast cancer. N Engl J Med 2005;353: 1659-72.
78. Perez EA, Romond EH, Suman VJ, et al. Four-year follow-up of trastuzumab plus adjuvant chemotherapy for operable human epidermal growth factor receptor 2-positive breast cancer: joint analysis of data from NCCTG N9831 and NSABP B-31. J Clin Oncol 2011;29(25): 3366-73.
79. Perez EA RE, Suman VJ, et al. Four-Year Follow-Up of Trastuzumab Plus Adjuvant Chemotherapy for Operable Human Epidermal Growth Factor Receptor 2-Positive Breast Cancer: Joint Analysis of Data From NCCTG N9831 and NSABP B-31. J Clin Oncol 2011;29(25).
80. Slamon DJ, Leyland-Jones B, Shak S, et al. Use of chemotherapy plus a monoclonal antibody against HER2 for metastatic breast cancer that overexpresses HER2. N Engl J Med 2001;344(11): 783-92.
81. Piccart-Gebhart MJ, Procter M, Leyland-Jones B, et al. Trastuzumab after adjuvant chemotherapy in HER2-positive breast cancer. N Engl J Med 2005;353(16): 1659-72.

82. Romond EH PE, Bryant J, et al. Trastuzuman plus adjuvant chemotherapy for operable HER2-positive breast cancer. N Engl J Med 2005;353: 1673-84.
83. Gianni L EW, Semiglazov V, et al. Neoadjuvant chemotherapy with trastuzumab followed by adjuvant trastuzumab followed by neoadjuvant chemotherapy alone, in patients with HER2-positive locally advanced breast cancer (the NOAH trial): a randomised controlled superiority trial with a parallel HER2-negative cohort. The Lancet 2010;375: 377-84.
84. Cho HS MK, Ramyar KX, Stanley AM, Gabelli SB, Denney JrDW, Leahy DJ. structure of the extracellular region of HER2 alone and in complex with the Herceptin Fab. Nature 2003;421.
85. Cuello M ES, Clark AS, Keane MM, Posner RH, Nau MM, Dennis PA, Lipkowitz S. Down-Regulation of the erbB-2 Receptor by Trastuzumab (Herceptin) enhances Tumor Necrosis Factor-related Apoptosis-inducing Ligand-mediated Apoptosis in Breast and Ovarian Cancer Cell Lines that Overexpress erbB-2. Cancer Res. 2001;61: 4892-900.
86. Dolloff NG MP, Hart LS, Dicker DT, Humphreys R, El-Deiry WS. Off-target lapatinib activity sensitizes colon cancer cells through TRAIL death receptor up-regulation. Sci Transl Med 2011;3(86).
87. Berns K (1st) HHs, Hennessy BT, et al: A functional genetic approach identifies the PI3K pathway as a major determinant of Trastuzumab resistance in breast cancer. Cancer Cell 12:395-402, 2007. A functional genetic approach identifies the PI3K pathway as a major determinant of Trastuzumab resistance in breast cancer. . Cancer Cell 2007;12: 395-402.
88. Molina MA C-SJ, Albanell J, Rojo F, Arribas J, Baselga J. Trastuzumab (Herceptin), a Humanized Anti-HER2 Receptor Monoclonal Antibody, Inhibits Basal and Activated HER2 Ectodomain Cleavage in Breast Cancer Cells. Cancer Research 2001;61: 4744-49.
89. Zagozdzon R GW, Crown J. Truncated HER2: implications for HER2-targeted therapeutics. Drug Discovery Today 2011;16(810-816).
90. Xiao-Feng Le F-XC, Amy Lammayot, Ling Tian, Deepa Deshpande, Ruth LaPushin, Ana M. Tari and Robert C. Bast Jr. The Role of Cyclin-dependent Kinase Inhibitor p27Kip1 in Anti-HER2 Antibody-induced G1 Cell Cycle Arrest and Tumor Growth Inhibition. Journal of Biological Chemistry 2003;278: 23441-50.
91. Arnould L GM, Penault-Llorca F, Benoit L, Bonnetain F, Migeon C, Cabaret V, Fermeaux V, Bertheau P, Garnier J, Jeannin J-F, Coudert B. Trastuzumab-based treatment of HER2-positive breast cancer: an antibody-dependent cellular cytotoxicity mechanism? British Journal of Cancer 2006;94: 259-67.
92. Clynes RA TT, Presta LG, Ravetch JV. Inhibitory Fc receptors modulate in vivo cytotoxicity against tumor targets. Nat Med 2000;6: 443-6.
93. D. M. Collins NOD, P. M. McGowan, F. O'Sullivan, M. J. Duffy & J. Crown. Trastuzumab induces antibody-dependent cell-mediated cytotoxicity (ADCC) in HER-2-non-amplified breast cancer cell lines. Annals of Oncology 2012;23: 1788–95.
94. Gennari R MS, Fagnoni F, Ponchio L, Scelsi M, Tagliabue E, Castiglioni F, Villani L, Magalotti C, Gibelli N, Oliviero B, Ballardini B, Da Prada G, Zambelli A, Costa A,. Pilot study of the mechanism of action of preoperative trastuzumab in patients with primary operable breast tumors overexpressing HER2. . Clin Cancer Res 2004;10(17): 5650 - 5.

95. Nahta R YD, Hung MC, Hortobagyi GN, Esteva FJ. . Mechanisms of Disease: understanding resistance to HER2-targeted therapy in human breast cancer. . Nature Clinical Practice Oncology 2006;3(5): 269-80.
96. Gril B, Palmieri D, Bronder JL, et al. Effect of lapatinib on the outgrowth of metastatic breast cancer cells to the brain. J Natl Cancer Inst 2008;100(15): 1092-103.
97. David W. Rusnak KL, Karen Affleck, et al. The Effects of the Novel, Reversible Epidermal Growth Factor Receptor/ErbB-2 Tyrosine Kinase Inhibitor, GW2016, on the Growth of Human Normal and Tumor-derived Cell Lines in Vitro and in Vivo. Mol Cancer Ther 2001;1: 85-94.
98. Cameron D, Casey M, Press M, et al. A phase III randomized comparison of lapatinib plus capecitabine versus capecitabine alone in women with advanced breast cancer that has progressed on trastuzumab: updated efficacy and biomarker analyses. Breast Cancer Res Treat 2008;112(3): 533-43.
99. Nahta R, Yuan LX, Du Y, Esteva FJ. Lapatinib induces apoptosis in trastuzumab-resistant breast cancer cells: effects on insulin-like growth factor I signaling. Mol Cancer Ther 2007;6(2): 667-74.
100. Scaltriti M, Chandarlapaty S, Prudkin L, et al. Clinical benefit of lapatinib-based therapy in patients with human epidermal growth factor receptor 2-positive breast tumors coexpressing the truncated p95HER2 receptor. Clin Cancer Res 2010;16(9): 2688-95.
101. Xia W, Mullin RJ, Keith BR, et al. Anti-tumor activity of GW572016: a dual tyrosine kinase inhibitor blocks EGF activation of EGFR/erbB2 and downstream Erk1/2 and AKT pathways. Oncogene 2002;21(41): 6255-63.
102. Xia W MR, Keith BR,Liu L-H, Ma H, Rusnak DW, Owens G, Alligood KJ, and Spector NL. Anti-tumor activity of GW572016: a dual tyrosine kinase inhibitor blocks EGF activation of EGFR/erbB2 and downstream Erk1/2 and AKT

pathways. Oncogene 2002;21: 6255-63.
103. Gilmer TM. Lapatinib: functional genomics study leads to insights into mechanism of action. Mol Cancer Ther 2011;10(11): 2025.
104. Lin NU, Dieras V, Paul D, et al. Multicenter phase II study of lapatinib in patients with brain metastases from HER2-positive breast cancer. Clin Cancer Res 2009;15(4): 1452-9.
105. Piccart-Gebhart MJ HA, Baselga J, et al. First results from the phase III ALTTO trial (BIG 2-06; NCCTG [Alliance] N063D) comparing one year of anti-HER2 therapy with lapatinib alone (L), trastuzumab alone (T), their sequence (T→L), or their combination (T+L) in the adjuvant treatment of HER2-positive early breast cancer (EBC). JCO 2014;32:5s.
106. Gelmon KA BF, Kaufman B, et al. . Open-label phase III randomized controlled trial comparing taxane-based chemotherapy (Tax) with lapatinib (L) or trastuzumab (T) as first-line therapy for women with HER2+ metastatic breast cancer: Interim analysis (IA) of NCIC CTG MA.31/GSK EGF 108919. JCO 2012;30(15_suppl).
107. Geyer CE FJ, Lindquist D, Chan S, Romieu CG, Pienkowski T, Jagiello-Gruszfeld A, Crown J, Chan A, Kaufman B, Skarlos D, Campone M, Davidson N, Berger M, Oliva C, Rubin SD, Stein S, Cameron D. Lapatinib plus Capecitabine for HER2-Positive Advanced Breast Cancer. N Engl J Med 2006;355(26).

108. Agus DB, Akita RW, Fox WD, et al. Targeting ligand-activated ErbB2 signaling inhibits breast and prostate tumor growth. Cancer Cell 2002;2(2): 127-37.
109. David B Agus RWA, William D Fox, Gail D Lewis, Brian Higgins, Paul I Pisacane, Julie A Lofgren, Charles Tindell, Douglas P Evans, Krista Maiese, Howard I Scher, Mark X Sliwkowski. Targeting ligand-activated ErbB2 signaling inhibits breast and prostate tumor growth. Cancer Cell 2002;2(2): 127-37.
110. Lee-Hoeflich ST, Crocker L, Yao E, et al. A central role for HER3 in HER2-amplified breast cancer: implications for targeted therapy. Cancer Res 2008;68(14): 5878-87.
111. Si Tuen Lee-Hoeflich LC, Evelyn Yao, Thinh Pham, Xander Munroe,, Klaus P. Hoeflich MXS, and Howard M. Stern. A Central Role for HER3 in HER2-Amplified Breast Cancer: Implications for Targeted Therapy. Cancer Res. 2008;68: 5878-87.
112. Werner Scheuer TF, Helmut Burtscher, Birgit Bossenmaier, Josef Endl, and Max Hasmann. Strongly Enhanced Antitumor Activity of Trastuzumab and Pertuzumab Combination Treatment on HER2-Positive Human Xenograft Tumor Models. Cancer Res. 2009;69: 9330.
113. Scheuer W, Friess T, Burtscher H, Bossenmaier B, Endl J, Hasmann M. Strongly enhanced antitumor activity of trastuzumab and pertuzumab combination treatment on HER2-positive human xenograft tumor models. Cancer Res 2009;69(24): 9330-6.
114. José Baselga JC, Sung-Bae Kim, Seock-Ah Im, Roberto Hegg, Young-Hyuck Im, Laslo Roman, José Luiz Pedrini, Tadeusz Pienkowski, Adam Knott, Emma Clark, Mark C. Benyunes, Graham Ross, and Sandra M. Swain, for the CLEOPATRA Study Group*. Pertuzumab plus Trastuzumab plus Docetaxel for Metastatic Breast Cancer. N Engl J Med 2011;366(2).
115. Luca Gianni TP, Young-Hyuck Im, Laslo Roman, Ling-Ming Tseng, Mei-Ching Liu, Ana Lluch, Elżbieta Staroslawska,, Juan de la Haba-Rodriguez S-AI, Jose Luiz Pedrini, Brigitte Poirier, Paolo Morandi, Vladimir Semiglazov, Vichien Srimuninnimit, Giulia Bianchi, Tania Szado, Jayantha Ratnayake, Graham Ross, Pinuccia Valagussa. Efficacy and safety of neoadjuvant pertuzumab and trastuzumab in women with locally advanced, inflammatory, or early HER2-positive breast cancer (NeoSphere): a randomised multicentre, open-label, phase 2 trial. Lancet Oncology 2012;13: 25-32.
116. Gianni L BG, Valagussa P, Belousov A, Thomas M, Ross G, Pusztai L. Adaptive Immune System and Immune Checkpoints Are Associated with Response to Pertuzumab (P) and Trastuzumab (H) in the NeoSphere Study. SABCS. San Antonio, 2012.
117. Loi S MS, Salgado R, Sirtaine N, Jose V, Fumagalli D, Brown DN, Kellokumpu-Lehtinen P-L, Bono P, Kataja V, Desmedt C, Piccart-Gebhart MJ, Loibl S, Untch M, Denkert C, Smyth MJ, Joensuu H, Sotiriou C. Tumor infiltrating lymphocytes (TILs) indicate trastuzumab benefit in early-stage HER2-positive breast cancer (HER2+ BC). SABCS. San Antonio, 2013.
118. Ravi V. J. Chari BAM, Jonathan L. Gross, et al. Immunoconjugates Containing Novel Maytansinoids: Promising Anticancer Drugs. Cancer Res. 1992;52: 127-31.
119. Kakkar SAHaR. The potential for trastuzumab emtansine in human epidermal growth factor receptor 2 positive metastatic breast cancer: latest evidence and ongoing studies. Therapeutic Advances in Medical Oncology 2012;4(5): 235-45.

120. Gail D. Lewis Phillips GL, Debra L. Dugger, Lisa M. Crocker, Kathryn L. Parsons, Elaine Mai, Walter A. Bla¨ttler, John M. Lambert, Ravi V.J. Chari, Robert J. Lutz, Wai Lee T. Wong, Frederic S. Jacobson, Hartmut Koeppen, Ralph H. Schwall, Sara R. Kenkare-Mitra, Susan D. Spencer, and Mark X. Sliwkowski. Targeting HER2-Positive Breast Cancer with Trastuzumab-DM1, an Antibody–Cytotoxic Drug Conjugate. Cancer Res. 2008;68: 9280-90.
121. Erickson HK, Park PU, Widdison WC, et al. Antibody-maytansinoid conjugates are activated in targeted cancer cells by lysosomal degradation and linker-dependent intracellular processing. Cancer Res 2006;66(8): 4426-33.
122. Junttila TT, Li G, Parsons K, Phillips GL, Sliwkowski MX. Trastuzumab-DM1 (T-DM1) retains all the mechanisms of action of trastuzumab and efficiently inhibits growth of lapatinib insensitive breast cancer. Breast Cancer Res Treat 2011;128(2): 347-56.
123. Boyraz B, Sendur MA, Aksoy S, et al. Trastuzumab emtansine (T-DM1) for HER2-positive breast cancer. Curr Med Res Opin 2013;29(4): 405-14.
124. Slamon D, Eiermann W, Robert N, et al. Adjuvant trastuzumab in HER2-positive breast cancer. N Engl J Med 2011;365(14): 1273-83.
125. Geyer CE FJ, Lindquist D, Chan S, Romieu CG, Pienkowski T, Jagiello-Gruszfeld A, Crown J, Chan A, Kaufman B, Skarlos D, Campone M, Davidson N, Berger M, Oliva C, Rubin SD, Stein S, Cameron D. Lapatinib plus Capecitabine for HER2-Positive Advanced Breast Cancer. N Engl J Med 2006;355(26): 2733-43.
126. Robidoux A, Tang G, Rastogi P, et al. Lapatinib as a component of neoadjuvant therapy for HER2-positive operable breast cancer (NSABP protocol B-41): an open-label, randomised phase 3 trial. Lancet Oncol 2013;14(12): 1183-92.
127. Guarneri V, Frassoldati A, Bottini A, et al. Preoperative chemotherapy plus trastuzumab, lapatinib, or both in human epidermal growth factor receptor 2-positive operable breast cancer: results of the randomized phase II CHER-LOB study. J Clin Oncol 2012;30(16): 1989-95.
128. Lisa A. Carey DAB, David Ollila, Lyndsay Harris, Ian E. Krop, Douglas Weckstein, Norah Lynn Henry, Carey K. Anders, Constance Cirrincione, Eric P. Winer, Charles M. Perou, Clifford Hudis. Clinical and translational results of CALGB 40601: A neoadjuvant phase III trial of weekly paclitaxel and trastuzumab with or without lapatinib for HER2-positive breast cancer. J Clin Oncol 2013;31(supl: abstract 500).
129. Piccart-Gebhart M HA, de Azambuja E, Di Cosimo S, Swaby R, Untch M, Jackisch C, Lang I, Smith I, Boyle F, Xu B, Barrios C, Gelber R, Eidtmann H, Baselga J. . The association between event-free survival and pathological complete response to neoadjuvant lapatinib, trastuzumab or their combination in HER2-positive breast cancer. Survival follow-up analysis of the NeoALTTO study (BIG 1-06). SABCS, 2013.
130. Gianni L, Eiermann W, Semiglazov V, et al. Neoadjuvant chemotherapy with trastuzumab followed by adjuvant trastuzumab versus neoadjuvant chemotherapy alone, in patients with HER2-positive locally advanced breast cancer (the NOAH trial): a randomised controlled superiority trial with a parallel HER2-negative cohort. Lancet 2010;375(9712): 377-84.
131. Sunil Verma DM, Luca Gianni, Ian E. Krop, Manfred Welslau, José Baselga, Mark Pegram, Do-Youn Oh, Véronique Diéras, Ellie Guardino, Liang Fang, Michael W. Lu, Steven Olsen, and Kim Blackwell. Trastuzumab Emtansine for HER2-Positive Advanced Breast Cancer. N Engl J Med 2012;367(19).

132. Krop IE, Kim SB, Gonzalez-Martin A, et al. Trastuzumab emtansine versus treatment of physician's choice for pretreated HER2-positive advanced breast cancer (TH3RESA): a randomised, open-label, phase 3 trial. Lancet Oncol 2014;15(7): 689-99.
133. Harold J. Burstein YS, Luc Y. Dirix, Zefei Jiang, Robert Paridaens, Antoinette R. Tan, Ahmad Awada, Anantbhushan Ranade, Shunchang Jiao, Gary Schwartz, Richat Abbas, Christine Powell, Kathleen Turnbull, Jennifer Vermette, Charles Zacharchuk, and Rajendra Badwe. Neratinib, an Irreversible ErbB Receptor Tyrosine Kinase Inhibitor, in Patients With Advanced ErbB2-Positive Breast Cancer. J Clin Oncol 2010;28(8).
134. Lin NU WE, Wheatley D, Carey LA, Houston S, Mendelson D, Munster P, Frakes L, Kelly S, Garcia AA, Cleator S, Uttenreuther-Fischer M, Jones H, Wind S, Vinisko R, Hickish T. A phase II study of afatinib (BIBW 2992), an irreversible ErbB family blocker, in patients with HER2-positive metastatic breast cancer progressing after trastuzumab. Breast Cancer Res Treat 2012;133: 1057-65.
135. Nagy P, Friedlander E, Tanner M, et al. Decreased accessibility and lack of activation of ErbB2 in JIMT-1, a herceptin-resistant, MUC4-expressing breast cancer cell line. Cancer Res 2005;65(2): 473-82.
136. Esteva FJ, Guo H, Zhang S, et al. PTEN, PIK3CA, p-AKT, and p-p70S6K status: association with trastuzumab response and survival in patients with HER2-positive metastatic breast cancer. Am J Pathol 2010;177(4): 1647-56.
137. Browne BC, Eustace AJ, Kennedy S, et al. Evaluation of IGF1R and phosphorylated IGF1R as targets in HER2-positive breast cancer cell lines and tumours. Breast Cancer Res Treat 2012;136(3): 717-27.
138. Zhang S, Huang WC, Li P, et al. Combating trastuzumab resistance by targeting SRC, a common node downstream of multiple resistance pathways. Nat Med 2011;17(4): 461-9.
139. Saez R, Molina MA, Ramsey EE, et al. p95HER-2 predicts worse outcome in patients with HER-2-positive breast cancer. Clin Cancer Res 2006;12(2): 424-31.
140. Miller TW RB, Garret JT, Arteaga CL. Mutations in the phosphatidylinositol 3-kinase pathway: role in tumor progression and therapeutic implications in breast cancer. Breast Cancer Research 2011;13(224).
141. Stemke-Hale KA G-AA, Lluch A, Neve RM, Davies MA, Carey MS, Sahin A, Symmans WF, Pusztai L, Nolden L, Horlings H, Berns K, Hung MC, van de Vijver MJ, Valero V, Gray JW, Bernards R, Mills GB, Hennessy BT An integrative genomic and proteomic analysis of PIK3CA, PTEN and AKT mutations in breast cancer. . Cancer Research 2008;68: 6084-91.
142. Samuels Y WZ, Bardelli A, et al. . High frequency of mutations of the PIK3CA gene in human cancers. Science 2004;304(554.).
143. Bachman KE AP, Samuels Y, et al. . The PIK3CA gene is mutated with high frequency in human breast cancers. . Cancer Biol Ther 2004;3.
144. Saal LH HK, Maurer M, et al PIK3CA mutations correlate with hormone receptors, node metastasis, and ERBB2, and are mutually exclusive with PTEN loss in human breast carcinoma. . Cancer Res 2005;65: 2554-59.
145. Hennessy BT, Smith DL, Ram PT, Lu Y, Mills GB. Exploiting the PI3K/AKT pathway for cancer drug discovery. Nat Rev Drug Discov 2005;4(12): 988-1004.

146. Loibl S DC, Schneeweis A, Paepke S, Lehmann A, Rezai M, Zahm D-M, Sinn P, Khandan F, Eidtmann H, Dohnal K, Huober J, Loi S, Pfitzner B, Fasching PA, Andre F, Lindner J, Sotiriou C, Guo S, Gade S, Nekljudova V, Untch M, von Minckwitz G. PIK3CA mutation predicts resistance to anti-HER2/chemotherapy in primary HER2-positive/hormone-receptor-positive breast cancer – Prospective analysis of 737 participants of the GeparSixto and GeparQuinto studies. SABCS. San Antonio, 2013.
147. Baselga J. PI3KCA mutations and correlation with pCR in the NeoALTTO trial. SABCS. San Antonio, 2013.
148. Zardavas D FD, Borwn DN, Desmedt C, Metzger-Filho O, Piccart M, Sotiriou C, Michieles S, Loi S. Understanding the biology and prognosis of PIK3CA gene mutations in primary breast cancer using gene expression profiling: A pooled analysis. SABCS. San Antonio, 2013.
149. Loi S, Michiels S, Lambrechts D, et al. Somatic mutation profiling and associations with prognosis and trastuzumab benefit in early breast cancer. J Natl Cancer Inst 2013;105(13): 960-7.
150. Gayle SS AS, O'Regan RM, Nahta R. Pharmacologic Inhibition of mTOR Improves Lapatinib Sensitivity in HER2-Overexpressing Breast Cancer Cells with Primary Trastuzumab Resistance. Anti-Cancer Agents in Medicinal Chemistry 2012;12(2): 151-62.
151. Stemke-Hale K, Gonzalez-Angulo AM, Lluch A, et al. An integrative genomic and proteomic analysis of PIK3CA, PTEN, and AKT mutations in breast cancer. Cancer Res 2008;68(15): 6084-91.
152. O'Brien NA BB, Chow L, et al. Activated Phosphoinositide 3-Kinase/AKT Signaling Confers Resistance to Trastuzumab but not Lapatinib. Molecular Cancer Therapeutics 2010;9: 1489-502.
153. Gayle SS AS, O'Regan RM, Nahta R. Pharmacologic Inhibition of mTOR Improves Lapatinib Sensitivity in HER2-Overexpressing Breast Cancer Cells with Primary Trastuzumab Resistance. Anti-Cancer Agents in Medicinal Chemistry 2012;12.
154. Christian D Young ECN, Andrew Lewis, Natalie J Serkova, and Steven M Andersoncorresponding Activated Akt1 accelerates MMTV-c-ErbB2 mammary tumourigenesis in mice without activation of ErbB3. Breast Cancer Res 2008;10(4).
155. Nagata Y LK, Zhou X, et al. PTEN activation contributes to tumor inhibition by trastuzumab, and loss of PTEN predicts trastuzumab resistance in patients. Cancer Cell 2004;6: 117-27.
156. Esteva FJ GH, Zhang S, Santa-Maria C, Stone S, Lanchbury JS, Sahin AA, Hortobagyi GN, Yu D. PTEN, PIK3CA, p-AKT, and p-p70S6K Status Association with Trastuzumab Response and Survival in Patients with HER2-Positive Metastatic Breast Cancer. Am J Pathol 2010;177(4).
157. Nahta R YL, Zhang B, et al Insulin-like Growth Factor-I Receptor/Human Epidermal Growth Factor Receptor 2 Heterodimerization Contributes to Trastuzumab Resistance of Breast Cancer Cells. Cancer Res 2005;65: 11118-28.
158. Xiaoping Huang LG, Shuiliang Wang, James L. McManaman, Ann D. Thor, XiaoHe Yang, Francisco J. Esteva, and Bolin Liu. Heterotrimerization of the Growth Factor Receptors erbB2, erbB3, and Insulin-like Growth Factor-I Receptor in Breast Cancer Cells Resistant to Herceptin. Cancer Res. 2010;70: 1204.

159. B. C. Browne JC, N. Venkatesan, M. J. Duffy, M. Clynes, D. Slamon & N. O'Donovan. Inhibition of IGF1R activity enhances response to trastuzumab in HER-2-positive breast cancer cells. Ann Oncol 2011;22: 68-73.
160. A. Esparıs-Ogando AO, R. Rodrıguez-Barrueco, L. Ferreira, J. Borges & A. Pandiella. Synergic antitumoral effect of an IGF-IR inhibitor and trastuzumab on HER2-overexpressing breast cancer cells. Ann Oncol 2008;19: 1860–69.
161. Brigid C. Browne AJE, Susan Kennedy, Neil A. O'Brien, Kasper Pedersen, Martina S. J. McDermott, Annemarie Larkin, Jo Ballot, Thamir Mahgoub, Francesco Sclafani, Stephen Madden, John Kennedy, Michael J. Duffy, John Crown, Norma O'Donovan. Evaluation of IGF1R and phosphorylated IGF1R as targets in HER2-positive breast cancer cell lines and tumours. Breast Cancer Res Treat 2012;136: 717-27.
162. THEODORA G. KALEMI KTP, ALEXANDROS F. LAMBROPOULOS, SOULTANA VOYATZI, ALEXANDROS KOTSIS, and ALEXANDROS H. KORTSARIS. Expression of the HER Family mRNA in Breast Cancer Tissue and Association with Cell Cycle Inhibitors p21waf1 and p27kip1. Anticancer Research 2007;27: 913-20.
163. Nahta R TT, Ueno NT, Hung M-C, Esteva FJ. P27KIP1 Down-Regulation is Associated with Trastuzumab Resistance in Breast Cancer Cells. Cancer Research 2004;64: 3981-86.
164. F. Michael Yakes WC, Christoph A. Ritter, Walter King, Steven Seelig, and Carlos L. Arteaga. Herceptin-induced Inhibition of Phosphatidylinositol-3 Kinase and Akt Is Required for Antibody-mediated Effects on p27, Cyclin D1, and Antitumor Action. Cancer Res. 2002;62: 4132.
165. Jun-ichi Yamashita MO, Shin-ichi Yamashita, Koichi Nomura, Masafumi Kuramoto, Tetsushi Saishoji, and Sadahito Shin. Immunoreactive Hepatocyte Growth Factor Is a Strong and Independent Predictor of Recurrence and Survival in Human Breast Cancer. Cancer Res. 1994;54: 1630-33.
166. Yan Yao LJ, Alexander Fuchs, Ansamma Joseph, Harold M. Hastings, Itzhak D. Goldberg, and Eliot M. Rosen. Scatter Factor Protein Levels in Human Breast Cancers. Am J Pathol 1996;149(5).
167. Hanane Khoury MAN, Dongmei Zuo, Veena Sangwan, Melanie M. Frigault, Stephanie Petkiewicz, David L. Dankort, William J. Muller, and Morag Park. HGF Converts ErbB2/Neu Epithelial Morphogenesis to Cell Invasion. Mol Biol Cell 2005;16(2): 550-61.
168. Todd W. Bauer RJS, Fan Fan, Wenbiao Liu, Marjorie Johnson, Donald P. Lesslie, Douglas B. Evans, Gary E. Gallick and Lee M. Ellis. Regulatory role of c-Met in insulin-like growth factor-I receptor–mediated migration and invasion of human pancreatic carcinoma cells. Mol Cancer Ther 2006;5: 1676.
169. David L. Shattuck JKM, Kermit L. Carraway III, et al. Met Receptor Contributes to Trastuzumab Resistance of Her2-Overexpressing Breast Cancer Cells. Cancer Res. 2008;68: 1471-77.
170. Judit Anido MS, Joan Josep Bech Serra, Bele´n Santiago Josefat, Federico Rojo Todo, Jose´ Baselga and Joaquı´n Arribas. Biosynthesis of tumorigenic HER2 C-terminal fragments by alternative initiation of translation. EMBO J. 2006;5: 3234-44.
171. Miguel A. Molina RS, Elizabeth E. Ramsey, Marıa-Jose Garcia-Barchino, Federico Rojo, Adam J. Evans, Joan Albanell, Edward J. Keenan, Ana Lluch, Javier

Garcıa-Conde, Jose Baselga, and Gail M. Clinton. NH2-terminal Truncated HER-2 Protein but not Full-Length Receptor Is Associated with Nodal Metastasis in Human Breast Cancer 2002;8: 347-53.
172. !!! INVALID CITATION !!!
173. Rosana Sáez MAM, Elizabeth E. Ramsey, et al. p95HER-2 Predicts Worse Outcome in Patients with HER-2-Positive Breast Cancer. Clin Cancer Res 2006;12: 424-31.
174. Maurizio Scaltriti FR, Alberto Ocaña , Judit Anido , Marta Guzman , Javier Cortes , Serena Di Cosimo , Xavier Matias-Guiu , Santiago Ramon y Cajal , Joaquin Arribas , José Baselga. Expression of p95HER2, a Truncated Form of the HER2 Receptor, and Response to Anti - HER2 Therapies in Breast Cancer. J Natl Cancer Institute 2007;99: 628-38.
175. Shari A. PRICE-SCHIAVI, Scott JEPSON, Peter LI, Maria ARANGO, Philip S. RUDLAND, Lisa YEE and Kermit L. CARRAWAY. RAT MUC4 (SIALOMUCIN COMPLEX) REDUCES BINDING OF ANTI-ERBB2 ANTIBODIES TO TUMOR CELL SURFACES, A POTENTIAL MECHANISM FOR HERCEPTIN RESISTANCE. Int J Cancer 2002.
176. Peter Nagy EF, Minna Tanner, Anita I. Kapanen, Kermit L. Carraway, Jorma Isola, and Thomas M. Jovin. Decreased Accessibility and Lack of Activation of ErbB2 in JIMT-1, a Herceptin-Resistant, MUC4-Expressing Breast Cancer Cell Line. Cancer Res. 2005;65: 473.
177. Trowe T, Boukouvala S, Calkins K, et al. EXEL-7647 inhibits mutant forms of ErbB2 associated with lapatinib resistance and neoplastic transformation. Clin Cancer Res 2008;14(8): 2465-75.
178. Rexer BN, Ghosh R, Narasanna A, et al. Human breast cancer cells harboring a gatekeeper T798M mutation in HER2 overexpress EGFR ligands and are sensitive to dual inhibition of EGFR and HER2. Clin Cancer Res 2013;19(19): 5390-401.
179. Boulbes DR JQ, Arold ST, Ladbury JE, Yu D, Esteva FJ. . 2011. SABCS. San Antonio.
180. Jaiswal BS, Kljavin NM, Stawiski EW, et al. Oncogenic ERBB3 mutations in human cancers. Cancer Cell 2013;23(5): 603-17.
181. Tvorogov D, Sundvall M, Kurppa K, et al. Somatic mutations of ErbB4: selective loss-of-function phenotype affecting signal transduction pathways in cancer. J Biol Chem 2009;284(9): 5582-91.
182. Berns K, Horlings HM, Hennessy BT, et al. A functional genetic approach identifies the PI3K pathway as a major determinant of trastuzumab resistance in breast cancer. Cancer Cell 2007;12(4): 395-402.
183. O'Brien NA, Browne BC, Chow L, et al. Activated phosphoinositide 3-kinase/AKT signaling confers resistance to trastuzumab but not lapatinib. Mol Cancer Ther 2010;9(6): 1489-502.
184. Scaltriti M, Rojo F, Ocana A, et al. Expression of p95HER2, a truncated form of the HER2 receptor, and response to anti-HER2 therapies in breast cancer. J Natl Cancer Inst 2007;99(8): 628-38.
185. Anido J, Scaltriti M, Bech Serra JJ, et al. Biosynthesis of tumorigenic HER2 C-terminal fragments by alternative initiation of translation. EMBO J 2006;25(13): 3234-44.

186. Molina MA, Saez R, Ramsey EE, et al. NH(2)-terminal truncated HER-2 protein but not full-length receptor is associated with nodal metastasis in human breast cancer. Clin Cancer Res 2002;8(2): 347-53.
187. Shattuck DL, Miller JK, Carraway KL, 3rd, Sweeney C. Met receptor contributes to trastuzumab resistance of Her2-overexpressing breast cancer cells. Cancer Res 2008;68(5): 1471-7.
188. Yamashita J, Ogawa M, Yamashita S, et al. Immunoreactive hepatocyte growth factor is a strong and independent predictor of recurrence and survival in human breast cancer. Cancer Res 1994;54(7): 1630-3.
189. Le XF, Claret FX, Lammayot A, et al. The role of cyclin-dependent kinase inhibitor p27Kip1 in anti-HER2 antibody-induced G1 cell cycle arrest and tumor growth inhibition. J Biol Chem 2003;278(26): 23441-50.
190. Kalemi TG, Papazisis KT, Lambropoulos AF, Voyatzi S, Kotsis A, Kortsaris AH. Expression of the HER family mRNA in breast cancer tissue and association with cell cycle inhibitors p21(waf1) and p27(kip1). Anticancer Res 2007;27(2): 913-20.
191. Hennessy BT SD, Ram PT, Lu Y, Mills GB. EXPLOITING THE PI3K/AKT PATHWAY FOR CANCER DRUG DISCOVERY. Nature Reviews Drug Discovery 2005;4: 988-1004.
192. Wander SA HB, Slingerland JM. Next-generation mTOR inhibitors in clinical oncology: how pathway complexity informs therapeutic strategy. Journal of Clinical Investigation 2011;121(4).
193. O'Regan R. Phase 3, Randomized, Double-Blind, Placebo-Controlled Multicenter Trial of Daily Everolimus Plus Weekly Trastuzumab and Vinorelbine in Trastuzumab-Resistant, Advanced Breast Cancer (BOLERO-3). ASCO, 2013.
194. Sun SY RL, Wang X, et al: . Activation of Akt and eIF4E survival pathways by rapamycin-mediated mammalian target of rapamycin inhibition. . Cancer Res 2005;65: 7052 - 58.
195. S C. Phase II study of temsirolimus (CCI-779), a novel inhibitor of mTOR, in heavily pretreated patients with locally advanced or metastatic breast cancer. J Clin Oncol 2005;23(23).
196. O'Brien NA, McDonald K, Tong L, et al. Targeting PI3K/mTOR overcomes resistance to HER2-targeted therapy independent of feedback activation of AKT. Clin Cancer Res 2014;20(13): 3507-20.
197. Violeta Serra BM, Maurizio Scaltriti, Pieter J.A. Eichhorn, Vanesa Valero, Marta Guzman, Maria Luisa Botero, Elisabeth Llonch, Francesco Atzori, Serena Di Cosimo, Michel Maira, Carlos Garcia-Echeverria, Josep Lluis Parra, Joaquin Arribas, and José Baselga. NVP-BEZ235, a Dual PI3K/mTOR Inhibitor, Prevents PI3K Signaling and Inhibits the Growth of Cancer Cells with Activating PI3K Mutations. Cancer Research 2008;68(8022).
198. Saskia M. Brachmann aIH, a Christian Schnell,a Christine Fritsch,a Susan Wee,b,1 Heidi Lane,a,2 Shaowen Wang,b Carlos Garcia-Echeverria,a and Sauveur-Michel Mairaa. Specific apoptosis induction by the dual PI3K/mTor inhibitor NVP-BEZ235 in HER2 amplified and PIK3CA mutant breast cancer cells. PNAS 2009;106(52).
199. Jeffrey J. Wallin KAE, Jane Guan, Megan Berry, Wei Wei Prior, Leslie Lee, John D. Lesnick, Cristina Lewis, Jim Nonomiya, Jodie Pang, Laurent Salphati, Alan G. Olivero, Daniel P. Sutherlin, Carol O'Brien, Jill M. Spoerke, Sonal Patel, Letitia Lensun, Robert Kassees, Leanne Ross, Mark R. Lackner, Deepak Sampath, Marcia

Belvin, and Lori S. Friedman. GDC-0980 Is a Novel Class I PI3K/mTOR Kinase Inhibitor with Robust Activity in Cancer Models Driven by the PI3K Pathway. Mol Cancer Ther 2011;10: 2426.
200. Liu N RB, Schneider C, Bull C, Hoffmann J, Kaekoenen S, Hentemann M, Scott W, Mumberg D, Ziegelbauer K. BAY 80-6946, a highly selective and potent pan-class I PI3K inhibitor, induces tumor apoptosis in vitro and tumor regression in vivo in a subset of tumor models. American Association for Cancer Research. Washington DC, USA, 2010.
201. Liu N HA, Bull C, Schatz C, Wiehr S, Pichler BJ, Hauff P, Mumberg D, Jenkins S, Schwarz T, Ziegelbauer K. BAY 80-6946, a highly potent and efficacious PI3K class I inhibitor, induces complete tumor regresion or tumor stasis in tumor xenograft models with PIK3CA mutant or PTEN deletion. American Association for Cancer Research. Washington DC, USA, 2010.
202. Lotze MT AL, Ramanathan RK, Tolcher AW, Beeram M, Papadopoulos KP, Rasco DW, Weiss GJ, Mountz JM, Toledo FGS, Alvarez RJ, Oborski MJ, Rajagopalan P, Jeffers M, Roth D, Duboxy RL, Patnaik A. Phase I study of intravenous PI3K inhibitor BAY 80-6946: activity in patients with advanced solid tumors and non-Hodgkin's lymphoma treated in MTD expansion cohorts. American Society of Clinical Oncology. Chicago, Illinois, USA, 2012.
203. Saura C, Bendell J, Jerusalem G, et al. Phase Ib Study of Buparlisib plus Trastuzumab in Patients with HER2-Positive Advanced or Metastatic Breast Cancer That Has Progressed on Trastuzumab-Based Therapy. Clin Cancer Res 2014.
204. Junttila TT, Akita RW, Parsons K, et al. Ligand-independent HER2/HER3/PI3K complex is disrupted by trastuzumab and is effectively inhibited by the PI3K inhibitor GDC-0941. Cancer Cell 2009;15(5): 429-40.
205. Liu N HA, Scholz A, Hoffmann J, Mumberg D, Ziegelbauer K. Combination of PI3K inhibitor BAY 80-6946 with allosteric MEK inhibitor BAY 86-9766 (RDEA119) and with erlotinib for the treatment of non-small-cell lung cancer. 22nd EORTC-NCI-AACR Symposium. Berlin, Germany, 2010.
206. Rabindran SK, Discafani CM, Rosfjord EC, et al. Antitumor activity of HKI-272, an orally active, irreversible inhibitor of the HER-2 tyrosine kinase. Cancer Res 2004;64(11): 3958-65.
207. Denis Collins NOD, Naomi Walsh, Kathy Gately, Connla Edwards, Anthony Davies, Kenneth John O'Byrne, John Crown. The effects of lapatinib and neratinib on HER2 protein levels in breast cancer cell lines. ASCO, 2012.
208. Canonici A, Gijsen M, Mullooly M, et al. Neratinib overcomes trastuzumab resistance in HER2 amplified breast cancer. Oncotarget 2013;4(10): 1592-605.
209. Awada A, Dirix L, Manso Sanchez L, et al. Safety and efficacy of neratinib (HKI-272) plus vinorelbine in the treatment of patients with ErbB2-positive metastatic breast cancer pretreated with anti-HER2 therapy. Ann Oncol 2013;24(1): 109-16.
210. R. Swaby KB, Z. Jiang, Y. Sun, V. Dieras, K. Zaman, C. Zacharchuk, C. Powell, R. Abbas and M. Thakuria. Neratinib in combination with trastuzumab for the treatment of advanced breast cancer: A phase I/II study. ASCO: J Clin Oncol (Meeting Abstracts), 2009.
211. Bose R, Kavuri SM, Searleman AC, et al. Activating HER2 mutations in HER2 gene amplification negative breast cancer. Cancer Discov 2013;3(2): 224-37.

212. D Li LA, T Shimamura, S Kubo, M Takahashi, LR Chirieac, RF Padera, GI Shapiro, A Baum, F Himmelsbach, WJ Rettig, M Meyerson, F Solca, H Greulich, and K-K Wong. BIBW2992, an irreversible EGFR/HER2 inhibitor highly effective in preclinical lung cancer models. Oncogene 2008;27(4702-4711).
213. Lin NU, Winer EP, Wheatley D, et al. A phase II study of afatinib (BIBW 2992), an irreversible ErbB family blocker, in patients with HER2-positive metastatic breast cancer progressing after trastuzumab. Breast Cancer Res Treat 2012;133(3): 1057-65.
214. Schuler M AA, Harter P, Canon JL, Possinger K, Schmidt M, De Gréve J, Neven P, Dirix L, Jonat W, Beckmann MW, Schutte J, Fasching PA, Gottschalk N, Besse-Hammer T, Fleischer F, Wind S, Uttenreuther-Fischer M, Piccart M, Harbeck N. A phase II trial to assess the efficacy and safety of afatinib in extensively pretreated patients with HER2-negative metastatic breast cancer. Breast Cancer Res Treat 2012;134: 1149-59.
215. Nancy U. Lin EPW, Duncan Wheatley, Lisa A. Carey, Stephen Houston, David Mendelson, Pamela Munster, Laurie Frakes, Steve Kelly, Agustin A. Garcia, Susan Cleator, Martina Uttenreuther-Fischer, Hilary Jones, Sven Wind, Richard Vinisko, Tamas Hickish. A phase II study of afatinib (BIBW 2992), an irreversible ErbB family blocker, in patients with HER2-positive metastatic breast cancer progressing after trastuzumab. Breast Cancer Res Treat 2012;133: 1057-65.
216. Rimawi MF AS, Rozas AA, Nunes Matos Neto J, Caleffi M, Vinholes JJF, Figueira AC, Cunha Souza S, Reiriz AB, Arantes H, Uttenreuther-Fischer MM, Osborne CK. A neoadjuvant, randomized, open-label phase II trial of afatinib (A) versus trastuzumab (T) versus lapatinib (L) in patients (pts) with locally advanced HER2-positive breast cancer (BC). J Clin Oncol 2012;30 (suppl; abstr 606).